The biotransformation of benzene derivatives

the influence of active site and substrate characteristics
on the metabolic fate

Promotor:	Dr. C. Veeger Emeritus Hoogleraar in de Biochemie
Co-promotor:	Dr. ir. I.M.C.M. Rietjens Universitair Hoofddocent, Vakgroep Biochemie

Janneke Koerts

The biotransformation of benzene derivatives

the influence of active site and substrate characteristics on the metabolic fate

Proefschrift
ter verkrijging van de graad van doctor
op gezag van de rector magnificus
van de Landbouwuniversiteit Wageningen,
dr. C.M. Karssen,
in het openbaar te verdedigen
op woensdag 18 december 1996
des namiddags te vier uur in de Aula.

Thesis University Wageningen. With summary in Dutch.
ISBN 90-5485-621-1

NN08201, 2197

Stellingen

1. De invloed van de interactie tussen het substraat en het reactieve ijzer-oxo deeltje op de orientatie van het substraat in het actieve centrum van cytochroom P450 tijdens de katalyse is van groter belang dan algemeen wordt aangenomen.
Paulsen and Ornstein, 1993, Protein Engineering 6, 359-365.
Dit Proefschrift

2. Het feit dat in tegenstelling tot een fluor, broom en chloor atoom er geen cytochroom P450 gekatalyseerde jood NIH shift is waargenomen komt door het feit dat de aanval van het ijzer-oxo deeltje op de ring koolstof atomen naast het gesubstitueerde atoom wordt gehinderd door de grootte van het jood atoom.
Dit proefschrift

3. De rol van areen oxide intermediairen in de cytochroom P450 gekatalyseerde aromatische ring hydroxylering van gehalogeneerde benzenen wordt ten onrechte overschat.
Korzekwa et al., 1989, Biochemistry 28, 9019-9027.
Rietjens et al., 1993, Biochemistry 32, 4801-4812.
Rizk and Hanzlik, 1995, Xenobiotica 25, 143-150.
Dit proefschrift

4. De invloed van de axiale ligand in heem-enzymen heeft minder invloed op het reactie mechanisme van het gevormde ijzer-oxo deeltje dan in de literatuur wordt gesuggereerd.
Du and Loew, 1992, International Journal of Quantum Chemistry 44, 251-261.
Zakharieva et al., 1996, Journal of Biological Inorganic Chemistry 1, 192-204.

5. Ab initio moleculaire orbitaal berekeningen zijn per definitie niet beter voor de voorspelling van chemische reacties dan semi-empirische berekeningen.

6. Bij het opstellen van QSAR's op basis van multivariatie technieken is het van belang om de variabelen in vergelijkbare eenheid weer te geven zodat uit de coëfficiënten de relatieve invloed van de verschillende parameters af te leiden is.
Yin et al., 1995, Proceedings of the National Academy of Sciences USA 92, 11076-11080.

7. Het is soms onbegrijpelijk dat er geen QSAR lijkt te bestaan tussen de precisie waarmee het experiment wordt uitgevoerd en de netheid op het lab.

8. Op grond van het feit dat de muis de meest gebruikte diersoort is voor onderzoek zou de uitdrukking 'Proefkonijn' beter vervangen kunnen worden door 'Proefmuis'.

9. Voor de financiële administratie van de LUW geldt hetzelfde als voor wetenschappelijk onderzoek: op het moment dat je denkt te weten hoe het ongeveer werkt is het toch net even anders.

10. Door de toename van de bevolking en diens activiteit worden de winters in Nederland mogelijk weer kouder ('Heinrich events'). Ondanks deze klimaatsverandering blijkt helaas toch dat door de omvang van deze populatie een officiële Elfstedentocht in het water valt.

11. Aan de houding van een violist(e) kan men zien of er de eerste viool gespeeld wordt.

12. De emancipatie van de vrouw is nabij als in de wasmiddelen-reclame een man, net zoals een vrouw nu, het 'belang' van een witte en schone was kan overdrijven.

13. Het feit dat liefdadigheidsacties vaak veel meer succes hebben wanneer deze gekoppeld zijn aan een loterij toont meer eigenliefde van de deelnemer dan liefde voor zijn medemens.

14. De enige geboden die de mens niet belemmeren maar uiteindelijk tot zijn bevrijding zullen leiden zijn De Tien Geboden.

Stellingen behorende bij het proefschrift:

The biotransformation of benzene derivatives
the influence of active site and substrate characteristics on the metabolic fate

Janneke Koerts
Wageningen, 18 december 1996

Contents

Chapter 1

Introduction to the biotransformation of xenobiotics

The progress in prosperity and welfare in modern industrial society can be partially ascribed to the enormous amount of chemical products which have been synthesized and used, and an even further increase in the development of new compounds is foreseen. These non-natural occurring xenobiotics (foreign to organisms) comprise chemical products such as agrochemicals, pharmaceutical products, industrial chemicals and food additives. The extensive use of these xenobiotics exposes organisms to a large number of these agents under widely varying conditions. Exposure results from industrial application of these chemicals and also from the presence of these chemicals as environmental pollutants. Organisms, like humans and animals, have an enzymatic system to protect themselves against these xenobiotics. In mammals small xenobiotics can principally become inactivated by enzymatic conversion. The biotransformation enzymes involved catalyse the modification of these xenobiotics to compounds which can be more easily excreted from the body. Although most of these biotransformation reactions result in detoxification of the chemical, some of these reactions appear to result in metabolites provoking toxic and/or mutagenic/carcinogenic effects in the organism (bioactivation). Therefore, a better insight in the mechanisms of biotransformation of (hazardous) xenobiotics would improve possibilities for the assessment of the risks of xenobiotics for organisms. For example, understanding of the biotransformation reactions of xenobiotics is a prerequisite for the development and registration of new industrial chemicals and drugs, as biotransformation reactions might have consequences for their bioavailability and/or the balance between their elimination or their conversion to metabolites that might bring about unintentional (toxic) side-effects.

The rate of development of new xenobiotics is such fast that it becomes more and more unfeasible to test the biotransformation patterns and toxic and/or mutagenic/carcinogenic effects of all newly developed chemical compounds individually. One way to reduce this problem is the development of QSARs

(Quantitative Structure-Activity Relationships). A QSAR describes a model in which structural characteristics of a chemical are linked to its biological activity. On the basis of these QSARs, predictions can be made for the biotransformation and/or biological activity of newly developed chemicals. This could help to set priorities in toxicological studies resulting in a decreased use of experimental animals. Furthermore, QSARs often give more insight in the mechanism of the biotransformation enzymes and/or the biological activity of xenobiotics. This knowledge can contribute to the development of chemicals which better fulfil their industrial, medical and/or agricultural requirements and are safer in use.

In this chapter the general principles of the biotransformation of xenobiotics and the development of QSARs in biotransformation research will be described in greater detail.

1 General principles of the biotransformation of xenobiotics
- 1.1 Phase I: General aspects of cytochromes P450
  - A. The mechanism of oxygen activation
  - B. The function and regulation of cytochrome P450 enzyme patterns
  - C. Factors controlling cytochrome P450 catalysis
  - D. Proposed mechanisms for cytochrome P450-catalysed oxidations
- 1.2 Phase II

2 Quantitative Structure-Activity Relationships in biotransformation studies
- A. Frontier Orbital Theory
- B. Review of frontier orbital based MO-QSARs for biotransformation of xenobiotics.

1 General principles of the biotransformation of xenobiotics

Since most xenobiotics are hydrophobic, they can readily be absorbed by human beings and animals through the skin, lungs and the gastro-intestinal tract. Also dependent on their physical characteristics compounds absorbed will be divided over the various tissues of the body. Organisms defend themselves against accumulation of the xenobiotics by enzymatic conversion of these chemicals to more

hydrophilic (water-soluble) products facilitating excretion in the urine or, through bile, in the faeces. The enzymes responsible for the biotransformation of xenobiotics are present in nearly all organs, but the liver appears to contain the highest amount of biotransformation enzymes. This is a logic consequence of the function of the liver: i.e. its capacity to extract substances readily from the blood which are absorbed from the gastro-intestinal tract and to store or distribute them after chemical modification.

The biotransformation reactions are roughly divided into two types, i.e. the Phase I (transformation or modification) and Phase II (conjugation) reactions. In Phase I reactions a functional group (e.g. -OH, -SH, $-NH_2$, -COOH) is introduced by oxidation, reduction or hydrolysis of the parent compound, generally increasing the hydrophilicity of the compound and making it more susceptible for Phase II reactions. In the Phase II reactions the parent compound or the Phase I-derivative is covalently linked to an endogenous agent (e.g. glucuronic acid, sulphate, glutathione, H_2O) thereby often further enhancing the hydrophilicity and making it possible to excrete the chemical by urinary and biliary faecal routes. There are also xenobiotics which are so hydrophilic that they can be excreted in their unmodified form. Figure 1 shows the process of Phase I and II biotransformation of xenobiotics and the main enzymes involved in these conversions.

1.1 Phase I

General aspects of cytochromes P450

The cytochrome P450 monooxygenases are important Phase I enzymes. It is an enzyme complex which in humans and animals consists of various cytochrome P450 enzymes, NADPH-cytochrome P450 reductase, NADH-cytochrome P450 reductase and cytochrome b_5, which are all embedded in the phospholipid matrix of mainly the endoplasmatic reticulum. The phospholipids are thought to facilitate the interaction between the various components of the enzyme system and/or to play a role in concentrating the hydrophobic substrates in the neighbourhood of this Phase I enzyme system [1]. The cytochromes P450 have a molecular weight of about 50 kDa and contain an iron (III)-protoporphyrin IX (heme) as the prosthetic group, the iron of which is coordinated by a cysteine-thiolate residue from the apoprotein (Figure 2). The cytochromes P450 owe their name to the fact that reduced cytochrome P450 (Fe^{2+}) liganded with carbon monoxide has an absorption spectrum with a maximum near 450 nm, a characteristic attributable to the ligation of the heme by the cysteine-

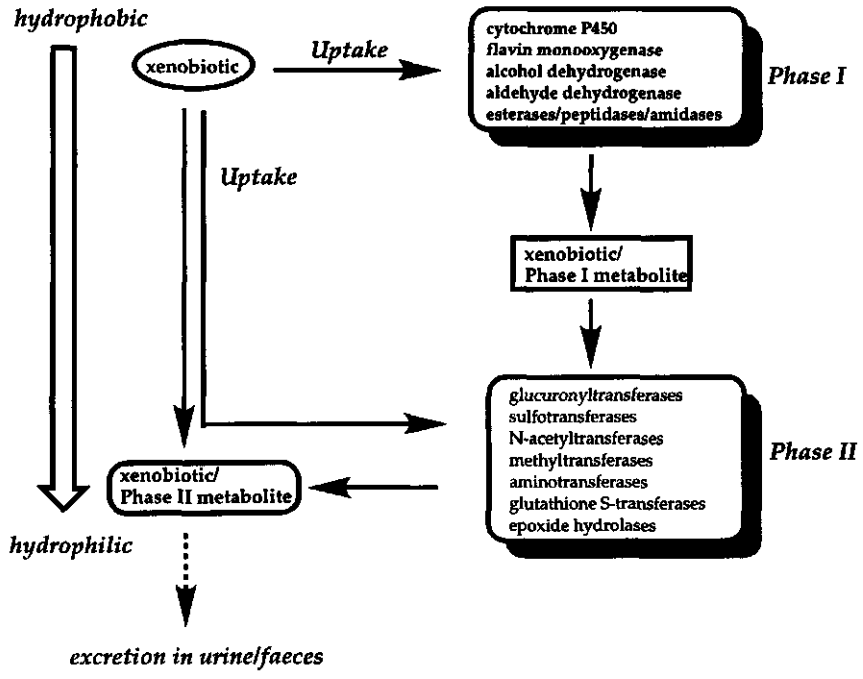

Figure 1 The process of Phase I and II biotransformation of xenobiotics and the main enzymes involved.

thiolate [2,3]. Absorption at 420 nm indicates inactivated cytochrome P450 due to a larger distance between the iron and the axial thiolate or replacement of the thiolate by another ligand (e.g. imidazole) [4,5].

The NADH- and NADPH-cytochrome P450 reductases are flavin containing enzymes (molecular weight about 78 kDa) and they catalyse the electron transport from NADH and NADPH respectively to the cytochromes P450. NADPH-cytochrome P450 reductase can directly donate the electrons to cytochrome P450 or via cytochrome b5 while NADH-cytochrome P450 reductase transfers the electrons to cytochrome b5. Cytochrome b5 (molecular weight about 17 kDa) is a hemeprotein and has been suggested that in some cases it can transfer electrons from NADH- and

NADPH-cytochrome P450 reductase to cytochrome P450 [6].

The cytochrome P450 enzyme system is widespread in nature and many different enzymes have been observed in animals, plants and microorganisms. In humans and animals the enzyme system has been found in every type of cell with the exception of red blood cells and skeletal muscle cells. The liver appears to have the highest amount of cytochromes P450 [6].

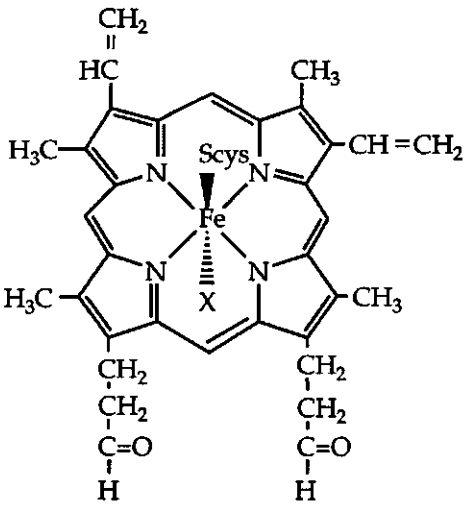

Figure 2 A schematic picture of the prosthetic group of cytochrome P450.

A. The mechanism of oxygen activation

The cytochrome P450 enzyme system is a monooxygenase. It catalyses dioxygen activation using two electrons (from NAD(P)H) and two protons, ultimately resulting in the insertion of one oxygen atom from O_2 into a substrate (S) and incorporation of the other oxygen atom in a water molecule (Equation 1):

$$S + O_2 + 2e^- + 2H^+ \text{----------} > SO + H_2O \qquad (1)$$

The mechanism proposed for oxygen activation and substrate conversion in a cytochrome P450 reaction cycle is depicted in the overall scheme in Figure 3 [7]. The individual steps in this cycle are discussed below.

Step 1. The oxidized state (ferric iron (III)) of cytochrome P450 exists in two forms which are in equilibrium: a hexacoordinated low-spin (S=1/2) or a pentacoordinated high-spin (S=5/2) complex. The hexacoordinated low-spin iron (III) complex has two axial ligands perpendicular to the plane of the porphyrin ring system; a proximal cysteine-thiolate residue of the apoprotein and the distal ligand, presumably an OH-containing residue (H_2O or a tyrosine). The pentacoordinated high-spin complex has only the cysteine-thiolate ligand which results in displacement of the Fe^{3+} out of the plane of the porphyrin ring system [8]. Binding of substrates in the active sites of cytochromes P450 induces a shift in the spin state of the heme resulting in a characteristic spectral change. Type I substrates preferentially bind to the high-spin form resulting in a shift of the absorption maximum of the free cytochrome P450 to lower wavelengths (± 390 nm (high-spin band)), while Type II substrates preferentially bind to the low-spin form resulting in a shift of the absorption maximum to higher wavelengths (425-435 nm (low-spin band)) [9]. So far, it is thought that Type I substrates bind at or near the catalytic site of cytochrome P450 while Type II substrates, especially nitrogen containing compounds, are suggested to coordinate directly to the heme iron occupying the sixth axial ligand position [10-12].

Step 2. The binding of substrate to the enzyme results in a conformational change in the apoprotein triggering an one-electron transfer via NADPH-cytochrome P450 reductase to reduce ferric iron-heme to Fe^{2+}. For some cytochromes P450 it has been observed that Type II substrates increase while Type I substrates decrease the redox-potential resulting in an increased and decreased rate of reduction of the ferric heme respectively [8]. However, this spin-redox coupling is not observed for all cytochromes P450 and the spin state is not correlated to catalytic activity [13].

Step 2[a]. Although the cytochromes P450 are classified as monooxygenases it is noteworthy that cytochromes P450 in the ferrous state are able to catalyse the reduction of some easily reducible compounds, especially under low oxygen pressure conditions. These reductions, which are considerably less important than monooxygenation reactions, have been reported for substrates like halogenated alkanes, azodyes, nitro compounds, benzoquinoneimines and quinones [14].

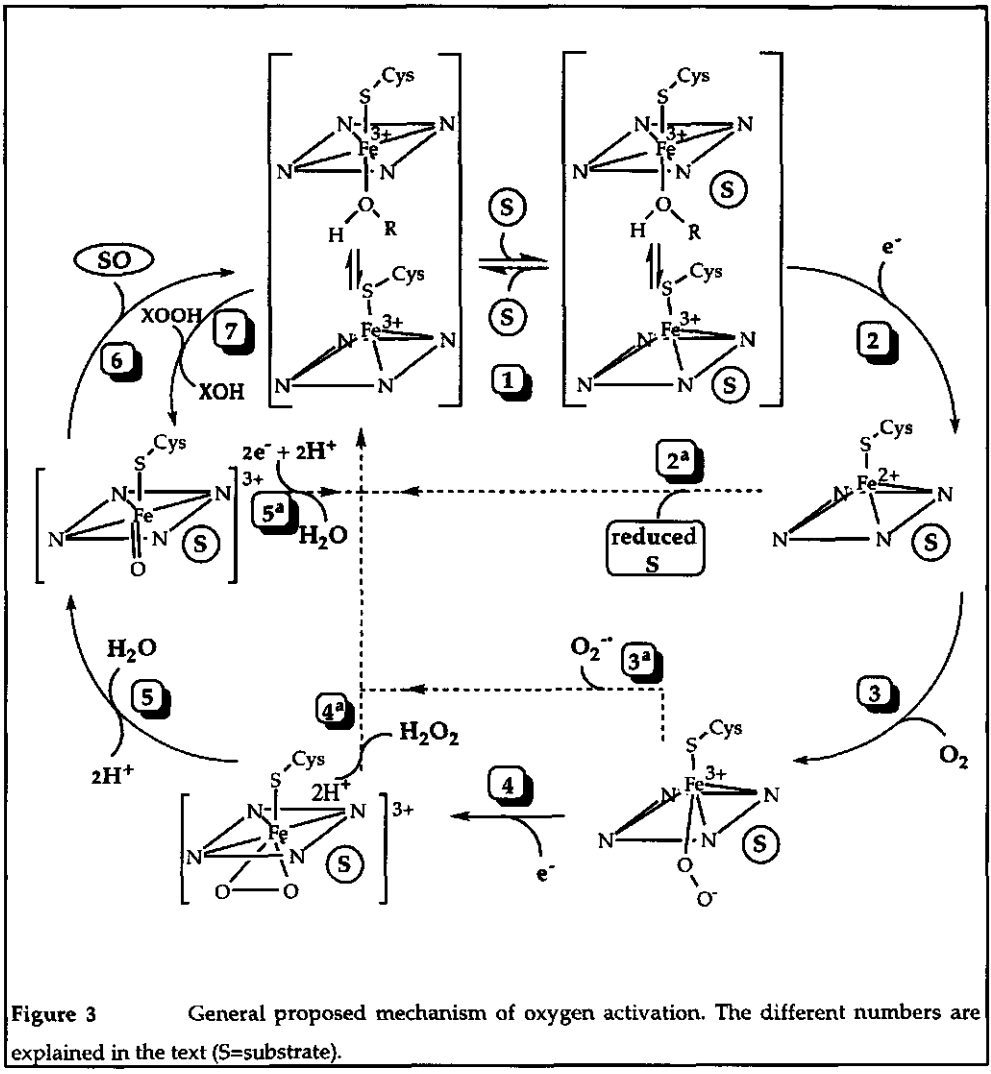

Figure 3 General proposed mechanism of oxygen activation. The different numbers are explained in the text (S=substrate).

Step 3. The reduction of the ferric cytochrome P450-substrate complex to the ferrous state initiates step 3, which represents the binding of molecular oxygen.

Step 3a. The cytochrome P450 oxygen cycle can be short circuited when an electron of the Fe^{2+} is transferred to O_2 producing $O_2^{-\bullet}$ that dissociates. This phenomenon is called uncoupling or futile

cycling of the cytochrome P450 oxygen cycle and is probably due to steric interference between water molecules and dioxygen as well as access of dioxygen to solvent protons [15]. Hydrogen peroxide may be formed by disproportionation of two superoxide anion molecules as follows:

$O_2^{-\bullet} + O_2^{-\bullet} \longrightarrow O_2 + H_2O_2$

Hydroxyl radicals can be produced from the hydrogen peroxide in a Fe^{2+} catalysed Fenton reaction [9,17]:

$Fe^{2+} + H_2O_2 \longrightarrow Fe^{3+} + OH^- + OH^\bullet$

Step 4. The ferrous cytochrome P450-substrate-oxygen complex receives another electron from NADPH via NADPH-cytochrome P450 reductase or, in some cases, from NADH via NADH-cytochrome reductase and cytochrome b_5 [5]. The structure of this intermediate depicted in Figure 3 is a hypothetical representation as its structure has not been established yet for example on the basis of model-compound analogues [16].

Step 4^a. Uncoupling of the oxygen cycle at this stage can occur in some bacterial and mammalian cytochromes P450, i.e. hydrogen peroxide is released, which is possibly due to the presence of disorderd water molecules [18-20]. In a Fe^{2+} catalysed Fenton reaction hydroxyl radicals might be formed (see step 3^a) [9, 17].

Step 5. In a series of reactions, which is not fully proved so far but which is thought to be facilitated by the thiolate ligand [21-23], heterolytic cleavage of the oxygen bond takes place and two electrons are transferred to the molecular oxygen atom, which is then reduced to water. The other oxygen is bound to the heme iron resulting in a high-valent iron-oxo porphyrin radical cation species $(FeO)^{3+}$ which is thought to have a structure similar to that of horseradish peroxidase (HRP) Compound I [8,24,25].

Step 5^a. The high-valent iron-oxo species can be reduced by two electrons to form a second water molecule. Formation of excess water is in competition with substrate oxidation [26,27]. This uncoupling pathway might prevent oxidation of active site amino acids and heme when the catalytic oxygen cycle is initiated but the substrate leaves the active site before catalysis. This phenomenon is seen with substrates of low reactivity for oxidation or pseudo substrates like perfluorinated hydrocarbons.

Step 6. The resulting high-valent iron-oxo species, whatever its exact electronic structure, is highly reactive and able to insert its oxygen into the substrate. The

mechanism of oxygen incorporation in the substrate is dependent on the atom or molecule to be oxidized [28] (see paragraph 1.1 D). The oxygenated substrate dissociates thereby regenerating the oxidized form of cytochrome P450 which is then available for the next cycle of oxygen activation.

Step 7. This reaction step depicted in Figure 3 involves the direct creation of the high-valent iron-oxo species of cytochrome P450 from its Fe^{3+} form using alternative oxygen donors such as iodosobenzene, cumene hydroperoxide, t-butyl hydroperoxide, and is called the "peroxidase shunt". Cytochrome P450-catalysed oxygenations by oxygen and peroxycompounds are thought to result in the same high-valent iron-oxo intermediate (Compound I). The rate of catalysis of a peroxidase supported cytochrome P450 conversion is generally faster than the normal NADPH/O_2 driven reaction because the reduction steps in the normal cytochrome P450 cycle are often the rate limiting steps in overall catalysis [24,29].

B. The function and regulation of cytochrome P450 enzyme patterns

Besides metabolizing endogenous compounds like signalling molecules (prostaglandins, thromboxanes, leukotrienes, $NO^{\bullet}$), steroids (e.g. pregnenolone and progesterone), alkaloids (morphine, codeine), bile acids and the fat soluble vitamins A and D, cytochromes P450 are able to modify a large range of structurally diverse xenobiotics. The number of known chemical substrates for cytochromes P450 extends to about 250,000 now. As it would be impractical for the body to produce elaborate and specific enzyme systems to deal with every new molecule that might enter the body, the cytochromes P450 comprise a superfamily of enzymes with a generally broad substrate specificity. All cytochrome P450 enzymes are thought to use a common heme perferryl $(FeO)^{3+}$ intermediate, and therefore the chemistry of cytochromes P450 oxidation reactions is proposed to be essentially identical among the different enzymes [30]. However, the cytochrome P450 enzymes differ in the three dimensional structure of their apoprotein due to differences in amino acid sequences. Based on the similarities in their amino acid sequences they have been classified into families and subfamilies [31]. Those complementary DNA sequences with at least 40% identity are grouped into families (1,2,3...). Sequences within a family that are at least 55% identical are grouped into subfamilies (A,B,C,...). The individual genes within a subfamily are denoted with an Arabic numeral (1,2,3...). The corresponding genes are given the prefix CYP (cyp for mouse). So far 221 cytochrome P450 genes have been characterized [31]. The known human and animal

cytochromes P450 comprise 12 gene families, which can be subdivided into two groups. One group contains the cytochromes P4501, 2, 3 and 4, which are mainly concerned with the oxidation of xenobiotics (Table 1) [32], and the other group consists of cytochrome P450 families 5, 7, 11, 17, 19, 21, 24 and 27 which are involved in hydroxylation of endogenous compounds. The latter group of enzymes is fairly restrictive in their substrate specificity while the former has a wide and overlapping substrate specificity. The cytochromes P4501, 2, 3 and 4 are proposed to have been evolved and diverged in animals due to their exposure to plant poisons over the last one billion years.

As organisms are not continuously exposed to the whole array of xenobiotics there is a cellular control mechanism to respond to certain substances (inducers) resulting in the increased biosynthesis and/or stabilization of specific cytochrome P450 enzymes. The induction of cytochromes P450 is accomplished by certain hormones and chemicals which increase the biosynthesis of cytochrome P450 apoproteins (Table 1). The enhancement of biosynthesis of apoproteins is initiated by elevation of the specific mRNA coding for the protein through either increased DNA transcription and/or mRNA stabilization [33]. The exact mechanisms of the increased rate of transcription are unknown. Most is known about the transcription of cytochrome P4501A1 which is regulated by a cytosolic (steroid like) receptor: the Ah receptor, which binds some carcinogens and other planar molecules. This complex is transported into the nucleus where it binds to a specific region of the P4501A1 gene inducing production of mRNA, which is the template for synthesis of the cytochrome P4501A1 enzyme [34,35]. Inducers of cytochrome P4501A1 are all potential substrates for this isoform, therefore the optimum spatial conformation of the active site of cytochrome P4501A1 and the binding site of the Ah receptor have been suggested to be similar [36,37]. The regulation of some other cytochromes P450 is known to proceed by a post-transcriptional mechanism, which includes the stabilization of mRNA and/or protein. This mechanism of induction is suggested for cytochromes P4502E, which are protected against degradation by the substrates acetone and imidazole [38,39]. Post-transcriptional regulation can also be accomplished by regulation of the pool of the necessary heme prosthetic cofactor [29]. Generally, it appears that, somewhat in contrast to the situation described above for P4501A1, there is little structural similarity between the cytochrome P450 inducer of a specific enzyme and the substrates for this enzyme.

Apart from cytochrome P450 induction, it is also known that cytochromes P450 can be inhibited by various chemical compounds. The most common type of inhibition is the competitive or non-competitive binding of substrates to the

Table 1 The nomenclature of the main cytochrome P450 enzymes, and their typical inducing agents, involved in the oxygenation of xenobiotics in humans and some experimental animals [31,52].

Subfamily	individual gene*	species	typical inducers
1A	1	rat, human rabbit, mouse	3-MC, β-NF
1A	2	rat, human rabbit, mouse	isosafrole
2A	1,2,3 4,5 6,7 10,11	rat mouse human rabbit	3-MC, β-NF
2B	1,2,3,8,14 4,5 6 9,10,13	rat rabbit human mouse	phenobarbital
2C	1-5,14-16 6,7,11-13,22-24 8,9,18,19	rabbit rat human	phenobarbital
2D	1-5 6 9-13	rat human mouse	non inducible
2E	1 2	rat human rabbit mouse rabbit	ethanol, isoniazid, acetone
3A	1,2,9 3,4,5,7 6 11,13	rat human rabbit mouse	PCN, dexamethasone
4A	1-3,8 4-7 9,11 10,12	rat rabbit human mouse	clofibrate

*Unfortunately, there is some ambiguity in the system concerning the last number when referring to different species-in some cases the last number is specific to the animal species, but in other instances the same nomenclature applies to all species.

3-MC= 3-methylcholanthrene, β-NF= β-naphtoflavone, PCN= pregnenolone 16α-carbonitrile

substrate binding site. In addition, irreversible inhibition may result from activation of a chemical upon its conversion by cytochrome P450, whereby reactive metabolites bind covalently to the pyrole nitrogens of heme, resulting in the destruction of the heme and loss of cytochrome P450 activity [40]. Cytochrome P450 inhibitors are often used in studies on the physiological role of cytochromes P450.

The cytochromes P450 which are involved in the metabolism of endogenous compounds are often constitutively expressed and sexually determined by neonatal imprinting and hormones. This means that the activity of these cytochromes P450 may vary in female and male species and in their activity during certain stages of the life cycle [33,41].

Finally, there might be cytochrome P450 differences between organisms due to polymorphism, i.e. some individuals might lack certain isozymes. Well-known examples of this phenomenon is cytochrome P4502D6 and P4502C19 which convert the drugs debrisoquine and S-mephenytoin respectively [42,43].

The regulation of cytochromes P450 is very important as especially the cytochromes P4501, 2, 3 and 4 are concerned with the detoxification of xenobiotics to more-polar, biologically-inactive, readily-excretable metabolites. However, the same microsomal enzymes can also catalyse the oxidative formation of reactive intermediates which might ultimately lead to carcinogens (epoxides, arene oxides, free (oxygen) radicals and N-hydroxy derivatives) through covalent binding to protein or DNA resulting in malignancy and other pathologic processes [37,44,45,46]. Especially the cytochrome P4501A family and to a lesser extent the cytochrome P4502E family of enzymes is concerned with the bioactivation of chemicals and carcinogens to reactive intermediates [32,37,47]. For example, the cytochrome P4501A subfamily selectively accepts planar molecules and oxygenates them in conformationally hindered positions, thus forming highly reactive arene oxides, which are not easily detoxified by other enzymes (Phase II) however [48]. The nitrosamines and other small molecules are mainly activated by cytochrome P4502E [32,49,50]. Furthermore, the cytochromes P4502E are also known to produce reactive oxygen species resulting in oxidative stress [47,51].

This catalysis of opposing pathways of detoxification and bioactivation of chemicals by the same group of enzymes has become of increasing importance with regard to biological consequences of biotransformation. Thus, the intensity and length of induction or inhibition of cytochromes P450 can have dramatic consequences for the detoxification or bioactivation of chemicals, but also for the availability of the compound. For example, co-administration of cytochrome P450 inhibitors with other drugs can prevent rapid drug metabolism.

C. Factors controlling cytochrome P450 catalysis

In the first part of this chapter the general proposed catalytic reaction cycle of cytochrome P450-catalysed oxygen activation resulting in a perferryl $(FeO)^{3+}$ intermediate was described. This catalytic active conformation relevant for the monooxygenation reactions catalysed by the enzymes is suggested to be similar for all cytochrome P450 enzymes [30]. However, this does not imply that all cytochrome P450 substrates are converted by all enzymes to the same extent or result in similar metabolic patterns. Although many cytochrome P450 enzymes have an overlapping substrate specificity, the extent and regio-/stereoselectivity of the cytochrome P450-catalysed conversion of chemicals might differ widely due to differences in the three-dimensional structure of cytochrome P450 enzymes. The chemical characteristics of the various substrates might also influence the cytochrome P450 catalysis. The apoprotein and substrate characteristics which control the cytochrome P450-catalysed biotransformation reactions have been investigated using various approaches. As more computing power has become available the development of many techniques accelerated enormously. Many attempts have been made to model the interactions between the substrate and the catalytic active site of cytochromes P450 through docking experiments, pharmacophore-3D representations, pattern recognitions or chemical and theoretical model systems. The influence of the chemical reactivity of the substrate on its cytochrome P450-catalysed conversion has been described by QSARs (see paragraph 2). In this session several factors controlling the cytochrome P450 catalysis of substrates are discussed in some more detail.

1. Accessibility of the active site for the substrate

Since the eukaryotic cytochromes P450 are embedded in a phospholipid matrix, the substrates might have to be dissolved in the membrane before they can enter the access channel which leads to the active site of the enzyme. Especially hydrophobic compounds will be able to dissolve in the lipophilic membrane, increasing their effective concentration in the neighbourhood of the enzyme and apparently increased affinity of the enzyme for the substrate [53].

For several bacterial cytochromes it has been shown that the hydrophobic substrates are recognized on the surface of the protein by a hydrophobic patch of amino acids adjacent to the substrate channel [54-56]. The substrates will partition down via the access chancel into the active site as a result of hydrophobic

interactions. This access route appears to be flexible, i.e. it has a large open/close motion [57-60]. This flexibility of the entrance channel is probably important in controlling substrate access to the active site and hence it is expected to exhibit wide variations between cytochromes P450, that have different substrate specificity [60,61].

2. Binding of the substrate in the active site

Cytochrome P450 substrates reach the active site by the entrance channel and will be bound in the catalytic cavity before catalysis. The binding affinity and orientation of the substrate in the active site is dependent on both the physicochemical properties of the active site as well as those of the substrate. Together, these factors will influence the extent and regio-/stereoselectivity of cytochrome P450 catalysis.

Much research so far has been centred on solving the three-dimensional structure of the active site of both bacterial as well as mammalian cytochromes P450. One of the best ways to resolve the three-dimensional structure of a protein is by X-ray analysis of its crystal structure. With the aid of computers these data are used to identify other molecules which fit into the same active site (docking) [62-64]. However, so far X-ray crystallographic analysis has only been successful for the cytosolic bacterial cytochromes P450, i.e. $P450_{cam}$, $P450_{terp}$, and $P450_{BM3}$ [18,54,55], mainly because technical difficulties are inherent to the crystallographic analysis of membrane-bound proteins due to the high hydrophobicity of these enzymes. Many attempts have been made to use the bacterial cytochromes P450 as a model for the mammalian systems like for example the elucidation of the substrate recognition regions in the cytochrome P4502C family based on amino acid sequence alignment with cytochrome $P450_{cam}$ [56]. However, this is a risky endeavour as the bacterial cytochromes P450 are not membrane bound, have low sequence homology with the mammalian cytochromes P450 and generally receive their electrons from a FAD reductase via a putidaredoxin instead of through the NAD(P)H cytochrome reductases [65,66]. In this respect, the tertiary structure of the bacterial cytochrome $P450_{BM3}$ from *Bacillus megaterium* which, similar to mammalian cytochromes P450, receives its electrons directly from NADPH-reductase and furthermore has a higher amino acid sequence homology to the mammalian bound enzymes is likely to provide better information as a standard template for three-dimensional models [54]. NMR analysis is also a good tool in solving protein structures. Unfortunately, elucidation of the tertiary structure of the cytochromes P450 by NMR analysis has

not been possible so far as the enzymes are relatively large for NMR analysis.

Therefore, up till now other techniques have been applied to obtain some insight in the three-dimensional structure of the active site of mammalian cytochromes P450. The topology and dynamics of the active sites of P4501A1, 1A2, 2B1, 2B2, 2E1 [67-71] and of the bacterial cytochromes $P450_{cam}$, $P450_{terp}$ and $P450_{BM3}$ [69,72] have been investigated by preparation of σ-bonded iron-aryl complexes of the heme-proteins. Exposure of these iron-aryl complexes to an oxidizing agent results in a covalent coupling of the aryl group to the porphyrin nitrogens in the original active site. The ratio of the four possible regioisomers gives information on the regions above the heme group that are (or are not) occupied by protein residues and thus are (not) accessible for substrates. The results obtained with this method for cytochromes $P450_{cam}$ and $P450_{terp}$ agreed with the resolved crystal structures of these enzymes showing the reliability of the approach. Additional results obtained showed that the topology of the bacterial and mammalian cytochromes P450 differs. For the mammalian cytochromes P450 the regions above the pyrole rings of the heme-cofactor are not accessible to a similar extent, i.e. two pyrole rings were found to be relatively exposed while the two others were occluded by protein residues, with subtle differences between the various cytochrome P450 enzymes. Thus, despite a gross difference in substrate specificity, the active sites of these cytochromes have a common architecture with respect to the accessibility of the pyrole rings of the heme, except for cytochrome P4501A2 for which the active site is open above all four rings [70]. The results of the iron-aryl complex studies have also been connected to results from previous studies on the proposed topology of the active site of cytochrome P4501A1 based on the molecular geometries of specific substrates for cytochrome P4501A1 [73] and the regio- and stereospecificity of P450 catalysis [74]. The conclusion was that the active site of P4501A1 is a relatively large but shallow region parallel to the heme plane and has a high area-to-depth ratio. In addition, it can be derived that if the aromatic hydrocarbon binding site is roughly parallel to the heme face, the data obtained with the iron-aryl complexes require that the bulk of the binding-site extends over two pyrole rings. This proposal is in accordance with the observation that the regions over the two other pyrole rings are masked by the protein.

Based on the homology between molecular geometries of other (cytochrome P450) substrates, it was concluded that the active sites of cytochromes P4502E are relatively small [75] and the active sites of phenobarbital induced cytochromes P450 accommodate bulky substrates with a relatively low area-to-depth ratio [37,76]. For acetanilide and acetaminophen it was shown, based on ^1H NMR T_1 relaxation

measurements, that the substrates were oriented differently with respect to the heme iron in two cytochrome P450 isozymes [77-80]. Acetaminophen was suggested to be oriented with its phenol group to the heme iron in cytochrome P4501A1, while in cytochrome P4502B1 it was oriented with its acetylamino to the heme iron [80]. Surprisingly, another study showed the opposite situation [79].
Altogether, the presently available data indicate that substrates might be differently bound in various cytochrome P450 enzymes.

Furthermore specific interactions between substrates and active site characteristics can be distinguished. By replacing specific amino acid residues through recombinant DNA technology (mutagenic changes at specific sites on the genes) it is possible to identify specific regions in the amino acid sequence which bind the substrate [81-84]. Interaction between the amino acids at the substrate binding site (distal region) and the bound substrate can be of ionic [85-89], hydrogen bonding [18,57,64,76] or hydrophobic [64,86,90] character and often result in a stereoselective orientation of the substrate in the active site. For example, based on pharmacophore space filling models, the human liver cytochrome P4502D6 binds compounds which have a positive charge on the nitrogen atom which is supposed to interact with a negatively charged carboxylate group of an amino acid [85,87,88,89].
Hydrogen bonding interactions are reported for the binding of camphor to cytochrome $P450_{cam}$. This substrate is bound through a hydrogen bond between its carbonyl group and a tyrosine residue [91].
Secondly, there are also possibilities of interactions with the Fe^{3+}-heme-cofactor in its resting state. The type II substrates, like arylamines [12], are known to bind near the heme-iron and act as a ligand to the heme-iron through their nitrogen atom; i.e. the sp^2 or sp^3 non-bonded electrons of the nitrogen are coordinating to the heme-iron [92]. Nearly all studies on substrate orientation in the active site reported so far neglect the possibility of interaction of the substrate with the catalytic active high-valent iron-oxo species, which is the ultimate reaction intermediate for cytochrome P450 catalysis. That this interaction can be important is shown for thiocamphor-bound to cytochrome $P450_{cam}$. The preferred substrate orientation was very different in the presence of the ferryl oxygen than in the absence of that oxygen and the orientation of thiocamphor in the presence of the oxygen was in agreement with the product profile found [64,93].

Although properties of the active site might impose a stereoselective orientation of the substrate there are also examples where binding of the substrate is aspecific with possibilities of high substrate mobility [18]. This means that a broad regioselectivity of catalysis might occur.

Altogether, the three-dimensional structure of the active site of cytochromes P450 and the specific interactions between properties of this active site and the substrate might result in the fact that specific substrates are better bound than others and that a stereoselective orientation of the substrate in the active site is induced. These binding characteristics influence the cytochrome P450-catalysed extent and regio-/stereoselectivity of substrate oxidation. The sometimes observed broad regioselectivity of substrate oxidation is consistent with multiple substrate orientations due to non-specific binding. In those cases the regioselectivity of the cytochrome P450-catalysed substrate conversion can be predominantly determined by intrinsic chemical reactivity characteristics of the substrate

3. Intrinsic chemical reactivity of the substrate

The intrinsic chemical reactivity of the substrate is particularly important for substrates which have a relatively large freedom of motion in the catalytic cavity, such as small non-polar hydrophobic xenobiotics which are substrates for the cytochromes P4501-4 family. This means that interactions between the substrate and the active site resulting in a stereoselective orientation of the chemical are not important factors in controlling the regioselectivity of catalysis. Thus, for these substrates the oxidation reaction catalysed by cytochromes P450 is predominantly determined by the properties of the substrate and the catalytic active iron-oxo species, i.e. the electronic characteristics of the reactants in the oxidation reaction. That this situation can indeed be relevant for cytochrome P450 catalysis is in accordance with the observations that i) most P450 oxidations are thought to involve radical reactions, and therefore charge stabilisation by the apoprotein may not be an important factor during the reaction and ii) the often broad regioselectivity suggests that the oxidation of the substrate is indeed 'chemical-like' and does not require specific substrate interactions with the apoprotein [66]. A clear example of this second phenomenon is the cytochrome P450-catalysed regioselectivity of aromatic ring hydroxylation of a series of fluorinated benzene and aniline derivatives [94,95]. In these studies it was demonstrated that the regioselectivity of aromatic ring hydroxylation was independent of the cytochrome P450 isozyme and could be correlated with the relative reactivity of the ring carbon atoms for an electrophilic attack by the cytochrome P450 high-valent iron-oxo species, ultimately resulting in the formation of the phenol derivative.

D. Proposed mechanisms for cytochrome P450-catalysed oxidations

There are various reactions known which are performed by cytochromes P450. Figure 4 shows a survey of the various known reactions and the mechanism by which these reactions are proposed to proceed. The following monooxygenation reactions are depicted: aliphatic hydroxylation [28,96-100], N-hydroxylation [100,101], heteroatom dealkylation [98,102-106], aromatic hydroxylation with or without an NIH shift [94,107-113], aromatic oxidative dehalogenation [114-116] and heteroatom oxidation [28,117].

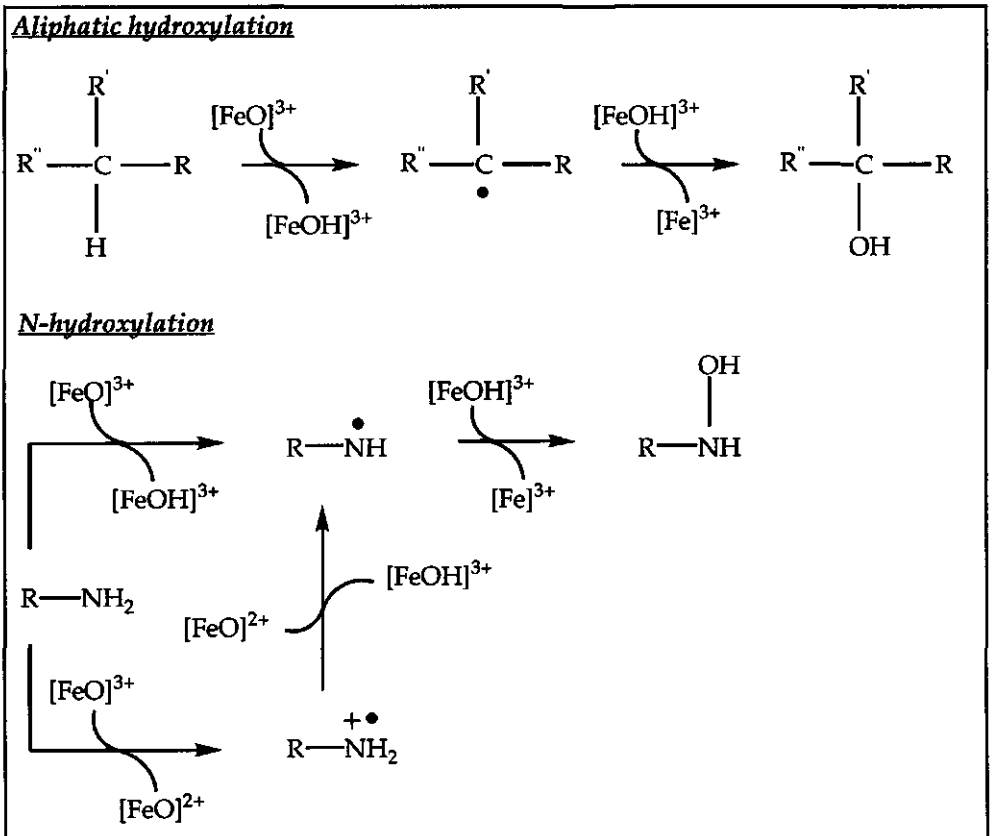

Figure 4 The mechanism of cytochrome P450-catalysed monooxygenation reactions: aliphatic hydroxylation, N-hydroxylation, heteroatom dealkylation, aromatic hydroxylation with or without an NIH shift, aromatic oxidative dehalogenation and heteroatom oxidation.

Heteroatom dealkylation

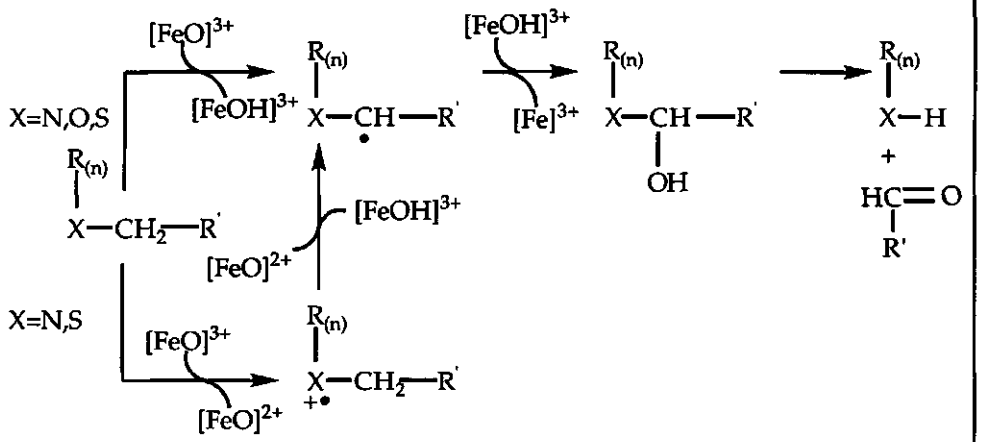

Aromatic hydroxylation/NIH-shift

1) proton/electron-abstraction mechanism (X=N,O,S)

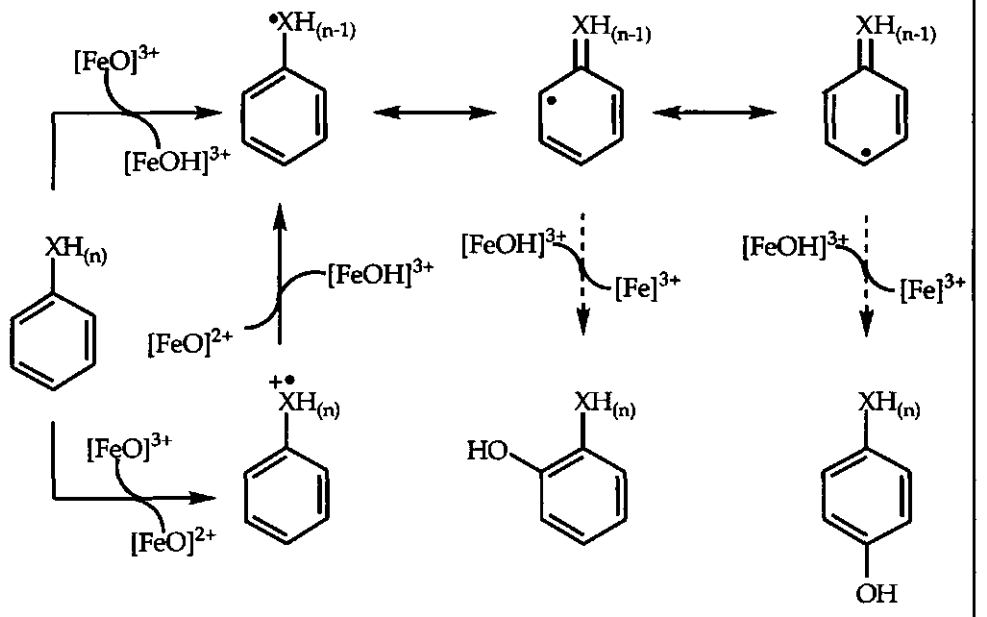

Figure 4 -continued-

2) σ-addition mechanism (X=H or halogen)

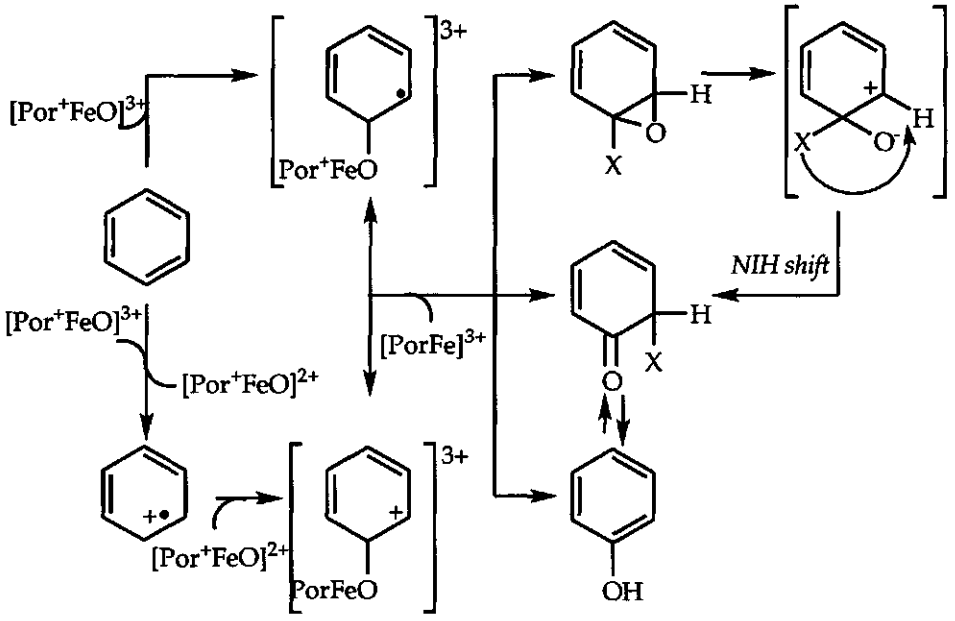

Aromatic oxidative dehalogenation

anilines and phenols (X=halogen)

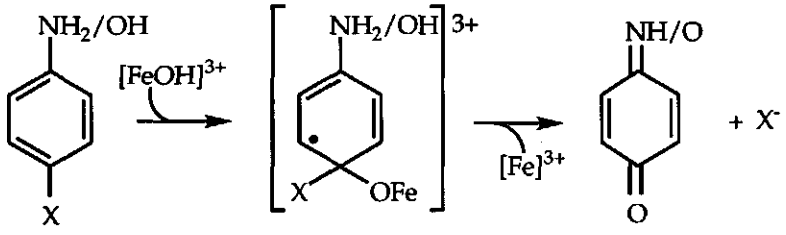

Heteroatom oxidation

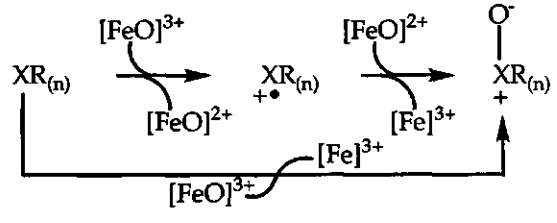

Figure 4 -continued-

1.2. Phase II

Contrary to the overwhelming knowledge about (cytochrome P450) Phase I reactions, less attention has been paid to Phase II reactions with perhaps the exception of the reactions catalysed by GSH S-transferases which have been extensively studied. The Phase II biotransformation reactions are conjugation reactions, i.e. the substrate is generally enzymatically linked to an endogenous agent. Phase II reactions are generally biosynthetic and often require energy which is obtained by activation of the cofactor or the substrate by ATP. This means that the chance that for some Phase II reactions a substrate undergoes a Phase II reaction depends on the availability of ATP and the cofactor. Often the Phase II reaction is preceded by a Phase I metabolic reaction to provide a metabolite with a group which is the reaction centre for conjugation. Phase II reactions can be subdivided in reactions with nucleophilic substrates, catalysed by UDP-glucuronyl-, sulfo-, acetyl-, methyl- and amino acid transferases and with electrophilic substrates catalysed by GSH S-transferases and epoxide hydrolases (see Table 2).

The enormous amount of different chemicals which can undergo a Phase II reaction is due to the presence of multiple forms of the various Phase II enzymes, which have overlapping and broad substrate specificity. They exist in soluble and microsomal cell fractions of different tissues, the liver generally being the organ with the highest amount of Phase II enzymes. However, as with Phase I enzymes the enzyme pattern present can differ widely from one organ to another, with age, between species or sexes, and with genotype. A well-known example of genetic polymorphism is the occurrence of so-called fast and slow acetylators, reflected in a different ability to acetylate isoniazid. It appears that 50% of the Caucasian population can be classified as slow acetylators due to a genetically dependent deficiency in a specific fast N-acetyl transferase [118]. As acetyl conjugation reactions are often detoxification reactions and thus important for organisms to defend themselves against toxic and mutagenic chemicals, slow acetylators are more susceptible for the toxic effects of chemicals such as arylamines [119].

As said earlier, the function of the Phase II enzymes in xenobiotic metabolism is detoxification of the chemical and facilitating its excretion. Well-known examples of these detoxification reactions are the detoxification of arene oxide metabolites from benzo(a)pyrene by epoxide hydrolases [120,121], the glutathione conjugation of epoxides and of halogenated benzenes such as bromobenzene 3,4-arene oxide [122] and the O-methylation of the glucuronide of 4-bromo-catechol [123]. As transport systems have evolved for the conjugated

2 Quantitative Structure-Activity Relationships in biotransformation studies

In order to predict and explain biotransformation reactions QSAR models (Quantitative Structure-Activity Relationships) have been developed. In these QSARs a correlation is described between parameters characterizing the structural electronic and/or reactivity properties of a series of chemicals and their biotransformation [95,126-128]. Based on these QSARs predictions for the biotransformation of non-tested related compounds can be made. Furthermore, these QSARs often give more insight in the mechanism of biotransformation reactions. In addition to QSARs for biotransformation reactions there are also examples of QSARs predicting the mutagenicity or carcinogenicity or other toxic characteristics of chemicals [37,129,130].

One of the main founders of the QSAR concept is Corwin Hansch, who extended models on linear energy relationships based on Hammett parameters (electronic effects) and Taft parameters (steric effects) by a hydrophobic parameter π, based on the logarithm of the experimental octanol/water partition coefficients [131]. This hydrophobic parameter turned out to be an important factor in the biological activity of chemicals. This can be rationalized as a mechanism in which a chemical is transported through cell membranes and across other biological barriers to reach its target. The work of Hansch has been extended and more than 200 parameters have been proposed to describe biological processes [132]. Due to the large amount of chemical and physical factors (physicochemical properties/parameters), other regression methods than the multiple linear regression methods were developed as these parameters might be collinear and not be important to a similar extent for a specific process. Along with the advent of high speed computers, multivariate statistical analyse techniques were developed, like Principal Components Analysis [133] and Partial Least Squares (PLS) to reduce the number of parameters [134] and to make it possible to test diverse type of groups of chemicals.

Most important for the reliability of QSARs is the choice of the right chemical parameters to describe the process and the right statistical method. The drawback of these methods is that there is the real risk of meaningless correlations, because the more parameters one selects to fit the biological process, the greater is the chance of a correlation arising [135]. Another problem arising is the fact that the more parameters used in a QSAR the more difficult it is to understand which chemical

property predominantly determines the process under investigation and thus the mechanism of the biological activity. In restricting the QSAR to the rate-limiting step, more insight can be obtained in the mechanism of the most important step of the whole biological process, because the rate-limiting step can be often described by only a few physicochemical parameters.

In addition to all experimental parameters, the availability of powerful and fast computers has accelerated the development of chemical parameters which are based on electronic and molecular structural properties obtained from quantum-chemical calculations [98,136-140]. Sometimes physicochemical parameters in QSARs are more easily obtained by quantum-chemical calculations than by experiments as determination of these experimental parameters require highly specific equipment, a lot of time and can be less accurate.

The quantum-chemical calculations are based on MO (Molecular Orbital) computer methods in which an approximate solution of the Schrödinger equation is obtained [141]:

$$\mathbf{H}\Psi = E\Psi \qquad (2)$$

H	Hamiltonian operator
Ψ	Electron wave function
E	Energy of the molecular orbital

As this equation can be solved exactly for a hydrogen atom only, various approximations are used to solve this equation for other molecules than hydrogen. There are roughly two methods to solve this equation, i.e. *ab initio* and semi-empirical methods, of which the latter use several approximations. Due to the additional approximations in semi-empirical calculations, the main difference between the *ab initio* and semi-empirical methods is that the semi-empirical methods require less computer time and space providing the advantage that they can also calculate some very large molecules. Although it seems that *ab initio* calculations are far more accurate as they are based on less approximations, this is not by definition the case. It appears that the choice of the most suitable MO method depends very much on the particular problem under consideration [142].

MO methods have given good results for (relative) prediction of experimental data such as molecular geometries, ionization energies, redox potentials, heat of formation and electron densities. However, as most of the MO calculation methods are applied to hypothetical motionless molecules in vacuo, this

means that the real biological situation under investigation is not taken into account as solvent or other characteristics of the surrounding are neglected. These differences involve effects such as entropy, the population of vibrational energy levels, solvation, and aggregation, of which each one is able to determine the selectivity of the reaction. Therefore, these calculations are most appropriate used to compare and study relative effects in series of closely related compounds or when relative differences in chemical properties in one molecule are investigated. Due to the developments in computer technology it is foreseen that in the future more complicated systems can be handled. For example, already commercial programs exist which can take into account solvation fields around the molecule.

A. Frontier Orbital Theory

In QSARs for chemical reactions the activation energy might be an important parameter. This activation energy can be approximated in two ways. When in a chemical reaction two molecules collide an activated complex (transition-state complex) of relatively high energy is formed. This transition-state complex decomposes into the product(s) (Figure 5). Enzymes are able to lower the activation energy, i.e. the energy difference between the starting situation and the transition state complex, thereby enhancing the reaction rate according to the equation of Arhenius:

$$k_{cat} = Ae^{-\Delta E_{act}/RT} \qquad (3)$$

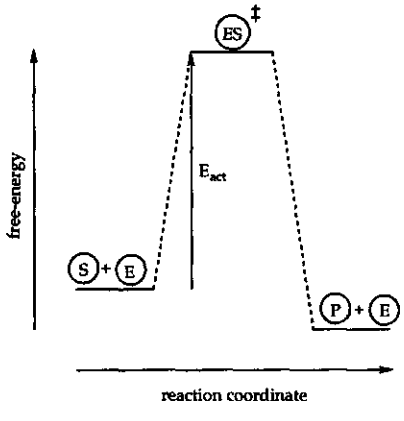

Figure 5 The energy profile of an enzymatic reaction (S=substrate, E=enzyme, E_{act}= activation energy, ‡=transition state, P=product).

However, it is difficult to assess or calculate the energy of the transition state since for many reactions a clear description of the transition state is unavailable. A possible way to overcome this problem is to investigate whether there exists a Brönsted relationship, i.e. a linear correlation between the activation energy ($\Delta H^{\ddagger}$) and the heat of the reaction (ΔH_R). The Brönsted relationship has been described for series of corresponding reactions for which the effects that stabilize or destabilize the reactants, the products and/or the transition state are similar [143]. In such a situation the ΔH_R which is the energy difference between reactants and products can be used as a relative approximation of the activation energy.

Another approach to assess the activation energy of a reaction is treating the interaction of two molecules as a pertubation which can be characterized by similar bonding and antibonding interactions as described by the valence bond theory. However, there are some limitations to this approach as finally the interaction is not merely a perturbation of two molecules on each other when they form the transition-state complex. Nevertheless, the Hammond postulate [144] says that the transition states for exothermic reactions are reactant-like, so a steeper slope is likely to lead to a higher-energy transition-state (Figure 5). Thus, it is possible to assess the relative activation energy by determining the slope of an early part of the path along the reaction coordinate.

Based on many approximations and assumptions, Klopman and Salem [145,146] derived an expression for the energy (ΔE) gain and loss when the orbitals of two reactants overlap:

$$\Delta E = - Q_{nucl} \cdot Q_{elec}/(\varepsilon \cdot r) + 2(c_{elec} \cdot c_{nucl} \cdot \beta)^2/(E_{HOMO}-E_{LUMO}) \quad (4)$$

Q_{nucl}, Q_{elec}	are the total charges on the reaction centre in the nucleophile or electrophile, respectively
ε	is the local dielectric constant
r	is the distance between the nucleophilic and electrophilic reaction centre
c^2_{nucl}, c^2_{elec}	orbital density of the HOMO or LUMO on the reaction centre of the nucleophile or electrophile, respectively
β	is the resonance overlap integral
E_{HOMO}	is the energy of the Highest Occupied Molecular Orbital of the nucleophile
E_{LUMO}	is the energy of the Lowest Unoccupied Molecular Orbital of the electrophile

This expression (equation 4) contains two terms, the Coulombic (first term) and the frontier orbital term (second term). The frontier orbital theory states that the interaction between molecules depends mainly on the electrons in the outer shell orbitals, i.e. the HOMO (Highest Occupied Molecular Orbital) and LUMO (Lowest Unoccupied Molecular Orbital). From Figure 6 it can be seen that an energy gain results from orbital interactions when the first reactant has a filled interacting frontier orbital (HOMO) and the other atom has an empty or partly filled interacting frontier orbital (LUMO or SOMO (Singly Occupied Molecular Orbital)). Two orbitals can combine to a bonding orbital and an antibonding orbital which are lower and higher in energy respectively. The energy needed to put two electrons into a bonding orbital costs more energy than in an antibonding orbital.

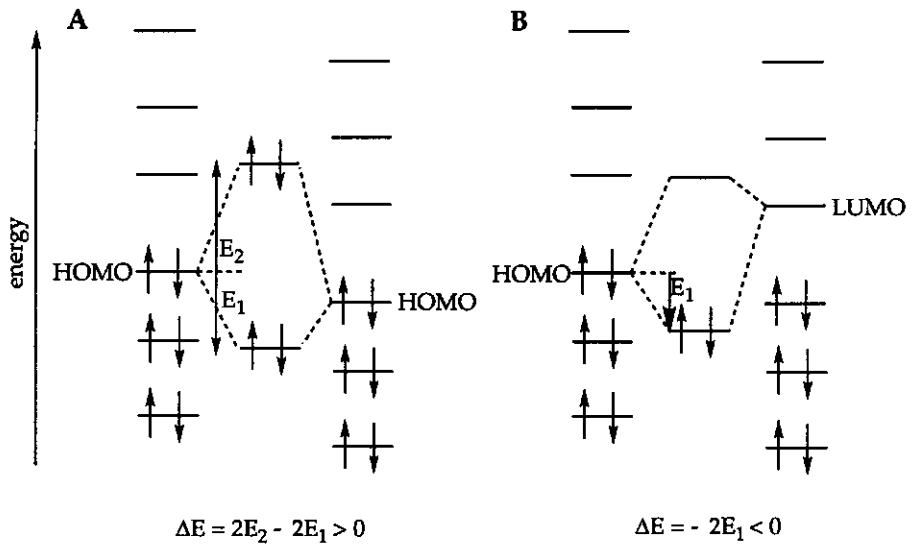

Figure 6 (A) Interaction of the HOMO orbitals of two molecules and (B) interaction of the HOMO orbital of one molecule with the LUMO orbital of another molecule.

The frontier orbital term in equation 4 is only valid when $E_{HOMO} \neq E_{LUMO}$. In case $E_{HOMO} \approx E_{LUMO}$ the interaction is better described in charge-transfer terms. It is obvious from equation 4 that a HOMO (nucleophile) and LUMO (electrophile) make

the largest contribution to the ΔE, especially to the frontier orbital term in ΔE when the value of E_{HOMO}-E_{LUMO} is smallest.

The frontier orbital density on the reaction centre (c^2) is also important in this term (equation 4). This frontier orbital density (c^2) can be calculated by an empirical derived equation from Fukui [147].

$$c^2 = 2\,(c^2_{HOMO} + c^2_{HOMO\text{-}1}\, e^{-3\Delta E}) \,/\, (1 + e^{-3\Delta E}) \qquad (5)$$

Fukui et al. experimentally determined that not only the HOMO but also the HOMO-1 (Molecular orbital below the HOMO) can contribute to the frontier orbital density. The extent of the contribution of the HOMO-1 to the frontier orbital density depends on the energy difference between the HOMO and the HOMO-1 (ΔE). This equation 5 is also valid for calculating the LUMO/LUMO+1 density on a reaction centre.

Nucleophiles and electrophiles are divided into hard and soft ones. Hard nucleophiles and electrophiles have relatively high-energy LUMOs and low energy HOMOs respectively. When they interact the energy difference between the HOMO and LUMO is large, so that the frontier orbital term can be neglected and the interaction can best described by charge interaction (Coulombic term). This situation is important for example for the reactions between ions and polar reactants. However, most reactants in enzymatic reactions are thought to be soft, i.e. they have low energy LUMOs and high energy HOMOs and are relatively uncharged. Thus for these reactants the frontier orbital term is most important. This also includes radicals which are soft as most are uncharged. Their frontier orbital is a SOMO [148].

The frontier orbital term of the high-valent iron-oxo species of cytochrome P450, which is involved in the catalysis of many xenobiotics, is supposed to be a SOMO as this species has been proposed to have radical character. This species might thus react with the HOMO of a substrate since the cytochrome P450$(FeO)^{3+}$ is considered to be an electrophilic species.

B. Review of frontier orbital based MO-QSARs for biotransformation of xenobiotics

In Table 3 a survey is presented of known frontier orbital based MO-QSARs/ or QSMRs (Quantitative Structure-Metabolism Relationships) for Phase I and II biotransformation reactions.

Table 3 Review of described frontier orbital based MO-QSARs* for the Phase I and II biotransformation of xenobiotics

enzyme(s) [references]	substrate	activity	relationship	mechanistic implication
P4501 [37]	aromatic amines	ethoxyresorufin O-dealkylation	logEROD=0.29 E(HOMO) (±0.12) + 0.80 length/width + 2.22 (± 0.26)	-
P450s [94]	(poly)fluorobenzenes	aromatic ring hydroxylation	regioselectivity of aromatic hydroxylation HOMO/HOMO-1 density distribution~ (r=0.96)	Electrophilic attack of $P450(FeO)^{3+}$ on π electrons of ring carbon atom resulting in a σ-adduct, which re-arranging to a phenol, without the intermediate involvement of epoxide intermediates.
P450s [95,149]	halogenated anilines	4-hydroxylation	$\ln k_{cat}$ ~ E(HOMO) (r=0.96)	Aromatic hydroxylation proceeds by an initial electrophilic attack of the $P450(FeO)^{3+}$ species on the frontier π-electrons of the substrate.
P450s [150]	secondary amines	binding to Pb-induced liver pig microsomes	$\log(1/K_s)$= 5.91 (HOMO) + 7.51 (r=0.871)	As for Type I substrates the K_s can be correlated to the K_m for hydroxylation, hydroxylation is suggested to proceed an an electrophilic mechanism.
GSH S-transferases (1-1, 3-3, A1-1, M1a-1a) [151,152]	fluoronitrobenzenes	GSH conjugation	$\ln k_{cat}$ ~ E(LUMO) (r=0.985-0.999)	Nucleophilic attack of the thiolate anion on the fluoronitrobenzenes, leading to formation of the Meisenheimer complex, which is the rate-limiting step in the overall catalysis.

*These QSARs are sometimes called Quantitative Structure-Metabolism Relationships (QSMRs) as they describe the correlation between the chemical characteristics of the substrate or intermediate in the biotransformation reaction and its product(s).

Aim of the present study

The starting point for this study is a MO-QSAR for the cytochrome P450-catalysed regioselectivity of aromatic ring hydroxylation of a series (poly)fluorobenzenes [94]. This MO-QSAR was obtained for benzene derivatives with fluorine substituents which are inert but also relatively small, so that steric effects due to these substituents or interactions between the substrate and the active site by these substituents are not expected. In the present study it is investigated whether this QSAR could also be applied to benzene derivatives with substituents which are more complicated and/or larger than a fluorine atom (*Chapters 2* and *3*). Additional experiments are performed when deviations between the predicted and observed regioselectivity of aromatic ring hydroxylation are observed. The possible influence of interactions between the substrate and properties of the active site on the regioselectivity of aromatic ring hydroxylation are investigated in *Chapters 4* and *5*. In *Chapter 4* the orientation of a series fluoromethylanilines in cytochromes P450 1A1 and 2B1 is investigated. The mechanism of aromatic ring hydroxylation by the mini-heme enzyme microperoxidase-8 (MP-8) is studied in order to determine whether this enzyme might be used as a model system for cytochrome P450-catalysed aromatic hydroxylation (*Chapter 5*). This mini-heme enzyme, containing only eight amino acids, lacks an active site, and, thus, can be used to determine the influence of the active site on the regioselectivity of aromatic ring hydroxylation assuming that it acts by a similar mechanism of aromatic hydroxylation as cytochrome P450.

In contrast to literature data about the extensive NIH shift upon cytochrome P450-catalysed aromatic ring hydroxylation of bromine and chlorine substituted benzenes, absence of such NIH shifted metabolites in the mainly fluorinated benzene derivatives in the previous chapters is observed. In *Chapter 6* the discrepancy in the occurrence of NIH shifted metabolites between chlorine and fluorinated benzenes is investigated.

Finally, in addition to all studies on model benzene derivatives, in *Chapter 7* the biotransformation of the insecticide Teflubenzuron is investigated. This study is performed to determine whether outcomes of studies on model benzene derivatives can be used to obtain more insight in the biotransformation of other benzene derivatives.

The summary and conclusions are presented in *Chapter 8*.

References

1 Strobel, H.W., Lu, A.Y.H., Heideman, J., and Coon, M.J. (1970) Phosphatidylcholine requirement in the enzymatic reduction of hemoprotein P-450 and in fatty acid, hydrocarbon, and drug hydroxylation. *J. Biol. Chem.* 245, 4851-4854.

2 Guengerich, F.P. (1992) Cytochrome P450: advances and prospects. *FASEB J.* 6, 667-705.

3 Omura, T., and Sato, R. (1964) The carbon monoxide pigment of liver microsomes, I. Evidence for its haemprotein nature. *J. Biol. Chem.* 239, 2370-2378.

4 Jefcoate, C.R. (1978) Measurement of substrate and inhibitor binding to microsomal cytochrome P-450 by optical-difference spectroscopy. *Methods Enzymol.* 52, 258-279.

5 Stern, J.O., Peisach, J., Blumberg, W.E., Lu, A.Y.H., and Levin, W. (1973) A low-temperature EPR study of partially purified, soluble ferric cytochromes P-450 and P-448 from rat liver microsomes. *Arch. Biochem. Biophys.* 156, 404-413.

6 Guengerich, F.P. (1993) Cytochrome P450 enzymes. *American Scientist* 81, 440-447.

7 Dawson, J.H. (1988) Probing structure-function relations in heme-containing oxygenases and peroxidases. *Science* 240, 433-439.

8 Gibson, G.G., and Tamburini, P.P. (1984) Cytochrome P-450 spin state: Inorganic biochemistry of haem iron ligation and functional significance. *Xenobiotica* 14, 27-47.

9 Schenkman, J.B. (1970) Studies on the nature of the Type I and Type II spectral changes in liver microsomes. *Biochemistry* 9, 2081-2091.

10 Schenkman, J.B., Cinti, D.L., Moldeus, P.W., and Orrenius, S. (1973) Newer aspects of substrate binding to cytochrome P-450. *Drug Metab. Dispos.* 1, 111-120.

11 Ullrich, V., Nastainczyk, W., and Ruf, H.H. (1975) Ligand reactions of cytochrome P-450. *Biochem. Soc. Trans.* 3, 803-807.

12 Golly, I., and Hlavica, P. (1992) Chemical modification of lysine residues in cytochrome P450LM2 (P450IIB4): Influence on heme liganding of arylamines. *Arch. Biochem. Biophys.* 292, 287-294.

13 Guengerich, F.P. (1983) Oxidation-reduction properties of rat liver cytochrome P-450 and NADPH-cytochrome P-450 reductase related to catalysis in reconstituted systems. *Biochemistry* 22, 2811-2820.

14 Goeptar, A.R., Scheerens, H., and Vermeulen, N.P.E. (1995) Oxygen and xenobiotic reductase activities of cytochrome P450. *Crit. Rev. Toxicol.* 25, 25-65.

15 Raag, R., Martinis, S.A., Sligar, S.G., and Poulos, T.L. (1991) Crystal structure of the cytochrome $P\text{-}450_{cam}$ active site mutant Thr252Ala. *Biochemistry* 30, 11420-11429.

16 Mansuy, D., Battioni, P., and Battioni, J.-P. (1989) Chemical model systems for drug-metabolizing cytochrome P450-dependent monooxygenases. *Eur. J. Biochem.* 184, 267-285.

17 Ingelman-Sundberg, M., and Johansson, I. (1984) Mechanisms of hydroxyl radical formation and ethanol oxidation by ethanol-inducible and other forms of rabbit liver microsomal cytochromes P-450. *J. Biol. Chem.* 259, 6447-6458.

18 Raag, R., and Poulos, T.L. (1991) Crystal structures of cytochrome $P\text{-}450_{CAM}$ complexed with camphane, thiocamphor, and adamantane: Factors controlling P-450 substrate hydroxylation. *Biochemistry* 30, 2674-2684.

19 Persson, J.-O., Terelius, Y., and Ingelman-Sundberg, M. (1990) Cytochrome P-450-dependent formation of reactive oxygen radicals: Isozyme-specific inhibition of P-450-mediated reduction of oxygen and carbon tetrachloride. *Xenobiotica* 20, 887-900.

20 Hanioka, N., Gonzalez, F.J., Lindberg, N.A., Liu, G., Gelboin, H.V., and Korzekwa, K.R. (1992) Site-directed mutagenesis of cytochrome P450s CYP2A1 and CYP2A2: Influence of the distal helix on the kinetics of testosterone hydroxylation. *Biochemistry* 31, 3364-3370.

21 Higuchi, T., Uzu, S., and Hirobe, M. (1990) Synthesis of a highly stable iron porphyrin coordinated by alkylthiolate anion as a model for the cytochrome P-450 and its catalytic activity in O-O bond cleavage. *J. Am. Chem. Soc.* 112, 7051-7053.

22 Adachi, S., Nagano, S., Ishimori, K., Watanabe, Y., and Morishima, I. (1993) Roles of proximal ligand in heme proteins: Replacement of proximal histidine of human myoglobin with cysteine and tyrosine by site-directed mutagenesis as models for P-450, Chloroperoxidase, and catalase. *Biochemistry* 32, 241-252.

23 Allenthoff, A.J., Bolton, J.L., Wilks, A., Thompson, J.A., and Ortiz de Montellano, P.R. (1992) Heterolytic versus homolytic peroxide bond cleavage by sperm whale myoglobin and myoglobin mutants. *J. Am. Chem. Soc.* 114, 9744-9749.

24 White, R.E., and Coon, M.J. (1980) Oxygen activation by cytochrome P450. *Ann. Rev. Biochem.* 49, 315-356.

25 Larroque, C., Lange, R., Maurin, L., Bienvenue, A., and Van Lier, J.E. (1990) On the nature of the cytochrome P450scc "ultimate oxidant": Characterization of a productive radical intermediate. *Arch. Biochem. Biophys.* 282, 198-201.

26 Atkins, W.M., and Sligar, S.G. (1987) Metabolic switching in cytochrome P-450$_{cam}$: Deuterium isotope effects on regioselectivity and the monooxygenase/oxidase ratio. *J. Am. Chem. Soc.* 109, 3754-3760.

27 Korzekwa, K.R., Gilette, J.R., and Trager, W.F. (1995) Isotope effect studies on the cytochrome P450 enzymes. *Drug Met. Rev.* 27, 45-59.

28 Guengerich, F.P., and Macdonald, T.L. (1990) Mechanisms of cytochrome P-450 catalysis. *FASEB J.* 4, 2453-2459.

29 Oritz de Montellano, P.R. (1986) Oxygen activation and transfer. In: Cytochrome P450-Structure, mechanism, and Biochemistry (Oritz de Montellano, P.R., Ed.), Plenum Press, New York, pp. 217-271.

30 Jones, J.P., Rettie, A.E., and Trager, W.F. (1990) Intrinsic isotope effects suggest that the reaction coordinate symmetry for the cytochrome P-450 catalyzed hydroxylation of octane is isozyme independent. *J. Med. Chem.* 33, 1242-1246.

31 Nelson, D.R., Kamataki, T., Waxman, D.J., Guengerich, F.P., Estabrook, R.W., Feyereisen, R., Gonzalez, F.J., Coon, M.J., Gunsalus, I.C., Gotoh, O., Okadu, K., and Nebert, D.W. (1993) The P450 superfamily: Update on new sequences, gene mapping, accession numbers, early trivial names of enzymes, and nomenclature. *DNA Cell Biol.* 12, 1-51.

32 Parkinson, A. (1996) Biotransformation of xenobiotics. In: Toxicology -The basic science of poisons, fifth edition- (Klaassen, C.D., Ed.), pp. 113-186.

33 Nebert, D.W., and Gonzalez, F.J. (1987) P450 genes: Structure, evolution, and regulation. *Ann. Rev. Biochem.* 56, 945-993.

34 Poland, A., and Glover, E. (1976) Stereospecific high affinity binding of 2,3,7,8-tetrachlorodibenzo-p-dioxin by hepatic cytosol. *J. Biol. Chem.* 251, 4936-4946.

35 Nebert, D.W., and Gonzalez, F. (1990) The P450 gene superfamily. In: Principles, mechanisms and biological consequences of induction (Ruckpaul, K., and Rein, H., Eds.), Akademie Verlag, Berlin, pp. 35-61.

36 Lewis, D.F.V., Ioannides, C., and Parke, D.V. (1986) Molecular dimensions of the substrate binding site of cytochrome P-448. *Biochem. Pharmacol.* 35, 2179-2185.

37 Lewis, D.F.V., Moereels, H., Lake, B.G., Ioannides, C., and Parke, D.V. (1994) Molecular modeling of enzymes and receptors involved in carcinogenesis: QSARs and COMPACT-3D. *Drug Met. Rev.* 26, 261-285.

38 Song, B.-J., Veech, R.L., Park, S.S., Gelboin, H.V., and Gonzalez, F.J. (1989) Induction of rat hepatic N-nitrosodimethylamine demethylase by acetone is due to protein stabilization. *J. Biol. Chem.* 264, 3568-3572.

39 Eliasson, E., Johansson, I., and Ingelman-Sundberg, M. (1990) Substrate-, hormone-, and cAMP-regulated cytochrome P450 degradation. *Proc. Natl. Acad. Sci. USA* 87, 3225-3229.

40 Oritz de Montellano, P.R., and Reich, N.O. (1986) Inhibition of cytochrome P450 enzymes In: Cytochrome P450-Structure, mechanism, and Biochemistry (Oritz de Montellano, P.R., Ed.), Plenum Press, New York, pp. 273-314.

41 Kato, R., and Yamazoe, Y. (1990) Sex-dependent regulation of cytochrome P-450 expression. In: Principles, mechanisms and biological consequences of induction (Ruckpaul, K., and Rein, H., Eds.), Akademie Verlag, Berlin, pp. 82-112.

42 De Morrais , S.M.F., Wilkinson, G.R., Blaisdell, J., Nakamura, K., Meyer, U.A., and Goldstein, J.A. (1994) The major genetic defect responsible for the polymorphism of (S)-mephenytoin metabolism in human. *J. Biol. Chem.* 269, 15419-15422.

43 Batt, A.M., Magdalou, J., Vincent-Viry, M., Ouzzine, M., Fournel-Gigleux, S., Galteau, M.M., and Siest, G. (1994) Drug metabolizing enzymes related to laboratory medicine: Cytochromes P450 and UDP-glucuronosyltransferases. *Clin. Chim. Acta* 226, 171-190.

44 Gonzalez, F.J., and Gelboin, H.V. (1994) Role of human cytochromes P450 in the metabolic activation of chemical carcinogens and toxins. *Drug Met. Rev.* 26, 165-183.

45 Epe, B. (1991) Genotoxicity of singlet oxygen. *Chem.-Biol. Interact.* 80, 239-260.

46 Ames, B.N., and Swirsky Gold, L. (1991) Endogenous mutagens and the causes of aging and cancer. *Mutat. Res.* 250, 3-16.

47 Parke, D.V., Ioannides, C., and Lewis, D.F.V. (1991) The role of the cytochromes P450 in the detoxication and activation of drugs and other chemicals. *Can. J. Physiol. Pharmacol.* 69, 537-549.

48 Ioannides, C., and Parke, D.V. (1987) The cytochrome P-448 -An unique family enzymes involved in chemical toxicity and carcinogenesis. *Biochem. Pharmacol.* 36, 4197-4207.

49 Yamazaki, H., Oda, Y., Funae, Y., Imaoka, S., Inui, Y., Guengerich, F.P., and Shimada, T. (1992) Participation of rat liver cytochrome P450 2E1 in the activation of N-nitrosodimethylamine and N-nitrosodiethylamine to products genotoxic in an acetyltransferase-overexpressing *Salmonella typhimurium* strain (NM2009). *Carcinogenesis* 13, 979-985.

50 Seaton, M.J., Schlosser, P.M., Bond, J.A., and Medinsky, M.A. (1994) Benzene metabolism by human liver microsomes in relation to cytochrome P450 2E1 activity. *Carcinogenesis* 15, 1799-1806.

51 Parke, D.V. (1994) The cytochromes P450 and mechanisms of chemical carcinogenesis. *Environ. Health Perspec.* 102, 852-853.

52 Guengerich, F.P. (1989) Structural multiplicity and functional versatility of cytochrome P450. In: Frontiers in Biotransformation, vol 1, basis and mechanisms of regulation of cytochromes P-450 (Ruckpaul, K., and Rein, H., Eds.), Taylor and Francis, London, pp. 101-150.

53 Taniguchi, H., and Pyerin, W. (1988) Phospholipid bilayer membranes play decisive roles in the cytochrome P-450-dependent monooxygenase system. *J. Cancer Res. Clin. Oncol.* 114, 335-240.

54 Ravichandran, K.G., Boddupalli, S.S., Hasemann, C.A., Peterson, J.A., and Deisenhofer, J. (1993) Crystal structure of hemoprotein domain of P450BM-3, a prototype for microsomal P450's. *Science* 261, 731-736.

55 Haseman, C.A., Ravichandran, K.G., Peterson, J.A., and Deisenhofer, J. (1994) Crystal structure and refinement of cytochrome P450terp at 2-3Å resolution. *J. Mol. Biol.* 236, 1169-1185.

56 Gotoh, O. (1992) Substrate recognition sites in cytochrome P450 family 2 (CUP2) proteins inferred from comparative analyses of amino acid and coding nucleotide sequences. *J. Biol. Chem.* 267, 83-90.

57 Graham-Lorence, S., Amarneh, B., White, R.E., Peterson, J.A., and Simpson, E.R. (1995) A three-dimensional model of aromatase cytochrome P450. *Protein Sci.* 4, 1065-1080.

58 Paulsen, M.D., and Ornstein, R.L. (1995) Dramatic differences in the motion of the mouth of open and closed cytochrome $P450_{BM-3}$ by molecular dynamics simulations. *Proteins* 21, 237-243.

59 Deprez, E., Gerber, N.C., Di Primo, C.D., Douzou, P., Sligar, S.G., and Joa, G.H.B. (1994) Electrostatic control of the substrate access channel in cytochrome $P450_{cam}$. *Biochemistry* 33, 14464-14468.

60 Li, H.Y., and Poulos, T.L. (1995) Modeling protein substrate interactions in the heme domain of cytochrome $P450_{BM-3}$. *Acta Crystallogr. [D]* 51, 21-32.

61 Li, H., and Poulos, T.L. (1994) Structural variation in heme enzymes: A comperative analysis of peroxide and P450 crystal structures. *Structure* 2, 461-464.

62 De Voss, J.J., and Ortiz de Montellano, P.R. (1995) Computer-assisted, structure-based prediction of substrates for cytochrome $P450_{cam}$. *J. Am. Chem. Soc.* 117, 4185-4186.

63 Harris, D., and Loew, G. (1995) Prediction of regioselective hydroxylation of camphor analogs by cytochrome $P450_{cam}$. *J. Am. Chem. Soc.* 117, 2738-2746.

64 Loida, P.J., Sligar., S., Paulsen, M.D., Arnold, G.E., and Ornstein, R.L. (1995) Stereoselective hydroxylation of norcamphor by cytochrome $P450_{cam}$. *J. Biol. Chem.* 270, 5326-5330.

65 Boddupalli, S.S., Haseman, C.A., Ravichandran, K.G., Lu, J.-Y., Goldsmith, E.J., Deisenhofer, J., and Peterson, J.A. (1992) Crystallization and preliminary x-ray diffraction analysis of $P450_{terp}$ and the hemoprotein domain of $P450_{BM-3}$, enzymes belonging to two distinct classes of the cytochrome P450 superfamily. *Proc. Natl. Acad. Sci.* 89, 5567-5571.

66 Korzekwa, K.R., and Jones, J.P. (1993) Predicting the cytochrome P450 mediated metabolism of xenobiotics. *Pharmacogenetics* 3, 1-8.

67 Swanson, B.A., Dutton, D.R., Lunetta, J.M., Yang, C.S., and Ortiz de Montellano (1991) The active sites of cytochromes P450IA1, IIB1, IIB2, and IIE1. *J. Chem. Biol.* 266, 19258-19264.

68 Tuck, S.F., and Ortiz de Montellano, P.R. (1992) Topological mapping of the active sites of cytochromes P4502B1 and P4502B2 by in situ rearrangement of aryl-iron complexes. *Biochemistry* 31, 6911-6916.

69 Ortiz de Montellano, P.R. (1995) Arylhydrazines as probes of hemoprotein structure and function. *Biochimie* 77, 581-593.

70 Tuck, S.F., Hiroya, K., Shimizu, T., Hatano, M., and Ortiz de Montellano, P.R. (1993) The cytochrome P450 1A2 active site: Topology and pertubations caused by glutamic acid-318 and threonine-319 mutations. *Biochemistry* 32, 2548-2553.

71 Mackman, R., Guo, Z., Guengerich, F.P., and Ortiz de Montellano, P.R. (1996) Active site topology of human cytochrome P4502E1. *Chem. Res. Toxicol.* 9, 223-226.

72 Tuck, S.F., Peterson, J.A., and Ortiz de Montellano, P.R. (1992) Active site topologies of bacterial cytochromes P450101 ($P450_{cam}$), P450108 ($P450_{terp}$), and P450102 ($P450_{BM3}$). *J. Biol. Chem.* 267, 5614-5620.

73 Bösterling, B., Trudell, J.R., and Galla, H.J. (1981) Phospholipid interactions with cytochrome P-450 in reconstituted vesicles. *Biochim. Biophys. Acta* 643, 547-556.

74 Van Bladeren, P.J., Balani, S.K., Sayer, J.M., Thakker, D.R., Boyd, D.R., Ryan, D.E., Thomas, P.E., Levin, W., and Jerina, D.M. (1987) Stereoselective formation of benzo(c)phenanthrene (+)-(3S,4R) and (+)-(5S,6R)-oxides by cytochrome P450c in a highly purified and reconstituted system. *Biochem. Biophys. Res. Commun.* 145, 160-167.

75 Guengerich, F.P., Kim, P., and Iwasaki, M. (1991) Role of human cytochrome P450IIE1 in the oxidation of many low molecular weight cancer suspects. *Chem. Res. Toxicol.* 4, 168-179.

76 Lewis, D.F.V., Ioannides, C., and Parke, D.V. (1987) Structural requirements for substrates of cytochromes P-450 and P-448. *Chem.-Biol. Interact.* 64, 39-60.

77 Crull, G.B., Kennington, J.W., Garber, A.R., Ellis, P.D., and Dawson, J.H. (1989) ^{19}F Nuclear magnetic resonance as a probe of the spatial relationship between the heme iron of cytochrome P-450 and its substrates. *J. Biol. Chem.* 264, 2649-2655.

78 Novak, R.F., and Vatsis, K.P. (1982) ^{1}H Fourier transform nuclear magnetic resonance relaxation rate studies on the interaction of acetanilide with purified isozymes of rabbit liver microsomal cytochrome P-450 and with cytochrome b_5. *Mol. Pharmacol.* 21, 701-709.

79 Myers, T.G., Thummel, K.E., Kalhorn, T.F., and Nelson, S.D. (1994) Preferred orientations in the binding of 4'-hydroxyacetanilide (acetaminophen) to cytochrome P450 1A1 and 2B1 isoforms as determined by ^{13}C- and ^{15}N-NMR relaxation studies. *J. Med. Chem.* 37, 860-867.

80 Van de Straat, R., De Vries, J., De Boer, H.J.R., Vromans, R.M., and Vermeulen, N.P.E. (1987) Relationship between paracetamol binding to and its oxidation by two cytochrome P-450 isoenzymes-a proton nuclear magnetic resonance and spectrophotometric study. *Xenobiotica* 17, 1-9.

81 Aoyama, T., Korzekwa, K., Nagata, K., Adesnik, M., Reiss, A., Lapenson, D.P., Gillette, J., Gelboin, H.V., Waxman, D.J., and Gonzalez, F.J. (1989) Sequence requirements for cytochrome P-450IIB1 catalytic activity-Alterations of the stereospecificity and regioselectivity of steroid hydroxylation by a simultaneous change of two hydrophobic amino acid residues to phenylalanine. *J. Biol. Chem.* 264, 21327-21333.

82 Kronbach, T., Larabee, T.D., and Johnson, E.F. (1989) Hybrid cytochromes P-450 identify a substrate binding domain in P-450IIC5 and P-450IIC4. *Proc. Natl. Acad. Sci. USA* 86, 8262-8265.

83 Szklarz, G.D., He, Y.-A., and Halperts, J.R. (1995) Site-directed mutagenesis as a tool for molecular modeling of cytochrome P450 2B1. *Biochemistry* 34, 14312-14322.

84 Furuya, H., Shimizu, T., Hatano, M., and Fujii-Kuriyama, Y. (1989) Mutations at the distal and proximal sites of cytochrome P-450$_d$ changed regio-specificity of acetanilide hydroxylations. *Biochem. Biophys. Res. Commun.* 160, 669-676.

85 Wolff, T., Distlerath, L.M., Worthington, M.T., Groopman, J.D., Hammons, G.J., Kadbular, F.F., Prough, R.A., Martin, M.V., and Guengerich, F.P. (1985) Substrate specificity of human liver cytochrome P-450 Debrisoquine 4-hydroxylase probed using immunochemical inhibition and chemical modeling. *Cancer Res.* 45, 2116-2122.

86 Smith, A., and Jones, B.C. (1992) Speculations on the substrate-activity relationship (SSAR) of cytochrome P450 enzymes. *Biochem. Pharmacol.* 44, 2089-2098.

87 Koymans, L., Vermeulen, N.P.E., Van Acker, S.A.B.E., Te Koppele, J.M., Heykants, J.J.P., Lavrijsen, K., Meuldermans, W., and Donné-Op den Kelder, G.M. (1992) A predictive model for substrates of cytochrome P450-Debrisoquine (2D6). *Chem. Res. Toxicol.* 5, 211-219.

88 Islam, S.A., Wolf, C.R., Lennard, M.S., and Sternberg, M.J.E. (1991) A three-dimensional molecular template for substrates of human cytochrome P450 involved in debrisoquine 4-hydroxylation. *Carcinogenesis* 12, 2211-2219.

89 Strobl, G.R., Von Kreudener, S., Stöckigt, J., Guengerich, F.P., and Wolf, T. (1993) Development of a pharmacophore for inhibition of human liver cytochrome P-450 2D6: Molecular and inhibition studies. *J. Med. Chem.* 36, 1136-1145.

90 Nakayama, A., Ikura, K., Katsuura, K., Hashimoto, S., and Nakata, A. (1989) Quantitative structure-activity relationships, conformational analyses and computer graphics study of triflumizole analogs, fungicidal N-(1-imidazol-1-ylalkylidene)anilines. *J. Pestic. Sci.* 14, 23-37.

91 Raag , R., and Poulos, T.L. (1992) X-ray crystallographic structural studies of cytochrome P450cam: Factors controlling substrate metabolism. In: Relationships between structure and function of cytochrome P450; experiments, calculations, models. Frontiers in Biotransformation, vol. 7 (Ruckpaul, K., and Rein, H., Eds.), Akademie Verlag, Berlin, pp. 1-44.

92 Hlavica, P. (1994) Regulatory mechanisms in the activation of nitrogenous compounds by mammalian cytochrome P-450 isozymes. *Drug Met. Rev.* 26, 325-348.

93 Paulsen, M.D., and Ornstein, R.L. (1993) Substrate mobility in thiocamphor-bound cytochrome P450$_{cam}$: An explanation of the conflict between the observed product profile and the X-ray structure. *Protein Engng.* 6, 359-365.

94 Rietjens, I.M.C.M., Soffers, A.E.M.F., Veeger, C., and Vervoort, J. (1993) Regioselectivity of cytochrome P-450 catalyzed hydroxylation of fluorobenzenes predicted by calculated frontier orbital substrate characteristics. *Biochemistry* 32, 4801-4812.

95 Cnubben, N.H.P., Peelen, S., Borst, J.-W., Vervoort, J., Veeger, C., and Rietjens, I.M.C.M. (1994) Molecular orbital-based quantitative structure-activity relationship for the cytochrome P450-catalyzed 4-hydroxylation of halogenated anilines. *Chem. Res. Toxicol.* 7, 590-598.

96 Korzekwa, K.R., Jones, J.P., and Gillette, J.R. (1990) Theoretical studies on cytochrome P-450 mediated hydroxylation: A predictive model for hydrogen atom abstractions. *J. Am. Chem. Soc.* 112, 7042-7046.

97 Riley, P., and Hanzlik, R.P. (1994) Electron transfer on P450 mechanisms. Microsomal metabolism of cyclopropylbenzene and p-cyclopropylanisole. *Xenobiotica* 24, 1-16.

98 Lewis, D.F.V., Ioannides, C., and Parke, D.V. (1995) A quantitative structure-activity relationship study on a series of 10 para-substituted toluenes binding to cytochrome P4502B4 (CYP2B4), and their hydroxylation rates. *Biochem. Pharmacol.* 50, 619-625.

99 Shea, J.P., Nelson, S.D., and Ford, G.P. (1983) MNDO calculation of kinetic isotope effects in model cytochrome P-450 oxidations. *J. Am. Chem. Soc.* 105, 5451-5454.

100 Hanzlik, R.P., and Ling, K.-H. (1990) Active site dynamics of toluene hydroxylation by cytochrome P-450. *J. Org. Chem.* 55, 3992-3997.

101 Guengerich, F.P., and Macdonald, T.L. (1990) Chemical mechanisms of catalysis by cytochromes P450: A unified view. *Acc. Chem. Res.* 17, 9-16.

102 Hall, L.R., and Hanzlik, R.P. (1991) N-dealkylation of tertiary amides by cytochrome P-450. *Xenobiotica* 21, 1127-1138.

103 Miwa, G.T., Walsh, J.S., and Lu, A.Y.M. (1984) Kinetic isotope effects on cytochrome P-450-catalyzed oxidation reactions-The oxidative *O*-dealkylation of 7-ethoxycoumarin. *J. Biol. Chem.* 259, 3000-3004.

104 Shea, J.P., Valentrine, G.L., and Nelson, S.D. (1982) Source of oxygen in cytochrome P-450 catalyzed carbinolamine formation. *Biochem. Biophys. Res. Commun.* 109, 231-235.

105 Pandey, R.N., Armstrong, A.P., and Hollenberg, P.F. (1989) Oxidative N-demethylation of *N,N*-dimethylaniline by purified isozymes of cytochrome P-450. *Biochem. Pharmacol.* 38, 2181-2185.

106 MacDonald, T.L., Guthem, W.G., Martin, R.B., and Guengerich, F.P. (1989) Oxidation of substituted *N,N*-dimethylanilines by cytochrome P-450: Estimation of the effective oxidation-reduction potential of cytochrome P-450. *Biochemistry* 28, 2071-2077.

107 Armstrong, R.N. (1987) Enzyme-catalyzed detoxication reactions: Mechanisms and stereochemistry. *CRC Crit. Rev. Biochem.* 22, 39-88.

108 Korzekwa, K., Swinney, D.C., and Trager, W.F. (1989) Isotopically labeled chlorobenzenes as probes for the mechanisms of cytochrome P450 catalyzed aromatic hydroxylation. *Biochemistry* 28, 9019-9027.

109 Rizk, P.N., and Hanzlik, R.P. (1995) Oxidative and non-oxidative metabolism of 4-iodoanisole by rat liver microsomes. *Xenobiotica* 25, 143-150.

110 Korzekwa, K., Trager, W., Gouterman, M., Sprangler, D., and Loew, G.H. (1985) Cytochrome P450 mediated aromatic oxidation: A theoretical study. *J. Am. Chem. Soc.* 107, 4273-4279.

111 Burka, L.T. (1983) Mechanism of cytochrome P-450 catalysis. Mechanism of N-dealkylation and amine oxide deoxygenation. *J. Am. Chem. Soc.* 107, 2549-2551.

112 Guroff, G., Daly, J.W., Jerina, D.M., Renson, J., Witkop, B., and Udenfriend, S. (1967) Hydroxylation-induced migration: The NIH shift. *Science* 157, 1524-1550.

113 Daly, J.W., Jerina, D.M., and Witkop, B. (1972) Arene oxides and the NIH shift: The metabolism, toxicity and carcinogenicity of aromatic compounds. *Experientia* 28, 1129-1264.

114 Rietjens, I.M.C.M., and Vervoort, J. (1991) Bioactivation of 4-fluorinated anilines to benzoquinoneimines as primary reaction products. *Chem.-Biol. Interact.* 22, 263-281.

115 Rietjens, I.M.C.M., and Vervoort, J. (1992) A new hypothesis for the mechanism for the cytochrome P450 dependent aerobic conversion of hexahalogenated benzenes to pentahalogenated phenols. *Chem. Res. Toxicol.* 5, 10-19.

116 Den Besten, C., Van Bladeren, P.J., Duizer, E., Vervoort, J., and Rietjens, I.M.C.M. (1993) Cytochrome P450-mediated oxidation of pentafluorophenol to tetrafluorobenzoquinone as the primary reaction product. *Chem. Res. Toxicol.* 6, 674-680.

117 Hanzlik, R.P., and Tullman, R.H. (1982) Suicidal inactivation of cytochrome P450 by cyclopropylamines. Evidence for cation radical intermediates. *J. Am. Chem. Soc.* 104, 2048-2050.

118 Gonzalez, F.J., and Idle, J.R. (1994) Pharmacogenitic phenotyping and genotyping-Present status and future potential-. *Clin. Pharmacokinet.* 26, 59-70.

119 Weber, W.W., and Levy, G.N. (1988) The pharmacogenetics of acyl transfer. In: Metabolism of xenobiotics (Gorrod, J.W., Oelschläger, H., and Caldwell, J., Eds.), Taylor and Francis, London, pp. 209-215.

120 Oesch, F., and Guenther, T.M. (1983) Effects of the modulation of epoxide hydrolase activity on the binding of benzo[a]pyrene metabolites to DNA in the intact nuclei. *Carcinogenesis* 4, 57-65.

121 Rossi, A.M., Migliore, L., Loprieno, N., Romano, M., and Salmona, M. (1983) Evaluation of epichlorhydrin (ECH) genotoxicity. *Mutat. Res.* 109, 41-52.

122 Hinson, J.A., and Kadlubar, F.F. (1988) Glutathione and glutathione transferases in the detoxication of drug and carcinogen metabolites. In: Glutathione conjugation. Mechanisms and biological significance (Sies, H., and Ketterer, B., Eds.), Academic Press Limited, London, pp. 236-280.

123 Monks, T.J., Lau, S.S., and Highet, R.J. (1984) Formation of nontoxic reactive metabolites of p-bromophenol. Identification of a new glutathione conjugate. *Drug Metab. Dispos.* 12, 432-437.

124 Dekant, W., Lash, L.H., and Anders, M.W. (1988) Fate of glutathione conjugates and bioactivation of cysteine S-conjugates by cysteine conjugate ß-lyase. In: Glutathione conjugation. Mechanisms and biological significance (Sies, H., and Ketterer, B., Eds.), Academic Press Limited, London, pp. 415-447.

125 Mulder, J. (Ed) (1990) Conjugation reactions in drug metabolism: An integrated approach. Taylor and Francis, London.

126 Temellini, A., Franchi, M., Giuliani, L., and Pacifici, G.M. (1991) Human liver sulphotransferase and UDP-glucuronosyltransferase: Structure-activity relationship for phenolic substrates. *Xenobiotica* 21, 171-177.

127 Van der Aar, E.M., De Groot, M.J., Bijloo, G.J., Van der Goot, H., and Vermeulen, N.P.E. (1996) Structure-activity relationships for the glutathione conjugation of 2-substituted 1-chloro-4-nitrobenzenes by rat glutathione S-transferase 4-4. *Chem. Res. Toxicol.* 9, 527-534.

128 Hansch, C., and Zhang, L. (1993) Quantitative structure-activity relationships of cytochrome P-450. *Drug Met. Rev.* 25, 1-48.

129 Magdó, I., Ferenczy, G.G., and Bencz, Z. (1994) Prediction of carcinogenicity from molecular structure; modification and reinvestigation of the method. *Cancer Lett.* 81, 201-207.

130 Ioannides, C., Lewis, D.F.V., and Park, D.V. (1994) The use of computers in the safety evaluation of drugs and other chemicals. *Eur. J. Drug Metab. Pharmacokinet.* 3, 225-233.

131 Hansch, C. (1962) Correlation of biological activity of phenoxyacetic acids with Hammett substituent constants and partion coefficients. *Nature* 194, 178-180.

132 Dearden, J.C. (1990) Physico-chemical descriptors. In: Practical applications of quantitative structure-activity relationships (QSAR) in environmental chemistry and toxicology (Karcher, W., and Devillers, J., Eds.), ECSC, EEC, EAEC, Brussels and Luxembourg, pp. 25-59.

133 Niemi, G.J. (1990) Multivariate analysis and QSAR: Applications of principal component analysis. In: Practical applications of quantitative structure-activity relationships (QSAR) in environmental chemistry and toxicology (Karcher, W., and Devillers, J., Eds.), ECSC, EEC,EAEC, Brussels and Luxembourg, pp. 153-169.

134 Geladi, P., and Tosato, M.-L. (1990) Multivariate latent variable projection methods: SIMCA and PLS. In: Practical applications of quantitative structure-activity relationships (QSAR) in environmental chemistry and toxicology (Karcher, W., and Devillers, J., Eds.), ECSC, EEC, EAEC, Brussels and Luxembourg, pp. 171-179.

135 Topliss, J.G., and Edwards, R.P. (1979) Chance factors in studies of Quantitative Structure-Activity Relationships. *J. Med. Chem.* 22, 1238-1244.

136 Harris, J.W., Jones, J.P., Martin, J.L., LaRosa, A.C., Olson, M.J., Pohl, L.R., and Anders, M.W. (1992) Pentahaloethane-based chlorofluorocarbon substitutes and halothane: Correlation of in vivo hepatic protein trifluoroacetylation and urinary trifluoroacetic acid excretion with calculated enthalpies of activation. *Chem. Res. Toxicol.* 5, 720-725.

137 Yin, H., Anders, M.W., Korzekwa, K.R., Higgins, L., Thummel, K.E., Kharasch, E.D., and Jones, J.P. (1995) Designing safer chemicals: Predicting the rates of metabolism of halogenated alkanes. *Proc. Natl. Acad. Sci. USA* 92, 11076-11080.

138 Lewis, D.F.V., Ioannides, C., and Parke, D.V. (1994) Interaction of a series of nitriles with the alcohol-inducible isoform of P450: Computer analysis of structure-activity relationship. *Xenobiotica* 24, 401-408.

139 Ghauri, F.Y., Blackledge, C.A., Glen, R.C., Sweatman, B.C., Lindon, J.C., Beddell, C.R., Wilson, I.D., and Nicholson, J.K. (1992) Quantitative structure-metabolism relationships for substituted benzoic acids in the rat. *Biochem. Pharmacol.* 44, 1935-1946.

140 Lewis, D.F.V. (1990) MO-QSARs: A review of molecular orbital-generated quantitative structure-activity relationships. In: Progress in drug metabolism (Gibson, G.G., Ed.), Taylor and Francis, London, pp. 205-255.

141 Schrödinger, E. (1926) An undulatory theory of the mechanics of atoms and molecules. *Phys. Rev.* 28, 1049-1070.

142 Dewar, M.J.S. (1983) Development and status of MINDO/3 and MNDO. *J. Mol. Structure* 100, 41-50.

143 Murdoch, J.R., and Magnoli, D.E. (1982) Kinetic and thermodynamic control in group transfer reactions. *J. Am. Chem. Soc.* 104, 3792-3800.

144 Hammond, G.S. (1955) A correlation of reaction rates. *J. Am. Chem. Soc.* 77, 334-338.

145 Klopman, G. (1968) Chemical reactivity and the concept of charge- and frontier-controlled reactions. *J. Am. Chem. Soc.* 90, 223-234.

146 Salem, L. (1968) Intermolecular orbital theory of the interaction between conjugated systems. General theory. *J. Am. Chem. Soc.* 90, 543-552.

147 Fukui, K., Yonezawa, T., Nagata, C., and Shingu, H. (1954) Molecular theory of orientation in aromatic, heteroaromatic, and other conjugated molecules. *J. Chem. Phys.* 22, 1433-1442.

148 Fleming, I. (1976) Molecular orbitals and frontier orbitals. In: Frontier Orbitals and Organic Chemical Reactions (Fleming, I., Ed.), John Wiley and Sons, New York, pp. 5-32.

149 Tyrakowska, B., Cnubben, N.H.P., Soffers, A.E.M.F., Wobbes, Th., and Rietjens, I.M.C.M. (1996) Comparative MO-QSAR studies in various species including man. *Chem.-Biol. Interact.* 100, 187-201.

150 Le Page, C., Schaeffer, M., Batt, A.M., and Siest, G. (1980) Q.S.A.R. in a series of secondary amines derived from perhexilline maleate with purified phenobarbital-induced pig liver microsomal cytochrome P-450. In: Biochemistry, biophysics and regulation of cytochrome P-450 (Gustafsson, J.-Å. et al., Eds.), Elsevier/North-Holland Biomedical Press, pp. 363-367.

151 Rietjens, I.M.C.M., Soffers, A.E.M.F., Hooiveld, G., Veeger, C., and Vervoort, J. (1995) Quantitative structure-activity relationships based on computer calculated parameters for the overall rate of glutathione S-transferase catalyzed conjugation of a series of fluoronitrobenzenes. *Chem. Res. Toxicol.* 8, 481-488.

152 Soffers, A.E.M.F., Ploemen, J.H.T.M., Moonen, M.J.H., Wobbes, Th., Van Ommen, B., Vervoort, J., Van Bladeren, P.J., and Rietjens, I.M.C.M. (1996) Regioselectivity and quantitative structure-activity relationships for the conjugation of a series of fluoronitrobenzenes by purified glutathione S-transferase enzymes from rat and man. *Chem. Res. Toxicol.* 9, 638-646.

Chapter 2

Influence of substituents in fluorobenzene derivatives on the cytochrome P450-catalysed hydroxylation at the adjacent *ortho* aromatic carbon centre

J. Koerts, M.M.C. Velraeds, A.E.M.F. Soffers, J. Vervoort and I. M.C.M. Rietjens

Chemical Research in Toxicology, accepted for publication.

Abstract

In a previous study the *in vivo* cytochrome P450-catalysed regioselectivity of aromatic ring hydroxylation for a series of (poly)fluorobenzenes could be quantitatively predicted by the calculated frontier orbital density distribution in the aromatic ring [Rietjens et al. (1993), Biochemistry 32, 4801-4812]. However, the relative small fluorine, its size almost comparable to a hydrogen, is not expected to influence the regioselectivity of aromatic hydroxylation due to steric hindrance. The aim of the present study was to investigate the influence of larger substituents than a hydrogen or fluorine on the possibilities for hydroxylation at the adjacent carbon centre. First, the *in vivo* regioselectivity of aromatic ring hydroxylation of a series of C4-substituted fluorobenzenes was investigated. The results obtained demonstrate that a chlorine and cyano C4 substituent do not hamper hydroxylation at the positions *ortho* to the C4 carbon atom. For 4-chloro- and 4-cyanofluorobenzene the observed regioselectivity of aromatic hydroxylation correlated with the regioselectivity predicted on the basis of the frontier orbital density distribution. In contrast, a bromine and iodine substituent affected the hydroxylation at the adjacent *ortho* carbon centres reducing it to respectively 40% and 6% of the calculated intrinsic reactivity of the carbon centres. Additional experiments were performed to investigate whether the regioselectivity of the aromatic hydroxylation of the C4-substituted fluorobenzene model compounds was influenced by changes in the cytochrome P450 enzyme pattern. Results obtained demonstrate that for these relatively small substrates the regioselectivity of their hydroxylation was not significantly influenced by several cytochrome P450 inducers. This suggests that the

active sites of the cytochromes P450 catalyzing the aromatic hydroxylation, do not impose a stereoselective orientation of the aromatic rings with respect to the iron-oxo porphyrin reaction centre. Thus, the working hypothesis for additional experiments was that the deviations for the regioselectivity of aromatic hydroxylation observed for 4-bromo- and 4-iodofluorobenzene may be ascribed to steric hindrance by the bromine and iodine substituents hampering the attack of the cytochrome P450 iron-oxo species on the adjacent carbon centres in the benzene derivative. This working hypothesis was further tested by investigating whether useful steric correction factors could be derived from the results obtained with the series C4-substituted fluorobenzenes. These correction factors should make it possible to correct calculated relative reactivities of carbon sites for steric hindrance by substituents positioned *ortho* with respect to the carbon to be hydroxylated. This will make it possible to better explain and predict the regioselectivities for other chlorine, bromine, iodine and cyano containing fluorobenzenes. The *in vivo* regioselectivity of aromatic ring hydroxylation of a series of five chlorine, bromine, iodine or cyano containing fluorobenzenes did not correlate with the non-corrected calculated reactivities (r=0.49). However, upon correction of the calculated reactivity values by using the steric correction factors, a correlation between the observed and calculated regioselectivity for the substrates of the present study was obtained (r=0.91). Together these results strongly indicate that for the fluorobenzenes studied main factors directing the regioselectivity of their aromatic hydroxylation are i) the nucleophilic chemical reactivity of the site to be hydroxylated and ii) steric influence of the substituent *ortho* with respect to the site of hydroxylation. This latter effect appears to be negligible for a fluorine, chlorine, and cyano substituent but significant for a bromine and iodine substituent.

Introduction

The regioselectivity and extent of the cytochrome P450-catalysed monooxygenation of benzene derivatives is an important factor influencing their conversion in either bioactivation or elimination pathways. The pathways leading to various ring hydroxylated metabolites of a single benzene derivative may differ in the type of toxic intermediates formed. For bromobenzene the pathway leading to 2-bromophenol appeared to be not as toxic as the metabolic pathway leading to formation of 4-bromophenol [1,2]. In addition, the formation of the various aromatic ring hydroxylated products might be dependent on the cytochrome P450 enzyme

pattern present [3-6]. For example, upon treatment of rats with 3-methylcholanthrene the biotransformation pattern of bromobenzene shifted in favour of the 2-bromophenol metabolic route [3,4].

In a previous study on the cytochrome P450-catalysed regioselectivity of aromatic ring hydroxylation of a series of (poly)fluorobenzenes the extent of aromatic ring hydroxylation on a non-substituted carbon centre correlated (r=0.96) with the calculated frontier orbital density on the respective carbon atom [7]. This observation is consistent with a reaction mechanism that proceeds by an initial electrophilic attack of the high-valent iron-oxo intermediate of cytochrome P450 on the reactive π-electrons of the aromatic ring. This means that formation of phenolic metabolites resulting from epoxide intermediates is not a main biotransformation route, as upon formation of epoxides the site of attack of the iron-oxo species does not need to be the site of hydroxylation [8-10]. Furthermore, for the tested series fluorobenzenes, containing the relatively small fluorine, it could be demonstrated that a change in the cytochrome P450 enzyme pattern did not significantly influence the regioselectivity of aromatic hydroxylation [7]. However, the cytochrome P450-catalysed regioselectivity of aromatic hydroxylation of benzene derivatives with larger substituents than a hydrogen or fluorine, for example a chlorine, bromine or iodine, might be influenced by factors originating from steric hindrance. This could be either i) steric hindrance in the active sites of the cytochromes P450 imposing a specific orientation of the substrate with respect to the activated heme cofactor and/or ii) steric hindrance of the substituent hampering the attack of the cytochrome P450 iron-oxo species on the carbon centres *ortho* with respect to the substituted carbon atom.

The aim of the present study was to investigate to what extent substituents, which are larger than a hydrogen or fluorine, influence possibilities for the cytochrome P450-catalysed aromatic hydroxylation of carbon atoms *ortho* with respect to the substituent. This was performed by studying the *in vivo* regioselectivity of aromatic hydroxylation of a series of fluorobenzenes, containing a chlorine, bromine, iodine or cyano substituent at the C4 position. Comparison of the observed regioselectivity of aromatic ring hydroxylation of the C4-substituted fluorobenzenes to the regioselectivity predicted on the basis of the frontier orbital calculations, will provide information on the actual influence of the various C4 substituents on possibilities for hydroxylation at the *ortho* aromatic carbon centres. Furthermore, possible deviations between the predicted and observed regioselectivities can result in steric correction factors for the extent of hydroxylation at a carbon atom adjacent to a substituent in a benzene derivative. Experiments

described in the present paper indicate to what extent such steric correction factors may actually affect and improve predictions for the cytochrome P450-catalysed regioselectivity of aromatic hydroxylation of benzene derivatives.

Materials and Methods

Chemicals

Fluorobenzene was purchased from Aldrich Chemie (Steinheim, Germany). 4-Cyanofluorobenzene was obtained from Fluka (Buchs, Switzerland). 4-Bromofluorobenzene, 4-chlorofluorobenzene, 2-bromo-4-fluorophenol, 2-bromo-5-fluorophenol, 4-bromo-2-fluorophenol, 2-chloro-4-fluorophenol, 2-chloro-5-fluorophenol, 4-chloro-2-fluorophenol, 4-chloro-1,2-difluorobenzene, 4-bromo-1,2-difluorobenzene, 4-cyano-1,2-difluorobenzene, 4-iodo-1,2-difluorobenzene and 2-chloro-5-bromofluorobenzene were all purchased from Fluorochem (Derbyshire, United Kingdom). 4-Iodofluorobenzene, 2-fluorophenol, 3-fluorophenol and 4-fluorophenol were obtained from Acros Chimica (Beerse, Belgium).

In vivo exposure of rats

Male Wistar rats (± 350 g) either untreated or pretreated with cytochrome P450 inducers, were exposed to 500 μmol/kg body weight of fluorobenzene, 4-chlorofluorobenzene, 4-bromofluorobenzene, 4-iodofluorobenzene, 4-cyanofluorobenzene, 4-chloro-1,2-difluorobenzene, 4-bromo-1,2-difluorobenzene, 4-iodo-1,2-difluorobenzene, 4-cyano-1,2-difluorobenzene or 2-chloro-5-bromo-fluorobenzene, administered in olive oil by oral injection. After dosing, 0-24 h urine samples were collected.

Pretreatment of rats with different cytochrome P450 inducers was carried out essentially as described before [11]: acetone (Merck, Darmstadt, Germany) (1.5 ml, using a stock solution of 30% in H_2O, p.o. 1 day), β-naphtoflavone (Sigma, St. Louis, MO, USA) (30 mg/kg body weight, using a stock solution of 10 mg/ml in olive oil, i.p. daily for 3 days) or phenobarbital (Brocacef, Maarssen, The Netherlands) (0.1% in drinking water for 7 days). The benzene derivatives were administered 24 h after administration of the final inducer injection.

Preparation of microsomes

Microsomes were prepared from the perfused livers of male Wistar rats (300-400 g) as described before [12].
Cytochrome P450 content of the microsomes was measured as described by Omura and Sato [13].

Microsomal incubations

Cytochrome P450 dependent conversion was studied *in vitro* in microsomal incubations containing (final concentrations) 0.1 M potassium phosphate pH 7.6, 2 mM microsomal cytochrome P450, 1 mM of the benzene added as 1% (v/v) of a 0.1 M cold stock solution in acetone, 1 mM ascorbic acid to prevent autoxidation of the hydroxylated reaction products and 1.0 mM NADPH. The reaction was started by the addition of the benzene and NADPH. The total reaction volume was 20 ml and the reaction was carried out at 37 °C for 10 min in a closed reaction vessel to prevent evaporation of the substrate. The reaction was terminated by the addition of 1 ml 12 N HCl and 5 ml ethyl acetate. Upon mixing and centrifugation (10 min 3000 rpm) the ethyl acetate layer was collected and 1.6 ml of the ethyl acetate extract was analysed by ^{19}F NMR as described hereafter.

Analysis of urine samples

Urine samples were diluted once in 0.2 M potassium phosphate buffer pH 7.6 for analysis by ^{19}F NMR. Phenolic metabolites, excreted in the urine in a sulphated or glucuronidated form, were converted to their non-conjugated forms by treatment of the urine with arylsulphatase/β-glucuronidase (from *Helix pomatia* (Boehringer, Mannheim, Germany) carried out essentially as described before [11].

Purification and identification of aromatic ring hydroxylated metabolites

The 0-24 h urine of rats exposed to 4-chloro-1,2-difluorobenzene, 4-bromo-1,2-difluorobenzene, 4-iodo-1,2-difluorobenzene, 4-cyano-1,2-difluorobenzene and 2-chloro-5-bromofluorobenzene was freeze-dried and resolved in 2 ml H_2O. 1.5 Ml of this fraction was applied on a Bio-Gel P2 column (Bio-Rad, Richmond, USA) (V=150 ml; d=1.5 cm) and eluted with 10 mM sodium acetate buffer pH 5.2 [14]. Fractions of 1.5 ml were collected and pooled based on ^{19}F NMR analysis. The pooled fractions were freeze-dried and resolved in 1 ml H_2O. The presence of phenolic products in

these fractions was proved by arylsulphatase/β-glucuronidase treatment of the fractions as previously described [11] and on the basis of the observation of characteristic shifts in the ^{19}F NMR ppm values of the phenolic metabolites compared to the ^{19}F NMR chemical shifts of other fluorobenzene substrates [7,15,16]. Unequivocal characterisation of the various conjugated ring hydroxylated metabolites in the pooled fractions was performed by analysing the proton-coupled and proton-decoupled ^{19}F NMR spectra of these samples (see Table 5 and results section for details).

^{19}F and ^{1}H NMR measurements

^{19}F NMR measurements of the urine samples were performed on a Bruker AMX 300 NMR spectrometer at 280 K. Spectra were recorded using 5 μs pulses and proton-decoupling was achieved with the Waltz-16 pulse sequence at -20dB from 50W. Samples contained 100 μl $^{2}H_2O$ for locking the magnetic field and 10 μl 8.4 mM 4-fluorobenzoic acid added as an internal standard. The total sample volume was 1.71 ml. Enzyme treated urine samples were made anaerobic by evacuating and filling with argon four times before analysis. This was done to prevent autoxidation of the phenolic metabolites. About 1500 scans were recorded. Chemical shifts are reported relative to $CFCl_3$. Quantification of the different metabolites was achieved by comparison of the integral of the ^{19}F NMR resonance of the added internal standard 4-fluorobenzoic acid to the integrals of the ^{19}F NMR peaks of the metabolites.

Proton-coupled ^{19}F NMR measurements of the Bio-Gel P2 column fractions were performed on a Bruker AMX 500 NMR spectrometer at 303 K. Spectra were recorded using 3 μs pulses. Samples contained 50 μl $^{2}H_2O$ for locking the magnetic field. The total sample volume was 0.5 ml. About 3000 scans were recorded.

^{19}F NMR HOMO-decoupling of these samples was performed on a Bruker DPX 400 NMR spectrometer at 303 K. Spectra were recorded using 5 μs pulses. About 200 scans were recorded for each spectrum.

Molecular orbital calculations

Semi-empirical molecular orbital calculations were performed on a Silicon Graphics Iris 4D/85 computer with the AM1 (Austin Method 1) Hamiltonian from the AMPAC program (Quantum Chemistry Program Exchange, program no. 506, Indiana University, Bloomington, IN, USA). The AM1 Hamiltonian was used since it

was reported to provide improved results for molecules containing heteroatoms compared to the MINDO/3 and MNDO methods [17]. Calculations were carried out with PRECISE criteria and self-consistent field was achieved for all calculations. Geometries were optimised for all bond lengths, bond angles and torsion angles using the Fletcher-Powell criteria.

Frontier electron densities for electrophilic attack on the π-electrons of the aromatic ring were calculated according to the equation of Fukui et al. [18]. In this equation the contribution of the HOMO (highest occupied molecular orbital) and the HOMO-1 (highest occupied molecular orbital below the HOMO) are both taken into account. The calculated electronic parameters are compared with the results from the *in vivo* biotransformation of the substrates upon their binding to the active sites of the cytochromes P450. Upon binding of the substrates to the active sites of the cytochromes P450, the intrinsic properties of the compounds might be changed due to solvation effects and a different dielectric constant. Because a series of closely related compounds is being compared and because the active sites of the mammalian cytochromes P450 are rather large aspecific hydrophobic pockets, it can be assumed that the relative differences calculated between the related compounds as well as between various sites in one molecule will not be influenced by binding of the substrates to the active sites of the cytochromes P450.

From the calculated HOMO/HOMO-1 density distributions the predicted regioselectivity of aromatic ring hydroxylation of the benzene derivatives was calculated by summation of frontier orbital densities of non-substituted aromatic ring carbon atoms and normalization of the sum of the values to 1.0. The predicted percentage of hydroxylation of an aromatic centre was calculated as the fraction of this normalized total frontier orbital density present on the respective non-substituted aromatic centre.

Results

In vivo regioselectivity of aromatic hydroxylation of the C4-substituted fluorobenzene derivatives

Figure 1 presents the ^{19}F NMR spectra of the arylsulphatase/β-glucuronidase treated 0-24 h urine samples of rats exposed to a series of C4-substituted fluorobenzenes (C4=H, Cl, Br, I and CN in Figures 1 a, b, c, d and e respectively). 1,4-Difluorobenzene was not included since the four non-substituted carbon positions in this substrate are identical. Metabolites were identified on the

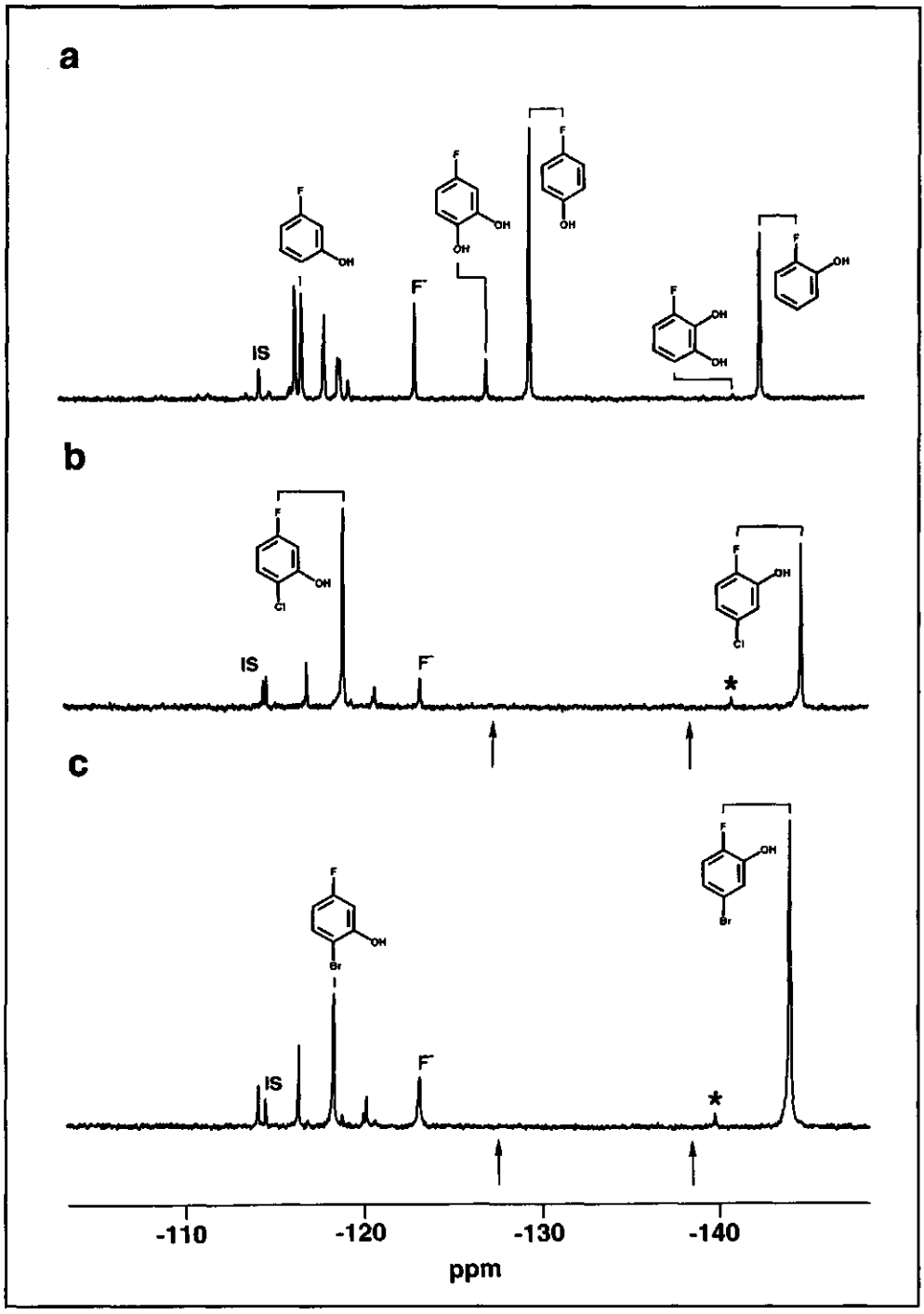
a
IS
F⁻
b
IS
F⁻
*
c
IS
F⁻
*
-110
-120
-130
-140
ppm

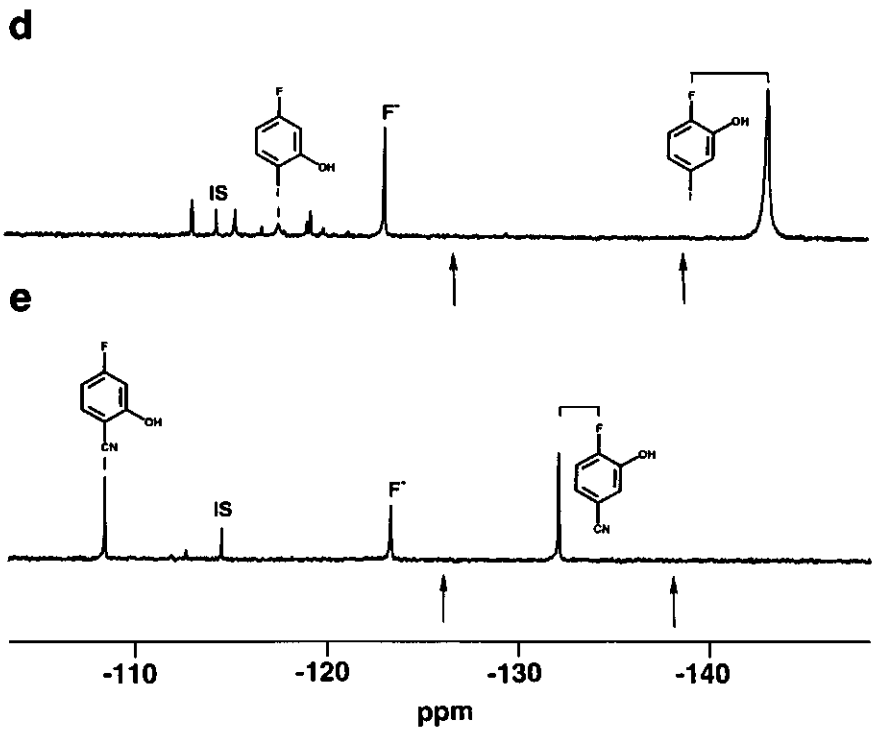

Figure 1 ^{19}F NMR spectra of the arylsulphatase/β-glucuronidase treated 0-24 h urine samples of rats exposed to (a) fluorobenzene, (b) 4-chlorofluorobenzene, (c) 4-bromofluorobenzene, (d) 4 iodofluorobenzene and (e) 4-cyanofluorobenzene. The arrows indicate the resonance positions of NIH shifted phenolic metabolites. The resonance marked "IS" is from the internal standard 4-fluorobenzoic acid. The resonances labelled with an asterisk in Figures b and c possibly belong to dihydroxylated products.

Table 1 *Chemical shifts of ^{19}F NMR resonances of identified aromatic ring hydroxylated products of the tested C4-substituted fluorobenzene derivatives (measured in 0.1 M potassium phosphate pH 7.6).* ^{19}F NMR resonances are presented relative to $CFCl_3$. Predicted ppm values were calculated on the basis of the characteristic ppm shifts observed in previous studies upon introduction of a hydroxyl moiety *ortho* (-23.1 ± 0.6 (n=7)), *meta* (+1.8 ± 1.2 (n=11)) or *para* (-11.0 ± 1.7 (n=6)) with respect to a fluorine substituent (see text for further details).

substrate metabolite	^{19}F NMR ppm value (in 0.1 M potassium phosphate) predicted	reference compound	metabolite peak observed in 0-24 h urine
fluorobenzene			
2-fluorophenol	-141.9 ± 0.6	-141.9	-141.9
3-fluorophenol	-116.5 ± 1.2	-116.5	-116.5
4-fluorophenol	-129.1 ± 1.7	-129.1	-129.1
3-fluoro-2-hydroxyphenol	-139.9 ± 1.2	-140.4[a]	-140.4
4-fluoro-2-hydroxyphenol	-127.4 ± 1.7	-126.7[a]	-126.7
2-fluoro-4-hydroxyphenol	-139.9 ± 1.2	-138.7[a]	no[b]
4-chlorofluorobenzene			
2-chloro-5-fluorophenol	-118.9 ± 1.2	-118.6	-118.6
5-chloro-2-fluorophenol	-143.8 ± 0.6	-	-144.0
4-chloro-2-fluorophenol	-138.8 ± 0.6	-138.5	no[b]
2-chloro-4-fluorophenol	-126.7 ± 1.7	-127.3	no[b]
6-chloro-3-fluoro-2-hydroxyphenol	-141.8 ± 1.2	-	-140.0[c]
5-chloro-2-fluoro-4-hydroxyphenol	-141.8 ± 1.2	-	-140.0[c]
4-bromofluorobenzene			
2-bromo-5-fluorophenol	-118.4 ± 1.2	-117.8	-117.8
5-bromo-2-fluorophenol	-143.3 ± 0.6	-	-143.3
4-bromo-2-fluorophenol	-138.5 ± 0.6	-138.3	no[b]
2-bromo-4-fluorophenol	-126.4 ± 1.7	-127.4	no[b]
6-bromo-3-fluoro-2-hydroxyphenol	-141.3 ± 1.2	-	-139.1[c]
5-bromo-2-fluoro-4-hydroxyphenol	-141.3 ± 1.2	-	-139.1[c]

Table 1 -continued-

substrate metabolite	^{19}F NMR ppm value (in 0.1 M potassium phosphate) predicted	reference compound	metabolite peak observed in 0-24 h urine
4-iodofluorobenzene			
2-iodo-5-fluorophenol	-117.5 ± 1.2	-	-117.4
5-iodo-2-fluorophenol	-142.4 ± 0.6	-	-142.6
4-iodo-2-fluorophenol	-138.6 ± 0.6	-	no[b]
2-iodo-4-fluorophenol	-126.5 ± 1.7	-	no[b]
6-iodo-3-fluoro-2-hydroxyphenol	-140.6 ± 1.2	-	no[b]
5-iodo-2-fluoro-4-hydroxyphenol	-140.6 ± 1.2	-	no[b]
4-cyanofluorobenzene			
2-cyano-5-fluorophenol	-105.2 ± 1.2	-	-108.1
5-cyano-2-fluorophenol	-130.1 ± 0.6	-	-131.7
4-cyano-2-fluorophenol	-138.2 ± 0.6	-	no[b]
2-cyano-4-fluorophenol	-126.1 ± 1.7	-	no[b]
6-cyano-3-fluoro-2-hydroxyphenol	-130.5 ± 1.2	-	no[b]
5-cyano-2-fluoro-4-hydroxyphenol	-130.5 ± 1.2	-	no[b]

[a] Taken from Rietjens et al. [7].

[b] Not observed.

[c] One of the two dihydroxylated products is possibly observed.

basis of added reference compounds, and/or on the basis of the consideration that the incorporation of a hydroxyl moiety in the benzene derivative results in a characteristic change in the ^{19}F NMR chemical shift of the fluorine at C1. Based on previous results with fluorinated anilines and benzenes converted to their phenolic metabolites [7,15,16] it can be calculated that the chemical shift of an aromatic fluorine substituent changes upon incorporation of a hydroxyl group at a position *ortho*, *meta* or *para* with respect to the fluorine by a value of -23.1 ± 0.6 (n=7), + 1.8 ±

1.2 (n=11) and -11.0 ± 1.7 ppm (n=6) respectively. On the basis of these results the ^{19}F NMR chemical shift values of the various phenolic metabolites could be predicted (Table 1). Table 1 also shows the values actually observed for phenolic derivatives that were commercially available. Comparison of the observed and predicted values indicates that the approach provides reliable results.

The arrows in Figure 1 indicate the resonance position of phenolic metabolites that would have resulted from hydroxylation accompanied by an NIH shift of either the fluorine or the C4 substituent [8,9]. Clearly, phenolic metabolites resulting from such an NIH shift were not observed. The unidentified peaks in Figure 1 do not belong to phenolic metabolites but might be ascribed to mercapturic acid metabolites or other sulphur containing metabolites because i) their resonance positions did not change upon enzyme treatment of the urine samples and ii) these type of metabolites were also observed for the *in vivo* metabolism of other halogenated benzenes [2,19-21]. Because the aim of the present study was the investigation of the influence of various substituents on the regioselectivity of aromatic ring hydroxylation at non-substituted positions, the resonances of non-phenolic metabolites were not identified at this stage. Since such mercapturic acid metabolites might arise from glutathione conjugation of epoxide intermediates their identification as such might even be an argument in favour of performing the predictive regioselectivity experiments *in vivo* and not in *in vitro* cytochrome P450 systems. This because *in vitro*, perhaps, phenolic metabolic profiles might to some extent become influenced by (partial) involvement of epoxide intermediate pathways. The latter would result in the situation where the site of the high-valent iron-oxo attack on the aromatic ring would be no longer necessarily the site of hydroxylation, eliminating possibilities for correlations between calculated reactivity parameters of the aromatic substrate and the regioselectivity of aromatic hydroxylation.

Based on the ^{19}F NMR results presented in Figure 1 the ratio of C2/6 : C3/5 : C4 or C2/6 : C3/5 hydroxylation of the C4-substituted fluorobenzenes could be calculated. The results (Table 2) show that the regioselectivity of aromatic ring hydroxylation varies with the type of the C4 substituent. One could argue that the observed urinary phenolic metabolic profiles might not reflect the actual outcome of the cytochrome P450-catalysed enzymatic conversion in the liver due to additional metabolic reactions of the phenols formed and/or their excretion through bile instead of urine. However, the urinary metabolic patterns of rats orally exposed to various substituted fluorophenols show that the fluorophenols were always efficiently excreted in the urine as their glucuronidated or sulphated conjugates at a

0-24 h recovery of nearly 100% [7,22]. Furthermore, results from *in vivo* experiments in part published in Rietjens et al. [16] with the cytochrome P450 inducer isosafrole showed that this compound effectively inhibits cytochrome P450-dependent metabolism, but that isosafrole is not able to inhibit other enzymes like the Phase II ones. When halogenated benzenes were orally dosed to rats pretreated with isosafrole, no urinary phenolic metabolites could be detected, showing that, indeed, cytochrome P450 Phase I catalysis is necessary for excretion of the halogenated benzenes. Clearly, this excludes biliary excretion and alternative biotransformation pathways of phenol derivatives formed. Further support for the assumption that the *in vivo* aromatic hydroxylation profile of the benzene derivatives is a proper reflection of the cytochrome P450-catalysed dependent formation of these metabolites comes from comparison between *in vitro* and *in vivo* regioselectivities which have been demonstrated to be similar for many benzene derivatives in previous studies reported in the literature [7,15,23]. In addition, this was experimentally checked and confirmed for two of the model benzenes of the present study. The C2/6 : C3/5 regioselectivity of aromatic hydroxylation of 4-chloro- and 4-bromofluorobenzene in incubations with microsomes from control rat livers amounted to 52 : 48 and 64 : 36 respectively which resembles the values observed *in vivo* with the generally observed margin of 10% [7,15,23].

From the ^{19}F NMR spectra presented in Figure 1 and the volumes of the respective 0-24 h urine samples the recovery of the various model C4-substituted fluorobenzenes was determined (Table 2). Table 2 also presents the percentage of the urine metabolites that could be ascribed to mono-phenolic metabolites. These results show that the total 0-24 h recovery is about 45-83% and that aromatic ring hydroxylation is a main pathway for urine excretion since 61-77% of the total amount of excreted metabolites are phenolic products.

Influence of the cytochrome P450 enzyme pattern on the regioselectivity of aromatic hydroxylation of the C4-substituted fluorobenzenes

Rats pretreated with specific cytochrome P450 enzyme inducers were also dosed with the C4-substituted fluorobenzenes. This was done to investigate the extent to which a variation in the cytochrome P450 enzyme pattern would influence the regioselectivity of aromatic hydroxylation of the various C4-substituted fluorobenzenes. The observation that ethoxyresorufin O-dealkylating, pentoxyresorufin O-dealkylating and aniline *para*-hydroxylation activity were increased 30, 60 [7], and 2 fold in the liver microsomes from rats receiving

pretreatments with β-naphtoflavone, phenobarbital and acetone respectively (data not shown) confirms a proper cytochrome P450 induction in the animals used. The regioselectivity of aromatic hydroxylation was determined from the ^{19}F NMR spectra of the arylsulphatase/β-glucuronidase treated urine samples. The results obtained are presented in Table 3 and clearly demonstrate that a variation in the cytochrome P450 enzyme pattern hardly influences the regioselectivity of the aromatic hydroxylation. The observed regioselectivities for a specific C4-substituted benzene, dosed to differently pretreated rats, vary by at most a few percent.

Table 2 The 0-24 h urine recovery, the percentage phenolic metabolites in the urinary metabolic pattern and the regioselectivity of the *in vivo* aromatic ring hydroxylation of a series C4-substituted fluorobenzene derivatives. Ratios were calculated from the enzyme treated 0-24 h urine samples of exposed rats (n=2). The fluorine atom is positioned at carbon atom C1.

benzene	0-24 h recovery (% of doses)	phenolic metabolites (% of total metabolites)	ring carbon atom	regioselectivity of aromatic ring hydroxylation
fluorobenzene	83	61	C2/6:C3/5:C4	33 : 20 : 47
4-chlorofluoro-	65	77	C2/6 : C3/5	46 : 54
4-bromofluoro-	67	75	C2/6 : C3/5	74 : 26
4-iodofluoro-	64	75	C2/6 : C3/5	96 : 4
4-cyanofluoro-	45	69	C2/6 : C3/5	64 : 36

Table 3 The regioselectivity of the *in vivo* aromatic ring hydroxylation of a series C4-substituted fluorobenzene derivatives in rats pretreated with cytochrome P450 inducers. Ratios were calculated from the enzyme treated 0-24 h urine samples of exposed rats. The fluorine atom is positioned at carbon atom C1.

benzene	inducer	ring carbon atom	regioselectivity of aromatic ring hydroxylation
fluorobenzene	none	C2/6 : C3/5 : C4	33 : 20 : 47
	β-naphtoflavone		34 : 15 : 51
	phenobarbital		34 : 19 : 47
	acetone		32 : 21 : 47
4-chlorofluoro-	none	C2/6 : C3/5	46 : 54
	β-naphtoflavone		47 : 53
	phenobarbital		47 : 53
	acetone		49 : 51
4-bromofluoro-	none	C2/6 : C3/5	74 : 26
	β-naphtoflavone		73 : 27
	phenobarbital		74 : 26
	acetone		76 : 24
4-iodofluoro-	none	C2/6 : C3/5	96 : 4
	β-naphtoflavone		88 : 12
	phenobarbital		95 : 5
	acetone		97 : 3
4-cyanofluoro-	none	C2/6 : C3/5	64 : 36
	β-naphtoflavone		60 : 40
	phenobarbital		59 : 41
	acetone		61 : 39

Calculated reactivity of the carbon centres of the C4-substituted fluorobenzenes for an electrophilic attack by the cytochrome P450 iron-oxo species

In a previous study it was demonstrated that the cytochrome P450-catalysed regioselectivity of aromatic hydroxylation of a series of (poly)fluorobenzenes correlated (r=0.96) with the calculated reactivity of the various non-substituted carbon centres in the aromatic ring for an electrophilic attack by the cytochrome P450 high-valent iron-oxo intermediate [7].

This reactivity can be calculated on the basis of the frontier electron density distribution, which is the distribution of the reactive π-electrons in the aromatic ring. Table 4 presents the regioselectivity of aromatic hydroxylation for the C4-substituted fluorobenzenes expected on the basis of the calculated reactivity of the aromatic centres. Comparison of the calculated regioselectivities to the regioselectivities observed demonstrates that for the fluorobenzenes with a chlorine or cyano C4 substituent, the expected values match the values actually observed within a few percent (Tables 2 and 4). However, for 4-bromofluorobenzene hydroxylation at the positions *ortho* to the bromine is only 40% of the calculated intrinsic reactivity of the sites for an electrophilic attack. For 4-iodofluorobenzene hydroxylation at C3/5 amounts to an even lower percentage (6%) of what would be expected on the basis of the calculated chemical reactivity (Tables 2 and 4). From these results steric correction factors of 1.0, 1.0, 0.4, 0.06 and 1.0 for hydroxylation at positions *ortho* with respect to a fluorine, chlorine, bromine, iodine and cyano respectively were derived.

The in vivo regioselectivity of aromatic hydroxylation of other substituted fluorobenzene derivatives

Additional experiments were performed in order to investigate whether the steric correction factors thus obtained would also improve the prediction of the regioselectivity of the aromatic hydroxylation of other substituted fluorobenzenes. Figure 2 presents the ^{19}F NMR spectra of the arylsulphatase/β-glucuronidase treated 0-24 h urine samples of five substituted fluorobenzenes. The ^{19}F NMR ppm values of the various aromatic ring hydroxylated products resulting from hydroxylation of non-substituted carbon centres were identified on the basis of the consideration that the incorporation of the hydroxyl moiety results in a characteristic change in the chemical shift of the fluorines [7,15,16] and on the proton-coupled and proton-decoupled ^{19}F NMR spectra of the pooled Bio-Gel P2 column fractions of the 0-24 h urine (Table 5). Phenolic metabolites resulting from hydroxylation

accompanied by an NIH shift were again not observed. The unidentified peaks in Figure 2 might be ascribed to mercapturic acid metabolites or other sulphur containing metabolites as outlined above for the C4-substituted fluorobenzenes. From the ^{19}F NMR spectra of the arylsulphatase/β-glucuronidase treated urine samples in Figure 2 the regioselectivity of aromatic ring hydroxylation could be calculated and the results are presented in Table 6. From the ^{19}F NMR spectra in Figure 2 and the volumes of the 0-24 h urine samples the recovery of the tested substituted fluorobenzenes and the percentage of mono-phenolic metabolites was calculated. About 63-72% of the benzene derivative is excreted in the urine within 24 h after dosage, except for 4-cyano-1,2-difluorobenzene and 2-chloro-5-bromofluorobenzene for which only 21% and 28% was excreted respectively. Aromatic ring hydroxylation was a main biotransformation route as 46-78% of the total amount of excreted metabolites were phenolic products.

Table 4 The calculated HOMO/HOMO-1 density distribution in the C4-substituted fluorobenzenes. From the HOMO/HOMO-1 density distribution at hydrogen substituted carbon centres the calculated regioselectivity of aromatic ring hydroxylation was derived. The fluorine atom is positioned at carbon atom C1.

benzene	HOMO/HOMO-1 density on carbon atom						calculated regioselectivity
	C1	C2	C3	C4	C5	C6	C2/6:C3/5:C4 or C2/6:C3/5
fluorobenzene	0.45	0.27	0.19	0.48	0.19	0.27	39 : 27 : 34
4-chlorofluoro-	0.43	0.18	0.17	0.47	0.17	0.18	51 : 49
4-bromofluoro-	0.39	0.18	0.17	0.47	0.17	0.18	53 : 47
4-iodofluoro-	0.37	0.19	0.15	0.44	0.15	0.19	56 : 44
4-cyanofluoro-	0.42	0.23	0.16	0.50	0.16	0.23	59 : 41

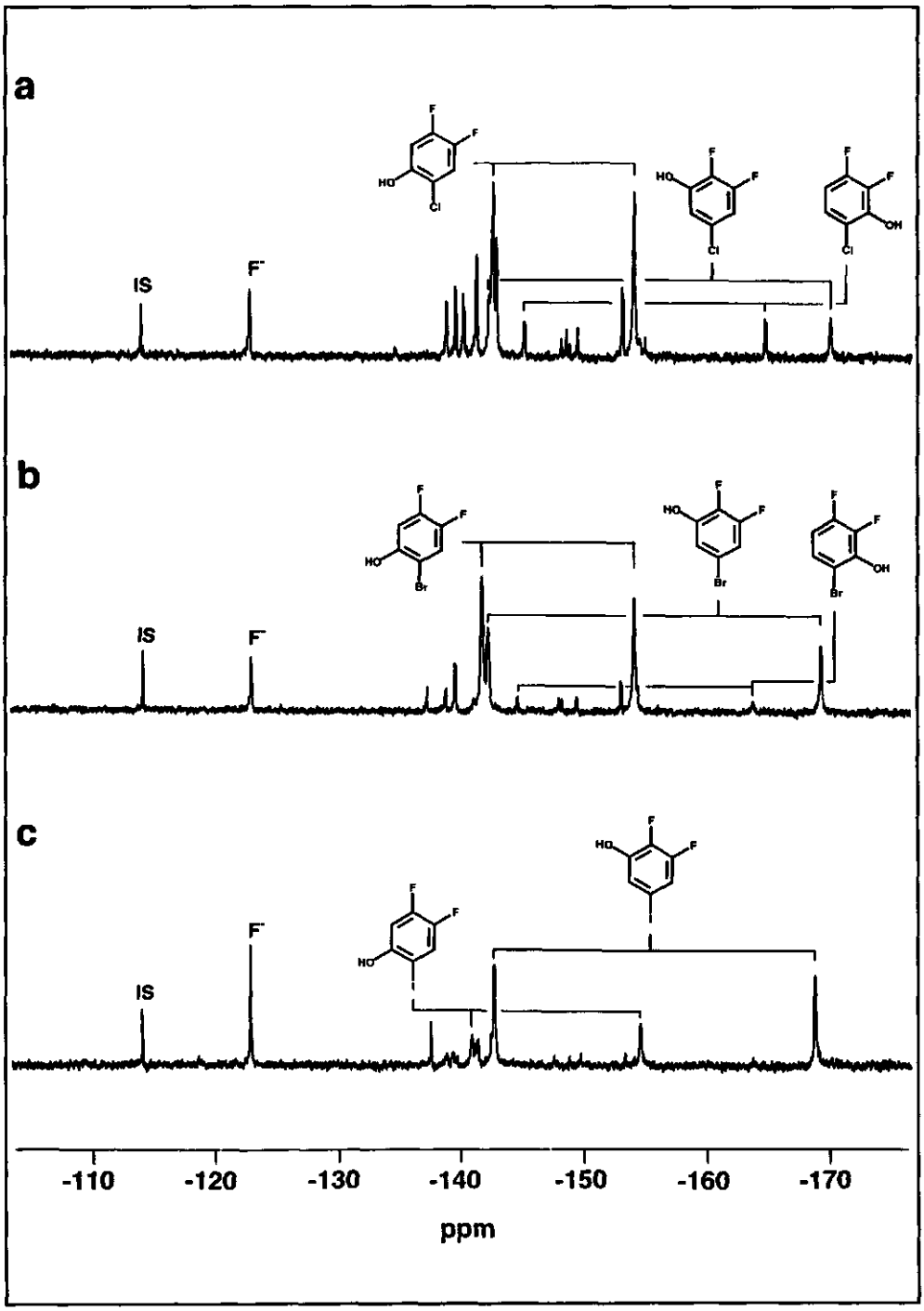
a
IS
F⁻
b
IS
F⁻
c
IS
F⁻
-110
-120
-130
-140
-150
-160
-170
ppm

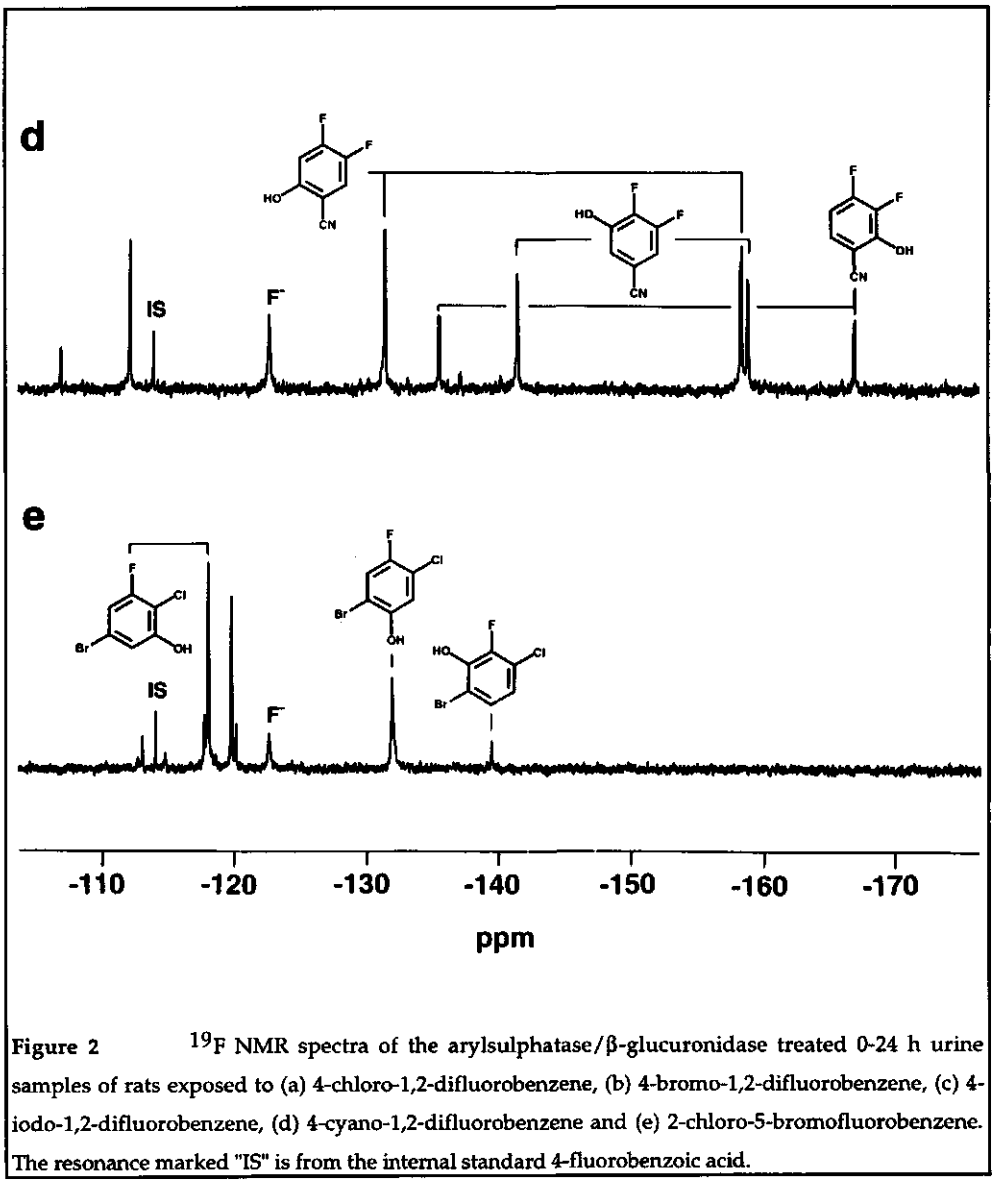

Figure 2 ^{19}F NMR spectra of the arylsulphatase/β-glucuronidase treated 0-24 h urine samples of rats exposed to (a) 4-chloro-1,2-difluorobenzene, (b) 4-bromo-1,2-difluorobenzene, (c) 4-iodo-1,2-difluorobenzene, (d) 4-cyano-1,2-difluorobenzene and (e) 2-chloro-5-bromofluorobenzene. The resonance marked "IS" is from the internal standard 4-fluorobenzoic acid.

Table 5 ^{19}F NMR resonances and J_{FF} and J_{HF} coupling constants of identified aromatic ring hydroxylated products of five substituted fluorobenzene derivatives (measured in 0.1 M potassium phosphate pH 7.6). ^{19}F NMR resonances are presented relative to $CFCl_3$.

substrate metabolite	^{19}F NMR ppm value	(J values) [Hz]
4-chloro-1,2-difluorobenzene		
6-chloro-2,3-difluorophenol	-164.1 (F2)	($^3J_{FF}$= 20.4, $^4J_{HF}$= 7.5)
	-144.9 (F3)	($^3J_{FF}$= 20.4, $^3J_{HF}$= 9.5, $^4J_{HF}$= 5.0)
6-chloro-3,4-difluorophenol	-142.4 (F3)	($^3J_{FF}$= 21.7, $^3J_{HF}$= 11.3, $^4J_{HF}$= 8.0)
	-153.7 (F4)	($^3J_{FF}$= 21.7, $^3J_{HF}$= 10.4, $^4J_{HF}$= 7.6)
5-chloro-2,3-difluorophenol	-169.3 (F2)	($^3J_{FF}$= 20.6, $^4J_{HF}$= 6.2, $^4J_{HF}$= 6.2)
	-142.1 (F3)	($^3J_{FF}$= 20.6, $^3J_{HF}$= 10.7)
4-bromo-1,2-difluorobenzene		
6-bromo-2,3-difluorophenol	-163.5 (F2)	($^3J_{FF}$= 20.0, $^4J_{HF}$= 5.9)
	-144.4 (F3)	($^3J_{FF}$= 20.0, $^3J_{HF}$= 9.4, $^4J_{HF}$= 4.7)
6-bromo-3,4-difluorophenol	-141.6 (F3)	($^3J_{FF}$= 21.6, $^3J_{HF}$= 11.0, $^4J_{HF}$= 8.3)
	-153.9 (F4)	($^3J_{FF}$= 21.6, $^3J_{HF}$= 9.8, $^4J_{HF}$= 7.4)
5-bromo-2,3-difluorophenol	-168.9 (F2)	($^3J_{FF}$= 20.0, $^4J_{HF}$= 5.9, $^4J_{HF}$= 5.9)
	-142.1 (F3)	($^3J_{FF}$= 20.0, $^3J_{HF}$= 9.4)
4-iodo-1,2-difluorobenzene		
6-iodo-2,3-difluorophenol	no[a]	
6-iodo-3,4-difluorophenol	-140.7 (F3)	($^3J_{FF}$= 21.1, $^3J_{HF}$= 11.2, $^4J_{HF}$= 8.9)
	-154.2 (F4)	($^3J_{FF}$= 21.1, $^3J_{HF}$= 9.7, $^4J_{HF}$= 7.3)
5-iodo-2,3-difluorophenol	-168.2 (F2)	($^3J_{FF}$= 19.6, $^4J_{HF}$= 6.5)
	-142.4 (F3)	($^3J_{FF}$= 19.6, $^3J_{HF}$= 8.7)
4-cyano-1,2-difluorobenzene		
6-cyano-2,3-difluorophenol	-166.8 (F2)	($^3J_{FF}$= 21.0, $^4J_{HF}$= 7.2)
	-135.6 (F3)	($^3J_{FF}$= 21.0, $^3J_{HF}$= 9.6, $^4J_{HF}$= 5.0)
6-cyano-3,4-difluorophenol	-131.5 (F3)	($^3J_{FF}$= 21.8, $^3J_{HF}$= 10.7, $^4J_{HF}$= 8.3)
	-158.3 (F4)	($^3J_{FF}$= 21.8, $^3J_{HF}$= 9.6, $^4J_{HF}$= 6.9)
5-cyano-2,3-difluorophenol	-158.8 (F2)	($^3J_{FF}$= 20.7, $^4J_{HF}$= 6.5)
	-141.5 (F3)	($^3J_{FF}$= 20.7, $^3J_{HF}$= 9.8)
2-chloro-5-bromofluorobenzene		
2-bromo-5-chloro-6-fluorophenol	-139.7 (F6)	($^4J_{HF}$= 7.0)
2-bromo-4-fluoro-5-chlorophenol	-132.1 (F4)	($^3J_{HF}$= 8.6, $^4J_{HF}$= 7.0)
2-chloro-3-fluoro-5-bromophenol	-118.2 (F3)	($^3J_{HF}$= 8.6)

[a] Not observed.

The calculated reactivity for aromatic ring hydroxylation of five substituted fluorobenzenes

Like for the C4-substituted fluorobenzenes, the HOMO/HOMO-1 density on the non-substituted aromatic ring carbon atoms of the five fluorobenzenes was calculated and from these results the expected regioselectivity of aromatic ring hydroxylation was derived. This calculated regioselectivity was further adjusted by taking into account the steric correction factors derived from the experiments with the C4-substituted fluorobenzenes. Thus, the expected extent of hydroxylation of carbon atoms *ortho* with respect to a hydrogen, fluorine, chlorine or cyano were not corrected (correction factor=1.0), whereas expected values obtained for carbon centres *ortho* with respect to a bromine or iodine were multiplied by a factor of 0.4 and 0.06 respectively, followed by normalization of the values then obtained. Thus for non-corrected positions the calculated relative reactivity increases due to their normalization. The corrected values for the regioselectivity of aromatic ring hydroxylation are also presented in Table 6.

Comparison of the non-corrected calculated frontier orbital density distribution with the observed regioselectivity of aromatic ring hydroxylation of the five substituted fluorobenzenes shows no correlation (r=0.49) (Figure 3A). However,

Table 6 Calculated and observed regioselectivity of *in vivo* aromatic hydroxylation of five substituted fluorobenzenes. The corrected values for the regioselectivity of aromatic hydroxylation were calculated using the steric correction factors derived from the results obtained with the C4-substituted fluorobenzenes (see Results section).

benzene	regioselectivity of aromatic ring hydroxylation			
	at carbon centres	calculated from HOMO/HOMO-1 density	corrected	observed *in vivo*
4-chloro-1,2-difluoro-	C3 : C5 : C6	20 : 60 : 20	20 : 60 : 20	12 : 71 : 17
4-bromo-1,2-difluoro-	C3 : C5 : C6	21 : 58 : 21	16 : 44 : 40	4 : 63 : 33
4-iodo-1,2-difluoro-	C3 : C5 : C6	22 : 57 : 21	5 : 13 : 82	0 : 24 : 76
4-cyano-1,2-difluoro-	C3 : C5 : C6	21 : 57 : 22	21 : 57 : 22	18 : 50 : 32
2-chloro-5-bromofluoro-	C3 : C4 : C6	20 : 55 : 25	39 : 42 : 19	53 : 42 : 5

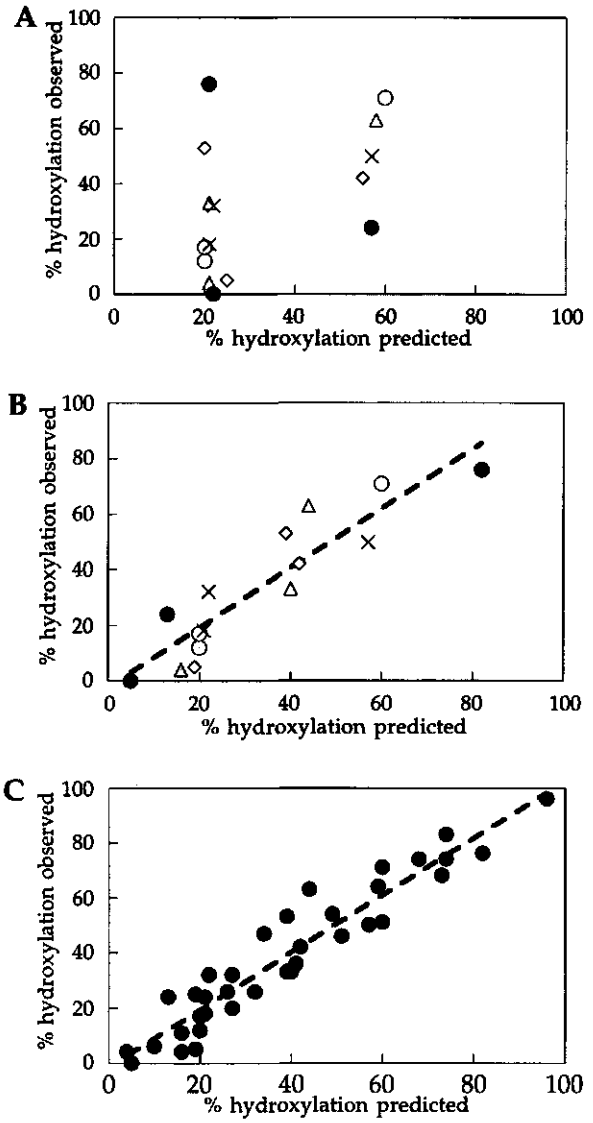

Figure 3 Plots of regioselectivity for aromatic hydroxylation observed in *in vivo* experiments and (A) predicted for the substituted fluorobenzenes of the present study without further correction (B) predicted for the substituted fluorobenzenes of the present study taking into account the steric correction factors of the present study and (C) predicted for all fluorobenzenes tested in this study and in a previous study [7] taking into account the steric correction factors of the present study. The correlation coefficients are A) 0.49, B) 0.91 and C) 0.95 respectively. In Figures 3A and B: O 4-chloro-1,2-difluorobenzene; Δ 4-bromo-1,2-difluorobenzene; • 4-iodo-1,2-difluorobenzene; × 4-cyano-1,2-difluorobenzene; ◊ 2-chloro-5-bromofluorobenzene.

taking into account the steric correction factors, the expected and observed regioselectivity of aromatic hydroxylation correlate well (r=0.91) (Figure 3B). Further, without taking into account the steric correction factors for prediction of the regioselectivity of aromatic ring hydroxylation of the bromine and iodine substituted fluorobenzenes, the absolute mean deviation between the predicted and observed regioselectivity of the five substituted fluorobenzenes was 16.8 ± 14.2%. However, upon correction of the predicted values for the regioselectivity of aromatic ring hydroxylation, the absolute mean deviation decreased to 8.7 ± 5.0%.

Discussion

In the present study the *in vivo* cytochrome P450-catalysed regioselectivity of aromatic ring hydroxylation of a series substituted fluorobenzenes with other than only fluorine substituents (i.e. Cl, Br, I and CN) was investigated. Special attention was focused on the possible steric hindrance of substituents on the possibilities for aromatic ring hydroxylation of the adjacent aromatic carbon atoms. First, the *in vivo* regioselectivity of aromatic ring hydroxylation of a series C4-substituted fluorobenzenes was investigated and compared with the predicted regioselectivity based on the frontier orbital density distribution. For the fluorobenzene derivatives substituted with a chlorine or cyano moiety, the observed *in vivo* regioselectivity of aromatic ring hydroxylation correlated well with the calculated reactivity of the carbon sites. However, for the bromine and iodine substituted fluorobenzenes the expected and observed regioselectivity of aromatic ring hydroxylation deviated significantly. For 4-bromofluorobenzene hydroxylation at C3/5 was 40% of the value expected on the basis of the calculated reactivity while for 4-iodofluorobenzene this was only 6%. These results suggest that bromine and iodine substituents hamper the attack of the iron-oxo species on the adjacent carbon atoms due to factors originating from steric hindrance. This could be either i) steric hindrance in the active sites of cytochromes P450 imposing a stereoselective orientation of the substrate with respect to the activated heme cofactor and/or ii) steric hindrance of the substituent hampering the attack of the iron-oxo species on the adjacent ring carbon atoms. Results of the *in vivo* regioselectivity of aromatic ring hydroxylation of the tested substrates in rats pretreated with different cytochrome P450 inducers showed that the regioselectivity of aromatic ring hydroxylation was not significantly influenced by the cytochrome P450 inducers. Altogether, the data of the present study indicate that the observed deviations between the predicted and observed

regioselectivity for 4-bromo- and 4-iodofluorobenzene should not be ascribed to a stereoselective positioning of the substrate in the cytochrome P450 active site, but might rather be ascribed to steric hindrance by the substituents hampering the attack of the cytochrome P450 iron-oxo species on the adjacent carbon atoms. The larger deviation between the predicted and observed regioselectivity of aromatic hydroxylation for the iodine than the bromine substituted fluorobenzene is in accordance with the fact that the Van der Waals radius of a iodine (2.15 Å) is larger than a bromine (1.95 Å), and thus a iodine substituent might be expected to cause greater steric hindrance than a bromine for attack of the cytochrome P450 iron-oxo species on the adjacent aromatic carbon atoms. The results obtained for 4-chlorofluorobenzene show that a chlorine, which is smaller (Van der Waals radius is 1.8 Å) than a bromine and iodine substituent, did not cause steric hindrance for attack of the iron-oxo species on the adjacent ring carbon atoms. The results obtained for 4-cyanofluorobenzene are interesting because the cyano group, consisting of a carbon and nitrogen atom with a Van der Waals radius of 1.85 and 1.5 Å respectively, might overall be larger than a bromine atom. However, in contrast to the observed significant steric hindrance by the bromine atom for aromatic ring hydroxylation of the adjacent carbon atoms, this was not observed for the cyano group. A possible explanation for these results is that the shape of the cyano group is such that only the steric hindrance by the carbon atom has to be taken into account. As the Van der Waals radius of a carbon atom is similar to that of a chlorine and smaller than a bromine and iodine, significant steric hindrance by the carbon substituent for attack of the cytochrome P450 iron-oxo species on the adjacent aromatic ring carbon atoms is not expected.

Altogether, comparison between the *in vivo* regioselectivity of aromatic hydroxylation of a series C4-substituted fluorobenzenes and their calculated reactivity for aromatic hydroxylation resulted in the hypothesis that a bromine or iodine, but not a fluorine, chlorine or cyano, cause steric hindrance for attack of the cytochrome P450 iron-oxo species on the adjacent aromatic carbon atom. Based on these results steric correction factors can be derived for prediction of the extent of aromatic carbon hydroxylation adjacent to a substituent, i.e. 1.0 for a fluorine, chlorine and cyano and 0.4 and 0.06 for a bromine and iodine substituent respectively. These results were further checked by investigating if and to what extent application of the steric correction factors would improve the prediction of the regioselectivity of aromatic ring hydroxylation of five other substituted fluorobenzenes. The observed regioselectivity of aromatic ring hydroxylation for these five substituted fluorobenzenes did not correlate with the calculated reactivity

(r=0.49). However, taking into account the correction factors as obtained for the C4-substituted fluorobenzenes, a correlation between the observed and predicted regioselectivity of aromatic hydroxylation (r=0.91) was observed. It is of importance to stress that the approach of the present study excludes epoxides as obligatory intermediates in the formation of phenolic metabolites. To do so is supported by the correlations obtained demonstrating that the site of attack is the site of hydroxylation which would not be the case when epoxide intermediates are involved. Furthermore other literature data support this view. First, Korzekwa et al. [24] also concluded, based on the results obtained from a study on the hydroxylation of deuterated chlorobenzenes, that the epoxide mechanism for hydroxylation of the chorobenzenes to phenols might be untenable. Second, in a study from Rizk and Hanzlik [25] the absence of any deuterium loss upon conversion of deuterated [3,5-$^2H_2$]-4-iodoanisole to 2-methoxy-5-iodophenol also suggested that this aromatic hydroxylation must occur almost entirely by direct aromatic hydroxylation instead of proceeding by an epoxide mechanism. Furthermore, it is known that NIH shifted phenolic metabolites can be formed from epoxide metabolites [8,9]. However, upon the *in vivo* aromatic hydroxylation of the substituted fluorobenzenes of the previous [7] and the present study, NIH shifted phenolic metabolites were not observed.

Figure 3C presents the correlation between the predicted and observed regioselectivity of aromatic ring hydroxylation of all the fluorobenzene derivatives now studied in the present and a previous study [7] taking into account the steric correction factors of the present study. The results in Figure 3C show that a good correlation (r=0.95) was obtained between the predicted and observed regioselectivity. These results show that for the tested fluorobenzenes (Figure 3C) the main factors directing the regioselectivity of their aromatic hydroxylation must be i) nucleophilic chemical reactivity of the site to be hydroxylated and ii) steric influence of the substituent *ortho* with respect to the site of hydroxylation. The latter was observed for a bromine and iodine substituent but not for a fluorine, chlorine or cyano substituent. The small deviations between the predicted and observed regioselectivities may be systematic and due to an interaction between the substrate and the cytochrome P450$(FeO)^{3+}$ species resulting in a stereoselective orientation of the substrate before the attack of the high-valent iron-oxo species [23,26] and/or to small contributions of epoxide intermediates.

Finally, one might address the toxicological significance of the predictions of regioselectivity of aromatic hydroxylation reported in the present study for the various congeners. This requires the identification of the ultimate reactive metabolite inducing the toxic effect. For halobenzenes the reactive metabolites involved could

be either epoxide intermediates or benzoquinone-type reactive metabolites formed upon oxidation of secondary diol metabolites [27,28]. Epoxide intermediates, as well as benzoquinone derivatives are known to be reactive and to bind to protein and DNA thereby possibly resulting in toxicologic and ultimately mutagenic/ carcinogenic responses [1,2]. Since the present study only relates to the primary phenolic metabolite profiles, the possible toxicological significance of the present results to the formation of benzoquinone-type reactive metabolites, has to await studies on prediction of regioselectivity of phenol hydroxylation, i.e. the secondary cytochrome P450-catalysed conversion of the benzenes. Furthermore, since the results of the present study argue against an important role for epoxide intermediates in the route leading to phenolic metabolites, the predictions presented can neither predict the type of reactive epoxide intermediates to be expected. Clearly, this absence for an intermediate role of toxic epoxide intermediates in the route leading to phenolic metabolites is to some extent opposite to what has been widely assumed. However, previous studies already reported additional evidence against an obligatory role for epoxides in aromatic hydroxylation. Based on studies of the hydroxylation of deuterated bromobenzenes [29], deuterated chlorobenzenes [24] and fluorobenzenes [7] it was also concluded that epoxides were not obligatory intermediates in the route leading to phenolic metabolites. This latter aspect seems to be a matter not yet well appreciated in biochemical toxicological studies on aromatic hydroxylation pathways.

Acknowledgements

The authors gratefully acknowledge Mr. G. van Tintelen for assistance with animal handling. Support from the TMR large scale NMR facility grant no. ERB-CHGE-CT94-0061 is also acknowledged.

References

1 Lau, S.S., Abrams, G.D., and Zannoni, V.G. (1980) Metabolic activation and detoxification of bromobenzene leading to cytotoxicity. *J. Pharmacol. Exp. Ther.* 214, 703-708.

2 Jollow, D.J., Mitchell, J.R., Zampaglione, N., and Gillette, J.R. (1974) Bromobenzene-induced liver necrosis. Protective role of glutathione and evidence for 3,4-bromobenzene oxide as the hepatotoxic metabolite. *Pharmacology* 11, 151-169.

3 Zampaglione, N., Jollow, D.J., Mitchell, J.R., Stripp, B., Hamrick, M., and Gillette, J.R. (1973) Role of detoxifying enzymes in bromobenzene-induced liver necrosis. *J. Pharmacol. Exp. Ther.* 187, 218-227.

4 Lau, S.S., and Zannoni, V.G. (1979) Hepatic microsomal epoxidation of bromobenzene to phenols and its toxicological implication. *Toxicol. Appl. Pharmacol.* 50, 309-318.

5 Selander, H.G., Jerina, D.M., and Daly, J.W. (1975) Metabolism of chlorobenzene with hepatic microsomes and solubilized cytochrome P-450 systems. *Arch. Biochem. Biophys.* 168, 309-321.

6 Bogaards, J.J.P., Van Ommen, B., Wolf, C.R., and Van Bladeren, P.J. (1995) Human cytochrome P450 enzyme selectivities in the oxidation of chlorinated benzenes. *Toxicol. Appl. Pharmacol.* 132, 44-52.

7 Rietjens, I.M.C.M., Soffers, A.E.M.F., Veeger, C., and Vervoort, J. (1993) Regioselectivity of cytochrome P-450 catalyzed hydroxylation of fluorobenzenes predicted by calculated frontier orbital substrate characteristics. *Biochemistry* 32, 4801-4812.

8 Daly, J.W., Jerina, D.M., and Witkop, B. (1972) Arene oxides and the NIH shift: The metabolism, toxicity and carcinogenicity of aromatic compounds. *Experientia* 28, 1129-1264.

9 Jerina, D.M., and Daly, J.W. (1974) Arene oxides: A new aspect of drug metabolism. *Science* 185, 573-582.

10 Korzekwa, K., Trager, W., Gouterman, M., Spangler, D., and Loew, G.H. (1985) Cytochrome P450 mediated aromatic oxidation: A theoretical study. *J. Am. Chem. Soc.* 107, 4273-4279.

11 Vervoort, J., De Jager, P.A., Steenbergen, J., and Rietjens, I.M.C.M. (1990) Development of a ^{19}F-n.m.r. method for studies on the *in vivo* and *in vitro* metabolism of 2-fluoroaniline. *Xenobiotica* 20, 657-670.

12 Rietjens, I.M.C.M., and Vervoort, J. (1989) Microsomal metabolism of fluoroanilines. *Xenobiotica* 19, 1297-1305.

13 Omura, T., and Sato, R. (1964) The carbon monoxide-binding pigment of liver microsomes. 1. Evidence for its hemoprotein nature. *J. Biol. Chem.* 239, 2370-2378.

14 Rietjens, I.M.C.M., Koerts, J., Boeren, S., and Vervoort, J. (1991) Biosynthesis and chemical determination of polyfluoro-4-hydroxyanilines. *Recl. Trav. Chim. Pays-Bas* 110, 216-221.

15 Cnubben, N.H.P., Vervoort, J., Veeger, C., and Rietjens, I.M.C.M. (1992) Study on the regioselectivity and mechanism of the aromatic hydroxylation of monofluoroanilines. *Chem.-Biol. Interact.* 85, 151-172.

16 Rietjens, I.M.C.M., Cnubben, N.H.P., Van Haandel, M., Tyrakowska, B., Soffers, A.E.M.F., and Vervoort, J. (1995) Different metabolic pathways of 2,5-difluoronitrobenzene and 2,5-difluoroaminobenzene compared to molecular orbital substrate characteristics. *Chem.-Biol. Interact.* 94, 49-72.

17 Dewar, M.J.S., Zoebisch, E.G., Healy, E.F., and Stewart, J.J.P. (1985) AM1: A new general purpose quantum mechanical molecular model. *J. Am. Chem. Soc.* 107, 3902-3909.

18 Fukui, K., Yonezawa, T., Nagata, C., and Shingu, H. (1954) Molecular orbital theory of orientation in aromatic, heteroaromatic and other conjugated molecules. *J. Chem. Phys.* 22, 1433-1442.

19 Lindsay Smith, J.R., Shaw, B.A., and Foulkes, D.M. (1972) Mechanisms of mammalian hydroxylation: Some novel metabolites of chlorobenzene. *Xenobiotica* 2, 215-226.

20 Zheng, J., and Hanzlik, R.P. (1992) Dihydroxylated mercapturic acid metabolites of bromobenzene. *Chem. Res. Toxicol.* 5, 561-567.

21 Griffeth, L.K., Rosen, G.M., and Rauchman, E.J. (1987) Effects of model traumatic injury on hepatic drug metabolism in the rat VI. Major detoxification/toxification pathways. *Drug Metab. Dispos.* 15, 749-759.

22 Soffers, A.E.M.F., Veeger, C., and Rietjens, I.M.C.M. (1994) Influence of the type of halogen substituent on *in vivo* and *in vitro* phase II metabolism of 2-fluoro-4-halophenol metabolites formed from 3-halo-fluorobenzenes. *Xenobiotica* 24, 759-774.

23 Koerts, J., Boeren, S., Vervoort, J., Weiss, R., Veeger, C., and Rietjens, I.M.C.M. (1996) Interaction between the substrate and the high-valent-iron-oxo porphyrin cofactor as a possible factor influencing the regioselectivity of cytochrome P450 catalysed aromatic ring hydroxylation of 3-fluoro(methyl)anilines. *Chem.-Biol. Interact.* 99, 129-146.

24 Korzekwa, K.R., Swinney, D.C., and Trager, W.F. (1989) Isotopically labeled chlorobenzenes as probes for the mechanism of cytochrome P-450 catalyzed aromatic hydroxylation. *Biochemistry* 28, 9019-9027.

25 Rizk, P.N., and Hanzlik, R.P. (1995) Oxidative and non-oxidative metabolism of 4-iodoanisole by rat liver microsomes. *Xenobiotica* 25, 143-150.

26 Koerts, J., Rietjens, I.M.C.M., Boersma, M.G., and Vervoort, J. (1995) ^{1}H NMR T_1 relaxation rate study on substrate orientation of fluoromethylanilines in the active sites of microsomal and purified cytochromes P450 1A1 and 2B1. *FEBS Lett.* 368, 279-284.

27 Van Ommen, B., Voncken, J.W., Müller, F., and Van Bladeren, P.J. (1988) The oxidation of tetrachloro-1,4-hydroquinone by microsomes and purified cytochrome P450b. Implications for covalent binding to protein and involvement of reactive oxygen species. *Chem.-Biol. Interact.* 65, 247-259.

28 Den Besten, C., Smink, M.M.C., De Vries, E.J., and Van Bladeren, P.J. (1991) Metabolic activation of 1,2,4-trichlorobenzene and pentachlorobenzene by rat liver microsomes: A major role for quinone metabolites. *Toxicol. Appl. Pharmacol.* 108, 223-233.

29 Hanzlik, R.P., Hogberg, K., and Judson, C.M. (1984) Microsomal hydroxylation of specifically deuterated monosubstituted benzenes. Evidence for direct aromatic hydroxylation. *Biochemistry* 23, 3048-3055.

Chapter 3

Interaction between the substrate and the high-valent iron-oxo porphyrin cofactor as a possible factor influencing the regioselectivity of cytochrome P450-catalysed aromatic ring hydroxylation of 3-fluoro(methyl)anilines

J. Koerts, S. Boeren, J. Vervoort, R. Weiss, C. Veeger and I.M.C.M. Rietjens

Chemico-Biological Interactions 99, 1996, 129-146.

Abstract

In the present study the *in vitro* and *in vivo* aromatic ring hydroxylation of a series of amino and/or methyl containing fluorobenzenes, i.e. 3-fluoro(methyl)-anilines, was investigated and compared to the calculated density distribution of the reactive frontier π-electrons of the aromatic substrate. This was done i) to study to what extent the regioselectivity of the aromatic ring hydroxylation of the 3-fluoro(methyl)anilines could be predicted on the basis of the calculated chemical reactivity, as was previously observed for a series of fluorinated benzenes and monofluoroanilines, and ii) to investigate which factors contribute to possible deviations from the predictions on the basis of the calculated chemical reactivity. Results obtained show that the *in vitro* and *in vivo* aromatic ring hydroxylation of the series 3-fluoro(methyl)anilines correlate qualitatively with the calculated frontier orbital density distribution for electrophilic attack by the cytochrome P450$(FeO)^{3+}$ species. These results indicate that the HOMO/HOMO-1 frontier orbital densities, i.e. the chemical reactivity of the carbon centres for an electrophilic attack, predict the preferential as well as the non-reactive sites for cytochrome P450-catalysed aromatic ring hydroxylation of the tested model compounds. The absolute values, however, deviated in a systematic way; C4 *para* hydroxylation being observed to a higher extent than expected on the basis of chemical reactivity and C2/C6 *ortho* hydroxylation being observed to a lower extent than expected. Additional experiments were performed using different microsomal preparations and microperoxidase-8. The latter is a mini heme protein of eight amino

acids without a substrate binding site. In incubations of the model compounds with different types of microsomal preparations, as well as with MP-8 and purified reconstituted cytochrome P450 2B1, similar systematic deviations between the predicted and observed regioselectivity of aromatic hydroxylation were observed. These results show that the regioselectivity of aromatic ring hydroxylation of the 3-fluoro(methyl)anilines cannot be predominantly ascribed to an interaction between the substrate and the substrate binding site of the cytochromes P450 dictating a specific stereoselective positioning of the substrate in the active site. More likely, the systematic deviations between the observed and predicted regioselectivity of hydroxylation of the tested model substrates should be ascribed to an (orienting) interaction between the substrate and the activated cytochrome P450$(FeO)^{3+}$ cofactor.

Introduction

In previous studies on the regioselectivity of the cytochrome P450-catalysed hydroxylation of monofluoroanilines [1] and a series of fluorinated benzenes [2] a qualitative and even a quantitative correlation was observed between the regioselectivity of the aromatic ring hydroxylation and the calculated density distribution of the reactive frontier π-electrons of the aromatic substrate. These results support a mechanism of hydroxylation of fluorinated benzene derivatives that proceeds through an initial electrophilic attack of the cytochrome P450$(FeO)^{3+}$ intermediate on the frontier π-electrons of the benzene derivative without an important role for epoxide intermediates [2]. The objective of the present study was to investigate to what extent this MO-QSAR (molecular orbital based quantitative structure activity relationship) would be applicable to fluorinated benzene derivatives containing additional methyl and/or amino substituents. Thus, fluorinated (methyl)anilines were used as model substrates. Insight into factors which determine the bioconversion of (methyl)aniline derivatives is of importance, because they are frequently used in the manufacture of agrochemicals, chemical dyes and drugs. In spite of the well-recognized implications of metabolic profiles of the methylanilines for their ultimate possibilities for excretion or bioactivation [3-14], only a limited number of studies are available on the metabolic pattern of these compounds [15-20].

In the present paper the biotransformation characteristics of 3-fluoromethylanilines were determined *in vitro* in incubations with microsomal

cytochromes P450 and *in vivo* on the basis of analysis of urine samples from exposed rats by ^{19}F NMR. A main objective of the present study was to investigate the influence of the cytochrome P450 substrate binding site, of activated cofactor-substrate interaction and of the chemical substrate reactivity on the regioselectivity of the aromatic ring hydroxylation. Thus, the outcomes of the biotransformation studies were compared to the calculated chemical reactivity parameters and additional studies were performed in which the conversion of the model compounds was studied in incubations with microperoxidase-8 (MP-8). MP-8 is a water soluble heme compound obtained by proteolytic digestion of horse heart cytochrome c, which consists of iron-protoporphyrin IX covalently bound to only eight residual cytochrome c amino acids [21]. Literature data report on the cytochrome P450 like catalytic properties of this MP-8 in a H_2O_2 but also in a NADPH/O_2/NADPH:cytochrome reductase driven system [22,23]. The axial histidine in MP-8 instead of a cysteine in cytochromes P450 is not expected to be crucial for the reaction chemistry that can be catalysed, also because the calculations of Du and Loew [24] reported similar electronic and spin properties in a cysteyl and histidyl coordinated high-valent iron-oxo porphyrin cofactor. Because the MP-8 model provides the activated porphyrin cofactor but has no substrate binding site, it was used in our study as a model to discriminate between the influences of the substrate binding site and of the cofactor-substrate interaction on the regioselectivity of the cytochrome P450-catalysed aromatic ring hydroxylation.

Materials and Methods

Chemicals

The substrates 3-fluoro-2-methylaniline, 3-fluoro-4-methylaniline and 3-fluoro-6-methylaniline were all purchased from Aldrich (Steinheim, Germany). 2-Amino-4-fluoro-5-methylphenylsulphate, 2-amino-6-fluoro-5-methylphenylsulphate and 2-amino-6-fluoro-3-methylphenylsulphate were synthesized according to a method described by Boyland et al. [25]. In short, 0.05 g of the corresponding 3-fluoromethylaniline and 0.25 ml (2 M) KOH were dissolved in 5 ml water under stirring. To this mixture 0.25 ml 0.2 M potassium persulphate was added over a period of 2 hours. The reaction mixture was analysed by ^{19}F NMR in 0.2 M potassium phosphate pH 7.6. For 3-fluoro-2-methylaniline the mixture appeared to contain the two possible fluorinated *ortho* phenylsulphate metabolites with the following ^{19}F NMR spectral characteristics; 2-amino-4-fluoro-5-methylphenyl-

sulphate δ = -123.8 ppm ($^3J_{HF}$=9.7 Hz, $^4J_{HF}$=8.9 Hz) and 2-amino-6-fluoro-5-methylphenylsulphate δ = -137.1 ppm ($^4J_{HF}$=8.5 Hz). For 3-fluoro-6-methylaniline formation of the *ortho* phenylsulphate metabolite 2-amino-6-fluoro-3-methylphenylsulphate at δ = -136.3 ppm ($^3J_{HF}$= 11.9 Hz, $^4J_{HF}$= 8.8 Hz) was observed.

3-Fluoro-2-hydroxy-4-methylaniline, 3-fluoro-6-hydroxy-4-methylaniline and 3-fluoro-2-hydroxy-6-methylaniline were obtained by acid hydrolysis (30 min 1 N HCl 100°C) of 2-amino-6-fluoro-5-methylphenylsulphate, 2-amino-4-fluoro-5-methylphenylsulphate and 2-amino-6-fluoro-3-methylphenylsulphate, respectively. The ^{19}F NMR spectral characteristics in 0.2 M potassium phosphate pH 7.6 were: 3-fluoro-2-hydroxy-4-methylaniline δ = -144.9 ppm ($^4J_{HF}$=8.5 Hz), 3-fluoro-6-hydroxy-4-methylaniline δ = -131.6 ppm ($^3J_{HF}$=9.6 Hz, $^4J_{HF}$=7.3 Hz) and 3-fluoro-2-hydroxy-6-methylaniline δ = -143.7 ppm ($^3J_{HF}$=11.2 Hz, $^4J_{HF}$=5.6 Hz).

In vivo exposure to the 3-fluoromethylanilines

Male Wistar rats (± 400 g) were exposed to 50 mg of the respective 3-fluoromethylaniline per kg body weight, administered in olive oil by oral injection. After oral dosing, 24 h urine samples were collected for two days. For ^{19}F NMR measurement, urine samples were diluted once in 0.2 M potassium phosphate pH 7.6.

Enzyme and acid hydrolysis of urine samples

In order to identify phenolic 3-fluoromethylaniline metabolites excreted in the urine in their glucuronidated, sulphated or N-acetylated form, urine samples were treated with acid, with β-glucuronidase (from *Escherichia coli* K12 (Boehringer, Mannheim, Germany)) or with arylsulphatase/β-glucuronidase (from *Helix pomatia* (Boehringer, Mannheim, Germany)). Enzyme treatments were carried out essentially as described before [26]. For acid hydrolysis of the urine samples 1.0 ml urine sample was incubated with 0.1 ml 37% (12 N) HCl for 1 hour in a boiling water bath. After acid hydrolysis the mixture was neutralised with 6 N NaOH and the sample was diluted 2 times in 0.2 M potassium phosphate pH 7.6 for analysis by ^{19}F NMR.

For ^1H NMR measurements on urinary metabolites the arylsulphatase/β-glucuronidase treated urine samples were extracted three times with an equal volume of ethyl acetate. The ethyl acetate phase was evaporated and the residue was dissolved in $CDCl_3$.

Chemical assay for the detection of 4-hydroxylated derivatives

4-Aminophenol derivatives present in the urine of 3-fluoromethylaniline exposed rats were determined using the method of Brodie and Axelrod [27]. Before chemical analysis, 4-aminophenol derivatives were extracted from the urine as follows; 400 µl urine of a methylaniline exposed rat was treated with arylsulphatase/β-glucuronidase as described above and extracted 2 times with 400 µl ethyl acetate. To 40 µl of the collected ethyl acetate extract 760 µl demi water and 240 µl trichloroacetic acid (20% w/v) were added. To 800 µl of this mixture 80 µl phenol reagent (5% w/v phenol in 2.5 M NaOH) and 160 µl 2.5 M Na_2CO_3 were added. The absorbance at 630 nm was measured after 45 min.

Microsomal preparations

Preparation of microsomes was carried out essentially as described previously [26]. Microsomes were obtained from perfused livers of male Wistar rats (300-400 g) which were untreated or pretreated with the following cytochrome P450 inducers: acetone (Merck, Darmstadt, Germany) (1.5 ml, 30% in water, orally dosed 24 h before liver perfusion), isosafrole (Janssen Chimica, Beerse, Belgium) (150 mg/kg body weight, using a stock solution of 100 mg/ml in olive oil, injected i.p. daily for 3 days), β-naphtoflavone (Sigma, St. Louis, MO, USA) (30 mg/kg body weight, using a stock solution of 12 mg/ml in olive oil, injected i.p. daily for 3 days) or phenobarbital (Brocacef, Maarssen, The Netherlands) (0.1% in drinking water for 7 days). The amount of cytochrome P450 in the microsomes was measured according to the method described by Omura and Sato [28].

Purification of microperoxidase-8 (MP-8)

MP-8 was purified after proteolytic digestion of horse heart cytochrome c (Sigma, St. Louis, MO USA) essentially as described in the literature [21]. The sample was over 96% pure based on HPLC analysis [21]. The HPLC analysis was performed on a Waters M600 HPLC with a Bakerbond WP-C4 column (25 cm × 4.6 mm). A linear gradient from 0 to 50% 0.1% trifluoroacetonitril in water and 50% 0.1% trifluoroacetic acid in acetonitril was applied in 50 min. Detection at 214 nm was performed on an ISCO V^4 absorbance detector and detection at 395 nm was performed on an Applied Biosystems 757 absorbance detector.

The heme content was determined essentially as described previously [29].

In vitro incubations

Microsomal P450

The incubation mixture contained (final concentrations) 0.1 M potassium phosphate pH 7.6, 3 mM substrate, added from a 0.3 M stock solution in dimethyl sulfoxide, 2.0 μM microsomal cytochrome P450, 1 mM ascorbic acid (Janssen Chimica, Beerse, Belgium) to prevent autoxidation of the ring-hydroxylated metabolites, added from a freshly prepared 20 mM stock solution in 0.1 M potassium phosphate pH 7.6.

The incubations were preincubated at 37 °C for 2 min and the reaction was started by the addition of NADPH (2 mM final concentration). The total sample volume was 2 ml. After 10 min the reaction was terminated by freezing the samples in liquid nitrogen. Blanks contained distilled water instead of NADPH or instead of microsomes.

The reaction rate was linear in time up to at least 10 min and with the amount of microsomal cytochrome P450 up to at least 2 μM. The regioselectivity of aromatic ring hydroxylation appeared to be unaffected by an increase in the cytochrome P450 concentration up to at least 2 μM (data not shown).

Microperoxidase-8 (MP-8)

The incubation mixture contained (final concentrations) 0.1 M potassium phosphate pH 7.6, 3 mM substrate, added from a 0.3 M stock solution in dimethyl sulfoxide, 7.5 μM MP-8, 2 mM ascorbic acid, added from a freshly prepared 20 mM stock solution in 0.1 M potassium phosphate pH 7.6. The incubations were preincubated at 37 °C for 1 min and the reaction was started by the addition of hydrogen peroxide (2.5 mM final concentration). The total sample volume was 2 ml. After 1 min the reaction was terminated by adding 6500 U catalase (Boehringer, Mannheim, Germany) and freezing the samples in liquid nitrogen. Blanks contained distilled water instead of hydrogen peroxide or instead of MP-8.

Cytochrome P4502B1

Cytochrome P4502B1 was purified and reconstituted as previously described [36].

^{19}F NMR and ^{1}H NMR measurements

^{19}F NMR measurements were performed on a Bruker AMX 300 NMR spectrometer at 280 K. Proton-decoupling was achieved with the Waltz-16 pulse sequence at -20dB from 50W.

Samples contained 100 µl $^{2}H_2O$ for locking the magnetic field and 10 µl 8.4 mM 4-fluorobenzoic acid added as an internal standard. The total sample volume was 1.71 ml. Enzyme treated urine samples and samples from *in vitro* incubations were made anaerobic by evacuating and filling with argon four times before analysis. This was done to prevent autoxidation of the phenolic metabolites. About 1500 scans for *in vivo* urine samples and 60 000 scans for the microsomal incubations samples were recorded. Chemical shifts are reported relative to $CFCl_3$. Quantification of the different metabolites was done by comparison of the integral of the ^{19}F NMR resonance of the added internal standard 4-fluorobenzoic acid to the integrals of the ^{19}F NMR peaks of the metabolites.

^{1}H NMR measurements were carried out on a Bruker AMX 500 NMR spectrometer at 296 K. Spectra were recorded using 30° pulses (3 µs), a 10 kHz spectral width, a repetition time of 1.9 s, quadrature phase detection and quadrature phase cycling (CYCLOPS). Samples contained $CDCl_3$ for locking the magnetic field. The total sample volume was 0.5 ml. About 2000 scans were recorded.

Molecular orbital calculations

Semi-empirical molecular orbital calculations were performed on a Silicon Graphics Iris 4D/85 computer with the AM1 (Austin Method 1) Hamiltonian from the AMPAC program (Quantum Chemistry Program Exchange, program no. 506, Indiana University, Bloomington, IN, USA). The AM1 Hamiltonian was used since it was reported to provide improved results for molecules containing heteroatoms compared to the MINDO/3 and MNDO methods [30]. Calculations were carried out with PRECISE criteria and self-consistent field was achieved for all calculations. Geometries were optimised for all bond lengths, bond angles and torsion angles using the Fletcher-Powell criteria.

Frontier electron densities of the substrates for electrophilic attack on the π-electrons of the aromatic ring were calculated according to the equation of Fukui et al. [31]. In this equation the contribution of the HOMO (highest occupied molecular orbital) and HOMO-1 (highest occupied molecular orbital below the HOMO) are both taken into account.

The calculated electronic parameters are compared with the results from the

in vivo and *in vitro* biotransformation of the substrates to aromatic ring hydroxylated products by cytochromes P450. Upon binding of the substrates to the active site of the cytochromes P450, the intrinsic properties of the compounds might be changed due to solvation effects and a different dielectric constant. Because a series of closely related compounds is being compared and because the active sites of the mammalian cytochromes P450 are rather large aspecific hydrophobic pockets, it can be assumed that the relative differences calculated between the related compounds as well as between various sites in one molecule will not be influenced by binding of the substrates to the active site of the cytochromes P450.

From the calculated HOMO/HOMO-1 density distributions the regioselectivity of aromatic ring hydroxylation of the 3-fluoro(methyl)anilines was calculated by summation of the frontier orbital densities of non-substituted aromatic ring carbon atoms and normalization of the sum of the values to 1.0. The predicted percentage of hydroxylation of an aromatic centre was calculated as the fraction of this normalized total frontier orbital density present on the respective non-substituted aromatic centre.

Statistical analysis of data

Values are presented as the mean ± S.D. (standard deviation).

Results

Identification of aromatic ring hydroxylated metabolites

Identification of the ^{19}F NMR resonances of the various hydroxylated metabolites of the 3-fluoromethylaniline model compounds was carried out on the basis of the following strategy. The effect of introduction of a hydroxyl moiety at an *ortho, meta* or *para* position with respect to the aromatic fluorine substituent can be expected to result in a relatively characteristic change in its ^{19}F NMR chemical shift [32]. The actual values for the change in a ^{19}F-chemical shift value as a result of introduction of a hydroxyl moiety at a position *ortho, meta* or *para* with respect to a specific fluorine substituent can be derived from the chemical shift values observed in previous studies with fluorinated anilines [1] and benzenes [2] converted to their hydroxylated derivatives. The mean value of these changes for introduction of a hydroxyl moiety at respectively the *ortho, meta* and *para* position with respect to the fluorine substituent amounts to -23.1 ± 0.6 (n=7), +1.8 ± 1.2 (n=11) and -11.0 ± 1.7

(n=6) ppm [33]. On the basis of these results the expected ^{19}F NMR chemical shifts of the various possible hydroxylated metabolites of the 3-fluoromethylanilines were calculated. The ppm values thus obtained are presented in Table 1. For example, introduction of a hydroxyl moiety *ortho* with respect to the fluorinated C3 in 3-fluoro-2-methylaniline can be expected to result in a shift of the ^{19}F NMR resonance by -23.1 ± 0.6 ppm from -121.9 to approximately -145.0 ± 0.6 ppm.

In order to check that this way of identification of ring hydroxylated metabolites was justified some of the hydroxylated 3-fluoromethylaniline metabolites were synthesized, i.e. 3-fluoro-2-hydroxy-4-methylaniline, 3-fluoro-6-hydroxy-4-methylaniline and 3-fluoro-2-hydroxy-6-methylaniline. The ^{19}F NMR ppm values of these synthesized reference compounds are -144.9, -131.6 and -143.7 ppm respectively, i.e. similar to the predicted values presented in Table 1. In one case, an *ortho* C2 and *para* C4 ring hydroxylated derivative were predicted to have similar ppm values, i.e. the *ortho* C2 and *para* C4 hydroxylated derivative of 3-fluoro-6-methylaniline (Table 1). Nevertheless, the actually observed urinary phenolic metabolite with its ppm value at -144.2 ppm could be identified as the C4 hydroxylated product. This follows from the observation that i) chemical synthesis of the *ortho* hydroxylated product demonstrated its ppm value to be -143.7 ppm and ii) the presence of the *para*-hydroxylated methylaniline could be demonstrated in the urine using a chemical assay for detection of 4-aminophenol metabolites (data not shown).

Table 1 also summarizes the actual resonances of metabolites observed in the ^{19}F NMR spectra from the *in vitro* microsomal incubations and from hydrolysed urine samples of exposed rats. Comparison of the calculated ^{19}F NMR resonances of phenolic metabolites (Table 1) to the ones observed in the ^{19}F NMR spectra (Figures 1 and 2) resulted in identification of the ^{19}F NMR resonances of the various phenolic compounds. The presence of these phenolic resonances in ^{19}F NMR spectra of urine samples only after treatment of the urine with arylsulphatase/β-glucuronidase further confirmed that these resonances belong to phenolic metabolites excreted as their sulphated or glucuronidated derivatives.

In vitro cytochrome P450-catalysed aromatic ring hydroxylation of 3-fluoro(methyl)anilines

The *in vitro* aromatic ring hydroxylation of the 3-fluoro(methyl)anilines was investigated in incubations with microsomes from isosafrole pretreated rats. From the incubations of 3-fluoro-2-methylaniline and 3-fluoroaniline with microsomes

Table 1 Identification of aromatic ring hydroxylated derivatives of 3-fluoromethylanilines. Chemical shift values presented are relative to $CFCl_3$. Estimated values were based on the changes in ^{19}F NMR chemical shifts observed upon introduction of a hydroxyl moiety in a series of fluorinated benzene [2] and aniline [1] derivatives [33].

substrate metabolite	ppm estimated	ppm observed *in vivo* and/or *in vitro*
3-fluoro-2-methylaniline	-	-121.9[a]
3-fluoro-4-hydroxy-2-methylaniline	-145.0 ± 0.6	-144.1
3-fluoro-5-hydroxy-2-methylaniline	-120.1 ± 1.2	no[b]
3-fluoro-6-hydroxy-2-methylaniline	-132.9 ± 1.7	-131.1
3-fluoro-6-methylaniline	-	-121.5[a]
3-fluoro-2-hydroxy-6-methylaniline	-144.6 ± 0.6	-143.7[a]
3-fluoro-4-hydroxy-6-methylaniline	-144.6 ± 0.6	-144.2[c]
3-fluoro-5-hydroxy-6-methylaniline	-119.7 ± 1.2	no[b]
3-fluoro-4-methylaniline	-	-121.5[a]
3-fluoro-2-hydroxy-4-methylaniline	-144.6 ± 0.6	-144.9[a]
3-fluoro-5-hydroxy-4-methylaniline	-119.7 ± 1.2	no[b]
3-fluoro-6-hydroxy-4-methylaniline	-132.5 ± 1.7	-131.6[a]

[a] Identified also on the basis of a synthesized or commercially available reference compound.

[b] No resonance observed at this position *in vivo* and/or *in vitro*.

[c] Identified also on the basis of a chemical assay for 4-hydroxylated aminobenzene derivatives and by the fact that the ^{19}F NMR resonance of the synthesized 3-fluoro-2-hydroxy-6-methylaniline, predicted to be at a similar value, was at -143.7 ppm.

from rats pretreated with different inducers ((vide infra) and [1]) it was observed that incubations with microsomes derived from isosafrole pretreated rats showed the highest rate of conversion. Figure 1 presents the ^{19}F NMR spectra of the 3-fluoromethylaniline model compounds with microsomes from isosafrole pretreated rats. The ^{19}F NMR spectrum of the incubation of 3-fluoroaniline with isosafrole microsomes was previously reported [1]. The amount of fluoride anions in the microsomal incubations equals the amount detected in the blank incubations

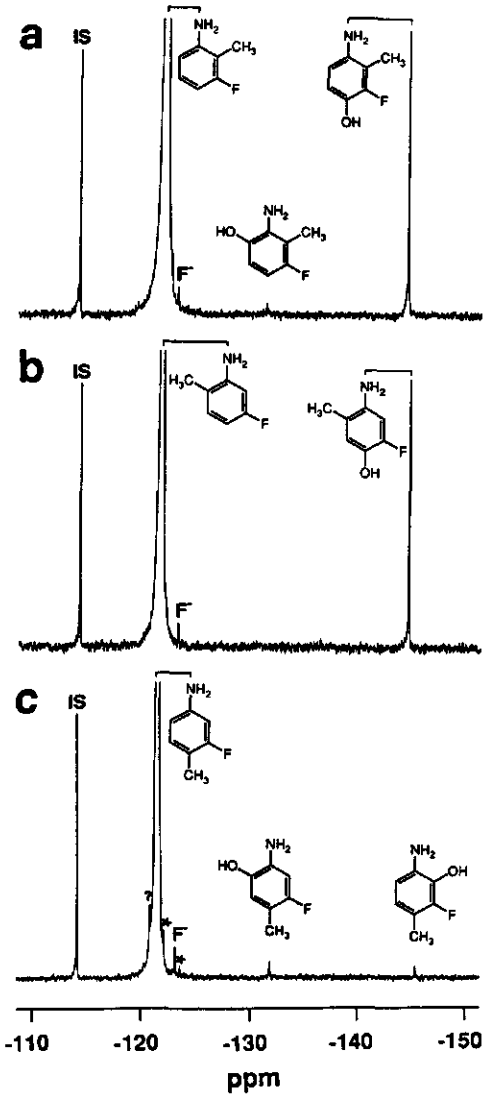

Figure 1 ^{19}F NMR spectra from incubations of (a) 3-fluoro-2-methylaniline, (b) 3-fluoro-6-methylaniline and (c) 3-fluoro-4-methylaniline with microsomes from isosafrole pretreated rats. Peaks marked with an asterisk were also found in the blank incubations without NADPH. The resonance peak of the internal standard 4-fluorobenzoic acid is marked "IS". Chemical shifts are recorded relative to $CFCl_3$. ^{19}F NMR resonances of possible metabolites resulting from CH_3 hydroxylation are masked by the relatively large resonance of the substrate. However, this is not of interest as the present study focuses on the regioselectivity of aromatic ring hydroxylation.

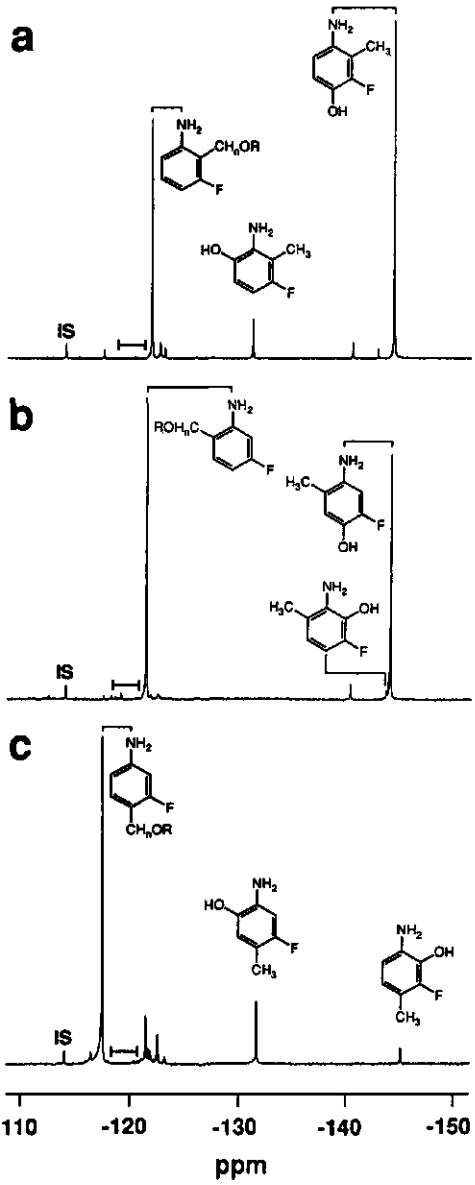

Figure 2 ^{19}F NMR spectra from acid treated 24 h urine samples of rats exposed to (a) 3-fluoro-2-methylaniline (b) 3-fluoro-6-methylaniline and (c) 3-fluoro-4-methylaniline. Chemical shifts are recorded relative to $CFCl_3$. The bar in the spectrum indicates the ppm range where the C5 hydroxylated metabolite can be expected (Table 1). Proton-coupled ^{19}F NMR analysis of peaks observed in this region demonstrated that they contain three aromatic protons indicating that they can not be ascribed to C_5 hydroxylated metabolites (data not shown). CH_nOR presents metabolites resulting from CH_3 hydroxylation with R=H and n=2 in case of a benzylalcohol and R=absent and n=1 for a benzaldehyde (see text for further details).

without NADPH. From this it can be concluded that hydroxylation accompanied by defluorination is not observed. Hydroxylation accompanied by an NIH shift of the fluorine was also not observed.

Table 2 presents the regioselectivity of the *in vitro* cytochrome P450 catalysed aromatic hydroxylation of the various model compounds as derived from the ^{19}F NMR results.

In vivo aromatic ring hydroxylation of 3-fluoro(methyl)anilines

The regioselectivity of the aromatic hydroxylation of the 3-fluoro(methyl)aniline derivatives upon their *in vivo* biotransformation was also determined. The regioselectivity of aromatic ring hydroxylation for the different substrates was derived from the ^{19}F NMR spectra of the acid treated urine samples of rats exposed to the various model compounds. In Figure 2 the ^{19}F NMR spectra of the acid treated urine samples of rats exposed to 3-fluoromethylanilines are shown. The ^{19}F NMR spectrum of urine from a 3-fluoroaniline exposed rat was previously reported [1]. From these ^{19}F NMR spectra it could be calculated that the 24 h recovery of the administered dose was 70-90% for all the model substrates. The amount of fluoride anions in the urine samples could be attributed to the fluoride anions originating from the food and/or drinking water, as a similar amount was observed in the ^{19}F NMR spectra of control urine samples of unexposed rats.

In addition to the resonances of the aromatic ring hydroxylated products the ^{19}F NMR spectra presented in Figure 2 contain additional resonances (-121.9 ppm (Figure 2a), -121.5 ppm (Figure 2b) and -117.6 ppm (Figure 2c)). These resonances can be ascribed to metabolites resulting from hydroxylation of the methyl moiety of the 3-fluoromethylanilines. This follows from the fact that ^{1}H NMR and ^{19}F NMR analysis of these metabolites, extracted into ethyl acetate after treatment of urine with arylsulphatase/β-glucuronidase, shows that they all still contain three aromatic protons, in addition to the fluorine substituent (data not shown). HPLC analysis of these samples show that these resonances can not be ascribed to the substrate (data not shown). Because metabolites resulting from hydroxylation of the amino moiety are generally not excreted into urine, it is most likely that these unidentified urinary metabolites result from a modification of the methyl group. Biotransformation of methylanilines to benzylalcohols and benzaldehydes, resulting from a modification of the methyl group, has been reported before [15,19,20]. Because the present study focuses on the regioselectivity of aromatic ring hydroxylation, the respective metabolites were not further identified at this stage.

Table 2 Regioselectivity of the *in vitro* and *in vivo* aromatic ring hydroxylation of 3-fluoro(methyl)anilines. The *in vitro* data were obtained from incubations with MP-8 or microsomes from isosafrole pretreated rats (n=2). *In vivo* results were obtained from analysis of acid treated 24 h urine samples of exposed rats (n=2). Ring carbon atoms are numbered in such a way that the amino moiety is at C1.

substrate	regioselectivity of aromatic ring hydroxylation			
ring carbon atom	observed[a]			predicted[b]
	in vitro		*in vivo*	
	cyt. P450	MP-8		
3-fluoro-2-methylaniline				
C4 : C5 : C6	94 : 0 : 6	71 : 0 : 29	89 : 0 : 11	53 : 10 : 37
3-fluoro-6-methylaniline				
C2 : C4 : C5	0 : 100 : 0	0 : 100 : 0	7 : 93 : 0	25 : 70 : 5
3-fluoro-4-methylaniline				
C2 : C5 : C6	25 : 0 : 75	30 : 0 : 70	20 : 0 : 80	32 : 11 : 57
3-fluoroaniline				
C2 : C4 : C5: C6	5 : 84 : 0 : 11[c]	8 : 59 : 0 : 33	0 : 75 : 0 : 25[c]	18 : 44 : 5 : 33

[a] % of total ring hydroxylated products.

[b] % of total HOMO/HOMO-1 density on non-substituted ring carbon atoms.

[c] Results taken from Cnubben et al. [1].

Table 2 presents the calculated regioselectivity of the *in vivo* aromatic ring hydroxylation, as derived from the ^{19}F NMR urine spectra. The data show that the cytochrome P450-catalysed regioselectivity of the ring hydroxylation observed *in vivo* resembles the regioselectivity observed *in vitro* (Table 2) (correlation=0.99, absolute mean deviation=4.8 ± 4.1%).

Influence of chemical reactivity on the regioselectivity of aromatic hydroxylation

Molecular orbital computer calculations were performed in order to find out to what extent electronic characteristics of the 3-fluoro(methyl)anilines can account for the regioselectivity of aromatic ring hydroxylation upon their biotransformation by the cytochromes P450.

If aromatic ring hydroxylation proceeds by an initial attack of the cytochrome P450$(FeO)^{3+}$ species on the π-electrons of the aromatic ring without the formation of epoxide intermediates, the regioselectivity may be directed by the HOMO/HOMO-1 density distribution in the parent substrate [2]. Table 2 presents the predicted regioselectivity of the aromatic ring hydroxylation of our model compounds calculated on the basis of the HOMO/HOMO-1 densities in the benzene ring according to the equation of Fukui et al. [31]. From the results presented in Table 2 it can be derived that the observed cytochrome P450-catalysed regioselectivity deviates with an absolute mean value of 18.6 ± 11.3% from the predicted regioselectivity. This deviation is much larger than the 6.5 ± 2.7% absolute mean deviation observed in a previous study for the fluorinated benzenes [2]. For comparison, in Figure 3A the regioselectivity of the *in vivo* aromatic ring hydroxylation for this series fluorinated benzenes is plotted against the percentage hydroxylation predicted on the basis of the molecular orbital calculations. Figure 3B presents these results for 3-fluoro-2-methylaniline, 3-fluoro-6-methylaniline and 3-fluoroaniline, substrates with a hydrogen-substituted *para* C4 and *ortho* C2 and/or C6 position. The dotted line in Figures 3A and 3B presents the theoretical perfect correlation between the percentage of hydroxylation and the predicted value (slope=1.00, intercept=0.00). As can been seen from Figure 3A the data obtained with the fluorinated benzenes (slope=1.03, intercept=-1.21, correlation=0.96) almost match this theoretical line. The data obtained for the two fluorinated *ortho* methylanilines and 3-fluoroaniline, however, deviate from this theoretical line in a systematic manner. Non-substituted (i.e. hydrogen containing) C4 positions are hydroxylated to a significantly higher extent than predicted, whereas non-substituted C2 and C6 positions are always below the theoretical line and are, thus, hydroxylated to a lower extent than their chemical reactivity would predict.

23 Nakamura, S., Mashino, T., and Hirobe, M. (1992) ^{18}O Incorporation from $H_2{}^{18}O_2$ in the oxidation of N-methylcarbazole and sulfides catalyzed by microperoxidase-11. *Tetrahedron Lett.* 33, 5409-5412.

24 Du, P., and Loew, G.H. (1992) Role of axial ligand in the electronic structure of model compound I complexes. *Int. J. Quantum Chem.* 44, 251-261.

25 Boyland, E., Manson, D., and Sims, P. (1953) The preparation of O-aminophenyl sulphates. *J. Chem. Soc.*, 3623-3628.

26 Vervoort, J., De Jager, P.A., Steenbergen, J., and Rietjens, I.M.C.M. (1990) Development of a ^{19}F-n.m.r. method for studies on the *in vivo* and *in vitro* metabolism of 2-fluoroaniline. *Xenobiotica* 20, 657-670.

27 Brodie, B.B., and Axelrod, J. (1948) The estimation of acetanilide and its metabolic products, aniline, N-acetyl p-aminophenol and p-aminophenol (free and conjugated) in biological fluids and tissues. *J. Pharmacol. Exp. Ther.* 94, 22-28.

28 Omura, T., and Sato, R. (1964) The carbon monoxide-binding pigment of liver microsomes, I. Evidence for its hemoprotein nature. *J. Biol. Chem.* 239, 2370-2378.

29 Falk, J.E. (Ed.), Phorphyrins and Metalloporphyrins. Elsevier, Amsterdam, pp. 181 and 240.

30 Dewar, M.J.S., Zoebisch, E.G., Healy, E.F., and Stewart, J.J.P. (1985) AM1: A new general purpose quantum mechanical molecular model. *J. Am. Chem. Soc.* 107, 3902-3909.

31 Fukui, K., Yonezawa, T., Nagata, C., and Shingu, H. (1954) Molecular orbital theory of orientation in aromatic, heteroaromatic and other conjugated molecules. *J. Chem. Phys.* 22, 1433-1442.

32 Wray, V. (1983) Fluorine bonded to a carbon of an aromatic system, including condensed alicyclic aromatic systems. In: Annual reports on NMR spectroscopy (Webb, G.A., Ed.), vol. 14, Academic press, New York, pp. 249-281.

33 Rietjens, I.M.C.M., Cnubben, N.H.P., Van Haandel, M., Tyrakowska, B., Soffers, A.E.M.F., and Vervoort, J. (1995) Different metabolic pathways of 2,5-difluoronitrobenzene and 2,5-difluoroaminobenzene compared to molecular orbital substrate characteristics. *Chem.-Biol. Interact.* 94, 49-72.

34 Novak, R.F., and Vatsis, K.P. (1982) Proton fourier transform nuclear magnetic resonance relaxation rate studies on the interaction of acetanilide with purified isoenzymes of rabbit liver microsomal cytochrome P-450 and with cytochrome b5. *Mol. Pharmacol.* 21, 701-709.

35 Van de Straat, R., De Vries, J., De Boer, H.J.R., Vromans, R.M., and Vermeulen, N.P.E. (1987) Relationship between paracetamol binding to and its oxidation by two cytochrome P-450 isoenzymes-a proton nuclear magnetic resonance and spectrophotometric study. *Xenobiotica* 17, 1-9.

36 Balvers, W.G., Boersma, M.G., Veeger, C., and Rietjens, I.M.C.M. (1993) Kinetics of cytochromes P-450 IA1 and IIB1 in reconstituted systems with dilauroyl- and distearoyl-glycerophosphocholine. *Eur. J. Biochem.* 215, 373-381.

Chapter 4

^{1}H NMR T_1 relaxation rate study on substrate orientation of fluoromethylanilines in the active sites of microsomal and purified cytochromes P4501A1 and 2B1

J. Koerts, I.M.C.M. Rietjens, M.G. Boersma and J. Vervoort

FEBS Letters 368, 1995, 279-284.

Abstract

The present study describes ^{1}H NMR T_1 relaxation rate studies on fluoromethylanilines bound to the active sites of microsomal and purified cytochromes P4501A1 and 2B1. From the data obtained, insights into the average orientation of the substrates with respect to the paramagnetic Fe^{3+} centre in the cytochromes P450 could be derived. Particular attention was paid to a possible extra relaxation pathway for methyl protons compared to the aromatic protons, due to the rotational motion of the CH_3 around the σ-C-CH_3 bond. However, this effect appeared to be minimal and to result in at most a few percent underestimation of the actual distance of the methyl protons to the Fe^{3+} centre. Furthermore, the data obtained demonstrate that all aromatic protons are at about the same average distance from the paramagnetic centre. The results also demonstrate that the fluoromethylanilines are bound to the active sites of cytochromes P4501A1 and 2B1 in a similar way. A time-averaged orientation of the substrate with the Fe^{3+} above the aromatic ring, with the π-orbitals of the aromatic ring and those of the porphyrin rings in a parallel position, providing possibilities for energetically favourable π-π interaction defines the orientation which best fits the results of the present study. Possibilities for a flip-flop rotation around an axis in the plane of the aromatic ring can be included in this picture, as such rotations would still result in a similar average distance of all aromatic protons to the Fe^{3+} paramagnetic centre. The results obtained also indicate that possible differences in metabolic patterns resulting from conversion of the fluoromethylanilines by different cytochromes P450, especially P4501A1 and 2B1, are unlikely to be caused by a specific orientation of the substrate

imposed by the substrate binding site of the enzyme.

Introduction

Several studies in the literature describe T_1 relaxation measurements investigating the manner of binding of substrates to the active sites of cytochromes P450 [1-5]. All of these studies report a stereoselective orientation of the substrate in the active site of the cytochrome P450, or even a link between the observed specific way of binding of the substrate and the regioselectivity of its hydroxylation by different P450 isozymes. However, some investigations have reported conflicting results. For example, the stereoselective orientation of 4-hydroxyacetanilide with respect to the Fe^{3+} centre in cytochromes P4501A1 and 2B1 was indicated to be different, but the actual difference reported appeared to be opposite in independent studies [2,3]. Using ^1H NMR T_1 relaxation rate measurements, the acetamino group was reported to be closer to the Fe^{3+} in P4502B1 than in P4501A1 [2], whereas in a study using ^{15}N and ^{13}C T_1 relaxation rate measurements the opposite was concluded, and the nitrogen atom of the acetamido group was reported to be closer to the Fe^{3+} in cytochrome P4501A1 than in P4502B1 [3].

Furthermore, recent results with various halogenated benzene derivatives have provided evidence for the hypothesis that relatively small substrates become bound to the relatively aspecific and large active sites of the mammalian cytochromes P450 in such a way that the active site does not impose a stereoselective positioning of the substrate with respect to the (activated) metal centre. This conclusion follows from the observation that the regioselectivity of the aromatic hydroxylation of fluorobenzene derivatives and fluoroanilines did not vary significantly with change in the cytochrome P450 enzyme pattern catalysing the hydroxylation [6,7]. Instead, the regioselectivity of the aromatic hydroxylation of a series of fluorobenzenes and fluoroanilines could be explained and even predicted on the basis of the calculated reactivity of the various carbon centres for an electrophilic attack. Together, these results rather suggest an orientation of the aromatic substrate in the active site of the cytochromes P450 with all protons at equal average distances from the Fe^{3+} centre, providing no distance limitations to hydroxylations at specific positions on the basis of a protein-imposed stereoselective orientation of the substrate in the active site of the cytochromes P450.

The objective of the present study was to gain greater insights into this question related to the presence or absence of a stereoselective positioning of

relatively small substrates in the active sites of cytochromes P450. Cytochrome P4501A1 and cytochrome P4502B1 were used as the P450 enzymes for the study. Fluoromethylanilines were chosen as the model substrates. These substrates were chosen for several reasons. First, insight into factors that determine the regioselectivity of the cytochrome P450-catalysed conversion of methylanilines is of importance because N-hydroxylation pathways lead to bioactivation and mutagenic metabolites, whereas aliphatic side chain methyl and aromatic ring hydroxylations lead to products that can be excreted upon Phase II conjugation [8-12]. Second, the fluoromethylanilines are relatively small molecules. Third, the molecules contain an amino group that may be especially suitable for a possible specific orienting interaction with active site amino acids. Such an orienting interaction between a cytochrome P450 amino acid residue and an amino moiety of the substrate has for example been reported for cytochrome P450 debrisoquine 4-hydroxylase [13]. Fourth, the molecules contain a methyl substituent, which makes it possible to study whether the distances obtained for methyl protons, which have a possible additional relaxation pathway due to the rotation of the methyl group around the σ-C-CH_3 bond [14], can actually be compared to distances obtained for aromatic protons which lack this additional relaxation pathway. In addition, preferential side-chain C-hydroxylation of the methyl moiety over aromatic ring hydroxylation has been reported for *para*-methylanilines and toluene [15-17], while for *ortho*-methylaniline the opposite is true [18]. Information on average proton distances for both the methyl and the aromatic protons may provide an answer to the question of whether the preferential site for hydroxylation originates from a closer proximity of the respective hydrogens to the active Fe^{3+} centre of the cytochromes P450. Finally, the substrates have a good water solubility making T_1 NMR relaxation measurements under saturating substrate condition possible.

Materials and Methods

Chemicals

4-Fluoro-2-methylaniline, 3-fluoro-4-methylaniline and 3-fluoro-2-methylaniline were all obtained from Aldrich (Steinheim, Germany). 2-Fluoro-4-methylaniline was purchased from Acros Chimica (Geel, Belgium).

Protein preparations

Preparation of purified cytochromes P4501A1 and 2B1 as well as preparation of microsomes was carried out essentially as previously described [19,20]. The amount of cytochrome P450 was measured according to the method of Omura and Sato [21].

^1H NMR T_1 relaxation rate measurements

^1H NMR T_1 relaxation rate measurements were performed on a Bruker CXP 500 NMR spectrometer at 296.2 K. The longitudinal relaxation time (T_1) was determined by a 180°-90° inversion recovery method. Irradiation of the water signal was employed to reduce the disturbance by this resonance. The delay time (τ) between the pulses for the samples containing purified or microsomal cytochromes P450 and for the samples containing only substrate was 0.1 and 0.2 sec respectively. About 12 τ values were applied and 32 scans for each τ value were recorded. Samples contained 0.1 M potassium phosphate pH 7.25 (containing 20% glycerol) or a solution of (microsomal) cytochrome P450 in this buffer (final concentration 1.26 µM cytochrome P450), or 0.4 M potassium phosphate pH 7.4 (containing 20% glycerol) or a solution of purified cytochrome P450 in this buffer (final concentration 1.26 µM cytochrome P450), 0.1 mM EDTA, 5 mM substrate added from a 0.25 M stock solution in dimethyl sulfoxide and 1% D_2O for locking the magnetic field. The total sample volume was 0.511 ml. Samples were made oxygen free by four cycles of evacuation and filling with argon.

To correct for the diamagnetic contribution to the longitudinal relaxation time the T_1 of a blank containing CO-dithionite-reduced cytochrome P450 was determined.

The corrected T_1 value ($1/T_1corr = 1/T_1$ observed - $1/T_1$blank) was used to calculate the distance (r) of the respective proton to the paramagnetic iron essentially as described by Novak and Vatsis [1], using the Solomon-Bloembergen equation, assuming the Fe^{3+} in both P4501A1 and 2B1 to be in the high spin conformation [1,22,23], and taking a τ_c value of 10^{-10} . This value for τ_c for cytochromes P450 may actually vary between 10^{-10} and 10^{-11} [24]. However, using a factor of 10^{-11} would result in values that are 68% of those obtained with a value of 10^{-10}. This changes the absolute values of the distances obtained by a constant factor, and does not influence relative differences obtained for protons in one substrate molecule bound to the active site of a specific cytochrome P450.

Calculation of optimised fluoromethylaniline geometry

The optimised geometry for the various fluoromethylanilines was calculated on a Silicon Graphics Indigo^2 using Insight (Biosym, CA, USA). The semi-empirical molecular orbital method was used, applying the AM1 Hamiltonian from the AMPAC program.

Results

^{1}H NMR T_1 relaxation measurements on fluoromethylanilines bound to β-naphtoflavone and phenobarbital induced microsomal cytochromes P450

Previous ^{1}H NMR relaxation rate studies on the interaction of benzo(a)pyrene with microsomal cytochromes P450 clearly demonstrated that differences in the orientation of a substrate in the active sites of cytochromes P4501A1 and 2B1 can be detected in studies with respectively β-naphtoflavone and phenobarbital induced microsomal preparations, respectively [5]. Thus, as a first approach, the binding of several fluoromethylanilines to cytochromes P450 was studied using β-naphtoflavone and phenobarbital induced microsomal preparations. The cytochrome P450 population in these microsomes contains 71% and 55% of cytochrome P4501A1 and cytochrome P4502B1, respectively [25].

Figure 1 presents the results of a ^{1}H NMR T_1 relation measurement for 3-fluoro-2-methylaniline bound to phenobarbital induced microsomal cytochromes P450. A plot of the natural logarithm of the peak at infinite delay time (M_∞) minus the peak area at the specific delay time τ (M_τ) against this delay time τ gives a straight line with a slope of $-1/T_1$, from which the T_1 relaxation time can be derived (Figure 2). Tables 1 and 2 present the T_1 values thus obtained for the various substrate protons in the presence of microsomes from β-naphtoflavone and phenobarbital treated rats, respectively. T_1 values for the CO-reduced blank samples are also listed. From these T_1 and T_1 CO-blank values the distances of the respective protons to the Fe^{3+} centre in the active site of the microsomal cytochromes P450 were calculated, the results obtained are also being presented in Tables 1 and 2. The distances of the various aromatic protons to the Fe^{3+} cytochrome P450 metal centre do not vary significantly for the aromatic protons of the various fluoromethylanilines. Based on these results as well as the calculated optimal geometry of the fluoromethylaniline molecules, the expected distance for the methyl protons to the Fe^{3+} centre can be calculated. This was carried out assuming the Fe^{3+} centre to be at the measured distance away from the aromatic protons and, thus,

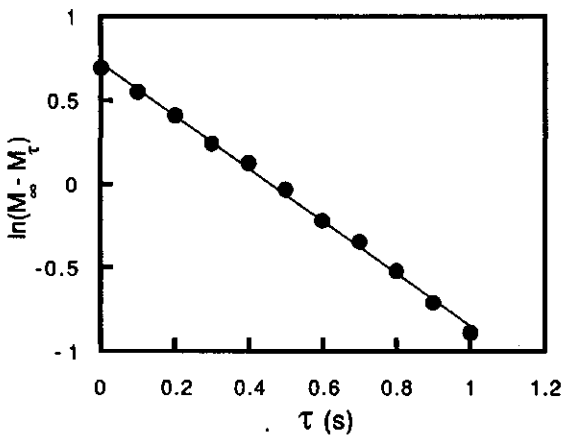

Figure 1 ^{1}H NMR spectra showing the inversion recovery sequence (180° - t -90° pulse sequence) of 3-fluoro-2-methylaniline in the presence of microsomal cytochrome P450 derived from phenobarbital pretreated rats. The water signal at 4.7 ppm is omitted.

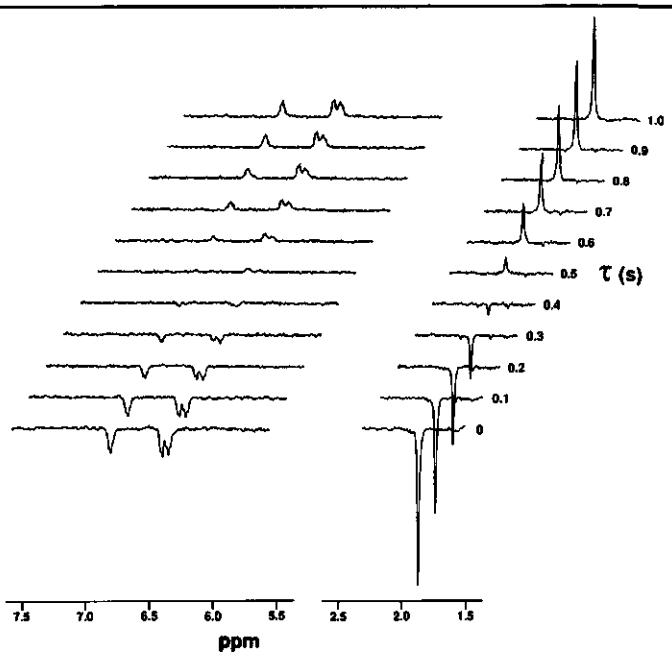

Figure 2 Plot showing ln (M_∞ - M_t) plotted against t for the H_4 proton of 3-fluoro-2-methylaniline in the presence of microsomal cytochrome P450 derived from phenobarbital pretreated rats (Figure 1). The slope of this curve equals $-1/T_1$.

Table 1 T_1 relaxation rates for protons of different fluoromethylanilines in a system containing microsomal cytochrome P450 from β-naphtoflavone pretreated rats, containing 71% P450 1A1 [25] and in a CO-dithionite reduced P450 blank sample (T_1 CO-blank). From these T_1 values the distances between the respective protons and the paramagnetic iron were calculated as described in Materials and Methods section.

substrate proton	T_1 (s)	T_1 CO-blank (s)	r (Fe-H) (Å)	r (Fe-Hmethyl) calculated (Å)
4-fluoro-2-methylaniline				
H_3	0.834 ± 0.034	1.187 ± 0.062	6.27 ± 0.39	
H_5	0.824 ± 0.087	1.202 ± 0.018	6.20 ± 0.06	
H_6	0.759 ± 0.013	1.086 ± 0.012	6.16 ± 0.04	
H_{CH3}	0.704 ± 0.004	0.848 ± 0.126	6.69 ± 0.62	6.65 ± 0.06
3-fluoro-2-methylaniline				
H_4	0.646 ± 0.065	0.908 ± 0.110	6.04 ± 0.08	
H_5	0.665 ± 0.120	0.927 ± 0.098	6.09 ± 0.70	
H_6	0.616 ± 0.074	0.846 ± 0.206	6.05 ± 0.07	
H_{CH3}	0.588 ± 0.019	0.727 ± 0.058	6.23 ± 0.21	6.51 ± 0.02
2-fluoro-4-methylaniline				
H_3	0.689 ± 0.109	0.955 ± 0.038	6.14 ± 0.36	
$H_5 + H_6$	0.609 ± 0.053	0.830 ± 0.093	6.06 ± 0.15	
H_{CH3}	0.564 ± 0.047	0.704 ± 0.084	6.28 ± 0.19	6.55 ± 0.05
3-fluoro-4-methylaniline				
H_2	0.482 ± 0.127	0.593 ± 0.067	6.18 ± 0.59	
$H_5 + H_6$	0.423 ± 0.001	0.561 ± 0.028	5.78 ± 0.08	
H_{CH3}	0.494 ± 0.033	0.597 ± 0.037	6.29 ± 0.07	6.44 ± 0.26

averaged in time above the centre of the aromatic ring. Comparison of the distances thus calculated and those actually observed demonstrates that the observed values are generally 96.5 ± 2.2% (n=8) of those calculated. This implies that, although the T_1 relaxation rate of the methyl protons in a fluoromethylaniline is generally faster than that of the aromatic protons, this effect is also observed in the blank and is independent of the presence of a paramagnetic centre. Thus, the distances obtained for the methyl protons can be well compared to those determined for the aromatic

protons.

Furthermore, comparison of the results presented in Tables 1 and 2 indicates that there are no significant differences between the distances observed with the two microsomal cytochrome P450 preparations, suggesting that the average way of binding and, more precisely, the average distance of the protons of a given substrate to the paramagnetic Fe^{3+} in the active site of the various cytochromes P450 are comparable.

Table 2 T_1 relaxation rates for protons of different fluoromethylanilines in a system containing microsomal cytochrome P450 from phenobarbital pretreated rats, containing 55% P450 2B1 [25] and in a CO-dithionite reduced P450 blank sample (T_1 CO-blank). From these T_1 values the distances between the respective protons and the paramagnetic iron were calculated as described in Materials and Methods section.

substrate proton	T_1 (s)	T_1 CO blank (s)	r (Fe-H) (Å)	r (Fe-Hmethyl) calculated (Å)
4-fluoro-2-methylaniline				
H_3	0.766 ± 0.033	1.100 ± 0.118	6.16 ± 0.26	
H_5	0.718 ± 0.035	1.033 ± 0.093	6.09 ± 0.30	
H_6	0.638 ± 0.004	0.944 ± 0.060	5.91 ± 0.10	
H_{CH3}	0.651 ± 0.014	0.838 ± 0.070	6.31 ± 0.04	6.50 ± 0.12
3-fluoro-2-methylaniline				
H_4	0.516 ± 0.106	0.958 ± 0.099	5.38 ± 0.25	
H_5	0.542 ± 0.164	0.893 ± 0.087	5.57 ± 0.55	
H_6	0.429 ± 0.064	0.794 ± 0.155	5.22 ± 0.19	
H_{CH3}	0.462 ± 0.096	0.743 ± 0.030	5.46 ± 0.34	5.89 ± 0.16
2-fluoro-4-methylaniline				
H_3	0.706 ± 0.152	0.941 ± 0.061	6.28 ± 0.47	
$H_5 + H_6$	0.646 ± 0.114	0.849 ± 0.081	6.23 ± 0.44	
H_{CH3}	0.581 ± 0.025	0.706 ± 0.052	6.44 ± 0.07	6.69 ± 0.03
3-fluoro-4-methylaniline				
H_2	0.398 ± 0.033	0.706 ± 0.035	5.20 ± 0.12	
$H_5 + H_6$	0.395 ± 0.007	0.691 ± 0.022	5.21 ± 0.06	
H_{CH3}	0.440 ± 0.064	0.664 ± 0.010	5.52 ± 0.31	5.72 ± 0.01

^1H NMR T_1 relaxation measurements on 4-fluoro-2-methylaniline and 2-fluoro-4-methylaniline bound to purified cytochromes P4501A1 and 2B1

To further support the observations obtained with the β-naphtoflavone and phenobarbital induced microsomal cytochromes P450, a ^1H NMR T_1 relaxation rate study was performed with purified cytochromes P4501A1 and 2B1 using two of the fluoromethylanilines as the substrate. The results obtained are presented in Table 3. Comparison of the results obtained with those listed in Tables 1 and 2 for the microsomal cytochromes P450 demonstrates that the average distances obtained with the purified enzymes are generally somewhat (17.7 ± 3.6%) longer than those observed with the microsomal cytochromes P450, however, the overall effects observed are similar. No significant differences are observed in the distances between the aromatic protons and the Fe^{3+} in the active site of the two enzymes.

Discussion

The ^1H NMR T_1 relaxation rate studies on fluoromethylanilines bound to the active sites of microsomal and purified cytochromes P4501A1 and 2B1 were used to investigate the presence or absence of a preferential orientation of the substrates in the active site of the cytochromes P450. Such a specific orientation would be reflected in different distances for the various protons in the substrates. An increased average distance of specific protons in the substrate molecule might result in an influence on the regioselectivity upon subsequent biotransformation to hydroxylated products. It should be mentioned that the actual orientation of the substrate bound to the Fe^{3+} resting state of the cytochrome P450 could be different from that of the substrate in the activated high-valent iron-oxo porphyrin form actually performing the hydroxylation step, as reported for thiocamphor bound to cytochrome $P450_{cam}$ [26]. However, an interaction between an active site amino acid and, for example the amino moiety of the substrate, could very well persist upon conversion of the Fe^{3+} form to the high-valent iron-oxo form of the enzyme and, thus, influence the regioselectivity of the hydroxylation by an effect on the actual distance of the possible reaction sites from the active metal centre. Such an influence of substrate orientation on the regioselectivity of the reaction imposed by the active site of the cytochrome P450 has been reported, for example, for amino-containing substrates converted by cytochrome P450 debrisoquine 4-hydroxylase [13], but have also been suggested for the conversion of, e.g., 4-hydroxyacetanilide by cytochrome P4501A1 or 2B1 [2,3]. However, from the data obtained in the present study for the binding of

Table 3 T_1 relaxation rates for 4-fluoro-2-methylaniline and 2-fluoro-4-methylaniline in a system containing purified cytochrome P4501A1 or 2B1 and in a CO-dithionite reduced P450 blank sample (T_1 CO-blank). From these T_1 values the distances between the respective protons and the paramagnetic iron were calculated as described in Materials and Methods section.

substrate proton	T_1 (s)	T_1 CO blank (s)	r (Fe-H) (Å)	r (Fe-Hmethyl) calculated (Å)
4-fluoro-2-methylaniline / cytochrome P4501A1				
H_3	1.638 ± 0.057	2.004 ± 0.034	7.61 ± 0.25	
H_5	1.649 ± 0.026	2.089 ± 0.078	7.44 ± 0.27	
H_6	1.424 ± 0.058	1.987 ± 0.389	6.91 ± 0.57	
H_{CH3}	1.084 ± 0.051	1.243 ± 0.007	7.54 ± 0.23	7.70 ± 0.35
4-fluoro-2-methylaniline / cytochrome P4502B1				
H_3	2.033 ± 0.155	2.858 ± 0.226	7.31 ± 0.81	
H_5	2.077 ± 0.176	2.926 ± 0.264	7.33 ± 0.74	
H_6	1.549 ± 0.436	2.694 ± 0.426	6.55 ± 0.47	
H_{CH3}	1.197 ± 0.137	1.465 ± 0.036	7.22 ± 0.40	7.45 ± 0.42
2-fluoro-4-methylaniline / cytochrome P4501A1				
H_3	1.191 ± 0.150	1.448 ± 0.090	7.25 ± 0.19	
$H_5 + H_6$	1.089 ± 0.133	1.305 ± 0.093	7.23 ± 0.23	
H_{CH3}	0.896 ± 0.103	1.008 ± 0.108	7.48 ± 0.42	7.62 ± 0.01
2-fluoro-4-methylaniline / cytochrome P4502B1				
H_3	1.718 ± 0.011	2.118 ± 0.030	7.63 ± 0.04	
$H_5 + H_6$	1.468 ± 0.039	1.814 ± 0.030	7.38 ± 0.18	
H_{CH3}	1.122 ± 0.038	1.220 ± 0.075	7.77 ± 0.39	7.87 ± 0.17

fluoromethylanilines to the active site of microsomal and purified cytochromes P4501A1 and 2B1, it follows that all aromatic protons are at about the same average distance from the paramagnetic centre. The results also demonstrate that the fluoromethylanilines are bound to the active sites of cytochromes P4501A1 and 2B1 in a similar way. Thus the binding characteristics of the relatively small fluoromethylanilines to the active sites of cytochrome P4501A1 and 2B1 provide no

indications for a stereoselective orientation that may influence the regioselectivity of the oxidation.

Special attention was paid to the average distance obtained from the T_1 relaxation measurements for the methyl protons in the fluoromethylanilines. This was done for two reasons, first, the existence of an extra relaxation pathway for methyl protons compared to aromatic protons, due to a rotational motion of the CH_3 around the σ-C-CH_3 bond, might hamper the comparison of distances obtained for aromatic protons to those determined for methyl protons. Second, preferential side-chain C-hydroxylation of the methyl moiety over aromatic ring hydroxylation has been reported for *para*-methylanilines. Information on average proton distances for both the methyl and the aromatic protons provides an answer to the question of whether this preferential side chain C-hydroxylation originates from a closer proximity of the methyl than of the aromatic protons to the active Fe^{3+} centre of the cytochromes P450. Clearly, the results of the present study provide support for the methyl protons having higher T_1 relaxation rates than the aromatic protons, but the same effect is observed in the T_1 relaxation rates of the CO-reduced blanks, resulting in calculated average distances for the methyl protons that can be reliably compared to distances obtained for aromatic protons. The actual distances observed indicate that the methyl protons are not closer to the Fe^{3+} paramagnetic centre than the aromatic protons, providing no basis for the easier hydroxylation of the *para*-methylanilines at the methyl group than in the aromatic ring.

Taken together, the results obtained support a time-averaged orientation of the substrate in the active site in which the location of the Fe^{3+} is above the aromatic ring, with the π-orbitals of the aromatic ring and the π-orbitals of the porphyrin rings in a parallel position providing possibilities for energetically favourable π-π interaction. Possibilities for a flip-flop rotation around an axis in the plane of the aromatic ring can be included in this picture, as such rotations would still result in a similar average distance of all aromatic protons to the Fe^{3+} paramagnetic centre.

Furthermore, the results obtained in the present study support the conclusion that possible differences in metabolic patterns resulting from conversion of the fluoromethylanilines by different cytochromes P450, especially P4501A1 and 2B1, and also the preferential sites for hydroxylation of the various sites in fluoro-methylanilines, are unlikely to be defined by a specific orientation of the substrate, imposed by the substrate binding site of the cytochromes P450. This conclusion supports previous conclusions from studies on regioselectivity of aromatic hydroxylation, from which it emerged that chemical reactivity instead of stereoselective binding imposed by the amino acids of the active site of the

cytochromes P450 is the major determinant in setting the outcomes of the regioselectivity of the hydroxylation of relatively small benzene derivatives by cytochromes P450 [6,7].

References

1 Novak, R.F., and Vatsis, K.P. (1982) Proton fourier transform nuclear magnetic resonance relaxation rate studies on the interaction of acetanilide with purified isoenzymes of rabbit liver microsomal cytochrome P-450 and with cytochrome b5. *Mol. Pharmacol.* 21, 701-709.

2 Van de Straat, R., De Vries, J., De Boer, H.J.R., Vromans, R.M., and Vermeulen, N.P.E. (1987) Relationship between paracetamol binding to and its oxidation by two cytochrome P-450 isoenzymes-a proton nuclear magnetic resonance and spectrophotometric study. *Xenobiotica* 17, 1-9.

3 Myers, T.G., Thummel, K.E., Kalhorn, T.F., and Nelson, S.D. (1994) Preferred orientations in the binding of 4'-hydroxyacetanilide (acetaminophen) to cytochrome P450 1A1 and 2B1 isoforms as determined by ^{13}C- and ^{15}N-NMR relaxation studies. *J. Med. Chem.* 37, 860-867.

4 Crull, G.B., Kennington, J.W., Garber, A.R., Ellis, P.D., and Dawson, J.H. (1989) ^{19}F Nuclear magnetic resonance as a probe of the spatial relationship between the heme iron of cytochrome P-450 and its substrate. *J. Biol. Chem.* 264, 2649-2655.

5 Castro-Maderal, L., and Sullivan, P.D. (1992) Proton NMR study of the interaction of benzo(a)pyrene with rat liver microsomal cytochrome P-450. *FEBS Lett.* 296, 249-253.

6 Cnubben, N.H.P., Vervoort, J., Veeger, C., and Rietjens, I.M.C.M. (1992) Study on the regioselectivity and mechanism of the aromatic hydroxylation of monofluoroanilines. *Chem.-Biol. Interact.* 85, 151-172.

7 Rietjens, I.M.C.M., Soffers, A.E.M.F., Veeger, C., and Vervoort, J. (1993) Regioselectivity of cytochrome P-450 catalyzed hydroxylation of fluorobenzenes predicted by calculated frontier orbital substrate characteristics. *Biochemistry* 32, 4801-4812.

8 Zimmer, D., Mazurek, J., Petzold, G., and Bhuyan, B.K. (1980) Bacterial mutagenicity and mammalian cell DNA damage by several substituted anilines. *Mutat. Res.* 77, 317-326.

9 Yoshimi, N., Sugie, S., Iwata, H., Niwa, K., Mori, H., Hashida, C., and Shimizu, H. (1988) The genotoxicity of a variety of aniline derivatives in a DNA repair test with primary cultured rat hepatocytes. *Mutat. Res.* 206, 183-191.

10 Arhenius, E. (1969/70) Effects of various *in vitro* conditions on hepatic microsomal *N*- and *C*-oxygenation of aromatic amines. *Chem.-Biol. Interact. 1*, 361-380.

11 Kiese, M. (1963) The effect of certain substituents upon the N-oxidation of aniline in vivo. *Naunyn-Schmiedebergs Arch. Exp. Pathol. Pharmakol.* 244, 387-404.

12 Pai, V., Bloomfield, S.F., Jones, J., and Gorrod, J.W. (1978) Mutagenicity testing of nitrogenous compounds and their N-oxidised products using TRP^+ reversion in E. coli. In: Biological Oxidation of Nitrogen (Gorrod, J.W., Ed.), Elsevier/Nort-Holland Biomedical Press, New York, pp. 375-382.

13 Wolff, T., Distlerath, L.M., Worthington, M.T., Groopman, J.D., Hammons, G.J., Kadbular, F.F., Prough, R.A., Martin, M.V. and Guengerich, F.P. (1985) Substrate specificity of human liver cytochrome P-450 desbrisoquine 4-hydroxylase probed using immunochemical inhibition and chemical modeling. *Cancer Res.* 45, 2116-2122.

14 Kalk, A., and Berendsen, H.J.C. (1976) Proton magnetic relaxation and spin diffusion in proteins. *J. Mag. Res.* 24, 343-366.

15 Boeren, S., Tyrakowska, B., Vervoort, J., De Hoffman, E., Teunis, K., Van Veldhuizen, A., and Rietjens, I.M.C.M. (1992) Rat liver microsomal metabolism of 2-halogenated 4-methylanilines. *Xenobiotica* 22, 1403-1423.

16 Tyrakowska, B., Boeren, S., Geurtsen, B., and Rietjens, I.M.C.M. (1993) Qualitative and quantitative influences of ortho chlorine substituents on the microsomal metabolism of 4-toluidines. *Drug Metab. Dispos.* 21, 508-519.

17 Hanzlik, R.P., and Ling, K-H.J. (1990) Active site dynamics of toluene hydroxylation by cytochrome P-450. *J. Org. Chem.* 55, 3992-3997.

18 Son, O.S., Everett, D.W., and Fiala, E.S. (1980) Metabolism of o-[methyl-^{14}C]toluidine in the F344 rat. *Xenobiotica* 10, 457-468.

19 Rietjens, I.M.C.M., and Vervoort, J. (1989) Microsomal metabolism of fluoroanilines. *Xenobiotica* 19, 1297-1305.

20 Balvers, W.G., Boersma, M.G., Veeger, C., and Rietjens, I.M.C.M. (1992) Differential cumene hydroperoxide sensitivity of cytochrome P450 enzymes IA1 and IIB1 determined by their way of membrane incorporation. *Biochim. Biophys. Acta* 1117, 179-187.

21 Omura, T., and Sato, R. (1964) The carbon monoxide-binding pigment of liver microsomes, I. Evidence for its hemoprotein nature. *J. Biol. Chem.* 239, 2370-2378.

22 Mildvan, A.S., and Gupta, R.K. (1978) Nuclear relaxation measurements of the geometry of enzyme-bound substrates and analogs. *Methods Enzymol.* 49, 322-359.

23 Wolf, C.R., and Oesch, F. (1983) Isolation of a high spin form of cytochrome P-450 induced in rat liver by 3-methylcholanthrene. *Biochem. Biophys. Res. Commun.* 111, 504-511.

24 Bertini, I., Banci, L., and Luchinat, C. (1989) Proton magnetic resonance metalloproteins. *Methods Enzymol.* 177, 246-263.

25 Thomas, P.E., Reik, L.M., Ryan, D.E., and Levin, W. (1983) Induction of two immunochemically related rat liver cytochrome P-450 isozymes, cytochromes P-450c and P-450d, by structurally diverse xenobiotics. *J. Biol. Chem.* 258, 4590-4598.

26 Paulsen, M.D., and Ornstein, R.L. (1993) Substrate mobility in thiocamphor-bound cytochrome $P450_{cam}$: An explanation of the conflict between the observed product profile and the X-ray structure. *Protein Engng.* 6, 359-365.

Chapter 5

Microperoxidase / H_2O_2-catalyzed aromatic hydroxylation proceeds by a cytochrome P450-type oxygen-transfer reaction mechanism

A.M. Osman, J. Koerts, M.G. Boersma, S. Boeren, C. Veeger and I.M.C.M. Rietjens

European Journal of Biochemistry 240, 1996, 232-238.

Abstract

The mechanism of aromatic hydroxylation of aniline and phenol derivatives in a H_2O_2 driven microperoxidase-8 (MP-8)-catalyzed reaction was investigated. It was shown that the reaction was not inhibited by the addition of scavengers of superoxide anion or hydroxyl radicals, which demonstrates that the reaction mechanism differs from that of the aromatic hydroxylation catalyzed by a horseradish peroxidase/dihydroxyfumarate system. Additional experiments with ^{18}O labelled $H_2{}^{18}O_2$ demonstrated that the oxygen incorporated into aniline to give 4-aminophenol originates from H_2O_2. Furthermore, it was found that the addition of ascorbic acid efficiently blocks all peroxidase-type of reactions that can be catalyzed by the MP-8/H_2O_2 system, but does not inhibit the aromatic hydroxylation of aniline and phenol derivatives. Together, these observations exclude reaction mechanisms for the aromatic hydroxylation that proceed through peroxidase-type of mechanisms in which the oxygen incorporated into the substrate originates from O_2 or H_2O. The mechanism instead seems to proceed by an initial attack of the high-valent iron-oxo intermediate of MP-8 on the π-electrons of the aromatic ring of the substrate leading to product formation by a cytochrome P450-type of σ-O-addition or oxygen-rebound mechanism. This implies that MP-8, which has a histidyl and not a cysteinate fifth axial ligand, is able to react by a cytochrome P450-like oxygen-transfer reaction mechanism.

Introduction

Microperoxidase-8 (MP-8) is a heme octapeptide obtained by enzymatic hydrolysis of horse-heart cytochrome c [1-3]. It contains a heme cofactor that is a protoporphyrin IX with an iron centre that exists in the ferric resting state, and is able to react with hydrogen peroxide to form high-valent iron-oxo intermediates that could be analogous to compounds I and II of horseradish peroxidase [4,5]. The ability of MP-8 to catalyze peroxidase-type of reactions has been well documented [6-9]. In addition to the peroxidase behaviour of MP-8, it has been claimed that MP-8 catalyzes cytochrome P450-like reactions such as the hydroxylation of aniline to give 4-aminophenol [10] and N-demethylations as well as S-oxygenations [11]. However, a major difference between the heme cofactor of (micro)peroxidases and cytochromes P450 is the nature of the axial ligand. In classical peroxidases and in MP-8, the iron retains histidine as its fifth ligand, whereas in cytochromes P450 the fifth ligand is a cysteinate. In the present study, the actual reaction pathway involved in the MP-8-catalyzed aromatic hydroxylation was investigated in more detail. This was done especially because the formation of 4-aminophenol from aniline in itself does not prove that MP-8 can react as a cytochrome P450.

Previously the hydroxylation of aromatic substrates was reported to be observed in a horseradish peroxidase/dihydroxyfumarate/oxygen system but not in a H_2O_2-driven horseradish peroxidase system [12,13]. The mechanism of this horseradish peroxidase-mediated hydroxylation has been demonstrated to be completely different from the reaction pathway for the peroxidase activity of the enzyme and also different from the reaction pathways for aromatic hydroxylation by cytochromes P450 [14]. For instance, the chemistry of high-valent iron-oxo compounds I and II is not involved in the horseradish peroxidase/ dihydroxyfumarate-mediated aromatic hydroxylations. Instead, the aromatic hydroxylation has been reported to proceed through the involvement of superoxide anion radicals [14,15].

Possible mechanisms for the aromatic hydroxylation that do include a role for the high-valent iron-oxo compounds I and II are depicted in Figure 1. The first pathway presented is analogous to the so-called oxygen-rebound mechanism suggested for cytochrome P450-mediated reactions [16] and proceeds through an initial one-electron oxidation of the substrate by compound I to give compound II and a substrate radical which easily loses a proton (step A, Figure 1). A so-called oxygen-rebound of compound II to the one-electron-oxidized substrate molecule (step B, Figure 1) provides a pathway leading to formation of a monooxygenated

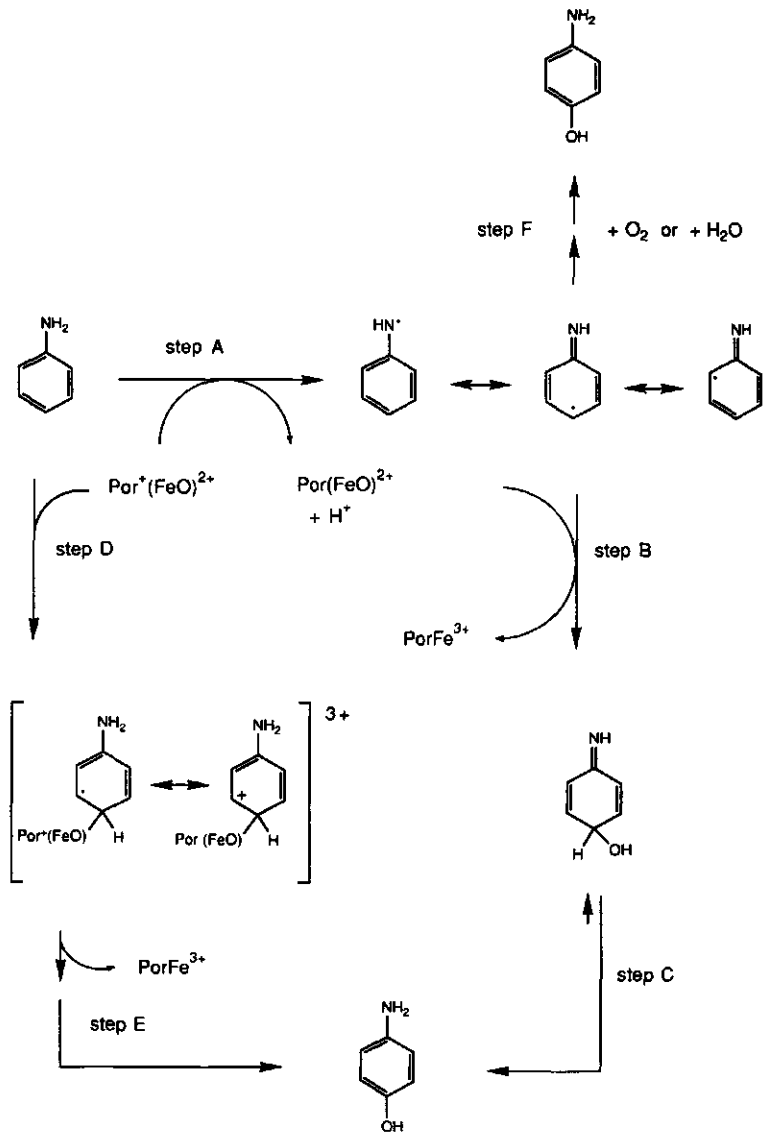

Figure 1 Schematic presentation of possible pathways for P450- and peroxidase-type of aromatic hydroxylation mechanisms by high-valent iron-oxo compound I (the exact nature and electron distribution in the high-valent iron-oxo species presented in this figure still requires unequivocal identification). Aniline is taken as an example, similar pathways can be presented for the aromatic hydroxylation of a phenol derivative. Steps A-C represent the so-called P450-type oxygen-rebound mechanism, whereas steps D and E represent the so-called σ-O-addition mechanism. Peroxidase-type of mechanisms are initiated by initial one-electron oxidation (step A) followed by oxygen incorporation through a reaction of the substrate radical with O_2 or H_2O (step F) [11]. See text for further details

product, which, upon keto-enol tautomerism (step C, Figure 1), gives rise to the 4-aminophenol. This pathway presents the so-called oxygen-rebound-type of P450 mechanism (steps A-C, Figure 1). In contrast, one-electron oxidation of a second substrate molecule by compound II would present the mechanism of a classical peroxidase reaction, in which dimerization or disproportionation of the two substrate radicals results in formation of the peroxidase-type products.

Another possible P450-type of reaction pathway depicted in Figure 1 is the so-called σ-O-addition mechanism proceeding by an initial addition of compound I to the reactive π-electrons of the aromatic substrate (step D, Figure 1). Rearrangement within the σ-O-adduct can give rise to the hydroxylated product (step E, Figure 1) [16,17].

Finally, peroxidase-type of reaction mechanisms can be considered. In these peroxidase-type mechanisms, the oxygen atom incorporated in the aromatic substrate is not derived from H_2O_2, but originates from O_2 or H_2O. They would proceed through an initial one electron oxidation of the substrate by compound I (step A, Figure 1) followed by reactions of the substrate radicals with O_2 or H_2O/OH^- [11] (step F, Figure 1).

In the present study, it was investigated whether the MP-8/H_2O_2-catalyzed aromatic hydroxylation proceeds by a peroxidase- or P450-type of reaction mechanism.

Materials and Methods

Chemicals

Microperoxidase (MP-8) was prepared by the proteolytic digestion of horse-heart cytochrome c essentially as described by Aron et al. [3] and concentrations were determined by the pyridine chromogen method [3]. Based on HPLC analysis, the purity of the MP-8 preparation used in this study is estimated at over 96%. Horseradish peroxidase, catalase and superoxide dismutase (SOD) were purchased from Boehringer (Mannheim, Germany). Aniline, 4-aminophenol, 2-aminophenol, 3-fluoroaniline and 2-fluorophenol were obtained from Janssen (Beerse, Belgium). Hydroquinone was from Aldrich (Steinheim, Germany), phenol from Merck (Darmstadt, Germany), and 2,2'-biphenol and 4,4'-biphenol from Sigma (St. Louis, MO). L-Ascorbic acid was obtained from Merck. All substrates were of 98-99% purity. Hydrogen peroxide (30%) was from Merck and was diluted in water to

obtain the required 50 mM stock solution. All other reagents used were analytical grade. $H_2{}^{18}O_2$ (2%) was obtained from Icon (Sunnit, New Jersey, USA).

Incubation conditions

A typical reaction mixture (total volume of 1.0 ml) contained the following (final concentrations): 3.0 mM ascorbic acid, 10 mM aniline (at 10 mM concentration of aniline the initial velocity of reaction approaches V_{max}, and is thus optimum for the product formation) or 1 mM 2-fluorophenol, 7.5 μM MP-8 or 5 μM horseradish peroxidase in 0.1 M potassium phosphate pH 7.6. The reaction mixture was preincubated at 37 °C for 2 min. The reaction was started by the addition of hydrogen peroxide (2.5 mM final concentration). The reaction was carried out for 1 min at 37 °C, and either injected directly onto the column or stopped by freezing the samples into liquid nitrogen until analysis was performed.

Aniline and phenol derivatives were added as 1% (v/v) of a 100 times concentrated stock solution in dimethyl sulfoxide to give the final concentration required. These optimized reaction conditions were chosen on the basis of experiments described hereafter (see Results section, Figure 2).

Chemical determination of the concentration of 4-aminophenol

For the chemical determination of 4-aminophenol, the reaction was terminated by adding 0.8 ml of the reaction mixture to 0.24 ml of 20% (w/v) of trichloroacetic acid. After centrifugation for 5 min at 13000 rpm, the supernatant was used for the determination of the concentration of 4-aminophenol following the procedure previously described [18]. It is important to note that the presence of ascorbic acid in the reaction mixture retarded the normal time of colour development. For this reason, the absorbance at 630 nm (the ε value at 630 nm is 30.5 $mM^{-1}cm^{-1}$) was measured after 4 h instead of 1 h incubation at room temperature. A calibration curve of 4-aminophenol in the presence of ascorbic acid demonstrated that the absorption coefficient of the indophenol was not affected by the addition of ascorbic acid.

^{19}F NMR analysis

The volume of the reaction mixture was increased to 2.0 ml for samples for NMR analysis, and at the end of the incubation 325 U of catalase were added to

prevent H_2O_2-driven product degradation during the overnight ^{19}F NMR measurement. The final NMR sample consisted of 1.60 ml reaction mixture to which 100 µl of ^2H_2O was added for locking the magnetic field and 10 µl 8.4 mM 4-fluorobenzoic acid was added as internal standard. The samples were made oxygen-free by four cycles of evacuation and filling with argon.

^{19}F NMR analysis was performed on a Bruker AMX 300 spectrometer as previously described [19]. Quantification of the fluorinated compounds in the samples was performed by comparing the integrals of their ^{19}F NMR resonances of 4-fluorobenzoic acid used as an internal standard.

High Performance Liquid Chromatography (HPLC)

50 µl of sample was injected into a HPLC system equipped with a reverse-phase Lichrosorb 5RP8 column (100 mm × 3 mm). Ultraviolet detection was performed with a Waters 996 diode array detector. Products were identified and quantified using commercially available standards (e.g. 4-aminophenol, 2-aminophenol, 2-2'-biphenol, 4-4'-biphenol, and hydroquinone). Elution was carried out at 1.0 ml/min starting with 100% water, maintaining 100% water for 1 min, followed by a linear gradient to give 27.7% of methanol in water in 10 min.

Analysis by Gas Chromatography-Mass Spectrometry (GC-MS)

For reaction mixtures analysed by GC-MS, the sample volume was increased to 10 ml, the MP-8 concentration was increased to 83.8 mM, and in some cases $H_2{}^{18}O_2$ instead of H_2O_2 was used. At the end of the incubations, 2600 U of catalase were added to prevent possible H_2O_2-driven product formation upon further processing of the sample. The reaction mixture was extracted four times with 1.0 ml of ethyl acetate. The collected ethyl acetate fractions were concentrated by evaporation to about 50 µl and the sample thus obtained was used for GC-MS (the yield of the ethyl acetate extraction step was more than 98%).

Of this preparation, a 2-µl or 5 µl-sample was injected into the GC-MS system. The gas chromatograph (Hewlett Packard 5890) was equipped with a 30 m × 250 µm capillary DB17 column. The carrier gas was helium at a flow of about 20 ml/min. A temperature gradient from 70 °C to 200 °C for 13 min was used. The column was connected to a Hewlett Packard 5970 mass spectrometer.

Results

Definition of reaction conditions

Figure 2 shows part of the results of experiments that were performed to define appropriate conditions for MP-8-catalyzed aromatic hydroxylation. Aniline was used as the model substrate to study product formation as a function of time, concentration of H_2O_2, concentration of MP-8, and pH. The 4-aminophenol formation increases linearly with increasing concentration of MP-8 up to at least 100 mM of MP-8 (data not shown). The dependence of 4-aminophenol formation on the concentration of H_2O_2 is presented in Figure 2a. Initially, the rate of the reaction increases with increasing concentration of hydrogen peroxide following saturation kinetics. At higher H_2O_2 concentrations the extent of product formation declines, most likely due to the rapid destruction of MP-8 and/or the reaction product by H_2O_2. Additional results (data not shown) demonstrate that the product formation is not linear in time. Following a non-linear increase in the first minute, product formation is no longer observed, due to inactivation of the mini-catalyst by an as yet unidentified mechanism. Similar peroxide-dependent inactivation has been reported for other heme-based enzymes [20,21].

Figure 2b shows the effect of varying pH on MP-8/H_2O_2-catalyzed aniline 4-hydroxylation. The optimum pH for aniline hydroxylation by MP-8/H_2O_2 in the presence of ascorbic acid is rather broad, in the range pH 7.6-9.5 (Figure 2b). No significant difference was observed using different buffers at overlapping pH values. At pH values below 6.2, activity was no longer observed. It is interesting to note that the rate versus pH profile is consistent with that reported for aniline hydroxylation by a cytochrome P450/cumene hydroperoxide system [22].

Based on these results, the standard reaction conditions for further experiments on the mechanism of the MP-8-catalyzed aromatic hydroxylation were chosen (final concentration): 7.5 μM MP-8, 2.5 mM H_2O_2, 0.1 M potassium phosphate pH 7.6, and 1 min incubation time.

Effect of radical scavengers on MP-8 /H_2O_2-mediated aromatic hydroxylation

To investigate a possible role of superoxide anions ($O_2^{-\bullet}$) and/or hydroxyl ($OH^\bullet$) radicals in the mechanism of MP-8-mediated aromatic hydroxylation, the effect of various radical scavengers on the 4-hydroxylation of aniline by MP-8 was investigated. The scavengers used were superoxide dismutase, mannitol, ethanol, formate, and Tris. All are reported to be effective, at the concentrations used in our

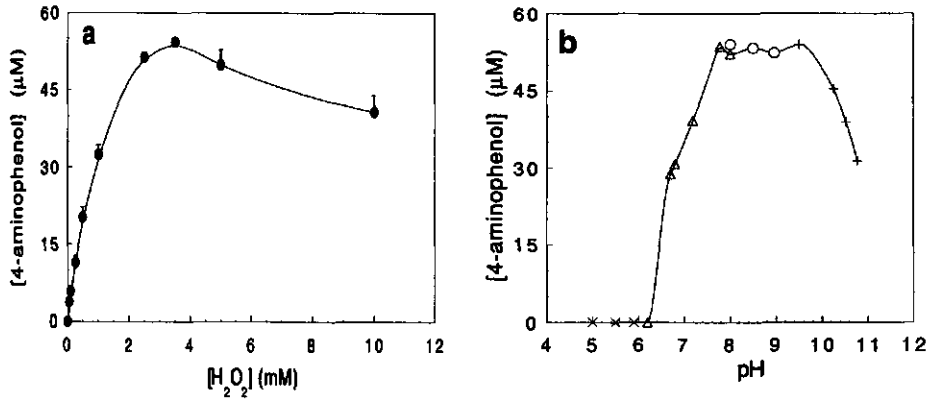

Figure 2 Dependence of 4-hydroxyaniline formation on (a) the concentration of H_2O_2 (10 mM aniline, 7.5 μM MP-8, 2 mM ascorbic acid, 1 min incubation time, 0.1 M potassium phosphate, pH 7.6), (b) pH (10 mM aniline, 2.5 mM H_2O_2, 7.5 μM MP8, 2 mM ascorbic acid, 1 min incubation time). The following buffers (0.1 M final concentration) were used: (×) sodium acetate; (Δ) potassium phosphate; (O) tricin; (+) potassium carbonate.

experiments, in the inhibition of aromatic hydroxylation by a horseradish peroxidase /dihydroxyfumarate system [14,15,23]. The rate constants reported for the reaction between the scavengers (mannitol, formate, ethanol) and hydroxyl radicals are in the order of 10^9 M^{-1} s^{-1}, indicating that the reaction is almost diffusion limited [15,24]. In addition, Mn^{2+} was used, because Mn^{2+} was also reported to be capable of inhibiting the horseradish peroxidase/dihydroxyfumarate-catalyzed reaction [13,15]. The results obtained from these experiments (Table 1) clearly show that none of the scavengers tested affects the MP-8/H_2O_2-catalyzed aniline hydroxylation either in the presence and or in the absence of ascorbic acid. These results indicate that the reaction mechanism of the MP-8/H_2O_2-catalyzed aromatic hydroxylation is different from that of the horseradish peroxidase/dihydroxyfumarate-catalyzed reaction and also that the MP-8/H_2O_2-catalyzed aromatic hydroxylation is unlikely to proceed through formation of $O_2^{-\bullet}$ and/or $OH^\bullet$ radicals.

The increased amount of 4-aminophenol observed in incubations with ascorbic acid as compared to the incubations without ascorbic acid most likely has to be ascribed to inhibition by ascorbic acid of the autoxidation of the 4-aminophenol.

Table 1 The effect of radical scavengers on MP-8/H_2O_2-catalyzed hydroxylation of aniline to 4-aminophenol.

Incubation conditions (final concentration of scavenger)		4-Aminophenol formed μM/min	%
MP-8 + ascorbic acid + H_2O_2		54.0	100
+ Mn^{2+}	(0.10 mM)	54.0	100
+ SOD	(0.01 mg/ml)	53.5	99.0
+ Mannitol	(10 mM ; 100 mM)	52.4 ; 54.1	97.0 ; 100
+ Ethanol	(10 mM ; 100 mM)	55.2 ; 56.0	102 ; 104
+ Formate	(10 mM ; 100 mM)	52.7 ; 55.6	97.6 ; 103
+ Tris	(50 mM ; 100 mM)	55.5 ; 54.8	103 ; 100
MP-8 + H_2O_2		14.5	100
+ Mn^{2+}	(0.10 mM)	14.8	102
+ SOD	(0.01 mg/ml)	15.6	108
+ Mannitol	(10 mM ; 100 mM)	14.5 ; 15.6	100 ; 108
+ Ethanol	(10 mM ; 100 mM)	15.0 ; 13.8	103 ; 95.2
+ Formate	(10 mM ; 100 mM)	15.0 ; 14.2	103 ; 97.9
+ Tris	(50 mM ; 100 mM)	15.5 ; 14.4	107 ; 99.3

Origin of the oxygen in 4-aminophenol formed from aniline by MP-8 /H_2O_2

Figure 3 shows the mass spectrum of molecular ion region of 4-aminophenol observed in an incubation of aniline with MP-8 in either the presence of unlabelled H_2O_2 (Figure 3a) or ^{18}O labelled $H_2{}^{18}O_2$ (Figure 3b). Comparison of the two mass spectra demonstrates that the mass of the 4-aminophenol is at m/z 109 for the incubation with unlabelled H_2O_2, but increases to m/z 111 when $H_2{}^{18}O_2$ is used. The mass spectrum in Figure 3b no longer contains a peak at m/z 109. This proves that the oxygen atom incorporated in aniline to give 4-aminophenol originates

fully from H_2O_2.

In addition, experiments carried out in the absence of molecular oxygen further confirmed that the oxygen did not arise from O_2, as product formation was not inhibited under anaerobic conditions (data not shown).

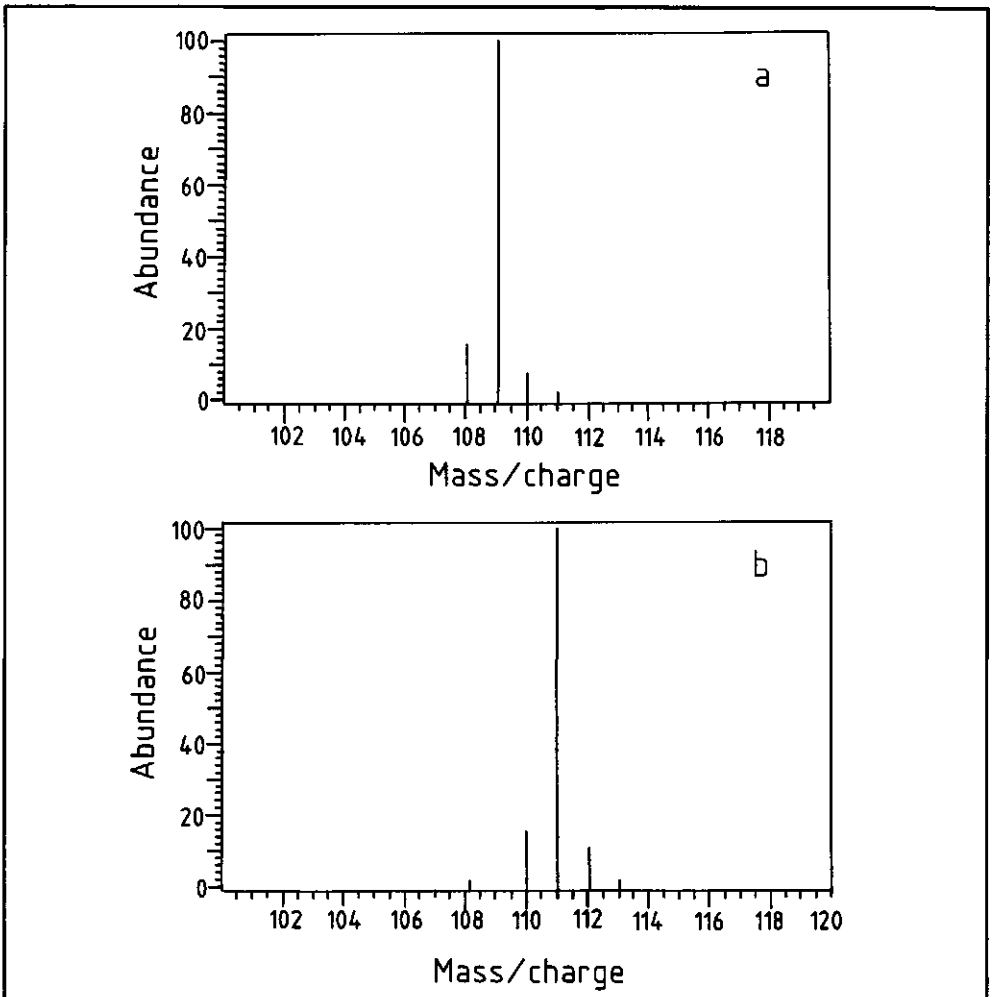

Figure 3 The mass spectra of the molecular ion region of 4-aminophenol obtained from the extraction of incubations of aniline with MP-8 in the presence of (a) unlabelled H_2O_2 or (b) ^{18}O-labelled $H_2{}^{18}O_2$.

Effect of ascorbic acid on MP-8/H_2O_2-catalyzed peroxidase activity

Ascorbic acid may inhibit peroxidase reactions by chemically reducing the initial substrate radical formed in step A Figure 1, back to the parent substrate [25,26]. Therefore, further experiments were performed in order to investigate whether ascorbic acid also inhibits peroxidase-type of conversions by MP-8/H_2O_2. For this purpose, the effect of ascorbic acid on model peroxidase-type of reactions was first investigated. When ascorbic acid was present in the incubation mixture in assays with *o*-dianisidine, acetaminophen and guaiacol, which are standard substrates for the measurement of peroxidase activity [3,8,26], formation of the peroxidative products was completely inhibited (data not shown). This capacity of ascorbic acid to inhibit peroxidase type of product formation was confirmed in incubations with horseradish peroxidase and H_2O_2. Thus, ascorbic acid is able to effectively block peroxidase-type of conversions by H_2O_2-driven MP-8 and H_2O_2-driven horseradish peroxidase systems.

These results were further confirmed by additional experiments. First, Figure 4 shows HPLC chromatograms that demonstrate the effect of ascorbic acid on MP-8/H_2O_2-catalyzed conversion of phenol. In the absence of ascorbic acid (Figure 4a), formation of dimeric products was observed which could be identified as 4,4'-diphenol and 2,2'-diphenol on the basis of added reference compounds. This conversion presents a classical peroxidative-type of conversion which could be confirmed by the observation that incubation of horseradish peroxidase with H_2O_2 and phenol, also in the absence of ascorbic acid, gave rise to an identical HPLC pattern and, thus, similar product formation. When ascorbic acid was present in the incubations formation of the peroxidative products was no longer observed (Figure 4b). In contrast, formation of the product resulting from monooxygenation of phenol, i.e. hydroquinone, is observed in the presence of ascorbic acid (Figure 4b).
Table 2 summarizes similar results obtained with aniline and 2-fluorophenol as the model substrates. It is clear from Table 2 that, in contrast to MP-8, HRP does not catalyze aromatic hydroxylation in the presence or in the absence of ascorbic acid. This difference between HRP and MP-8, HRP being unable but MP-8 being able to catalyze oxygen incorporation in an aromatic substrate, can most likely be best explained by a barrier between the substrate and the high-valent iron-oxo species of HRP [20,21]. There are very likely quite different steric constraints in getting to the oxygen of the activated iron porphyrin of MP-8 and HRP. The iron complex of MP-8 is much more accessible than that of HRP and this could in fact explain the lower reactivity of HRP.

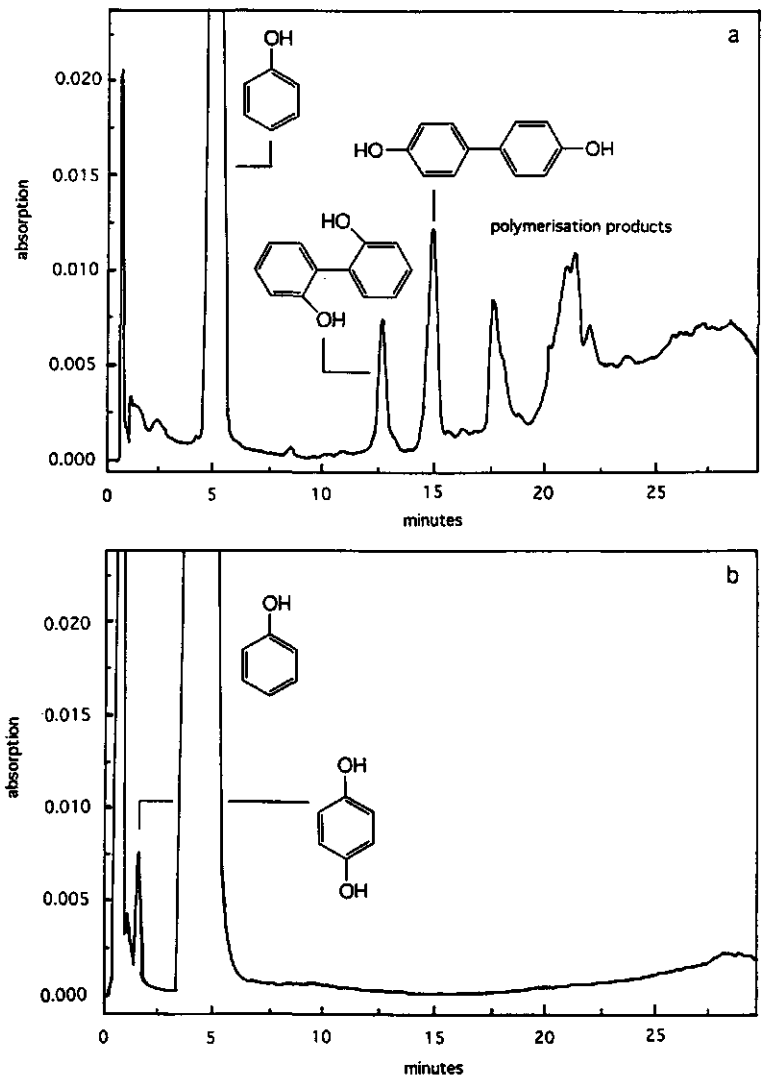

Figure 4 Conversion of phenol by MP-8/H_2O_2 in (a) the absence and (b) the presence of ascorbic acid. The dimerization products were identified on the basis of commercially available 4,4'-diphenol and 2,2'-diphenol. The peaks of the polymerization products were ascribed on the basis of the fact that incubation of phenol with horseradish peroxidase/H_2O_2 gave rise to similar complex polymeric metabolite patterns as presented in Figure a. The hydroquinone in Figure b was identified on the basis of comparison of the UV spectrum and retention time to that of a commercially available reference compound.

Table 2 Effect of ascorbic acid on MP-8/H_2O_2 and horseradish peroxidase/H_2O_2-mediated conversion of aniline and 2-fluorophenol. Product patterns were analyzed by HPLC.

Incubation condition	Hydroxylated product formed μM/min	Polymerization products[a]
aniline + MP-8 + H_2O_2	14.5	+
aniline + MP-8 + H_2O_2 + ascorbic acid	54.0	-
aniline + HRP + H_2O_2	0	+
aniline + HRP + H_2O_2 + ascorbic acid	0	-
2-fluorophenol + MP-8 + H_2O_2	0	+
2-fluorophenol + MP-8 + H_2O_2 + ascorbic acid	14.8	-
2-fluorophenol + HRP + H_2O_2	0	+
2-fluorophenol + HRP + H_2O_2 + ascorbic acid	0	-

a) Polymerization products could not be quantified due to the fact that not all of them were characterized. They were identified as polymerization products on the basis of their higher retention times compared to the parent compound on reverse-phase HPLC, their formation in a horseradish peroxidase/H_2O_2 system, and their disappearance in patterns of incubations in the presence of ascorbic acid (for an example see Figure 4).

Effect of ascorbic acid on MP-8/H_2O_2-catalysed aromatic hydroxylation

Although ascorbic acid effectively blocked peroxidase-catalyzed dimerization of phenol, aniline and 2-fluorophenol (Figure 4, Table 2), incubation of these model substrates with MP-8/H_2O_2 in the presence of ascorbic acid still results in the formation of the hydroxylated reaction products. Figure 4b and Figures 5-7 show this for phenol, aniline, 2-fluorophenol, and 3-fluoroaniline, respectively. Figure 5 shows the HPLC chromatogram of the incubation of aniline in the presence of MP-8/H_2O_2 and ascorbic acid. Formation of two hydroxylated products is clearly observed which were identified as 4- and 2-aminophenol on the basis of commercially available reference compounds. The ratio between the formation of 4- and 2-aminophenol was 0.85 : 0.15, which is similar to what has been reported for cytochrome P450-mediated conversions of aniline [27].

Discussion

In the present study, the mechanism of MP-8/H_2O_2-catalyzed aromatic hydroxylation was investigated. The results obtained provide conclusive evidence that the MP-8/H_2O_2-dependent hydroxylation of the model substrates proceeds by a reaction mechanism that differs from the reaction pathway proposed for the hydroxylation reaction of aromatic compounds mediated by a horseradish peroxidase/dihydroxyfumarate system. This conclusion is derived from the following observations of the present study. First, the MP-8-catalyzed hydroxylation requires H_2O_2 while H_2O_2 is unable to support horseradish peroxidase-mediated hydroxylation. Second, the radical scavengers (Table 1) had no effect on the MP-8-catalyzed hydroxylation reaction, whereas they are known to inhibit, at the concentrations used in our investigations, the horseradish peroxidase/dihydroxyfumarate-catalyzed hydroxylation [14,15] and are known to be extremely effective hydroxyl and superoxide anion radical scavengers [15]. Third, manganese, a powerful inhibitor of peroxidase hydroxylation [13,15,23], shows no effect on the MP-8/H_2O_2-catalyzed hydroxylation.

In additional experiments, ascorbic acid was demonstrated to fully inhibit horseradish peroxidase-catalyzed-type of conversions of model compounds like guaiacol, *o*-dianisidine, and also of aniline and phenol. Such an inhibitory effect of ascorbic acid on peroxidase reactions is in accordance with results reported by Potter et al. [26], who used ascorbic acid to prevent the polymerization reaction of acetaminophen catalyzed by horseradish peroxidase, and also with studies reported by Subrahmanyam and O'Brien [25] who reported inhibition of horseradish peroxidase/H_2O_2-mediated oxidation of phenol to reactive DNA binding products by ascorbic acid. Thus, the results with ascorbic acid are an indication that the aromatic hydroxylation might not result from peroxidase-type reaction chemistry. Experiments with ^{18}O-labelled $H_2{}^{18}O_2$ further support this conclusion, because all oxygen incorporation into aniline to give 4-aminophenol was demonstrated to originate from $H_2{}^{18}O_2$. In addition, the $H_2{}^{18}O_2$ experiment excludes that the reactive entity formed from $H_2{}^{18}O_2$ and MP-8 exchanges its oxygen with H_2O or O_2 on the time scale of the experiments. Together, the results of the present study strongly support a mechanism of aromatic hydroxylation by MP-8/H_2O_2 through a P450-type of oxygen-transfer mechanism and not through a peroxidase-type reaction chemistry.

This result of the present study implies that the nature of the axial ligand of the heme cofactor, which is histidyl in MP-8 but a cysteinate in the cytochromes

P450, does not play a dominant role in setting the type of reaction chemistry possible. Although MP-8 has a histidyl axial ligand, the results of the present study clearly show that the catalyst is able to support aromatic hydroxylations by a cytochrome P450 oxygen-transfer mechanism rather than a peroxidase-type reaction chemistry in which oxygen incorporated in the structural substrate originates from O_2 or H_2O [11]. This conclusion would be in agreement with conclusions from other studies in which the hypothesis is put forward that a barrier between the substrate and the oxygen of the high-valent iron-oxo species of HRP is responsible for the fact that horseradish peroxidase and other classical peroxidases differ from the monooxygenases in that they do not incorporate the oxygen of their high-valent iron-oxo intermediate into the product [20,21,29]. Another possibility would be that the type of ligand is not decisive for the type of reaction chemistry that can occur, but influences the ratio between the possible different reaction pathways. Thus, a histidyl ligand may favour peroxidase-type reaction chemistry over P450-type of oxygen transfer chemistry, whereas a cysteinate ligand may favour the latter. Clearly, further studies are required to solve this problem to a further extent.

Acknowledgements

The present work was financially supported by the EU Human Capital and Mobility grant MASIMO no. ERBCHRXCT, by the Biotech grant no. BIO2-CT942052, and by the TMR large scale NMR facility grant no. CHGE-CT94-0061.

References

1 Harbury, H.A., Cronin, J.R., Fanger, M.W., Hettinger, T.P., Murphy, A.J., Myer, Y.P., and Vinogradov, S.N. (1965) Complex formation between methionine and a heme peptide from cytochrome c. *Proc. Natl. Acad. Sci. USA* 54, 1658-1664.

2 Kraehenbuhl, J.P., Galardy, R.E., and Jamieson, J.D. (1974) Preparation and characterization of an immuno-electron microscope tracer consisting of a heme octapeptide coupled. *J. Exp. Med.* 139, 208-223.

3 Aron, J., Baldwin, D.A., Marques, M.M., Pratt, J.M., and Adams, P.A. (1986) Hemes and hemoproteins. 1. Preparation and analysis of the heme-containing octapeptide (microperoxidase-8) and identification of the monomeric form in aqueous solution. *J. Inorg. Biochem.* 27, 227-243.

4 Wang, J.S., and Van Wart, H.E. (1989) Resonance Raman characterization of the heme c group in *N*-acetyl-microperoxidase-8: A thermal intermediate spin-high spin state mixture. *J. Phys. Chem.* 93, 7925-7931.

5 Wang, J.S., Baek, H.K., and Van Wart, H.E. (1991) High-valent intermediates in the reaction of N^a-acetyl-microperoxidase-8 with hydrogen peroxide: Models for compounds O, I and II of horseradish peroxidase. *Biochem. Biophys. Res. Commun.* 179, 1320-1324.

6 Cunningham, I.D., Bachelor, J.L., and Pratt, J.M. (1991) Kinetic study of the H_2O_2 oxidation of phenols, naphthols and anilines catalyzed by the heme octapeptide microperoxidase-8. *J. Chem. Soc. Perkin Trans.* 2, 1839-1843.

7 Baldwin, D.A., Marques, M.M., and Pratt, J.M. (1985) Mechanism of activation of H_2O_2 by peroxidases: Kinetic studies on a model system. *FEBS Lett.* 183, 309-312.

8 Baldwin, D.A., Marques, M.M., and Pratt, J.M. (1987) Hemes and hemoproteins. 5: Kinetics of the peroxidatic activity of microperoxidase-8: model for the peroxidase enzymes. *J. Inorg. Biochem.* 30, 203-217.

9 Marques, H.M., Baldwin, D.A., and Pratt, J.M. (1987) Heme and hemoproteins 3. The reaction of microperoxidase-8 with cyanide: Comparison with aquocobalmin and heme proteins. *J. Inorg. Biochem.* 29, 77-91.

10 Rusvai, E., Vegh, M., Kramer, M., and Horvath, I. (1988) Hydroxylation of aniline mediated by heme bound oxy-radicals in a heme peptide model. *Biochem. Pharmacol.* 37, 4574-4577.

11 Nakamura S., Mashino, T., and Hirobe, M. (1992) ^{18}O incorporation from $H_2{}^{18}O_2$ in the oxidation of *N*-methylcarbazole and sulfides catalyzed by microperoxidase-11. *Tetrahedron Lett.* 33, 5409-5412.

12 Mason, H.S., Onoprienko, I., and Buhler, D. (1957) Hydroxylation: The activation of oxygen by peroxidase. *Biochem. Biophys. Acta* 24, 225-226.

13 Buhler, D.R., and Mason, H.S. (1961) Hydroxylation catalyzed by peroxidase. *Arch. Biochem. Biophys.* 92, 424-437.

14 Dordick, J.S., Klibanov, A.M., and Marletta., M.A. (1986) Horseradish peroxidase catalyzed hydroxylation: Mechanistic studies. *Biochemistry* 25, 2946-2951.

15 Halliwell, B. (1977) Generation of hydroperoxide, superoxide and hydroxyl radicals during the oxidation of dihydroxyfumaric acid by peroxidase. *Biochem. J.* 163, 441-448.

16 Guengerich, F.P., and MacDonald, T.L. (1990) Mechanisms of cytochrome P-450 catalysis. *FASEB J.* 4, 2453-2459.

17 Rietjens, I.M.C.M., Soffers, A.E.M.F., Veeger, C., and Vervoort, J. (1993) Regioselectivity of cytochrome P-450 catalyzed hydroxylation of fluorobenzenes predicted by calculated frontier orbital substrate characteristics. *Biochemistry* 32, 4801-4812.

18 Brodie, B.B., and Axelrod, J. (1948) The estimation of acetanilide and its metabolic products, aniline, *N*-acetyl *p*-aminophenol and *p*-aminophenol (free and conjugated) in biological fluids and tissues. *J. Pharmac. Exp. Ther.* 94, 22-28.

19 Vervoort, J., De Jager, P.A., Steenbergen, J., and Rietjens, I.M.C.M. (1990) Development of a ^{19}F n.m.r. method for studies on the *in vivo* and *in vitro* metabolism of 2-fluoroaniline. *Xenobiotica* 20, 657-670.

20 Ortiz de Montellano, P.R., Choe, S.Y., Depillis, G., and Catalano, E.C. (1987) Structure-mechanism relationships in hemoproteins: Oxygenations catalyzed by chloroperoxidase and horseradish peroxidase. *J. Biol. Chem.* 262, 11641-11646.

21 Ortiz de Montellano, P.R. (1992) Catalytic sites of hemoproteins: Peroxidases. *Annu. Rev. Pharmacol. Toxicol.* 32, 89-107.

22 Rahimtula, A.D., and O'Brien, P.J. (1974) Hydroperoxide catalyzed liver microsomal aromatic hydroxylation. *Biochem. Biophys. Res. Commun.* 60, 440-447.

23 Halliwell, B., and Ahluwalia, S. (1976) Hydroxylation of *p*-coumaric acid by horseradish peroxidase. *Biochem. J.* 153, 513-518.

24 Ingelman-Sundberg, M., and Johansson, I. (1984) Mechanism of hydroxyl radical formation and ethanol oxidation by ethanol-inducible and other forms of rabbit liver microsomal cytochrome P-450. *J. Biol. Chem.* 259, 6447-6458.

25 Subrahmanyam, V.V., and O'Brien, P.J. (1985) Peroxidase-catalyzed binding of [U-^{14}C]phenol to DNA. *Xenobiotica* 15, 859-871.

26 Potter, D.W., Miller, D.W., and Hinson, J.A. (1984) Identification of acetaminophen polymerization products catalyzed by horseradish peroxidase. *J. Biol. Chem.* 260, 12174-12180.

27 Esclade, L., Guillochon, D., and Thomas, D. (1985) Determination of metabolites of cytochrome P-450 model systems using high-performance liquid chromatography. *J. Chromatogr.* 341, 373-382.

28 Cnubben, N.H.P., Vervoort, J., Veeger, C., and Rietjens, I.M.C.M. (1992) Study on the regioselectivity and mechanism of the aromatic hydroxylation of monofluoroanilines. *Chem.-Biol. Interact.* 85, 151-172.

29 Ozaki, S., and Ortiz de Montellano, P.R. (1995) Molecular engineering of horseradish peroxidase: Thioether sulfoxidation and styrene epoxidation by Phe-41 leucine and threonine mutants. *J. Am. Chem. Soc.* 117, 7056-7064.

Chapter 6

The occurrence of the NIH shift upon the cytochrome P450-catalysed *in vivo* and *in vitro* aromatic ring hydroxylation of fluorobenzenes

J. Koerts, A.E.M.F. Soffers, A. de Jager and I.M.C.M. Rietjens

Chemical Research in Toxicology, submitted.

Abstract

The *in vivo* cytochrome P450-catalysed aromatic hydroxylation of a series of fluorobenzenes was investigated with special emphasis on the importance of the fluorine NIH shift. The results obtained demonstrate a minor role for the NIH shift in the metabolism of the fluorobenzenes to phenolic metabolites in control male Wistar rats. These results are different from data reported in the literature for their chlorinated analogues for which significant involvement of the NIH shift has been reported [Kohli et al. (1976) Can. J. Biochem. 54, 203-208; Chu et al. (1984) J. Toxicol. Environ. Health 13, 777-786; Schwartz et al. (1987) J. Toxicol. Environ. Health 22, 341-350]. Additional experiments presented in this paper provide an explanation for this discrepancy. Assuming that NIH shifted metabolites are likely to originate from arene oxide intermediates the actual *in vivo* occurrence of the NIH shifted metabolites will be -at least in part- dependent on i) the ease of arene oxide rearrangement to give the ring-opened intermediate preceding the NIH shifted phenol and ii) the ease and relative rate of the reaction of the arene oxide in competing biotransformation pathways such as GSH conjugation.
Results of the present study show that the formation of NIH shifted phenolic metabolites from fluorine substituted benzenes is hampered relative to the corresponding chlorinated analogues. Calculations indicate that the reduced tendency of fluorine substituted benzenes to undergo an NIH shift can -at least in part- be ascribed to i) the reduced chance of fluorine rather than chlorine arene oxide intermediates on ring opening generating NIH shifted phenolic metabolites and ii) the provision of an alternate pathway by the more efficient GSH conjugation of fluorine over chlorine containing arene oxides.

Introduction

During mammalian metabolism aromatic compounds can be converted to ring hydroxylated metabolites which can subsequently be conjugated and excreted from the body. Upon hydroxylation at an aromatic position the substituent originally present at this aromatic carbon atom might shift to the carbon atom adjacent to the site of hydroxylation. This phenomenon is believed to proceed via arene oxides and/or keto intermediates, and has been termed the NIH shift (Figure 1) [1-4]. The NIH type of migration has not only been reported for substituents like deuterium and tritium, but also for halo- and alkyl substituents [1-3]. The extent to which a substituent actually shifts upon aromatic hydroxylation is known to be dependent both on the nature of the substituent itself and also on the nature of other substituents that may be present in the molecule [2]. For example, the percentage of migration of a deuterium or tritium is generally higher than that of a chlorine substituent. Similarly, the deuterium shift observed upon C4 hydroxylation of 4-deuteromethoxybenzene is significantly higher than the deuterium shift reported for the C4 hydroxylation of 4-deuteroaminobenzene, revealing the effect of a *para* substituent [2,5,6].

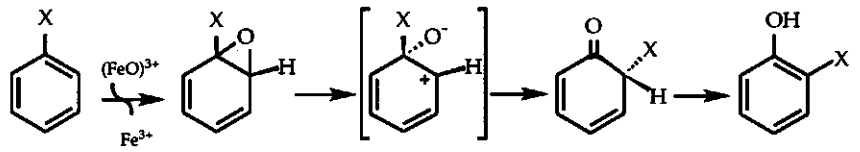

Figure 1 Schematic presentation of the reaction pathway proposed for the cytochrome P450-catalysed formation of NIH shifted phenolic metabolites through arene oxide intermediates. The pathway presented is that for the reaction which predominates at physiological pH where ring opening of the arene oxide intermediate to the carbonium ion is suggested to be the rate-limiting step in the formation of NIH shifted phenolic metabolites [1-4].

Generally, the importance of the NIH shift of halogen substituents in the course of aromatic hydroxylation is less well documented than the NIH shift of deuterium or tritium substituents. Studies on the conversion of 4-halogenated phenylalanines to 4-hydroxylated metabolites by the enzyme phenylalanine hydroxylase report migration of chlorine and bromine substituents, resulting in formation of 3-substituted tyrosines in contrast to fluorine or iodine substituents which were preferentially lost from the molecule [7,8]. For cytochrome P450-

catalysed hydroxylation of halogenated aromatic compounds evidence of the NIH shift has been presented primarily for substrates containing chlorine or bromine substituents [2;9-14]. The migration of fluorine or iodine substituents is far less well documented. Based on *in vitro* studies of the cytochrome P450-catalysed 4-hydroxylation of 4-fluoroaniline, 4-fluoroacetanilide and 4-iodoanisole it has even been reported that, by analogy to the phenyl alanine hydroxylase reaction, an iodine or fluorine substituent is preferentially lost from the molecule rather than giving rise to an NIH shift [15-18]. However, the inability of a fluorine substituent to give rise to an NIH shift in a cytochrome P450-catalysed conversion has only been reported for 4-fluoroaniline and 4-fluoroacetanilide so far [15,16]. Since, the involvement of the NIH shift is also dependent on other substituents present in the aromatic ring [2], it is uncertain whether the results obtained for the 4-fluorinated aniline derivatives are indicative of a general inability of a fluorine substituent to undergo the rearrangement. This uncertainty becomes even stronger if one takes into account the mechanism suggested for the cytochrome P450-catalysed C4 hydroxylation and subsequent dehalogenation of 4-fluorinated anilines and phenols. The presence of a substituent at C1 with electron donating capacities increases the possibilities to eliminate the fluorine as a fluoride anion [19,20]. Thus, the fact that the cytochrome P450-catalysed hydroxylation of 4-fluoroaniline and 4-fluoroacetanilide is preferentially accompanied by fluoride anion elimination instead of by an NIH shift, may be ascribed to the electron donating character of the amino or acetamido substituent opposite the fluorine, instead of to the inability of the fluorine to rearrange to the adjacent carbon atom.

Based on these considerations, the aim of the present study was to investigate the possible (in)ability of a fluorine substituent to give rise to an NIH shift in cytochrome P450-catalysed conversions to a greater extent when a series of compounds without substituents that would favour fluoride anion elimination was used. The following model compounds were used, 1,4-difluorobenzene, 1,2,3-trifluorobenzene, 1,2,4-trifluorobenzene, 1,2,3,4-tetrafluorobenzene and 1,2,3,5-tetrafluorobenzene. This series of fluorinated benzenes was chosen because their chlorinated analogues have been reported to be converted to NIH shifted phenolic metabolites to a significant extent upon their *in vivo* and/or *in vitro* conversion [9-14]. A second reason to use these fluorinated benzenes is that, in contrast to an amino, acetamido or phenolic moiety, the additional fluorine substituents in the molecule are unable to support an efficient fluoride anion elimination [21].

Materials and Methods

Chemicals

1,4-Difluorobenzene, 1,2,3-trifluorobenzene, 1,2,4-trifluorobenzene, 1,2,3,4-tetrafluorobenzene, 1,2,3,5-tetrafluorobenzene, 1,3,5-trifluorobenzene, 2,3-difluorophenol, 2,4-difluorophenol, 2,6-difluorophenol, 2,3,6-trifluorophenol, 2,3,5-trifluorophenol, 2,3,4-trifluorophenol, 3,4,5-trifluorophenol and 2,3,5,6-tetrafluorophenol were obtained from Fluorochem (Derbyshire, United Kingdom).

2,5-Difluorophenol and 3,4-difluorophenol were obtained from Aldrich Chemie (Steinheim, Germany). 4-Fluorophenol was purchased from Acros Chimica (Beerse, Belgium).

In vivo exposure of rats

Male Wistar rats (300-400 g) were exposed to 200 µmol of the desired fluorobenzene, administered in olive oil by oral injection. After dosing, 0-24 h urine samples were collected.

For glutathione (GSH) depletion the rats (230 g) were pretreated with buthionine sulfoximine (Aldrich Chemie, Steinheim, Germany) as follows [22]. Rats were exposed to 4 mmol buthionine sulfoximine/kg i.p. and 2 mmol buthionine sulfoximine/kg i.v. (administered in 0.9% NaCl) at 6 h and 1 h respectively before oral dosage of 200 µmol of 1,4-difluorobenzene. After dosing of 1,4-difluorobenzene, 0-16 h urine samples were collected. In contrast to the 0-24 h urine for non-depleted rats, the 0-16 h urine was taken because a previous study showed that liver tissue GSH levels of mice were restored between 10 and 24 h after administration of buthionine sulfoximine [22]. For comparison, the 0-16 h urine of a control rat exposed to 1,4-difluorobenzene was collected as well.

Analysis of urine samples

Urine samples were analysed by ^{19}F NMR after 1:1 dilution in 0.2 M potassium phosphate pH 7.6. Enzymatic hydrolysis was carried out as described previously [23] using arylsulphatase/β-glucuronidase from *Helix pomatia* (Boehringer Mannheim, Germany). Samples were routinely made oxygen-free by four cycles of evacuation and filling with argon to prevent autoxidation of the phenol derivatives.

Preparation of microsomes

Microsomes were prepared from the perfused livers of male Wistar rats (300-400 g) either untreated or treated with isosafrole as described before [16].

Cytochrome P450 content of the microsomes was measured as described by Omura and Sato [24].

Microsomal incubations

Cytochrome P450 dependent conversion was studied *in vitro* in microsomal incubations containing (final concentrations) 0.1 M potassium phosphate pH 7.6, 2 mM microsomal cytochrome P450, 1 mM of the benzene added as 1% (v/v) of a 0.1 M cold stock solution in acetone, 1 mM ascorbic acid to prevent autoxidation of the hydroxylated reaction products and 1.0 mM NADPH. The reaction was started by the addition of the benzene and NADPH. The total reaction volume was 20 ml and the reaction was carried out at 37 °C for 10 min in a closed reaction vessel to prevent evaporation of the substrate. The reaction was terminated by the addition of 1 ml 12 N HCl and 5 ml ethyl acetate. Upon mixing and centrifugation (10 min 3000 rpm) the ethyl acetate layer was collected and 1.6 ml of the ethyl acetate extract was analysed by ^{19}F NMR as described hereafter.

Purification of phenol hydroxylase from Trichosporon cutaneum

Phenol hydroxylase was isolated from the yeast *Trichosporon cutaneum* essentially as described by Sejlitz and Neujahr [25]. The final preparation had a specific activity of 5 U/mg protein.

Incubations with isolated phenol hydroxylase

Phenol hydroxylase incubations were carried out in closed reaction vessels to prevent evaporation of the fluorophenol and contained (final concentrations) 50 mM potassium phosphate pH 7.6, 1 mM (poly)fluorophenol, added from 100 times concentrated stock solution in dimethyl sulfoxide, 0.1 mM phenol hydroxylase, 0.1 mM EDTA, 10 mM flavin adenine dinucleotide (FAD) and 1 mM ascorbic acid to prevent autoxidation of the (poly)fluorocatechols formed. The incubations were started by the addition of 0.17 mM (final concentration) NADPH. Reactions were carried out at 25 °C for 15 min and terminated by freezing the samples in liquid nitrogen.

^{19}F NMR measurements

^{19}F NMR measurements were performed on a Bruker AMX 300 spectrometer as previously described [23]. Between 1500 and 100,000 scans were recorded, depending on the concentrations of the fluorine containing compounds and the signal to noise ratio required. The urinary sample volume was 1.71 ml containing 100 µl $^{2}H_2O$ for locking the magnetic field and 10 µl of a 8.4 mM 4-fluorobenzoic acid solution, added as internal standard.

The ethyl acetate extracts from the microsomal incubations were analysed using a coaxial insert containing a known amount of the internal standard dissolved in $^{2}H_2O$, instead of adding $^{2}H_2O$ and the internal standard to the 1.6 ml ethyl acetate extract in the NMR tube. Chemical shifts are reported relative to $CFCl_3$. Concentrations of the various metabolites could be calculated by comparison of the integrals of the ^{19}F NMR resonances of the metabolites to the integral of the ^{19}F NMR resonance of the internal standard, 4-fluorobenzoic acid.

Proton-coupled, proton-decoupled and HOMO-decoupling ^{19}F NMR of urine samples were acquired on a Bruker DPX 400 NMR spectrometer at 303 K. Spectra were recorded using 5 µs pulses. About 1000 scans were recorded for each spectrum.

Molecular orbital calculations

Semi-empirical molecular orbital calculations were performed on a Silicon Graphics Indigo^2 using InsightII (Biosyn, San Diego, CA, USA). The PM3 Hamiltonian from the MOPAC program was used. All calculations were carried out with PRECISE criteria and for all calculations the self-consistent field (SCF) was achieved. Geometries were optimised for all bond lengths, bond angles and torsion angles using BFGS criteria. The outcomes of the semi-empirical calculations on molecules in vacuum are related to the electronic characteristics of the substrates in the active site of cytochromes P450 or GSH S-transferases. Due to solvation effects and a different dielectric constant, the intrinsic properties of the compounds might be influenced upon binding to the active site. However, it is assumed that this phenomenon will not influence the relative differences of parameters between a series of closely related compounds or between similar centres within one molecule, to a significant extent. Electrophilic reactivity of the halogenated arene oxides was characterised by the calculated energy of their LUMO [26]. Heats of formation calculated for formation of the ring-opened intermediate from the arene oxide precursor of the benzene derivatives (Figure 1), i.e. ΔHF values, were calculated as

follows. The heat of formation of the arene oxides as well as of the ring-opened intermediates were calculated. The heat of formation of an arene oxide was then substracted from the heat of formation of the ring-opened intermediate leading to a ΔHF value. The relative ΔHF values, i.e. ΔΔHF, were obtained by setting the lowest ΔHF value to zero. The ΔΔHF values, calculated from the computer program in kcal per mole were converted to eV to provide values in the same unit as used for the E(LUMO).

Frontier electron densities for electrophilic attack on the π-electrons of the aromatic ring were calculated according to the equation of Fukui et al. [27]. In this equation the contribution of the HOMO (highest occupied molecular orbital) and the HOMO-1 (highest occupied molecular orbital below the HOMO) are both taken into account.

Results

In vivo conversion of fluorobenzenes to phenolic metabolites

Figure 2 presents the ^{19}F NMR spectra of the arylsulphatase/β-glucuronidase treated 0-24 h urine from rats exposed to a) 1,4-difluorobenzene, b) 1,2,3-trifluorobenzene, c) 1,2,4-trifluorobenzene, d) 1,2,3,4-tetrafluorobenzene and e) 1,2,3,5-tetrafluorobenzene. ^{19}F NMR resonances of the fluorophenols were identified on the basis of i) added reference compounds, ii) literature data [28], iii) analysis of proton-coupled and proton-decoupled ^{19}F NMR spectra and/or iv) incubation of fluorophenols with purified phenol hydroxylase from the yeast *Trichosporon cutaneum*, an enzyme known to catalyse hydroxylation of phenols at the position *ortho* with respect to the hydroxyl moiety [25] (see figure legend for further details).

Table 1 presents the ^{19}F NMR ppm values of the identified phenolic metabolites together with the quantified phenolic metabolite patterns as obtained from the ^{19}F NMR spectra of the 0-24 h urine samples (n=2) (Figure 2). Urinary recoveries (0-24 h) were between 65 and 75% of the dose administered and phenolic metabolites resulting from hydroxylation at a non-halogenated position make up a major part (36 to 75%) of the total amount of fluorinated metabolites (Figure 2 and Table 1). Phenolic metabolites resulting from hydroxylation accompanied by an NIH shift of a fluorine substituent are generally observed if at all to a very limited extent (≤ 1.2% of the total amount of fluorinated metabolites, and ≤ 3.3% of all identified phenolic metabolites) (Table 1). Hydroxylation accompanied by defluorination was also observed to only a limited extent (generally ≤ 1.9% of all identified metabolites, and

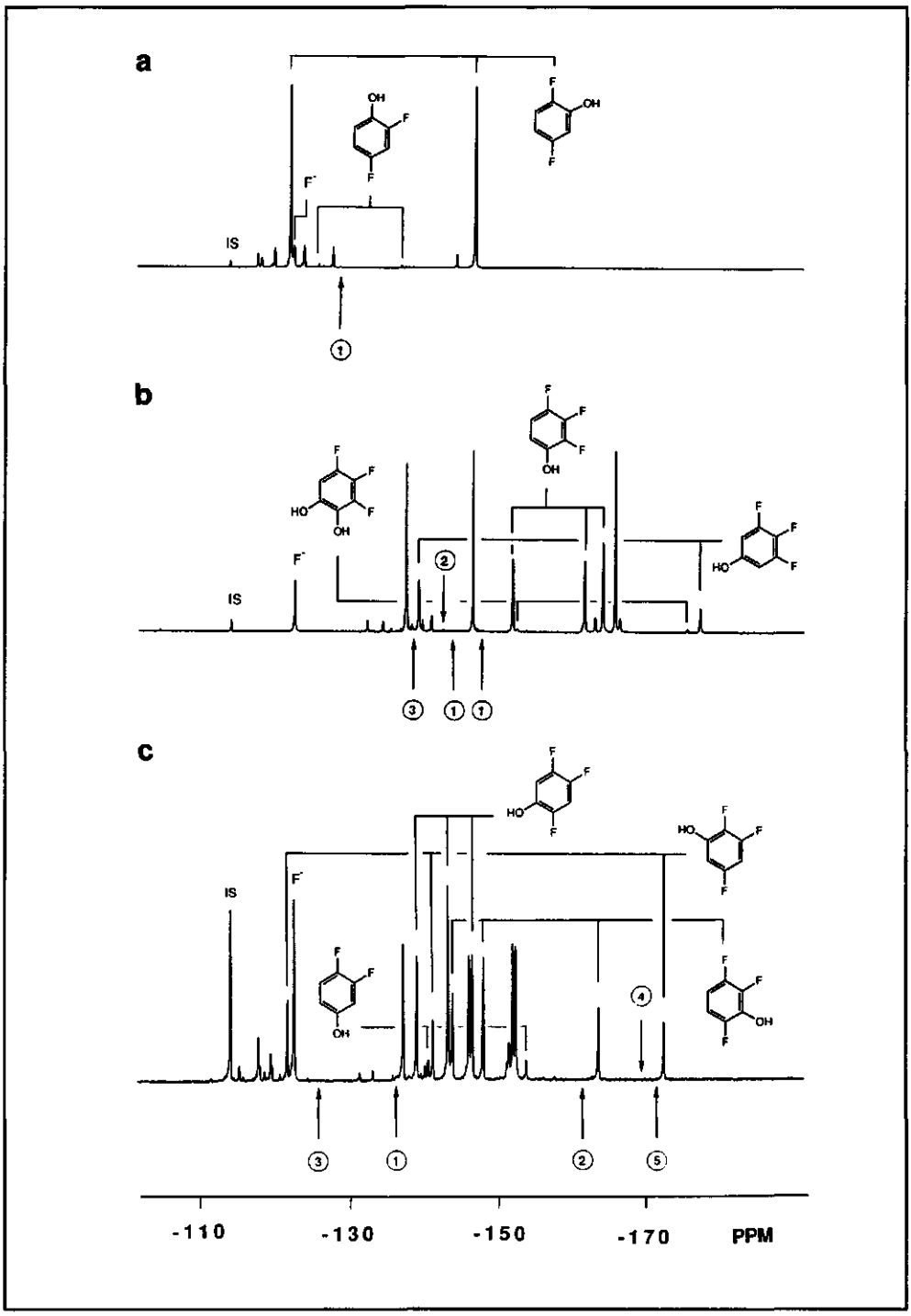
a
IS
F⁻
b
IS
F⁻
c
IS
F⁻
-110
-130
-150
-170
PPM

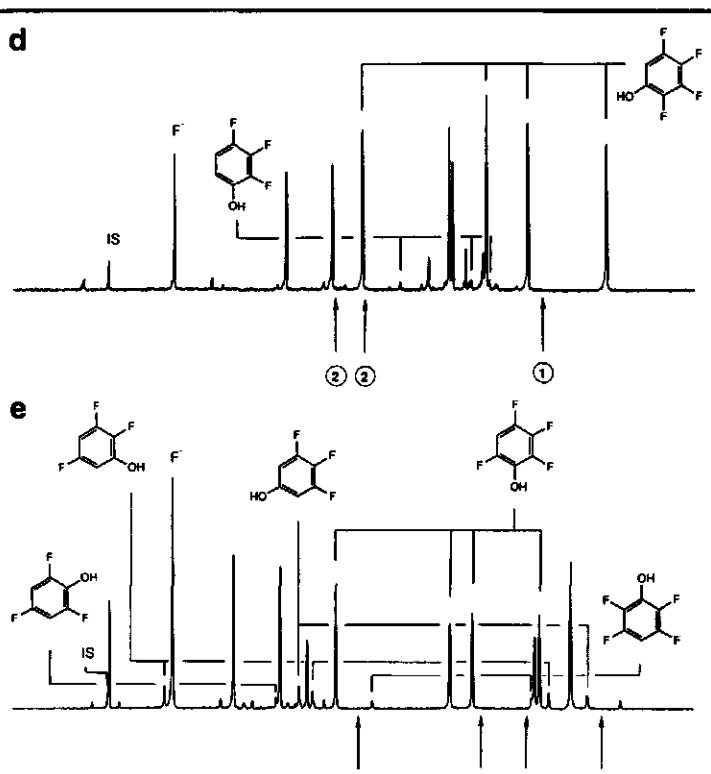

Figure 2 ^{19}F NMR spectra of the arylsulphatase/β-glucuronidase treated 0-24 h urine from male Wistar rats exposed to (a) 1,4-difluorobenzene, (b) 1,2,3-trifluorobenzene, (c) 1,2,4-trifluorobenzene, (d) 1,2,3,4-tetrafluorobenzene and (e) 1,2,3,5-tetrafluorobenzene. 19F NMR resonances were identified on the basis of i) added reference compounds, ii) literature data [28], iii) analysis of proton-coupled and proton-decoupled 19F NMR spectra or iv) incubation of fluorophenols with purified phenol hydroxylase from the yeast *Trichosporon cutaneum*, an enzyme known to catalyse hydroxylation of phenols at the position ortho with respect to the hydroxyl moiety [25]. In Figure 2a the arrow labelled 1) marks the resonance position of 4-fluorophenol, the metabolite that would result from hydroxylation accompanied by dehalogenation. In Figure 2b the arrows mark the resonance positions of 1) 2,3,6-trifluorophenol (the third resonance of this phenol at -164.0 ppm is masked by one of the resonances of 2,3,4-trifluorophenol), 2) 2,3-difluorophenol and 3) 2,6-difluorophenol, metabolites that (would) result from hydroxylation accompanied by an NIH shift or dehalogenation. In Figure 2c the arrows mark 1) 2,4,6-trifluorophenol, 2) 2,3,4-trifluorophenol, 3) 2,4-difluorophenol, 4) 2,3,5-trifluoro-4-hydroxyphenol and 5) 2,3,5-trifluoro-6-hydroxyphenol, metabolites that would result from hydroxylation accompanied by an NIH shift or dehalogenation. Both resonance positions of 2,5-difluorophenol (-122.3 and -147.2 ppm) are masked by peaks from unidentified metabolites that do not belong to phenolic metabolites. In Figure 2d the arrows mark the resonance positions of 1) 2,3,4,6-tetrafluorophenol and 2) 2,3,6-trifluorophenol, metabolites that would result from hydroxylation accompanied by an NIH shift or dehalogenation. In Figure 2e the arrows labelled 1) marks 2,3,4,5-tetrafluorophenol, the metabolite that would result from hydroxylation accompanied by an NIH shift. The resonance marked "IS" is from the internal standard 4-fluorobenzoic acid.

Table 1 Phenolic metabolite pattern of rats exposed to different fluorobenzenes as determined in the urine by ^{19}F NMR (n=2). Chemical shifts of the phenols were determined in urine 1:1 diluted in 0.2 M potassium phosphate pH 7.6. Chemical shifts are reported relative to $CFCl_3$. NIH shifted and defluorinated metabolites are indicated with (NIH) and ($-F^-$) respectively.

fluorobenzene possible metabolite	chemical shift (ppm)	% of total fluorine containing metabolites	% of identified phenolic metabolites
1,4-difluorobenzene			
2,5-difluorophenol	-122.3 ; -147.2	72.6 ± 0.4	96.5
2,4-difluorophenol (NIH)	-126.1 ; -137.3	0.6 ± 0.2	0.7
4-fluorophenol ($-F^-$)	-129.1	< 0.1	< 0.1
2,5-difluoro-6-dihydroxyphenol	-144.7[a]	2.1 ± 0.4[a]	2.7[a]
2,5-difluoro-4-dihydroxyphenol	-144.7[a]	2.1 ± 0.4[a]	2.7[a]
total		75.4 ± 1.0	100
1,2,3-trifluorobenzene			
2,3,4-trifluorophenol	-152.5 ; -161.9 ; -164.5	26.0 ± 1.1	67.7
3,4,5-trifluorophenol	-139.6 ; -177.6	10.3 ± 0.4	26.8
2,3,6-trifluorophenol (NIH)	-144.3 ; -148.4 ; -164.0	< 0.1	< 0.3
2,3-difluorophenol ($-F^-$)	-142.8 ; -166.9	0.4 ± 0.1	1.0
2,6-difluorophenol ($-F^-$)	-138.9	< 0.1	< 0.3
2,3,4-trifluoro-6-hydroxyphenol	-153.6 ; -162.0 ; -176.0	1.5 ± 0.1	3.9
total		38.4 ± 1.7	100

[a] The resonance is due to one of the two possible dihydroxylated products.

[b] The presence of 2,5-difluorophenol could not be determined because its resonance positions were masked by resonances from unidentified metabolites.

Table 1 -continued-

fluorobenzene possible metabolite	chemical shift (ppm)	% of total fluorine containing metabolites	% of identified phenolic metabolites
1,2,4-trifluorobenzene			
2,3,6-trifluorophenol	-144.3 ; -148.4 ; -164.0	10.2 ± 0.1	24.8
2,4,5-trifluorophenol	-139.4 ; -143.6 ; -146.9	20.1 ± 1.3	48.8
2,3,5-trifluorophenol	-121.9 ; -141.6 ; -172.7	8.6 ± 0.0	20.9
2,3,4-trifluorophenol (NIH)	-152.5 ; -161.9 ; -164.5	< 0.1	< 0.2
2,4,6-trifluorophenol (NIH)	-123.0 ; -136.6	< 0.1	< 0.2
3,4-difluorophenol (-F^-)	-140.9 ; -154.2	1.8 ± 0.4	4.4
2,5-difluorophenol (-F^-)	-122.3 ; -147.2	- [b]	- [b]
2,4-difluorophenol (-F^-)	-126.1 ; -137.3	< 0.1	< 0.2
2,3,5-trifluoro-4-hydroxyphenol	-144.4 ; -162.2 ; -169.7	< 0.1	< 0.2
2,3,5-trifluoro-6-hydroxyphenol	-146.0 ; -153.1 ; -171.5	< 0.1	< 0.2
total		41.2 ± 1.8	100
1,2,3,4-tetrafluorobenzene			
2,3,4,5-tetrafluorophenol	-147.5 ; -163.8 ; -169.3 ; -179.2	49.0 ± 0.4	96.5
2,3,4,6-tetrafluorophenol (NIH)	-144.5;-159.8;-162.6;-171.4	< 0.1	< 0.2
2,3,4-trifluorophenol (-F^-)	-152.5 ; -161.9 ; -164.5	1.6 ± 0.0	3.1
2,3,6-trifluorophenol (-F^-)	-144.3 ; -148.4 ; -164.0	< 0.1	< 0.2
total		50.8 ± 0.4	100
1,2,3,5-tetrafluorobenzene			
2,3,4,6-tetrafluorophenol	-144.5 ; -159.8 ; -162.6 ; -171.4	29.2 ± 1.8	80.4
2,3,4,5-tetrafluorophenol (NIH)	-147.5;-163.8;-169.3;-179.2	< 0.1	< 0.3
2,3,5,6-tetrafluorophenol (NIH)	-149.3 ; -170.6	1.1 ± 0.1	3.0
3,4,5-trifluorophenol (-F^-)	-139.6 ; -177.6	3.0 ± 0.1	8.3
2,3,5-trifluorophenol (-F^-)	-121.9 ; -141.6 ; -172.7	1.7 ± 0.1	4.7
2,4,6-trifluorophenol (-F^-)	-123.0 ; -136.6	1.2 ± 0.1	3.3
total		36.3 ± 2.2	100

≤ 4.6% of all identified phenolic metabolites). Only for 1,2,3,5-tetrafluorobenzene was formation of small amounts of defluorinated phenolic metabolites observed; 5.9% of the total amount of fluorinated metabolites, and 16.3% of all identified phenolic metabolites.

^{19}F NMR analysis of the parent fluorobenzenes demonstrated that the presence of NIH shifted or dehalogenated metabolites was not the result of other fluorobenzene or fluorophenol impurities in the parent compounds (data not shown).

The unidentified resonances in Figure 2 do not represent phenolic metabolites but they most likely belong to mercapturic acid metabolites or other sulphur containing metabolites. This follows from the fact that i) their resonance positions did not change upon enzyme treatment of the urine and ii) these type of derivatives are well known to be formed upon *in vivo* metabolism of halogenated benzenes [29-31]. However, as the objective of the present paper was the investigation of the occurrence of the NIH shift upon the formation of phenolic metabolites, these resonances were not further identified at this stage.

Altogether, the data presented in Figure 2 and Table 1 clearly indicate the absence of a significant amount of NIH shifted phenolic metabolites formed from the fluorobenzenes.

In vitro conversion of fluorobenzenes to phenolic metabolites

In addition to the *in vivo* studies the possible formation of NIH shifted phenolic fluorobenzene metabolites was also investigated in *in vitro* microsomal studies. Only 1,4-difluorobenzene gave detectable levels of conversion in the microsomal incubations. The lower reactivity of the tri- and tetrafluorobenzenes toward microsomal conversion can be explained by the decreased nucleophilicity of these substrates, reducing the rate of reaction between the activated cytochrome $P450(FeO)^{3+}$ and their π-systems [32].

Figure 3 presents the ^{19}F NMR spectrum of a microsomal incubation with 1,4-difluorobenzene. The results from incubations with microsomes from isosafrole pretreated rats are presented because they show a higher rate of conversion than the control microsomes, but results with control microsomes were comparable. In contrast to the results obtained *in vivo*, formation of a significant amount of the NIH shifted 2,4-difluorophenol can be observed, amounting to 26.8 ± 1.4% (n=4) of the total amount of phenolic metabolites (Figure 3). *In vivo* this percentage amounted to less than 1% of the total amount of phenolic metabolites (Table 1).

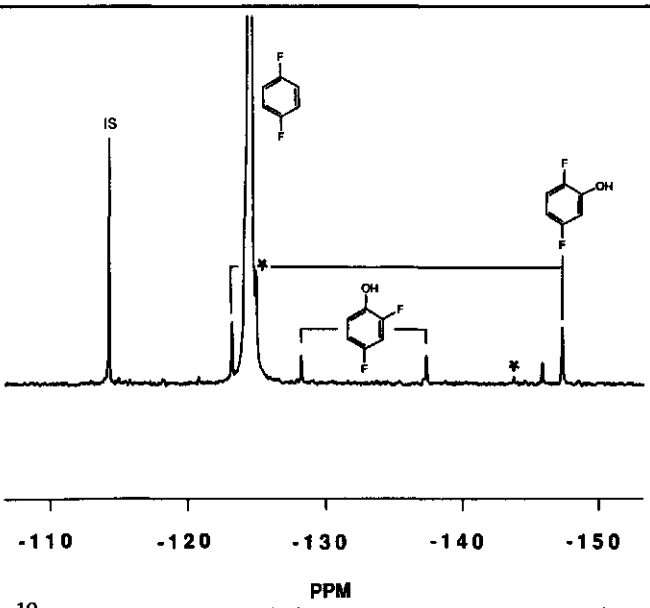

Figure 3 ^{19}F NMR spectra of the ethyl acetate extract of a microsomal incubation with 1,4-difluorobenzene. The resonance marked "IS" is from the internal standard 4-fluorobenzoic acid. The resonances marked with an asterisk were also present in samples from blank incubations carried out in the absence of NADPH.

The effect of GSH on the extent of the fluorine NIH shift for the in vitro metabolism of 1,4-difluorobenzene

The observed discrepancy between the relative importance of the fluorine NIH shift *in vivo* and *in vitro* was further investigated by performing an *in vitro* microsomal incubation in the presence of liver cytosol, containing glutathione S-transferases, and GSH. The rationale behind this experiment was that a possible efficient GSH conjugation of the arene oxide intermediates could explain the minor role of NIH shifted phenolic metabolites upon *in vivo* metabolism [2,3]. In microsomal incubations such reaction pathways are absent giving rise to possibilities for the conversion of the arene oxides to NIH shifted phenolic metabolites. Thus, *in vitro* microsomal incubations in the presence of GSH and cytosol were performed. ^{19}F NMR analysis from such microsomal incubations of 1,4-difluorobenzene in the presence of 1 mM GSH and liver cytosol fraction (^{19}F NMR spectrum not shown) showed that the amount of the NIH shifted 2,4-difluorophenol amounted to 19.9 ±

1.6% (n=6) of the total amount of phenolic metabolites. Compared to the microsomal incubations of 1,4-difluorobenzene without GSH and cytosol, which amounted to 26.8 ± 1.4% (n=4), this implies a relative reduction in the percentage of NIH shifted phenolic metabolites by around 26%.

The effect of GSH on the extent of the fluorine NIH shift for the in vivo metabolism of 1,4-difluorobenzene

The possible influence of GSH conjugation on the formation of NIH shifted phenolic metabolites was further investigated by studying the metabolism of 1,4-difluorobenzene in GSH-depleted rats. The ^{19}F NMR spectra of the arylsulphatase/β-glucuronidase treated urine samples of GSH-depleted rats exposed to 1,4-difluorobenzene were compared to the ^{19}F NMR urine spectra of non-depleted rats exposed to 1,4-difluorobenzene. The results show that for the GSH-depleted rats the amount of the NIH shifted phenolic metabolite 2,4-difluorophenol was 2.8 ± 0.1% of the total phenolic metabolites while this amount was 1.0 ± 0.0% for the non-depleted rats, indicating an almost 3-fold increase in the absolute amount of NIH shifted phenolic metabolites due to the partial GSH depletion.

Calculated reactivity for an NIH shift and GSH conjugation

Finally, computer calculations were performed to investigate possible reasons underlying the reduced probability of forming NIH shifted phenolic metabolites from fluorobenzenes compared to chlorobenzenes [9-11]. At physiological pH, the formation of NIH shifted phenolic metabolites is postulated as proceeding by the pathway presented in Figure 1 [1-4]. In this reaction pathway formation of the carbonium ion, i.e. the ring-opened intermediate, from the arene oxide intermediate, is believed to be the rate-limiting step [2,3]. Table 2 presents the calculated relative heats of formation of the ring-opened intermediates from the arene oxide precursors. Results in Table 2 show that the heat of formation for the ring opening of the arene oxide intermediate for fluorine derivatives is in all cases energetically more costly than it is for the chlorine analogues.

Table 2 also presents the E(LUMO) values of the various arene oxides. This parameter has been demonstrated to be representative of the relative rate and ease of the reaction of the arene oxide with GS^- [33,34]. The computational results indicate that rates of GS^- conjugation are predicted to be faster for fluorine than for chlorine substituted arene oxides.

Table 2 Relative heat of formation of the ring-opened intermediate from the arene oxide precursor and the E(LUMO) value of this arene oxide for a series fluorine or chlorine containing benzenes.

arene oxide	ΔΔHF for formation of the ring-opened intermediate from the arene oxide precursor (eV)		E(LUMO) arene oxide (eV)	
	nature of halogen substituent			
	F	Cl	F	Cl
1,4-dihalobenzene 1,2-arene oxide	0.62	0.35	-0.84	-0.66
1,2,3-trihalobenzene 3,4-arene oxide	0.69	0.11	-1.15	-0.85
1,2,4-trihalobenzene 2,3-arene oxide	0.66	0.25	-1.13	-0.89
1,2,4-trihalobenzene 3,4-arene oxide	0.49	0.43	-1.15	-0.88
1,2,4-trihalobenzene 4,5-arene oxide	0.75	0.40	-1.17	-0.86
1,2,4-trihalobenzene 1,6-arene oxide	0.43	0.00	-1.15	-0.88
1,2,3,4-tetrahalobenzene 4,5-arene oxide	0.56	0.02	-1.47	-1.03
1,2,3,5-tetrahalobenzene 3,4-arene oxide	0.73	0.31	-1.45	-1.07
1,2,3,5-tetrahalobenzene 4,5-arene oxide	0.88	0.48	-1.47	-1.05

Finally, a difference in the chances for attack by the $(FeO)^{3+}$ species on a chlorinated respectively a fluorinated aromatic carbon centre might be another reason underlying the greater tendency of a chlorine than a fluorine to give an NIH shift. To investigate this at least to some extent parameters that may influence the chance on such an $(FeO)^{3+}$ attack were calculated. In a previous study it was shown that the cytochrome P450-catalysed regioselectivity of aromatic ring hydroxylation of a series of fluorobenzenes was predicted well by the frontier orbital density (HOMO/HOMO-1 density) on an aromatic carbon centre indicating this to be a

parameter of influence [28]. In addition, in theory, reactivity of a carbon centre might also be influenced by its Coulombic interactions with the $(FeO)^{3+}$ species on the chances for $(FeO)^{3+}$ attack. Therefore, the frontier orbital and net charge density on the ring carbon atoms of the tested series of fluorobenzenes and their chlorinated analogues were calculated (Table 3). The results in Table 3 show that a chlorinated carbon centre is less positively, even negatively, charged than a fluorinated carbon centre. Taking into account the negative partial charge of the oxygen in a cysteinate-coordinated $Por^{+}Fe(IV)O$ species [35], these data indicate that Coulombic interactions can be expected to favour an iron-oxene attack on a fluorinated over a chlorinated aromatic carbon atom. Table 3 presents also the frontier orbital density on the carbon centres of a series of halobenzenes. From these data it can be concluded that not only the Coulombic factor, but also the frontier orbital parameter favour an iron-oxene attack on a fluorinated over a chlorinated carbon centre.

Discussion

In the present study the importance of the fluorine NIH shift for the cytochrome P450-catalysed aromatic ring hydroxylation of fluorobenzenes was investigated. The fluorobenzenes studied were the analogues of chlorobenzenes for which literature data report the formation of significant amounts (4-79% of the total amount of phenolic metabolites) of NIH shifted phenolic metabolites both *in vivo* and *in vitro* [9-14]. The results obtained in the present study for the *in vivo* cytochrome P450-catalysed aromatic hydroxylation of the fluorobenzenes show an extent of formation of NIH shifted phenolic metabolites that is significantly lower (0.3-3.3% of the total phenolic metabolites) than reported in the literature for their chlorinated analogues [9-11]. In contrast to the *in vivo* results, *in vitro* conversion of 1,4-difluorobenzene resulted in significant formation of the NIH shifted 2,4-difluorophenol (26.8% of the total amount of phenolic metabolites), which demonstrates the inherent ability of a fluorine atom to migrate.

Formation of NIH shifted phenolic metabolites is believed to proceed through arene oxide intermediates which rearrange to NIH shifted phenolic products via a ring-opened intermediate (Figure 1). Ring opening of the arene oxide has been reported as the rate-limiting step in the reaction [1-4]. However, it is also known that arene oxide intermediates, besides reacting in a rearrangement reaction to phenolic metabolites, are reactive electrophiles and can add to protein and DNA

Table 3 The frontier orbital density (HOMO/HOMO-1) and net charge on the ring carbon atoms of a series fluorine and chlorine containing benzenes.

benzene	C1	C2	C3	C4	C5	C6
1,4-difluoro-						
HOMO/HOMO-1	0.50	0.20	0.20	0.50	0.20	0.20
net charge	0.05	-0.11	-0.11	0.05	-0.11	-0.11
1,4-dichloro-						
HOMO/HOMO-1	0.32	0.13	0.13	0.32	0.13	0.13
net charge	-0.13	-0.09	-0.09	-0.13	-0.09	-0.09
1,2,3-trifluoro-						
HOMO/HOMO-1	0.29	0.36	0.29	0.30	0.28	0.30
net charge	0.07	0.01	0.07	-0.12	-0.06	-0.12
1,2,3-trichloro-						
HOMO/HOMO-1	0.18	0.23	0.18	0.18	0.15	0.18
net charge	-0.13	-0.15	-0.13	-0.09	-0.08	-0.09
1,2,4-trifluoro-						
HOMO/HOMO-1	0.49	0.30	0.14	0.41	0.31	0.13
net charge	0.03	0.07	-0.14	0.08	-0.12	-0.08
1,2,4-trichloro-						
HOMO/HOMO-1	0.30	0.18	0.09	0.14	0.19	0.08
net charge	-0.14	-0.13	-0.10	-0.12	-0.09	-0.08
1,2,3,4-tetrafluoro-						
HOMO/HOMO-1	0.39	0.25	0.25	0.39	0.23	0.22
net charge	0.05	0.04	0.04	0.05	-0.10	-0.10
1,2,3,4-tetrachloro-						
HOMO/HOMO-1	0.22	0.16	0.16	0.22	0.13	0.13
net charge	-0.13	-0.14	-0.14	-0.13	-0.08	-0.08
1,2,3,5-tetrafluoro-						
HOMO/HOMO-1	0.22	0.47	0.22	0.25	0.35	0.25
net charge	0.09	0.09	0.09	-0.16	0.11	-0.16
1,2,3,5-tetrachloro-						
HOMO/HOMO-1	0.13	0.28	0.13	0.15	0.19	0.15
net charge	-0.12	-0.15	-0.12	-0.10	-0.11	-0.10

[29,36], and/or undergo conjugation with GSH, resulting in mercapturic acids and other sulphur containing metabolites as final products [1,2,29-31]. Based on these facts, it can be anticipated that the *in vivo* formation of NIH shifted phenolic metabolites will be dependent on i) the chances for attack of the activated high-

valent iron-oxo form of cytochrome P450 on the halogenated aromatic carbon centre, but also on ii) the ease of ring opening of the arene oxide intermediates preceding the formation of the NIH shifted phenol and/or iii) the ease and relative rate of the reaction of the arene oxide in competing alternative biotransformation pathways such as GSH conjugation. Additional experiments in the present study were performed to investigate whether these considerations could explain the relatively low extent of formation of NIH shifted phenolic metabolites for fluorobenzenes compared to chlorobenzenes. For these studies 1,4-difluorobenzene was used as model compound and microsomal studies were performed in addition to the *in vivo* experiments. First, it was demonstrated that microsomal incubations of 1,4-difluorobenzene in contrast to the results observed for its *in vivo* metabolism, result in significant formation (26.8 ± 1.4% of the total amount of phenolic metabolites) of the shifted phenolic 2,4-difluorophenol. In the presence of GSH and liver cytosol a significantly ($P < 0.02$) lower extent of formation of the shifted phenolic metabolite 2,4-difluorophenol (19.9 ± 1.6% of the total amount of phenolic products) was observed. This result clearly points at GSH conjugation as a competing pathway for the route leading to formation of NIH shifted phenolic metabolites. This was further investigated in an *in vivo* experiment in which the formation of NIH shifted phenols in GSH-depleted rats was determined. From this experiment it appeared that the metabolic pattern of 1,4-difluorobenzene in GSH-depleted rats shows an almost 3-fold significantly ($P < 0.01$) higher level of the NIH shifted metabolite 2,4-difluorophenol (2.8 ± 0.1% of all phenolic metabolites) compared to non-depleted rats (1.0 ± 0.0% of all phenolic metabolites). Upon interpreting these *in vivo* results it should be kept in mind that treatment of experimental animals with buthionine sulfoximine generally does not result in a full depletion of liver GSH levels; in studies with mice it was demonstrated that a reduction by about 50% could be reached. Furthermore, GSH levels were fully restored within 24 h [22]. Thus, it can be anticipated that in our *in vivo* metabolism study GSH depletion and, thus, also the influence of GSH depletion on formation of NIH shifted metabolites from 1,4-difluorobenzene can only partly reflect the theoretical maximum effect of full GSH depletion.

Together, the results of the *in vitro* GSH/glutathione S-transferase addition and *in vivo* GSH depletion experiment show that GSH conjugation is a competing pathway for the formation of NIH shifted phenolic metabolites.

In additional investigations, molecular orbital calculations were performed to further study possible mechanisms underlying the observed difference in the *in vivo* formation of NIH shifted phenolic metabolites for fluorobenzenes compared to

chlorobenzenes. The relative heats of formation calculated for the process of ring opening of the arene oxide precursors (Figure 1) shows that for fluorobenzenes the heats of formation were always higher than for the chlorinated analogues (Table 2). This indicates that the chances for ring opening of the arene oxides to NIH shifted phenolic metabolites are higher for chlorine than fluorine substituted benzene analogues. Furthermore, calculation of the E(LUMO) of these arene oxides, indicative of their relative ease of GSH conjugation [32,33], show that E(LUMO) values for fluorinated arene oxides are generally lower than for the chlorinated analogues suggesting higher rates of GS^- conjugation for fluorine than chlorine containing arene oxide analogues.

Finally, a difference in the chances for attack by the $(FeO)^{3+}$ species on a chlorinated respectively a fluorinated aromatic carbon centre might be another reason underlying the greater tendency of a chlorine than a fluorine to give an NIH shift. Experimental support for this came previously from the fact that the site of cytochrome P450-catalysed aromatic hydroxylation of a series of polyfluorobenzenes could be even predicted with 6% accuracy and a correlation of 0.96 on the basis of frontier orbital, not Coulombic, parameters [28]. In addition, in theory, reactivity of a carbon centre might also be influenced by its Coulombic interactions with the $(FeO)^{3+}$ species on the chances for $(FeO)^{3+}$ attack. Therefore, the frontier orbital and net charge density on the ring carbon atoms of the tested series of fluorobenzenes and their chlorinated analogues were calculated. The results of these calculations show that a chlorinated carbon centre is less positively, even negatively, charged than a fluorinated carbon centre. Taking into account the negative partial charge of the oxygen in a cysteinate-coordinated $Por^+Fe(IV)O$ species [35], these data indicate that Coulombic interactions can be expected to favour an iron-oxene attack on a fluorinated over a chlorinated aromatic carbon atom. Furthermore, based on previous results [28] and the fact that the reaction is a radical-type interaction, and radical-type reactions are usually frontier-orbital controlled, the frontier orbital density was calculated as well [26]. Results of the calculated frontier orbital densities in the aromatic ring show that not only the Coulombic factor, but also the frontier orbital parameter favour an iron-oxene attack on a fluorinated over a chlorinated carbon centre. Thus, these data argue strongly against the hypothesis that differences in the charge for an iron-oxene attack on a chlorinated and fluorinated aromatic carbon centre are the reason underlying the higher tendency of a chlorine than a fluorine to give NIH shifted metabolites.

Altogether, results of the present study show that the formation of NIH shifted phenolic metabolites from fluorine substituted benzenes is hampered as

compared to their chlorinated analogues. Calculations indicate that the reduced tendency of fluorine substituted benzenes to undergo an NIH shift can-at least in part- be ascribed to i) the reduced chance of fluorine rather than chlorine arene oxide intermediates on ring opening generating NIH shifted phenolic metabolites and ii) the provision of an alternate pathway by the more efficient GSH conjugation of fluorine over chlorine containing arene oxides.

Acknowledgements

The authors gratefully acknowledge Mr G. van Tintelen, Mrs M.A.W. Faassen and Mr J.W.M. Haas for help with animal handling.
This work was supported by the "Wageningen NMR Center" (EU contract: CHGE-CT94-0061).

References

1 Guroff, G., Daly, J.W., Jerina, D.M., Renson, J., Witkop, B., and Udenfriend, S. (1967) Hydroxylation-induced migration: The NIH shift. *Science* 157, 1524-1530.

2 Daly, J.W., Jerina, D.M., and Witkop, B. (1972) Arene oxides and the NIH shift: The metabolism, toxicity and carcinogenicity of aromatic compounds. *Experientia* 28, 1129-1264.

3 Jerina, D.M., and Daly, J.W. (1974) Arene oxides: A new aspect of drug metabolism. *Science* 185, 573-582.

4 Korzekwa, K., Trager, W., Gouterman, M., Spangler, D., and Loew, G.H. (1985) Cytochrome P450 mediated aromatic oxidation: A theoretical study. *J. Am. Chem. Soc.* 107, 4273-4279.

5 Reed, D.J., Vimmerstedt, J., Jerina, D.M., and Daly, J.W. (1973) Formation of phenols from aromatic substrates by plant and animal mono-oxygenases: The effect of adjacent deuteriums on the magnitude of the NIH shift of tritium. *Arch. Biochem. Biophys.* 154, 642-647.

6 Daly, J., Jerina, D., and Witkop, B. (1968) Migration of deuterium during hydroxylation of aromatic substrates by liver microsomes: I. Influence of ring substituents. *Arch. Biochem. Biophys.* 128, 517-527.

7 Guroff, G., Kondo, K., and Daly, J. (1966) The production of meta-chlorotyrosine from *para*-chlorophenylalanine by phenylalanine hydroxylase. *Biochem. Biophys. Res. Commun.* 25, 622-628.

8 Counsell, R.E., Chan, P.S., and Weinhold, P.A. (1970) Lack of hydroxylation-induced migration with 4-iodophenylalanine. *Biochim. Biophys. Acta* 215, 187-188.

9 Kohli, J., Jones, D., and Safe, S. (1976) The metabolism of higher chlorinated benzene isomers. *Can. J. Biochem.* 54, 203-208.

10 Chu, I., Villeneuve, D.C., Viau, A., Barnes, C.R., Benoit, F.M., and Qin, Y.H. (1984) Metabolism of 1,2,3,4-, 1,2,3,5-, and 1,2,4,5-tetrachlorobenzene in the rat. *J. Toxicol. Environ. Health* 13, 777-786.

11 Schwartz, H., Chu, I., Villeneuve, D.C., and Benoit, F.M. (1987) Metabolism of 1,2,3,4-, 1,2,3,5-, and 1,2,4,5-tetrachlorobenzene in the squirrel monkey. *J. Toxicol. Environ. Health* 22, 341-350.

12 Den Besten, C., Ellenbroek, M., Van der Ree, M.A.E., Rietjens, I.M.C.M., and Van Bladeren, P.J. (1992) The involvement of primary and secondary metabolism in the covalent binding of 1,2- and 1,4-dichlorobenzenes. *Chem.-Biol. Interact.* 84, 259-275.

13 Den Besten, C., Smink, M.C.C., De Vries, E.J., and Van Bladeren, P.J. (1991) Metabolic activation of 1,2,4-trichlorobenzene and pentachlorobenzene by rat liver microsomes: A major role for quinone metabolites. *Toxicol. Appl. Pharmacol.* 108, 223-233.

14 Bogaards, J.J.P., Van Ommen, B., Wolf, C.R., and Van Bladeren, P.J. (1995) Human cytochrome P450 enzyme selectivities in the oxidation of chlorinated benzenes. *Toxicol. Appl. Pharmacol.* 132, 44-52.

15 Renson, J., and Bourdon, V. (1968) Hydroxylation et défluorination des dérivés fluores de l'aniline. *Arch. Int. Pharmacodyn.* 171, 240-242.

16 Rietjens, I.M.C.M., and Vervoort, J. (1989) Microsomal metabolism of fluoroanilines. *Xenobiotica* 19, 1297-1305.

17 Daly, J. (1970) Metabolism of acetanilides and anisoles with rat liver microsomes. *Biochem. Pharmacol.* 19, 2979-2993.

18 Rizk, P.N., and Hanzlik, R.P. (1995) Oxidative and non-oxidative metabolism of 4-iodoanisole by rat liver microsomes. *Xenobiotica* 25, 143-150.

19 Rietjens, I.M.C.M., and Vervoort, J. (1991) Bioactivation of 4-fluorinated anilines to benzoquinoneimines as primary reaction products. *Chem.-Biol. Interact.* 77, 263-281.

20 Den Besten, C., Van Bladeren, P.J., Duizer, E., Vervoort, J., and Rietjens, I.M.C.M. (1993) Cytochrome P450-mediated oxidation of pentafluorophenol to tetrafluorobenzoquinone as the primary reaction product. *Chem. Res. Toxicol.* 6, 674-680.

21 Rietjens, I.M.C.M., and Vervoort, J. (1992) A new hypothesis for the mechanism for cytochrome P-450 dependent aerobic conversion of hexahalogenated benzenes to pentahalogenated phenols. *Chem. Res. Toxicol.* 5, 10-19.

22 Griffith, O.W. (1982) Mechanism of action, metabolism, and toxicity of buthionine sulfoximine and its higher homologs, potent inhibitors of glutathione synthesis. *J. Biol. Chem.* 257, 13704-13712.

23 Vervoort, J., De Jager, P.A., Steenbergen, J., and Rietjens, I.M.C.M. (1990) Development of a ^{19}F-n.m.r. method for studies on the *in vivo* and *in vitro* metabolism of 2-fluoroaniline. *Xenobiotica* 20, 657-670.

24 Omura, T., and Sato, R. (1964) The carbon monoxide-binding pigment of liver microsomes. 1. Evidence for its hemoprotein nature. *J. Biol. Chem.* 239, 2370-2378.

25 Sejlitz, T., and Neujahr, H.Y. (1987) Phenol hydroxylase from yeast. A model for phenol binding and an improved purification procedure. *Eur. J. Biochem.* 170, 343-349.

26 Fleming, I. (1976) Molecular orbitals and frontier orbitals. In: Frontier Orbitals and Organic Chemical Reactions (Fleming, I., Ed.), John Wiley and Sons, New York, pp 5-32.

27 Fukui, K., Yonezawa, T., Nagata, C., and Shingu, H. (1954) Molecular orbital theory of orientation in aromatic, heteroaromatic and other conjugated molecules. *J. Chem. Phys.* 22, 1433-1442.

28 Rietjens, I.M.C.M., Soffers, A.E.M.F., Veeger, C., and Vervoort, J. (1993) Regioselectivity of cytochrome P-450 catalyzed hydroxylation of fluorobenzenes predicted by calculated frontier orbital substrate characteristics. *Biochemistry* 32, 4801-4812.

29 Jollow, D.J., Mitchell, J.R., Zampaglione, N., and Gillette, J.R. (1974) Bromobenzene-induced liver necrosis. Protective role of glutathione and evidence for 3,4-bromobenzene oxide as the hepatotoxic metabolite. *Pharmacology* 11, 151-169.

30 Zheng, J., and Hanzlik, R.P. (1992) Dihydroxylated mercapturic acid metabolites of bromobenzene. *Chem. Res. Toxicol.* 5, 561-567.

31 Lindsay Smith, J.R., Shaw, B.A.J., and Foulkes, D.M. (1972) Mechanisms of mammalian hydroxylation: Some novel metabolites of chlorobenzene. *Xenobiotica* 2, 215-226.

32 Cnubben, N.H.P., Peelen, S., Borst, J.-W., Vervoort, J., Veeger, C., and Rietjens, I.M.C.M. (1994) Molecular orbital-based quantitative structure-activity relationship for the cytochrome P450-catalyzed 4-hydroxylation of halogenated anilines. *Chem. Res. Toxicol.* 7, 590-598.

33 Rietjens, I.M.C.M., Soffers, A.E.M.F., Hooiveld, G.J.E.J., Veeger, C., and Vervoort, J. (1995) Quantitative structure-activity relationships based on computer calculated parameters for the overall rate of glutathione S-transferase catalyzed conjugation of a series of fluoronitrobenzenes. *Chem. Res. Toxicol.* 8, 481-488.

34 Soffers, A.E.M.F., Ploemen, J.H.T.M., Moonen, M.J.H., Wobbes, Th., Van Ommen, B., Vervoort, J., Van Bladeren, P.J., and Rietjens, I.M.C.M. (1996) Regioselectivity and quantitative structure-activity relationships for the conjugation of a series fluoronitrobenzenes by purified glutathione S-transferase enzymes from rat and man. *Chem. Res. Toxicol.* 9, 638-646.

35 Zakharieva, O., Grodzicki, M., Trautwein, A.X., Veeger, C., and Rietjens, I.M.C.M. (1996) Molecular orbital study of the hydroxylation of benzene and monofluorobenzene catalysed by iron-oxo porphyrin π cation radical complexes. *JBIC* 1, 192-204.

36 Monks, T.J., Lau, S.S., and Gillette, J.R. (1984) Diffusion of reactive metabolites out of hepatocytes: Studies with bromobenzene. *J. Pharmacol. Exp. Ther.* 228, 393-399.

Chapter 7

Metabolism of the insecticide Teflubenzuron in rats

J. Koerts, A.E.M.F. Soffers, J.-W. de Kraker, N.H.P. Cnubben and I.M.C.M. Rietjens

Xenobiotica, submitted.

Abstract

The metabolic fate of the insecticide teflubenzuron, orally dosed to male Wistar rats, was investigated. Particular attention was paid to the metabolic fate of the benzoate and aniline moiety after hydrolysis of the urea bridge. The 0-48 h urinary and faecal metabolite patterns and recoveries showed that for a dose range of 4-53 μmol (1.5-20 mg) teflubenzuron 90% of the dose was excreted in the faeces mainly in unmodified form, approximately 4.6% was absorbed from the lumen and excreted in the urine and 5.4% was retained in the body. Metabolites excreted in the urine could be identified as benzoate and aniline derivatives originating from the two aromatic rings of teflubenzuron liberated from the parent molecule by hydrolysis of the urea bridge. The amount of urinary benzoate-type metabolites was about eight times the amount of aniline-type metabolites, indicating significant differences in efficiency of urinary excretion of the benzoate moiety as compared to the aniline ring. To further investigate the possible reason underlying this difference in urinary excretion efficiency between the two aromatic derivatives formed from teflubenzuron, dose-recovery studies of these aniline- and benzoate-type metabolites were performed. These studies confirmed the discrepancy observed between the urinary recovery of the benzoate and the aniline moiety of teflubenzuron. Additional results of the present study indicate that the discrepancy can be explained by the fact that the benzoate derivative is excreted mainly in its unmetabolized form whereas the aniline derivative needs additional Phase I and II modifications before it can be excreted from the body. Furthermore, conversion of the halogenated aniline derivative in Phase I metabolism might result in a reactive benzoquinone-type primary metabolite that can be withheld in the body due to a reaction with cellular macromolecules.

Introduction

In the past twenty years the development of fluorinated agrochemicals has increased considerably and an even further increase in fluorinated agrochemicals is foreseen for the years ahead [1]. Replacement of an atom by a fluorine can change the properties of a chemical and affect its metabolism, chemical reactivity and lipophilicity [1-3].

An example of such a series of fluorinated agrochemicals consists of the benzoylphenyl urea insect growth regulants which act by inhibiting the enzyme responsible for the chitin synthesis in larves [4]. Diflubenzuron which is the active component in the product named Dimilin (Figure 1), which was introduced in 1975 and used as larvicide for fruit, cotton and soybeans, was the first benzoylphenyl urea insect growth regulant commercialized. Teflubenzuron, the active component in the insecticide commercialized as Nomolt (Figure 1), was introduced in 1984, and is another benzoylphenyl urea larvicide used for the protection of fruit and vegetables.

Upon development of an agrochemical it is important to investigate the metabolic fate and disposition of the compound in target [4,5] but also in non-target organisms [4,6-9]. Non-target organisms, including man, are exposed to these chemicals upon the manufacture of these compounds but also when these chemicals are released into the environment or are present as a residue in food following crop treatment.

Previous studies on the bioavailability and metabolism of diflubenzuron in various non-target species, i.e. rat, sheep, cattle, swine and chicken, showed that upon a 4-10 mg/kg (13-32 μmol/kg) oral dose of diflubenzuron more than 50% of the dose was excreted unchanged in the faeces [7-10]. The remainder of the dose was absorbed from the gastro-intestinal tract. Part of the diflubenzuron absorbed was metabolized to conjugated aromatic ring hydroxylated diflubenzuron derivatives and excreted in the bile. The remainder of the dose absorbed was excreted in the urine mainly as derivatives from products resulting from hydrolysis of the urea bridge, which were identified especially as 2,6-difluorobenzoic acid derived metabolites. However, there were relatively many unidentified metabolites in the urine pattern and especially a lot of uncertainty remained about the recovery and metabolic fate of the aniline moiety which must also have been formed upon the hydrolytic splitting of the parent compound. Metabolites of this second scission product 4-chlorophenylurea, containing the aniline ring, could not be detected in the urine or bile although unidentified metabolites observed in the urine were taken as

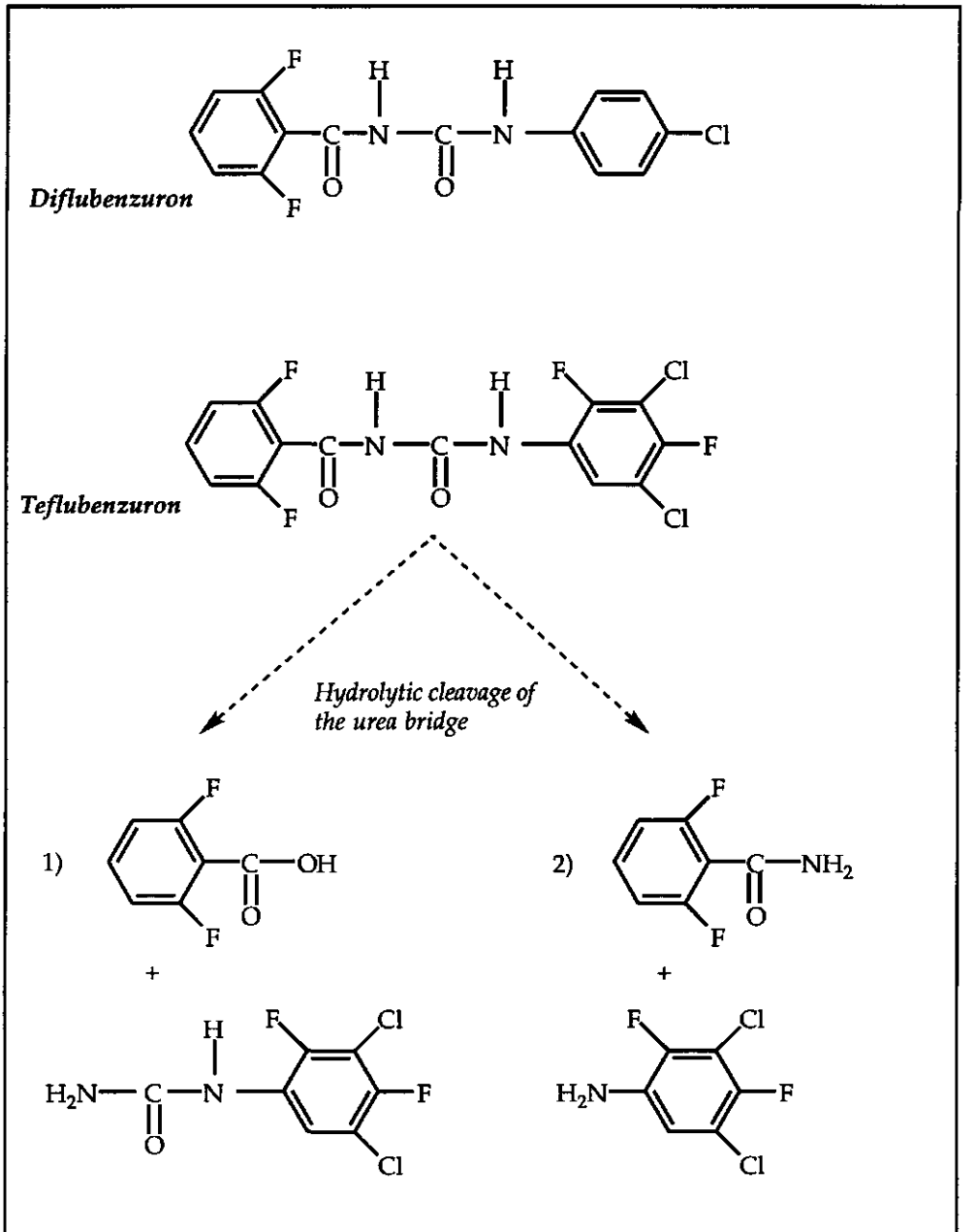

Figure 1 The molecular structure of the insecticides diflubenzuron and teflubenzuron and the proposed scission products formed by hydrolytic cleavage of the phenylurea bridge of teflubenzuron, pathway 1 being the major route [4].

being suggestive of further metabolism of the 4-chlorophenylurea moiety [8].

Altogether, the metabolic fate of benzoylphenylurea insecticides is not well described and especially the fate of the aniline part of the insecticide upon hydrolysis of the urea bridge has not been well investigated. Therefore, the aim of the present study was to investigate the differences in the recovery and metabolic fate of the two aromatic scission products of the benzoylphenyl urea insecticides formed upon hydrolysis of the urea bridge. To do so the benzoylphenyl urea larvicide teflubenzuron was taken as the model compound because the presence of fluorine substituents in both the benzoate but also the aniline moiety (Figure 1) provides a way to actually detect the metabolic fate of both parts of the molecule, since the fluorine containing metabolites can be identified and quantified by the use of ^{19}F NMR.

Materials and Methods

Chemicals

Teflubenzuron, the active compound in Nomolt (purchased from Shell BV, The Netherlands), was obtained by extracting Nomolt with chloroform in an 1:2 (v:v) ratio. The chloroform phase was evaporated and white powder was obtained which was dissolved in dimethyl sulfoxide. (3,5-Dichloro-2,4-difluorophenyl)urea and 3,5-dichloro-2,4-difluoroaniline were a generous gift from Shell Forschung (Schwabenheim, Germany). 2,6-Difluorobenzamide was purchased from Aldrich Chemie (Steinheim, Germany) and 2,6-difluorobenzoic acid was obtained from Fluorochem Limited (Derbyshire, United Kingdom). Synthesis of 2,6-difluorobenzoylglycine from 2,6-difluorobenzoic acid was performed according to Vogel, 1989 [11]. Synthesis of 2-amino-3,5-difluoro-4,6-dichlorophenylsulphate was carried out according to a method for synthesis of O-aminophenyl sulphates described by Boyland et al. [12].

In vivo metabolism

Male Wistar rats (350-400 g) were exposed to 1-53 µmol (as indicated) of teflubenzuron, 2,6-difluorobenzoic acid, 2,6-difluorobenzamide, 3,5-dichloro-2,4-difluoroaniline or (3,5-dichloro-2,4-difluorophenyl)urea, all administered in olive oil with 20% dimethyl sulfoxide by oral injection. After dosing, 0-24 h, 24-48 h urine and 0-48 h faeces samples were collected.

For ^{19}F NMR measurement, urine samples were either diluted once in 0.2 M potassium phosphate pH 7.6 or, when necessary, concentrated by freeze-drying and subsequent dissolving in 0.1 M potassium phosphate pH 7.6.

Faeces samples were homogenized by extensive (o/n) stirring in 25 ml ethyl acetate using a magnetic stirrer. The homogenate obtained was filtered over glass mineral wool and the residue was washed 3 times with 25 ml ethyl acetate. The ethyl acetate filtrate was evaporated to dryness. The residue was dissolved in 4 ml ethyl acetate and analysed by ^{19}F NMR.

Acid and enzyme hydrolysis of urine samples

In order to identify phenolic metabolites excreted in the urine in their N-acetylated, glucuronidated or sulphated form, urine samples were treated with acid, with β-glucuronidase (from *Escherichia coli* K12 (Boehringer, Mannheim, Germany)) or with arylsulphatase/β-glucuronidase (from *Helix pomatia* (Boehringer, Mannheim, Germany)). Enzyme treatments were carried out essentially as described before by Vervoort and Rietjens [13].

For acid hydrolysis of the urine samples 1.0 ml urine sample was incubated with 0.1 ml 37% (12 N) HCl for 1 hour in a boiling water bath. After acid hydrolysis the mixture was neutralised with 6 N NaOH and the sample was diluted once in 0.2 M potassium phosphate pH 7.6 for analysis by ^{19}F NMR.

Microsomal preparations

Preparation of microsomes was carried out essentially as described previously [13]. Microsomes were obtained from perfused livers of male Wistar rats (300-400 g) which were exposed to 150 mg/kg body weight of the cytochrome P450 inducer isosafrole (Janssen Chimica, Beerse, Belgium) by i.p. injection daily for three days using a stock solution of 100 mg/ml in olive oil. The amount of cytochrome P450 in the microsomes was measured according to the method described by Omura and Sato [14].

In vitro microsomal incubations

In vitro microsomal incubations contained (final concentrations): 0.1 M potassium phosphate pH 7.6, 0-5 mM 3,5-dichloro-2,4-difluoroaniline, added from a 100 times concentrated stock solution in dimethyl sulfoxide and 2 μM microsomal

cytochrome P450. Microsomes from isosafrole pretreated rats were used to allow comparison of the results to those of microsomal metabolism of aniline derivatives reported in a previous study [15], which also demonstrated that these microsomes are most effective in metabolism of aniline derivatives [15,16]. The total sample volume was 1 ml. The reaction was started by the addition of NADPH (1 mM final concentration) and the incubation mixture was incubated at 37 °C for 10 min. The reaction was stopped by the addition of 0.3 ml 20% (w/v) trichloroacetic acid after which the mixture was centrifuged for 3 min at 13,000 rpm.

Chemical assay for the detection of 4-hydroxy-3,5-dichloro-2-fluoroaniline

4-Hydroxy-3,5-dichloro-2-fluoroaniline present in the urine and microsomal incubations was determined using the method of Brodie and Axelrod [17] for chemical determination of 4-aminophenol derivatives. Arylsulphatase/β-glucuronidase treated urine samples were extracted with ethyl acetate. To 40 µl of this ethyl acetate fraction, 760 µl demi water and 240 µl trichloroacetic acid (20% w/v) were added. To 800 µl of this mixture 80 µl phenol reagent (5% w/v phenol in 2.5 M NaOH) and 160 µl 2.5 M Na_2CO_3 were added. The absorbance at 630 nm was measured after 1 h at room temperature. Ethyl acetate extract from non-enzyme treated urine was used as a blank.

For the *in vitro* microsomal incubations 100 µl phenol reagent and 200 µl Na_2CO_3 were added to 1 ml of the trichloroacetic acid mixture. A microsomal incubation with water instead of substrate was used as blank.

The ε_{630} value of the 4-hydroxy-3,5-dichloro-2-fluoroaniline derived indophenol is not known. Therefore, based on a previous study on the cytochrome P450-catalysed 4-hydroxylation of halogenated aniline derivatives in which the ε_{630} values of various halogenated aminophenol-derived indophenols were determined [15], the ε_{630} of the 4-hydroxy-3,5-dichloro-2-fluoroaniline-derived indophenol could be set to 20 $mM^{-1}\ cm^{-1}$.

Data analysis

The apparent Michaelis-Menten constant K_m (mM) and the apparent maximum reaction rate k_{cat} (nmol 4-hydroxy-3,5-dichloro-2-fluoroaniline/min/nmol cytochrome P450) for the *in vitro* microsomal cytochrome P450-catalysed 4-hydroxylation of 3,5-dichloro-2,4-difluoroaniline were calculated by fitting the

obtained data of the *in vitro* incubations to the Michaelis-Menten equation $v=V_{max} \cdot [S]/(K_m + [S])$. Fitting the experimental data to the Michaelis-Menten equation resulted in correlation coefficients > 0.97.

^{19}F NMR measurements

^{19}F NMR measurements were performed on a Bruker AMX 300 NMR spectrometer at 280 K. Proton-decoupling was achieved with the Waltz-16 pulse sequence at -20dB from 50W.

Samples contained 100 µl $^{2}H_2O$ for locking the magnetic field and 10 µl 8.4 mM 4-fluorobenzoic acid added as an internal standard. The total sample volume was 1.71 ml. Enzyme and acid treated urine samples were made anaerobic by evacuating and filling with argon four times before analysis. This was done to prevent autoxidation of the phenolic metabolites. Quantification of the different metabolites was done by comparison of the integral of the ^{19}F NMR resonance of the added internal standard 4-fluorobenzoic acid to the integrals of the ^{19}F NMR peaks of the metabolites. The ethyl acetate extract of the faeces was analysed with a coaxial insert containing 4-fluorobenzoic acid dissolved in $^{2}H_2O$. The total sample volume was 1.6 ml. Chemical shifts are reported relative to $CFCl_3$.

Molecular orbital calculations

Semi-empirical molecular orbital calculations were performed on a Silicon Graphics Iris 4D/85 computer with the AM1 (Austin Method 1) Hamiltonian from the AMPAC program (Quantum Chemistry Program Exchange, program no. 506, Indiana University, Bloomington, IN, USA). Calculations were carried out with PRECISE criteria and self-consistent field was achieved for all calculations. Geometries were optimised for all bond lengths, bond angles and torsion angles using the Fletcher-Powell criteria.

Results

Urine and faeces metabolic patterns of 2,6-difluorobenzoic acid, 2,6-difluorobenzamide, 3,5-dichloro-2,4-difluoroaniline, (3,5-dichloro-2,4-difluorophenyl)urea and teflubenzuron

The *in vivo* metabolism of 2,6-difluorobenzoic acid, 2,6-difluorobenzamide, 3,5-dichloro-2,4-difluoroaniline and (3,5-dichloro-2,4-difluorophenyl)urea was investigated in order to identify the metabolites from teflubenzuron that result from hydrolysis of the phenylurea bridge (Figure 1) and subsequent metabolism of the scission products.

2,6-Difluorobenzoic acid

Figure 2a shows the ^{19}F NMR spectrum of the 0-24 h urine of a rat exposed to 10 µmol of 2,6-difluorobenzoic acid. Metabolites were identified on the basis of commercially available 2,6-difluorobenzoic acid and its synthesized glycine conjugate. The ^{19}F NMR spectrum shows that urinary excretion of 2,6-difluorobenzoic acid occurs mainly (96%) in the form of the unmodified parent compound 2,6-difluorobenzoic acid and to a minor extent (4%) as 2,6-difluorobenzoylglycine. The amount of F^- observed could be fully accounted for by the F^- present in blank urine samples from unexposed rats. The total urinary recovery was 86%.

The ^{19}F NMR spectra of the ethyl acetate extracts of the 0-48 h faeces of the 2,6-difluorobenzoic acid exposed rat show no resonance peaks (detection limit 1 µM for an o/n run) (^{19}F NMR spectrum not shown).

2,6-Difluorobenzamide

Figure 2b shows the ^{19}F NMR spectrum of the 0-24 h urine of a rat exposed to 10 µmol of 2,6-difluorobenzamide. Metabolites were identified on the basis of commercially available or synthesized reference compounds. The ^{19}F NMR spectrum shows that urinary excretion of 2,6-difluorobenzamide mainly occurs in the form of 2,6-difluorobenzoic acid (94%) while a minor extent was excreted as 2,6-difluorobenzoylglycine (4%) and unmodified 2,6-difluorobenzamide (2%). The amount of F^- observed could be fully accounted for by the F^- present in blank urine samples from unexposed rats. The 24 h urinary recovery was 100%.

The ^{19}F NMR spectra of the ethyl acetate extracts of the 0-48 h faeces of the 2,6-difluorobenzamide exposed rat show no metabolite or substrate resonances (detection limit 1 µM for an o/n run) (^{19}F NMR spectra not shown).

3,5-Dichloro-2,4-difluoroaniline

Figure 2c shows the ^{19}F NMR spectrum of the 0-24 h urine of a rat exposed to 10 μmol of 3,5-dichloro-2,4-difluoroaniline. ^{19}F NMR resonances of conjugated metabolites, i.e. sulphated, glucuronidated or acetylated products, were identified on the basis of the shift of their ^{19}F NMR resonance in the spectrum upon arylsulphatase and/or β-glucuronidase, or acid treatment of the urine. The aromatic ring hydroxylated product 2-amino-3,5-difluoro-4,6-dichlorophenylsulphate was identified on the basis of its synthesized reference compound. Identification of 4-hydroxy-3,5-dichloro-2-fluoroaniline, formed from its N-acetylated, sulphated and/or glucuronidated conjugate upon acid, arylsulphatase and/or β-glucuronidase treatment of the urine, was achieved on the basis of the chemical assay for detection of 4-aminophenol derivatives. The amount of 4-hydroxy-3,5-dichloro-2-fluoroaniline detected by this chemical assay correlated with the amount of the metabolite giving rise to the ^{19}F NMR resonance at -136.5 ppm which could thus be identified. This latter result was supported by the following observation. In a previous study it was demonstrated that the introduction of a hydroxyl group *meta* with respect to a fluorine in a fluorinated benzene derivatives results in a ^{19}F NMR chemical shift of 1.8 ± 1.2 ppm [16]. Based on this result, the ^{19}F NMR chemical shift of 4-hydroxy-3,5-dichloro-2-fluoroaniline was predicted to be -136.3 ± 1.2 ppm clearly supporting the identification of the ^{19}F NMR resonance value at -136.5 ppm as 4-hydroxy-3,5-dichloro-2-fluoroaniline.

The results in Figure 2c show that the urinary excretion of 3,5-dichloro-2,4-difluoroaniline is mainly in the form of the N-acetylated, sulphated and/or glucuronidated conjugates of its *ortho* and *para*-hydroxylated metabolites. Only one of the metabolite peaks in the ^{19}F NMR spectrum could not be further identified. However, its presence in the urine spectrum of 3,5-dichloro-2,4-difluoroaniline exposed rats clearly identifies this metabolite as derived from the aniline moiety of teflubenzuron. The total 24 h urinary recovery was 59.5% of the administered dose.

The ^{19}F NMR spectra of the ethyl acetate extracts of the 0-48 h collected faeces reveal the presence of some parent aniline compound excreted in the faeces to about 2% of the dose administered (^{19}F NMR spectrum not shown).

(3,5-Dichloro-2,4-difluorophenyl)urea

Figure 2d shows the ^{19}F NMR spectrum of the 0-24 h urine of a rat exposed to 10 μmol (3,5-dichloro-2,4-difluorophenyl)urea. Metabolites were identified in a similar way as described for 3,5-dichloro-2,4-difluoroaniline. The results in Figure 2d demonstrate that (3,5-dichloro-2,4-difluorophenyl)urea is excreted in the urine as the

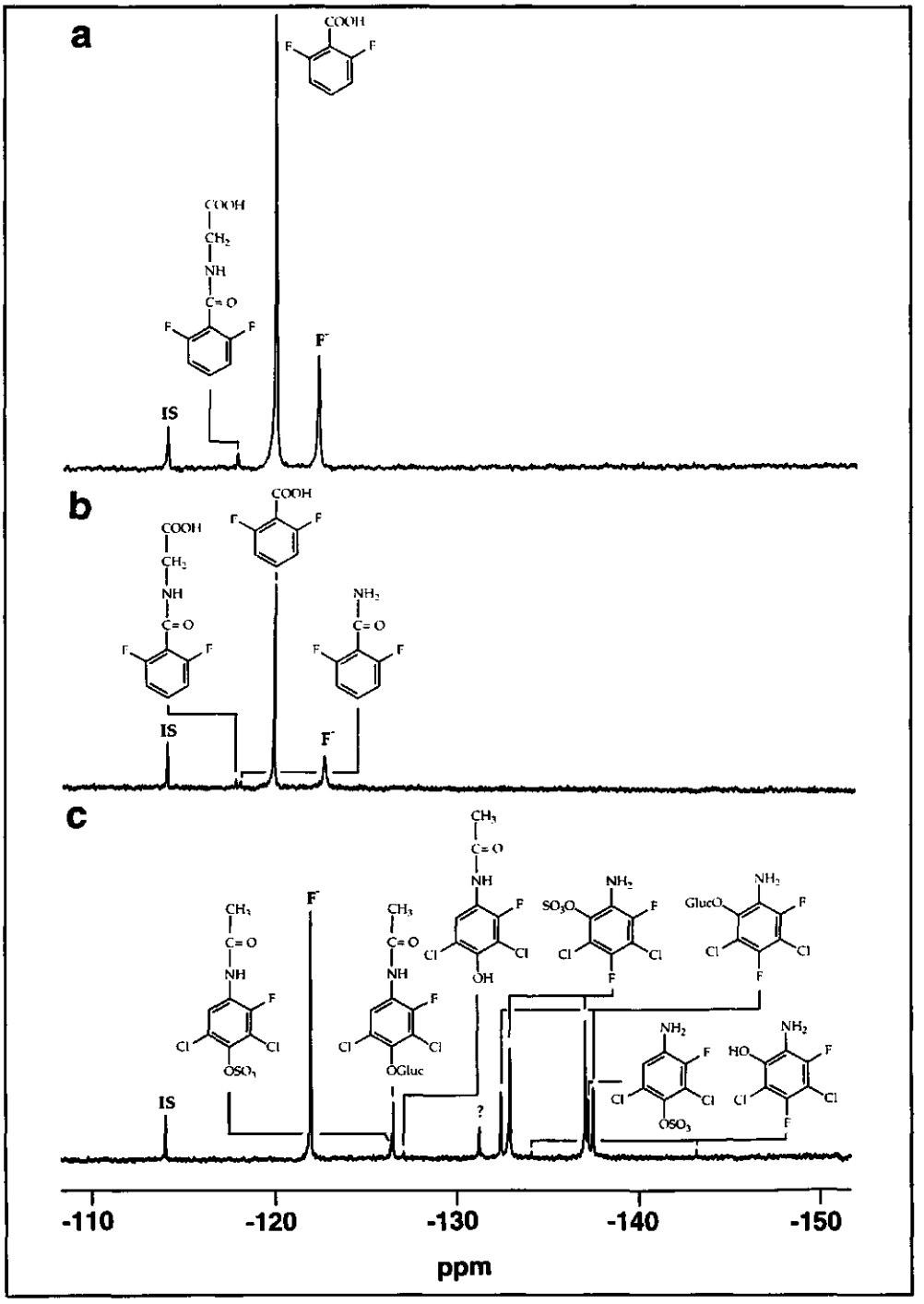
a
b
c
IS
F⁻
?
-110
-120
-130
-140
-150
ppm

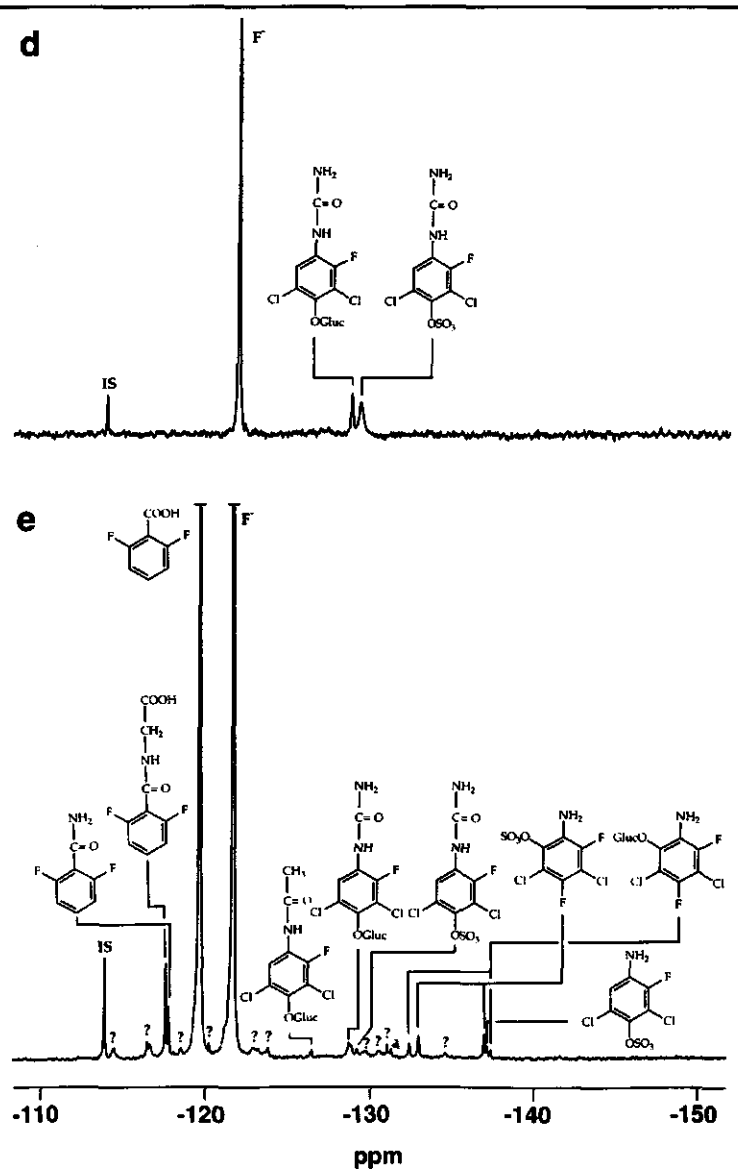

Figure 2 The ^{19}F NMR spectra of the 0-24 h urine samples of rats exposed to (a) 2,6-difluorobenzoic acid, (b) 2,6-difluorobenzamide, (c) 3,5-dichloro-2,4-difluoroaniline, (d) (3,5-dichloro-2,4-difluorophenyl)urea and (e) teflubenzuron. The resonance peak marked with an "a" in Figure 2e belongs to a metabolite derived from biotransformation of 3,5-dichloro-2,4-difluoroaniline, which is one of the scission products of teflubenzuron after hydrolysis of the urea bridge. The fluorine resonances in the spectra a-d are not similar in size due to the different volumes of the 0-24 h urine samples produced by the rats. The resonance peak marked IS is from the internal standard 4-fluorobenzoic acid. Chemical shifts values are reported relative to $CFCl_3$.

sulphated and glucuronidated conjugates of (4-hydroxy-3,5-dichloro-2-fluorophenyl)urea. The total 24 h urinary recovery was 54.5% of the administered dose.

The ^{19}F NMR spectra of the ethyl acetate extracts of the 0-48 h faeces sample reveal the presence of some parent compound excreted in the faeces to about 6% of the dose administered (^{19}F NMR spectrum not shown).

Teflubenzuron

Figure 2e shows the ^{19}F NMR spectrum of the 0-24 h urine of a rat exposed to 53 µmol (20 mg) teflubenzuron. Based on the *in vivo* urinary metabolic patterns of 2,6-difluorobenzoic acid, 2,6-difluorobenzamide, 3,5-dichloro-2,4-difluoroaniline and (3,5-dichloro-2,4-difluorophenyl)urea (Figures 2a-d), metabolites resulting from hydrolysis of the urea bridge of teflubenzuron and further metabolism of the aromatic scission products could be identified. The metabolic profiles thus identified shows that the benzoate part of teflubenzuron is mainly excreted as 2,6-difluorobenzoic acid, and, to a minor extent, as 2,6-difluorobenzoylglycine and 2,6-difluorobenzamide. The aniline ring of teflubenzuron was excreted as the sulphated and glucuronidated conjugates of (4-hydroxy-3,5-dichloro-2-fluorophenyl)urea and 6-hydroxy-3,5-dichloro-2,4-difluoroaniline, the sulphated conjugate of 4-hydroxy-3,5-dichloro-2-fluoroaniline and the glucuronidated conjugate of 4-hydroxy-3,5-dichloro-2-fluoroacetamido. In addition to all these identified metabolites, the ^{19}F NMR spectrum of the urine of the teflubenzuron exposed rats shows several unidentified resonance peaks, one of which has the same chemical shift value as the unidentified resonance peak observed in the urine of rats exposed to 3,5-dichloro-2,4-difluoroaniline indicating that this metabolite can also be ascribed to a metabolite derived from the aniline part of teflubenzuron. The percentage of unidentified peaks amounts to only 12.3% of the total metabolic pattern.

Although a similar amount of benzoate and aniline metabolites should originate from the hydrolytic cleavage of teflubenzuron, the amount of benzoate derived metabolites thus identified in the urine made up 91.3% of the total identified metabolic pattern whereas the amount of aniline derivatives was 8.7%, indicating that the amount of benzoate derived metabolites was eight times the amount of aniline derived metabolites. Thus, the 12.3% of unidentified minor metabolites will not alter the conclusion that there is a remarkable difference in urinary recovery of the two aromatic moieties derived from teflubenzuron. The 24-48 h urine sample of the rat exposed to 53 µmol was also analysed in order to investigate whether due to retarded excretion the remainder of the aniline moiety was excreted in the 24-48 h urine. However, the amount of metabolites in this 24-48 h urine was only 1.5% of the

amount excreted in the 0-24 h urine. Altogether, these data show that part of the aniline moiety is withheld in the body. Since total recovery in 0-24 h urine, 24-48 h urine and 0-48 h faeces amounted to 4.5%, 0.1% and 90% respectively, approximately 5.4% of the dose of teflubenzuron could not be accounted for. Taking into account that recovery of the dose of teflubenzuron administered as benzoate and aniline derived urinary metabolites amounts to 7.5% and 0.9% respectively, indicates that a significant amount of the dose withheld in the body in the first 48 h might indeed have to be ascribed to aniline moiety containing metabolites.

The ^{19}F NMR spectra of the ethyl acetate extracts of the 0-48 h faeces sample of the teflubenzuron exposed rats showed mainly (91%) unchanged teflubenzuron. Scission products of teflubenzuron or metabolites derived from them were not observed. The recovery of teflubenzuron in the faeces was about 90% of the dose.

Dose-recovery studies of teflubenzuron, 2,6-difluorobenzoic acid, 2,6-difluorobenzamide, 3,5-dichloro-2,4-difluoroaniline and (3,5-dichloro-2,4-difluorophenyl)urea

To investigate whether the amount of teflubenzuron administered and of the scission products derived from it would affect the extent of absorption and excretion via urinary and faecal excretion routes dose-recovery studies of teflubenzuron and its possible scission products were performed. Analysis of the 0-48 h urinary samples showed that over the whole dose-range tested, i.e. 4-53 µmol for teflubenzuron and 1-10 µmol for the scission products, for all these compounds their urinary recoveries did not vary significantly. For the scission products this dose range of 1-10 µmol was chosen because the results obtained from the dose-recovery study of teflubenzuron showed that about 0.5-4.0 µmol of teflubenzuron was absorbed from the gastro-intestinal tract and excreted in the 0-24 h urine indicating that the range of 1-10 µmol of aromatic scission products would be in the range to be actually expected to be formed in the rats exposed to 4-53 µmol of teflubenzuron.

At all dose-levels of teflubenzuron about 4.5% of the dose of teflubenzuron is excreted in the 0-24 h urine mainly as metabolites derived from the scission products resulting from hydrolysis of the urea bridge of teflubenzuron, while about 90% of the dose is excreted in the faeces mainly as unmodified teflubenzuron. Furthermore, the urinary recovery of the aniline moiety was only about 12% of the excreted benzoate moiety at the whole 4-53 µmol dose range.

The dose-recovery studies of the benzoate and aniline scission products of teflubenzuron (Figure 3) show that, for a dose range of 1-10 µmol, the 0-24 h urinary

recovery of 2,6-difluorobenzoic acid and of 2,6-difluorbenzamide was always significantly ($P<0.001$) higher and about twice the recovery observed for similar doses of 3,5-dichloro-2,4-difluoroaniline or (3,5-dichloro-2,4-difluorophenyl)urea. This two-fold difference thus explains only part of the eight-fold difference in recovery of the benzoate and aniline moiety in case of their formation from teflubenzuron. This discrepancy might be due to the fact that at the doses tested the rate-limiting Phase I metabolism of the aniline-type scission products is still operating at almost saturating aniline derivative concentrations, whereas upon their formation in situ by hydrolysis of teflubenzuron their steady-state concentration for Phase I metabolism is below V_{max} conditions. Because dose-recovery studies at lower doses of the aniline derivatives were not feasible due to the detection limit of the ^{19}F NMR urine analysis, further experiments were performed to actually determine the kinetic values for this Phase I aromatic hydroxylation of the aniline derivatives.

In vitro microsomal incubations

Figure 4 presents the Michaelis-Menten plot for the microsomal cytochrome P450-catalysed 4-hydroxylation of 3,5-dichloro-2,4-difluoroaniline. The K_m and k_{cat} value derived from these data were 0.58 ± 0.06 mM and 0.24 ± 0.01 nmol/min/nmol P450 respectively.

Molecular orbital computer calculations

Since the microsomal conversion of (3,5-dichloro-2,4-difluorophenyl)urea could not be followed by the sensitive chemical assay available for the aniline derivative, support for its equally low k_{cat} value was derived from theoretical studies. Molecular orbital computer calculations on 3,5-dichloro-2,4-difluoroaniline and (3,5-dichloro-2,4-difluorophenyl)urea were performed to find theoretical support for the low rate of Phase I aromatic hydroxylation of these teflubenzuron-derived splitting products.

The energy of the HOMO (Highest Occupied Molecular Orbital) of 3,5-dichloro-2,4-difluoroaniline and (3,5-dichloro-2,4-difluorophenyl)urea is -9.0 and -9.3 eV respectively, indicative of a k_{cat} for (3,5-dichloro-2,4-difluorophenyl)urea that can not be higher than that obtained for the aniline derivative [15] since the lower E(HOMO) indicates an even lower reactivity of this compound for an electrophilic attack by the activated $(FeO)^{3+}$ species of cytochromes P450.

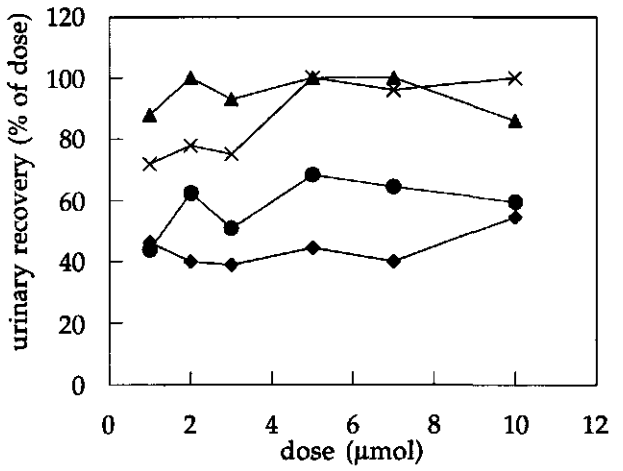

Figure 3 Dose-recovery curves of (▲) 2,6-difluorobenzoic acid, (x) 2,6-difluorobenzamide, (•) 3,5-dichloro-2,4-difluoroaniline and (♦) (3,5-dichloro-2,4-difluorophenyl)urea. The recovery is presented as the percentage of the dose excreted in the urine 24 h after an oral dose of the chemical.

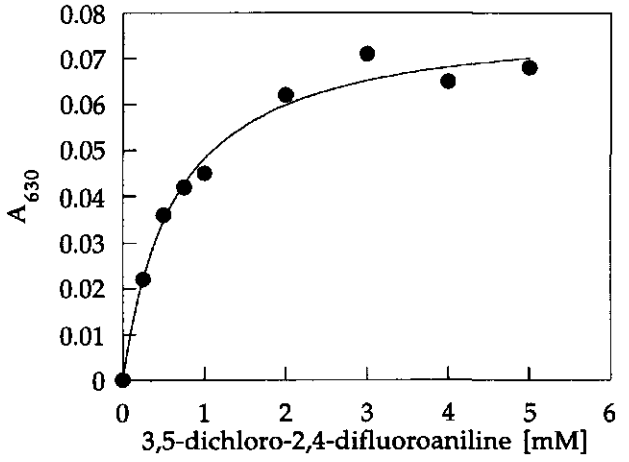

Figure 4 The Michaelis-Menten plot for the microsomal cytochrome P450-catalysed 4-hydroxylation of 3,5-dichloro-2,4-difluoroaniline. From this plot the K_m and k_{cat} values were derived.

Discussion

The aim of the present study was to investigate the biotransformation of the insecticide teflubenzuron in rats. Particular attention was focused on the metabolic fate of the aniline part of teflubenzuron because in previous studies on the biotransformation of diflubenzuron, which is an analogue of teflubenzuron, a lot of uncertainty remained about the recovery and metabolic fate of the aniline derivative formed after hydrolysis of the urea bridge [4,7-10].

Male Wistar rats were orally exposed to different dose levels of teflubenzuron and urine samples as well as faecal extracts were analysed by ^{19}F NMR. The ^{19}F NMR spectra of urine samples of rats orally exposed to teflubenzuron (Figure 2e) mainly showed metabolites derived from products resulting from hydrolysis of the urea bridge. Analysis of faecal extracts of teflubenzuron exposed rats revealed the presence of mainly unmodified teflubenzuron. Within 48 h almost the total dose of teflubenzuron was recovered, partly as metabolites in the urine (4.6% of the dose administered) and mainly in unmodified form in the faeces extract (90% of the dose administered). Independent of the dose of teflubenzuron, the amount of urinary aniline derived metabolites observed amounted to only 12% of the amount of benzoate derived metabolites, in spite of the fact that hydrolytic cleavage of the urea bridge in teflubenzuron will generate equal amounts of benzoate and aniline derivatives. This observation of inefficient excretion of especially the aniline part of teflubenzuron, formed upon hydrolytic cleavage of the urea bridge in the benzoylphenyl urea agrochemical, is in agreement with the qualitative results described previously for diflubenzuron [4,7-10].
Further experiments described in the present study were performed to find a rationale for this significant difference between the urinary recovery of the benzoate- and aniline-type scission products.

First, it was investigated to what extent the observed discrepancy might be ascribed to a difference in excretion efficiency of the benzoate and aniline derivatives themselves. Dose-recovery studies were performed for the four possible scission products, i.e. 2,6-difluorobenzoic acid, 2,6-difluorobenzamide, 3,5-dichloro-2,4-difluoroaniline and (3,5-dichloro-2,4-difluorophenyl)urea. The results obtained showed a difference in the excretion efficiency between the benzoate-type derivatives on the one hand, which were, at all dose levels investigated, almost fully excreted within the first 24 h following administration and the aniline-type derivatives on the other hand, which were excreted, also independent of the dose, to about 50% of the dose administered. Based on these data, excretion efficiencies of the

aniline-type compounds is demonstrated to be at least two-fold lower than that of the benzoates. However, the difference observed in the excretion efficiency of the benzoate- and aniline-type compounds when compounds are formed in situ from teflubenzuron is eight-fold. This discrepancy between the excretion efficiency of the benzoate- and aniline-type compounds of teflubenzuron compared to the experiments when the compounds were dosed as such might be explained on the basis of the following additional observations of the present study.

First, is of importance to notice that the benzoate moiety is almost exclusively excreted in its unmodified form, suggesting that after hydrolysis no further metabolism is required to obtain efficient excretion of the 2,6-difluorobenzoate or the 2,6-difluorobenzamide. In contrast, the metabolites derived from the aniline part of teflubenzuron, i.e. from 3,5-dichloro-2,4-difluoroaniline or from (3,5-dichloro-2,4-difluorophenyl)urea require further metabolism in both Phase I and II metabolism before they can be excreted from the body. Especially the aromatic hydroxylation of such aniline derivatives catalysed by cytochromes P450 to give the aminophenol metabolites suitable for Phase II conjugation and formation of the products that can be efficiently excreted, could be a relatively slow reaction. It is likely that the rate of this cytochrome P450-catalysed aromatic ring hydroxylation is relatively low because cytochrome P450-catalysed aromatic hydroxylation is often the rate-limiting step in biotransformation and generally much slower than Phase II conjugation reactions [15,18].

If the rate of cytochrome P450 conversion of the aniline derivative would indeed be the rate-limiting factor for excretion of the aniline-type derivatives, the actual concentrations of the aniline derivatives in relation to especially the K_m for the reaction might be a factor influencing the actual efficiency of the conversion to a large extent. Especially when the concentration is around or below the K_m values, variation in the actual concentration of the compound will affect the efficiency of its conversion and excretion. This may then be the explanation for the fact that upon direct administration of 1-10 µmol of the aniline derivatives their excretion is more efficient, than when a similar dose is formed over a long time interval upon the hydrolytic cleavage of teflubenzuron. The latter might result in a lower time averaged concentration of the compound.

Comparison of the actual K_m and V_{max} values determined for the cytochrome P450-catalysed C4-hydroxylation of 3,5-dichloro-2,4-difluoroaniline in the present study, to estimate the concentrations expected in the liver, supports this hypothesis. Assuming a liver volume of 5-10 ml, and full absorption and transport of a 1-10 µmol aniline dose from the gastro-intestinal tract to the liver, a maximum

concentration of 3,5-dichloro-2,4-difluoroaniline in the liver of about 0.1-2.0 mM can be foreseen. This is around the K_m value for the cytochrome P450-catalysed oxidative C4-dehalogenation determined to be 0.58 ± 0.06 mM. When in the teflubenzuron exposed animals the same amount of aniline is liberated from the parent compound over a time interval that is for example four times longer than the time interval required for the efficient uptake of the single dose, this will result in lower liver concentrations that will be below the K_m resulting in lower rates of conversion. Such an effect could explain that in the teflubenzuron exposed rats the efficiency for excretion of the aniline-type metabolites is eight-fold lower than for the benzoate-type of metabolites whereas in the direct exposure experiments this difference is only two-fold.

Although this difference in excretion efficiency of the benzoate and aniline-type compounds can explain the observed difference in their urinary recovery, one can not neglect the fact that even upon a single dose of the aniline derivative about 50% of the dose can not be recovered in the 0-48 h urine or faeces. This means that part of the aniline derivative remains in the body. An explanation for this observation might be related to the mechanism by which the cytochrome P450-catalysed oxidative dehalogenation of these halogenated anilines to 4-aminophenol derivatives occur. This oxidative dehalogenation represents the first step required for formation of the 4-hydroxylated urinary metabolites observed. Figure 5 presents the reaction pathway suggested for this reaction. The primary product formed in such a cytochrome P450-catalysed oxidative dehalogenation of a C4-halogenated aniline derivative is the reactive benzoquinoneimine and not its two-electron reduced aminophenol form [19,20]. Swift binding of this reactive benzoquinoneimine to tissue macromolecules instead of its chemical and/or enzymatic reduction to the non-toxic aminophenol, might cause the compound to be withheld in the body. The possibility of such a mechanism causing covalent binding of the aniline part of teflubenzuron to tissue macromolecules seems to be supported by several other observations. First, about 5.4% of the dose of teflubenzuron could not be recovered in urine or faeces. At least part of this 5.4% was expected to be excreted in the form of urinary aniline-type of metabolites since the urinary recovery in the form of benzoate-type metabolites was 7.5% compared to only 0.9% in the form of aniline-type of metabolites. Furthermore, the amount of the fluorine in the 24 h urine of (3,5-dichloro-2,4-difluorophenyl)urea exposed rats was above the amount that could be accounted by the fluorine originating from food and/or drinking water and from the amount of dehalogenated products observed. This observation suggests that part of the aniline moiety is dehalogenated but not excreted from the

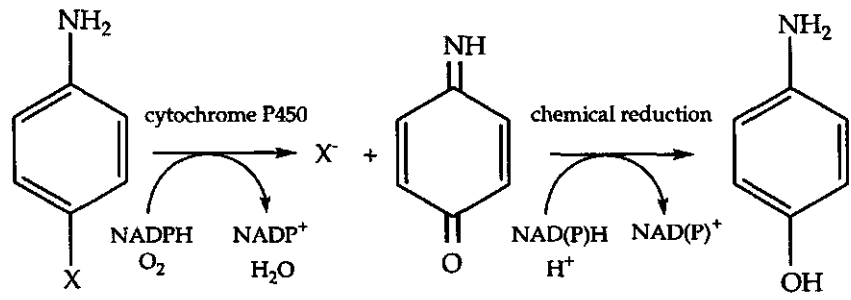

Figure 5 The proposed reaction pathway for the cytochrome P450-catalysed dehalogenation of 4-halogenated anilines [19].

body. Finally, the absence of full excretion of the urea agrochemical from the body would be in line with the results obtained in a study with rats orally exposed to 5 mg/kg diflubenzuron for which 4% of the dose was eventually recovered in the carcass [8]. Finally, the observation of the present study that the 24-48 h urine recovery of teflubenzuron was significantly below the 0-24 h recovery to some extent argues against the slow cytochrome P450-catalysed conversion of the aniline moiety as the main reason for its relatively low recovery. Slow metabolism of a circulating amount of 3,5-dichloro-2,4-difluoroaniline would imply that even after 24 h metabolism and excretion would continue at a level comparable to that observed in 0-24 h. Since this is not what is observed the explanation for low aniline recovery due to covalent interaction of a reactive metabolite derived from it with tissue macromolecules provides the best explanation for this phenomenon. Altogether, the mechanism depicted in Figure 5 might provide the best explanation for the low recovery of the C4-halogenated aniline part of the molecules, both in case of teflubenzuron, but also in case of diflubenzuron, where the C4 position in the aniline moiety is chlorinated. Clearly, such a process resulting in formation of a reactive benzoquinone-type metabolite may be of importance also from a toxicological point of view, especially when taking into account that diflubenzuron was reported to elicit hepatocellular changes in mice [21].

Acknowledgements

The authors gratefully acknowledge Mr. G. van Tintelen for assistance with animal handling. Support from the TMR large scale NMR facility grant no. ERB-CHGE-CT94-0061 is also acknowledged.

References

1 Blanks, R.E. (Ed) (1994) Fluorine in Agriculture 9-11 January 1995. Conference Papers University of Manchester 1995, (United Kingdom: Fluorochem Limited).

2 Park, B.K., and Kitteringham, N.R. (1994) Effects of fluorine substitution on drug metabolism: Pharmacological and toxicological implications. *Drug Met. Rev.* 26, 605-643.

3 Luteijn, J.M., and Tipker, J. (1986) A note on the effects of fluorine substituents on the biological activity and environmental chemistry of benzoylphenylureas. *Pestic. Sci.* 17, 456-458.

4 Verloop, A., and Ferell, C.D. (1977) Benzoylphenyl ureas - A new group of larvicides interfering with chitin deposition. In: Pesticide Chemistry in the 20th Century (Plimmer, J.R., Ed.) (ACS Symposium series, Washington), Vol. 37, pp. 237-270.

5 Van Laecke, K., and Degheele, D. (1991) Detoxification of diflubenzuron and teflubenzuron in the larvae of beet armyworm (*Spodoptera exigua*) (lepidoptera: Noctuidae). *Pestic. Biochem. Physiol.* 40, 181-190.

6 Metcalf, R.L., Lu, P., and Bowlus, S. (1975) Degradation and environmental fate of (2,6-difluorobenzoyl)-3-(4-chlorophenyl)urea. *J. Agric. Food Chem.* 23, 359-364.

7 Ivie, G.W. (1978) Fate of diflubenzuron in cattle and sheep. *J. Agric. Food Chem.* 26, 81-89.

8 Willems, A.G.M., Overmars, H., Scherpenisse, P., De Lange, N., and Post, L.C. (1980) Diflubenzuron: Intestinal absorption and metabolism in the rat. *Xenobiotica* 10, 103-112.

9 Opdycke, J.C., Miller, R.W., and Menzer, R.E. (1982) Metabolism and fate of diflubenzuron in swine. *J. Agric. Food Chem.* 30, 1223-1227.

10 Opdycke, J.C., Miller, R.W., and Menzer, R.E. (1982) In vivo and liver microsomal metabolism of diflubenzuron by two breeds of chickens. *J. Agric. Food Chem.* 30, 1227-1233.

11 Vogel, A.J. (1989) In: Vogel's Textbook of Practical Organic Chemistry, Fourth Edition (Furniss, B.S., Hannaford, A.J., Smith, P.W.G., and Tatchell, A.R., Eds.), Longman Scientific and Technical, England, pp. 1074 and 1274.

12 Boyland, E., Manson, D., and Sims, P. (1953) The preparation of O-aminophenyl sulphates. *J. Chem. Soc.*, 3623-3628.

13 Vervoort, J., De Jager, P.A., Steenbergen, J., and Rietjens, I.M.C.M. (1990) Development of a ^{19}F-n.m.r. method for studies on the *in vivo* and *in vitro* metabolism of 2-fluoroaniline. *Xenobiotica* 20, 657-670.

14 Omura, T., and Sato, R. (1964) The carbon monoxide pigment of liver microsomes, I. Evidence for its haemprotein nature. *J. Chem. Biol.* 239, 2370-2378.

15 Cnubben, N.H.P., Peelen, S., Borst, J.-W., Vervoort, J., Veeger, C., and Rietjens, I.M.C.M. (1994) Molecular orbital-based quantitative structure-activity relationship for the cytochrome P450-catalyzed 4-hydroxylation of halogenated anilines. *Chem. Res. Toxicol.* 7, 590-598.

16 Koerts, J., Boeren, S., Weiss, R., Veeger, C., and Rietjens, I.M.C.M. (1996) Interaction between the substrate and the high-valent iron-oxo porphyrin cofactor as a possible factor influencing the regioselectivity of cytochrome P450-catalysed aromatic ring hydroxylation of 3-fluoro(methyl)anilines. *Chem.-Biol. Interact.* 99, 129-146.

17 Brodie, B.B., and Axelrod, J. (1948) The estimation of acetanilide and its metabolic products, aniline, N-acetyl p-aminophenol and p-aminophenol (free and conjugated) in biological fluids and tissues. *J. Pharmacol. Exp. Ther.* 94, 22-28.

18 Soffers, A.E.M.F., Veeger, C., and Rietjens, I.M.C.M. (1994) Influence of the type of halogen substituent on *in vivo* and *in vitro* phase II metabolism of 2-fluoro-4-halophenol metabolites formed from 3-halo-fluorobenzenes. *Xenobiotica* 24, 759-774.

19 Cnubben, N.H.P., Vervoort, J., Boersma, M.G., and Rietjens, I.M.C.M. (1995) The effect of varying halogen substituent patterns on the cytochrome P450-catalyzed dehalogenation of 4-halogenated anilines to 4-aminophenol metabolites. *Biochem. Pharmacol.* 49, 1235-1248.

20 Rietjens, I.M.C.M., and Vervoort, J. (1991) Bioactivation of 4-fluorinated anilines to benzoquinoneimines as primary reaction products. *Chem.-Biol. Interact.* 22, 263-281.

21 Young, M.F., Trombetta, L.D., and Carson, S. (1986) Effects of diflubenzuron on the mouse liver. *J. Appl. Toxicol.* 6, 343-348.

Chapter 8

Summary and Conclusions

The amount of newly developed chemicals such as agrochemicals, drugs and food additives in our modern society is ever increasing. The industrial production, use and also the release in the environment of these chemicals expose organisms to these xenobiotics. Due to the often hydrophobic character of these xenobiotics they can be easily absorbed and accumulated in the body. However, organisms defend themselves against these agents by converting them enzymatically to more hydrophilic easily excretable products. Sometimes these biotransformation reactions can lead to reactive intermediates which cause cell damage, toxicity, malignancy and/or ultimately carcinogenicity. This indicates why a lot of toxicological screening and safety tests have to be performed during the development of these agents.

However, modern society still requires new compounds with better properties. As it is unfeasible to test the biological activity and toxic effects of all newly developed chemicals in experimental animals, many *in vitro* systems have been developed in which these chemicals can be quickly tested for various biological and/or toxicological effects. To diminish the use of experimental test systems the QSAR concept has been developed, describing so-called Quantitative Structure-Activity Relationships. This QSAR approach should make it possible to predict the biological effect, the biotransformation pattern and/or the toxicity of a chemical based on its physical and chemical characteristics. In this respect the application of MO (Molecular Orbital) computer calculations to describe at least some of these chemical characteristics appears to become more and more useful.

The present thesis focuses on the use of these computer calculated MO parameters for the prediction of biotransformation characteristics of benzene derivatives. Benzene derivatives play an important role as precursors for the synthesis of many xenobiotics and industrially relevant chemicals. The cytochrome P450-catalysed biotransformation of various substituted benzenes was studied and the results were evaluated to determine whether (MO-based) computer calculated chemical parameters of benzenes could explain the results obtained. Where results could not be described well by the chemical reactivity of the substrate itself,

additional experimental work was performed to investigate to which factors and/or interactions the observed deviations could be ascribed. This information can then be used to adopt and improve the predictive model.

Biotransformation of xenobiotics by higher organisms is an enzymatic process in which cytochromes P450 play a major role. This system is able to handle an enormous amount of very structurally different chemicals. The cytochrome P450 enzymes differ in their substrate specificity, metabolic activity and their extent of contribution to the production of toxic metabolites. As outlined in the introduction of this thesis (*Chapter 1*), there are several factors which control the cytochrome P450-catalysed biotransformation. These factors include for example, electron donation to cytochrome P450, the accessibility of the active $(FeO)^{3+}$ species in the active site of the enzyme, the interaction between the substrate and the active site and the chemical reactivity of the substrate itself. In cases where the latter factor controls the outcomes of the cytochrome P450-catalysed biotransformation, one could describe a QSARs for the reaction. Based on these QSARs the cytochrome P450-catalysed biotransformation of other chemicals might be predicted. Furthermore, these QSARs might give more insight in the mechanistic background of the biotransformation reaction for which it has been developed.

An example of this approach is described in *Chapter 2* of this thesis. In this chapter *in vivo* cytochrome P450-catalysed aromatic ring hydroxylation of various substituted benzene derivatives was determined using ^{19}F NMR. Previous reported results on the regioselectivity of cytochrome P450-catalysed aromatic ring hydroxylation of a series (poly)fluorobenzenes [1] demonstrated a clear QSAR (correlation 0.96) relating the site of hydroxylation of the site of the reactive HOMO π-electrons in the benzene substrate. Thus, in *Chapter 2* the same parameter was tested for its ability to predict the regioselectivity of aromatic hydroxylation of a series C4-substituted fluorobenzenes. It turned out that the MO-QSAR approach could well predict the regioselectivity of the series of 4-X-substituted fluorobenzenes when X was a H, F, Cl, and CN group. However, this approach of predicting the regioselectivity of aromatic hydroxylation ran into problems when the *para* substituent was a bromine or iodine. The extent to which the hydroxylation adjacent to a bromine and iodine substituent was reduced, correlated qualitatively with the size of the substituents as given by their Van der Waals radius, i.e. the larger the substituent the greater the deviation between the predicted and observed

hydroxylation at the adjacent aromatic carbon centre. Additional experiments showed that the observed deviations could not be ascribed to a stereoselective orientation of these substrates in the active sites of cytochromes P450. These results led to the hypothesis that bromine and iodine substituents sterically hamper the electrophilic attack of the cytochrome P450 high-valent iron-oxo species on the carbon atoms adjacent to the substituted carbon centres. This hypothesis was supported by calculating the steric effects of bromine and iodine substituents, thus defining a steric correction factor for prediction of the aromatic ring hydroxylation at sites *ortho* with respect to a bromine or iodine substituent. In a second series of regioselectivity experiments using a series of tri-substituted benzenes containing fluorine, chlorine, bromine, iodine and cyano substituents, these steric correction factors were validated. Without using the steric correction factors for bromine and iodine substituents no correlation between the predicted and observed regioselectivity was obtained. However, upon application of the correction factors a correlation factor of 0.91 was obtained for prediction and actually observed regioselectivity of cytochrome P450-catalysed aromatic hydroxylation of the series tri-substituted benzenes. These results show that the QSAR which was initially developed for a series of (poly)fluorobenzenes was still valid for other substituted benzenes taking into account the steric hindrance by relatively large substituents such as bromine and iodine. Furthermore, from a mechanistic point of view these MO-QSARs suggest that the cytochrome P450-catalysed aromatic ring hydroxylation of at least the benzene derivatives tested proceeds by an initial attack of the iron-oxo species on the ring carbon atom, without the formation of arene oxide intermediates as a major route [2,3].

The question remains why going from a chlorine to a bromine substituent, steric hindrance is observed rather abrupt. A possible explanation might be found in the observation that when two molecules approach each other the potential energy goes through a minimum and thereafter increases rapidly with decreasing distance.

Surprisingly, it was found that steric hindrance by the cyano group was not observed although this group is definitely larger than a bromine. However, with respect to steric hindrance of the electrophilic attack of the $(FeO)^{3+}$ species, only the atom closest to the aromatic ring might have to be taken into account. Steric hindrance of this atom, a carbon, is not expected since a carbon, has a size similar to that of a chlorine.

More complicated substituents than H, F, Cl, Br, I and CN were investigated in *Chapter 3* where the regioselectivity of aromatic ring hydroxylation of 3-fluoro(methyl)anilines was investigated. Little is known about the cytochrome P450-catalysed biotransformation of such methylanilines. Results from the *in vivo* and *in vitro* cytochrome P450-catalysed regioselectivity of aromatic hydroxylation showed that the frontier orbital density distribution in the aromatic ring could only qualitatively predict the observed regioselectivity. Again, as for the bromine and iodine substituents the observed regioselectivity of aromatic ring hydroxylation for the various amino and methyl substituted substrates showed systematic deviations from the predicted regioselectivity, i.e. hydroxylation at the ring carbon C4 *para* with respect to the amino moiety was always higher than predicted while hydroxylation at the carbon atoms *ortho* with respect to the amino group (C2 and C6) was lower than expected. Further research was performed to investigate why for this series of amino and/or methyl substituted benzene derivatives the intrinsic chemical reactivity did not predict the observed regioselectivity of aromatic hydroxylation quantitatively. Three different experimental approaches were used to investigate possible reasons underlying the systematic deviations between predicted and observed regioselectivity for the cytochrome P450-catalysed aromatic hydroxylation of amino-containing benzenes. These results are discussed in some more detail hereafter.

1. As a first approach, incubations of 3-fluoro-2-methylaniline with different microsomal preparations containing various cytochrome P450 enzyme patterns as well as with purified cytochrome P4502B1 were performed. The regioselectivity for aromatic hydroxylation of 3-fluoro-2-methylaniline observed in all these incubations were similar. This result indicates that cytochromes P450 with different active sites give similar regioselectivities and, thus, in case of 3-fluoro-2-methylaniline similar deviations for predicted values. This suggests that the observed discrepancy between predicted and observed aromatic hydroxylation patterns can not be ascribed to a stereoselective orientation of the 3-fluoro(methyl)anilines imposed by the active sites of the cytochromes P450 catalysing its conversion.

2. Further support for this conclusion was obtained from ^{1}H NMR T_1 relaxation studies on fluoromethylanilines. These studies are described in *Chapter 4*. It appears that the orientation of the tested fluoromethylanilines in the active sites of cytochromes P4501A1 and 2B1 is similar. Based on the observation that all aromatic protons are at about the same average distance from the catalytic Fe^{3+} centre, these

results are most compatible with a time-averaged orientation of the substrates with the Fe^{3+} above the aromatic ring and the π-orbitals of the aromatic ring and those of the porphyrin rings in a parallel position. This latter aspect would provide possibilities for energetically favourable π-π interactions. Possibilities for a flip-flop rotation around an axis in the plane of the aromatic ring of the substrate can be included in this picture, as such rotations would still result in a similar average distance of all aromatic protons to the Fe^{3+} centre. Altogether, the data strongly suggest that, independent of the cytochrome P450 enzyme these substrates can rotate freely in the active site and are not hindered and/or specifically orientated by interactions with specific amino acid residues of the active site.

3. Finally, the possible influence of the active site on the cytochrome P450-catalysed aromatic hydroxylation was tested by using microperoxidase-8 as a model system for cytochrome P450-catalysed aromatic ring hydroxylation. Microperoxidase-8 is a so-called mini-enzyme prepared by proteolytic digestion of horse-heart cytochrome c. MP-8 contains a heme covalently attached to a peptide chain of only eight amino acids and thus it lacks an active site. MP-8 is well known to perform peroxidase-like reactions. However, experimental evidence has been obtained described in *Chapter 5* of this thesis that the MP-8-catalysed aromatic ring hydroxylation of aniline and phenol derivatives in a H_2O_2-driven system proceeds by a cytochrome P450-like oxygen-transfer mechanism. This could be concluded from the fact that ^{18}O incorporation from $H_2{}^{18}O_2$ into the 4-aminophenol formed from aniline was 100%. Thus, the H_2O_2-driven MP-8 system was used as a model to study regioselectivity of oxygen-transfer in a heme-based catalyst without an active site.

The results of such experiments demonstrated that the MP-8-catalysed aromatic ring hydroxylation of 3-fluoro(methyl)anilines (*Chapter 3*) results in similar regioselectivities of aromatic ring hydroxylation as those observed for cytochrome P450-catalysis. As a specific substrate binding site in MP-8 can be excluded, these results, together with those obtained from different microsomal preparations (*Chapter 3*) and the ^1H NMR T_1 relaxation measurements (*Chapter 4*), clearly eliminates the possibility that the regioselectivity of aromatic ring hydroxylation is predominantly dictated by a stereoselective orientation of the substrate in the active site of cytochromes P450. Thus for these relatively small and non-polar substrates specific interactions between molecular sides in the substrate and amino acid side chains present in the active site are not dictating a stereoselective orientation of these substrates.

Since the MP-8-catalysed reactions showed similar deviations between predicted and observed regioselectivity of aromatic hydroxylation of 3-fluoro(methyl)anilines, it was concluded that the deviations must result from an orientating interaction between the substrate and the high-valent iron-oxo species $(FeO)^{3+}$ itself, resulting in a stereoselective orientation of the substrate towards the catalytically active species. This interaction can be expected to be quite similar for different cytochromes P450 and might also be comparable in the active MP-8 system. This implies that, in contrast to what was observed by ^1H NMR for substrates bound to the Fe^{3+} resting state of the enzyme, the $(FeO)^{3+}$ form of the protein would impose a preferential orientation of the amino-containing substrate in such a way that on the average C4 (*para* to the amino) is closer to whereas C2/6 (*ortho* to the amino) are further away from the $(FeO)^{3+}$ species. Support for a different substrate orientation in the Fe^{3+} resting state and the $(FeO)^{3+}$ activated form respectively can be found in a study of Paulsen and Ornstein [4]. They showed that the orientation of camphor in the presence and absence of the high-valent iron-oxo species $(FeO)^{3+}$ was different and that orientation in the presence of the catalytically active form of the enzyme ($(FeO)^{3+}$) was in accordance with the observed regioselectivity of oxidation.

Altogether, results from all studies on the regioselectivity of aromatic hydroxylation of the various benzene derivatives show that the regioselectivity of the H, F, Cl, Br, I, CN, CH_3 and NH_2 substituted benzene derivatives investigated is predominantly determined by their chemical reactivity. However, especially for amino-containing benzene derivatives interactions between the substrate and the high-valent iron-oxo species, resulting in a stereoselective orientation of the substrate, might also play a role. This means that the QSAR for aromatic ring hydroxylation in the case of amino-containing benzenes predicts only qualitatively the regioselectivity of aromatic ring hydroxylation for these series of substrates.

An additional result obtained in all regioselectivity studies was the absence of formation of NIH shifted phenolic metabolites. The formation of such NIH shifted phenolic metabolites has been well documented especially for the biotransformation of chlorinated and brominated benzene derivatives. As the benzenes in our studies were mainly fluorinated, we decided to investigate whether there was a (chemical) reason for this discrepancy.

In Chapter 6 the possibility of a cytochrome P450-catalysed fluorine NIH shift in a series of polyfluorobenzenes was investigated and compared with the

literature data of the chlorinated analogues. The *in vivo* biotransformation of a series polyfluorobenzenes showed that formation of NIH shifted metabolites was not a significant biotransformation route. As outlined above, this is in contrast to the results reported in the literature for the chlorinated analogues. However, in contrast to the *in vivo* data, in *in vitro* microsomal studies with 1,4-difluorobenzene formation of a significant amount of fluorine NIH shifted phenolic metabolite was observed. Unfortunately, the *in vitro* microsomal conversion of the other used polyfluorobenzenes could not be detected, possibly due to the fact that the HOMO energy of these substrates was too low for an efficient conversion by cytochromes P450 [5]. It is generally accepted that formation of NIH shifted metabolites proceeds via arene oxide intermediates and that these arene oxides, especially *in vivo*, but not *in vitro* in a microsomal system, might react in competing conjugation pathways such as GSH conjugation. Additional *in vivo* and *in vitro* experiments showed that indeed GSH conjugation was a competing pathway for the arene oxide intermediates, its presence or absence resulting in an influence on the amount of NIH shifted phenolic metabolites observed.

Nevertheless, the results thus obtained also clearly illustrated and confirmed the reduced capacity for formation of NIH shifted phenolic metabolites for fluoro- as compared to chlorobenzenes. This differences between the NIH shift for fluorine and chlorine containing benzenes was further investigated and could be explained by MO computer calculations on the proposed reaction intermediates in the two biotransformation pathways. Epoxide ring opening, supposed to be the rate-limiting step in the formation of NIH shifted metabolites, appeared easier for chlorinated benzenes compared to their fluorinated analogues. Furthermore, these MO calculations in combination with a MO-QSAR for the rate of GS-conjugation of electrophilic model compounds [6] were indicative for higher rates of GSH conjugation for the fluorinated benzene arene oxides than the chlorinated analogues. The detoxifying pathway of GSH conjugation is very important for assessing the risks of these kind of substrates as arene oxides are known to react with protein and DNA provoking toxic and/or mutagenic/carcinogenic responses.

Altogether, the results from this study show that MO calculations can not only explain and thus predict the regiospecificity of biotransformation in a molecule but also explain the relative rates, i.e. chances, on different biotransformation routes.

Finally, in addition to all studies on model benzene derivatives, the last chapter of this thesis (*Chapter 7*) describes studies on the biotransformation of a halogenated benzene derived compound that is used as an insecticide, i.e. teflubenzuron. This may provide some insight in the possibilities to use outcomes from studies on model compounds to obtain insights also in the biotransformation of other compounds. Teflubenzuron, which is used for the protection of fruit and vegetables against larves, contains two aromatic benzene-derived rings connected via an urea bridge. These aromatic rings are differently substituted and are a suitable starting point to evaluate the influence of various substituents on the metabolic fate of the chemical. Basically, they are an aniline and a benzoate derived moiety. Results of this study on the biotransformation of teflubenzuron demonstrate that upon an oral dose of the insecticide to male Wistar rats the metabolic fate of the two aromatic rings is significantly different. Though about 90% of the dose was excreted unchanged in the faeces, the remainder of the dose was absorbed from the gastro-intestinal tract and -in part- excreted in the urine mainly after hydrolysis of the urea bridge. Interestingly, the urinary recovery of the benzoate moiety was about 8 times higher than that of the aniline moiety of teflubenzuron. Dose-recovery studies on the scission products of teflubenzuron confirmed these results as the urinary recovery of the metabolites from the benzoate moiety were nearly 100% while the recovery of the aniline derivatives was only about 50%. The benzoate moiety is excreted unchanged or after a Phase II reaction, while the aniline moiety has to undergo both a Phase I and II reaction before it can be excreted. The significant difference between the recovery of the benzoate and aniline moiety can be best explained by the formation of a cytochrome P450-catalysed reactive benzoquinoneimine from the C4 halogenated aniline derivatives. Swift binding of these reactive benzoquinoneimines to tissue macromolecules might cause the compound to be withheld in the body. This is also important from a toxicological point of view as binding of these reactive benzoquinoneimines might provoke toxic and/or mutagenic/carcinogenic effects in the body.

Altogether, the results described in this thesis show that QSARs are very useful in explaining the biotransformation pattern of relatively small and non-polar benzene derivatives. Their biotransformation pattern was demonstrated to be predominantly determined by the chemical reactivity of the benzenes and - although to a much lesser extent for bromine, iodine and amino containing derivatives- more than by steric factors (Br,I) and/or electronic dipole-dipole interactions with the

activated $(FeO)^{3+}$ cofactor (NH_2). However, the further extension of the presently developed QSARs to more complicated and especially to larger molecules might require the incorporation of computer techniques that take into account preferential stereoselective substrate orientations imposed by the active sites. Although the molecular modelling computer techniques to do these type of additional orientation analyses are available, such studies also require the availability of the enzyme crystal structures. Since such 3-D structures for cytochromes P450 are at present restricted to some bacterial cytochromes P450 and not available for mammalian cytochromes P450 the studies may have to await the elucidation of the mammalian cytochrome P450 structures. Nevertheless, the concept as such might be developed using either molecular modelling combined with quantum chemical calculations for the bacterial cytochrome P450 system as done recently by Zakharieva et al. [7] and Freutel et al. [8], or by performing similar studies for other biotransformation enzymes, such as for example the glutathione S-transferases for which several 3-D structures have been described.

In general, QSARs can be used to predict the biological activity of non-tested chemicals but they can also give more insight in the mechanistic rules of biotransformation of molecules. This knowledge can be very helpful for example when the technical ability of cloning cytochromes P450, and thus producing these enzymes in large quantities, is increasing. Cytochromes P450 could then be used for the synthesis of chemical products (P450 biotechnology). Especially cytochromes P450 are suitable as they are able to convert many structural diverse substrates. The advantage of enzymatic synthesis compared to chemical synthesis is that it causes among others less waste problems.

References

1 Rietjens, I.M.C.M., Soffers, A.E.M.F., Veeger, C., and Vervoort, J. (1993) Regioselectivity of cytochrome P-450 catalyzed hydroxylation of fluorobenzenes predicted by calculated frontier orbital substrate characteristics. *Biochemistry* 32, 4801-4812.

2 Korzekwa, K.R., Swinney, D.C., and Trager, W.F. (1989) Isotopically labeled chlorobenzenes as probes for the mechanism of cytochrome P-450 catalyzed aromatic hydroxylation. *Biochemistry* 28, 9019-9027.

3 Rizk, P.N., and Hanzlik, R.P. (1995) Oxidative and non-oxidative metabolism of 4-iodoanisole by rat liver microsomes. *Xenobiotica* 25, 143-150.

4 Paulsen, M.D., and Ornstein, R.L. (1993) Substrate mobility in thiocamphor-bound cytochrome $P450_{cam}$: An explanation of the conflict between the observed product profile and the X-ray structure. *Protein Engng.* 6, 359-365.

5 Cnubben, N.H.P., Peelen, S., Borst, J.-W., Vervoort, J., Veeger, C., and Rietjens, I.M.C.M. (1994) Molecular orbital-based Quantitative Structure-Activity Relationship for the cytochrome P450-catalyzed 4-hydroxylation of halogenated anilines. *Chem. Res. Toxicol.* 7, 590-598.

6 Soffers, A.E.M.F., Ploemen, J.H.T.M., Moonen, M.J.H., Wobbes, Th., Van Ommen, B., Vervoort, J., Van Bladeren, P.J., and Rietjens, I.M.C.M. (1996) Regioselectivity and quantitative structure-activity relationships for the conjugation of a series fluoronitrobenzenes by purified glutathione S-transferase enzymes from rat and man. *Chem. Res. Toxicol.* 9, 638-646.

7 Zakharieva, O., Grodzicki, M., Trautwein, A.X., Veeger, C., and Rietjens, I.M.C.M. (1996) Molecular orbital study of the hydroxylation of benzene and monofluorobenzene catalysed by iron-oxo porphyrin π cation radical complexes. *JBIC* 1, 192-204.

8 Freutel, J.A., Collins, J.R., Camper, D.L., Loew, G.H., and Ortiz de Montellano, P.R. (1992) Calculated and experimental absolute stereochemistry of the styrene and β-methylstyrene epoxides formed by cytochrome P450cam. *J. Am. Chem. Soc.* 114, 6987-6993.

Abbreviations and Symbols

AcetylcoA	acetyl coenzyme A
AM1	Austin method 1
ATP	adenosine triphosphate
c^2	frontier orbital density
CO	carbonmonoxide
CYP/cyp	cytochrome P450 gene
Cys	cysteine
DNA	deoxyribonucleic acid
E	energy
EDTA	ethylenediaminetetraacetate
E(HOMO)	energy of the HOMO
elec	electrophile
E(LUMO)	energy of the LUMO
EROD	ethoxyresorufin O-dealkylation
FAD	flavin adenine dinucleotide
GC-MS	gaschromatography-mass spectrometry
FeO(H)	high-valent iron-oxo species
GSH	glutathione
H	Hamiltonian operator
H_r	heat of formation of a reaction
H‡	activation energy
ΔHF	heat of formation
HPLC	high performance liquid chromatography
HOMO	highest occupied molecular orbital
HRP	horseradish peroxidase
IS	internal standard
JHF	coupling constant
k_{cat}	first-order rate constant of enzymatic conversion
kDa	kilodalton
K_m	Michaelis-Menten constant, substrate concentration at 1/2 V_{max}
K_s	binding affinity constant
LUMO	lowest unoccupied molecular orbital
3-MC	3-methylcholanthrene
MINDO/3	modified intermediate neglect of differential overlap/3
MNDO	modified neglect of differential overlap
MP-8	microperoxidase-8
mRNA	messenger ribonucleic acid
MO	molecular orbital
MO-QSAR	molecular orbital based quantitative structure-activity relationship
M_τ	nmr peak area at delay time τ

NAD(P)H	reduced nicotinamide adenine dinucleotide (phosphate)
NIH	national institute of health, USA
NMR	nuclear magnetic resonance
nucl	nucleophile
o/n	overnight
$P450_{cam}$	cytochrome P450 camphor
$P450_{BM3}$	cytochrome P450 *Bacillus megaterium*
$P450_{terp}$	cytochrome P450 terpineol
PAPS	3'-phosphoadenosine-5'-phosphosulfate
PCN	pregnenolone 16α-carbonitrile
PCA	principal components analysis
PLS	partial least squares
ppm	parts per million
Q	charge
QSAR	quantitative structure-activity relationship
QSMR	quantitative structure-metabolism relationship
r	distance or correlation coefficient
R	molar gas constant
S	substrate
SAM	S-adenosylmethionine
S.D.	standard deviation
SO	oxygenated substrate
SOD	superoxide dismutase
SOMO	singly occupied molecular orbital
t	time
T_1	longitudinal relaxation time
UDP	uridine diphosphate
UDP-GA	uridine-5'-diphospho-α-D-glucuronic acid
V_{max}	maximal enzymatic velocity
β	resonance overlap integral
β-NF	β-naphtoflavone
ε	local dielectric constant
ε_x	extinction coefficient at wavelength x
τ	delay time
τ_c	correlation time
Y	electron wave function

Samenvatting
(ook voor niet-ingewijden)

De welvaart in de westerse samenleving is mede te danken aan de ontwikkeling van vele chemische verbindingen zoals gewasbeschermingsmiddelen (b.v. pesticiden en herbiciden), farmaceutische verbindingen, plastics en kunstmatige voedseladditieven. Deze niet van nature voorkomende verbindingen zijn voor organismen, zoals mens en dier, lichaamsvreemd en worden xenobiotica genoemd. Organismen worden aan deze verbindingen onder zeer verschillende omstandigheden blootgesteld, zoals tijdens de fabricage en het gebruik van xenobiotica, maar ook doordat zij als verontreinigingen in het milieu voorkomen.

Veel xenobiotica zijn hydrofoob (vet oplosbaar) en kunnen dus makkelijk in het vetweefsel van het lichaam opgehoopt worden. Gelukkig zijn organismen in staat om zich te verdedigen tegen ophoping van deze chemicaliën in het lichaam doordat enzymen ("kleine chemische fabriekjes") deze componenten kunnen omzetten in meer hydrofiele (water oplosbare) verbindingen die het lichaam kunnen verlaten via de urine en/of faeces. Het enzymatisch omzetten van verbindingen wordt biotransformatie genoemd. Deze biotransformatie reakties voor lichaamsvreemde stoffen kunnen ingedeeld worden in Fase I (transformatie) en II (conjugatie) reakties. In Fase I reakties wordt meestal een groep ingebracht of vrijgemaakt die het molecuul vatbaar maakt voor een Fase II reaktie waarin het gemodificeerde molecuul wordt gekoppeld aan een endogene (van nature in het lichaam aanwezige) component (b.v. glutathion). Meestal leiden deze biotransformatie reakties tot verbindingen die niet alleen beter wateroplosbaar zijn maar ook minder giftig zijn dan de uitgangsverbinding (detoxificatie). Echter, in sommige gevallen leiden deze reakties tot voor het lichaam giftige (toxische) verbindingen (bioactivatie) die schade kunnen aanrichten doordat zij reageren met eiwitten, DNA en/of andere celcomponenten en daardoor de normale functies van cellen verstoren.

Eén van de belangrijkste Fase I enzymen verantwoordelijk voor de biotransformatie van lichaamsvreemde stoffen is het cytochroom P450 dat in vele lichaamsdelen voorkomt, vooral in de lever. Het lichaamsvreemde molecuul wordt

op een bepaalde plaats in het enzym gebonden (actieve centrum) en aldaar omgezet. Bij deze omzetting wordt in het algemeen een zuurstof atoom van een geactiveerde ijzer-oxo porphyrine (heem) groep ($(FeO)^{3+}$) in het substraat gezet. Bij de omzetting van lichaamsvreemde stoffen door dit enzym spelen diverse factoren een rol. De chemische reactiviteit van het substraat bepaalt voor een belangrijk deel de omzetting. Daarnaast kunnen interacties tussen specifieke chemische of sterische eigenschappen van het substraat en het actieve centrum resulteren in een specifieke oriëntatie van het substraat in het actieve centrum. Hierdoor is het mogelijk dat het substraat niet vrij draaibaar is en zullen bepaalde plaatsen in het molecuul beter bereikbaar zijn voor een aanval door het $(FeO)^{3+}$ deeltje dan andere plaatsen.

Het feit dat sommige verbindingen schade kunnen aanrichten in organismen betekent dat nieuw gesynthetiseerde chemicaliën eerst goed getest moeten worden voordat zij op de markt kunnen komen. Daar het aantal nieuw ontwikkelde componenten groot is, is het onmogelijk om alle nieuw gesynthetiseerde verbindingen te testen in proefdieren op hun toxische eigenschappen. Een geld- en tijdbesparende methode die de laatste jaren is ontwikkeld om de reactiviteit van deze verbindingen te kunnen voorspellen is het beschrijven van QSAR's (Quantitatieve Structuur-Activiteits Relaties). Een QSAR beschrijft een correlatie tussen bijvoorbeeld de chemische, fysische of geometrische eigenschappen van een verbinding en zijn biologische activiteit. Deze eigenschappen van een verbinding worden tegenwoordig steeds meer bepaald met behulp van vaak snelle en eenvoudige computer programma's. Op basis van eenmaal opgestelde QSAR's kunnen voorspellingen gedaan worden voor de biologische activiteit van nog niet onderzochte verbindingen (*Hoofdstuk 1*).

In dit proefschrift is onderzocht in hoeverre een QSAR voor de cytochroom P450 gekatalyseerde aromatische ring hydroxylering van fluorbenzenen (zie Figuur 1) toepasbaar is op benzeen derivaten die substituenten bevatten die ingewikkelder zijn dan het relatieve kleine en inerte fluor atoom. Het blijkt dat de QSAR geldig kan zijn voor substituenten zoals Cl, Br, I en CN, maar dat voor Br en I wel een correctie factor nodig is om de regioselectiviteit van aromatische ring hydroxylering quantitatief te kunnen voorspellen (*Hoofdstuk 2*). Deze substituenten zijn zo groot dat zij sterische hinder veroorzaken voor de aanval van het $(FeO)^{3+}$ deeltje op de koolstof atomen in de aromatische ring naast het gesubstitueerde koolstof atoom. Geconcludeerd kon worden dat de QSAR die is opgesteld voor de regioselectiviteit van aromatische ring hydroxylering van fluorbenzenen ook kan worden gebruikt voor benzeen derivaten met een Cl, Br, I, en CN groep, rekening houdend met

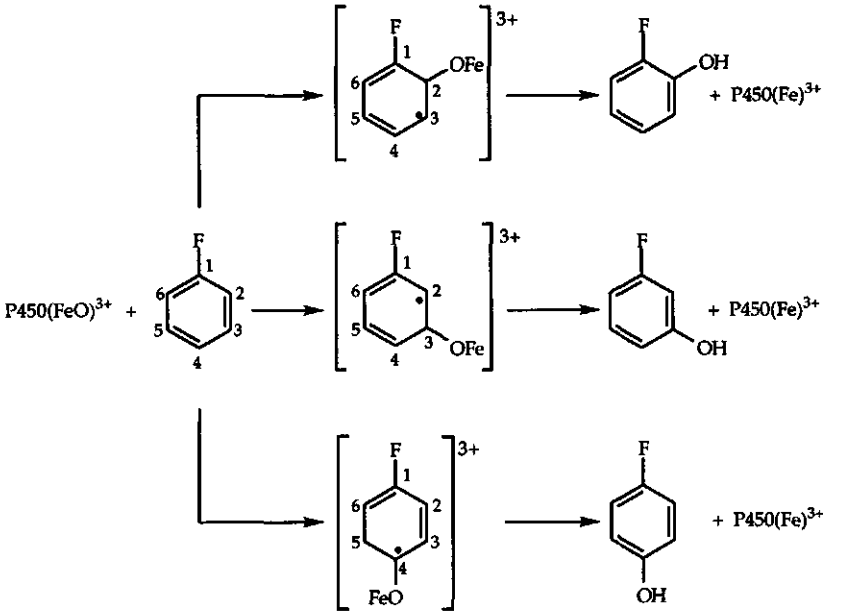

Figuur 1 De cytochroom P450 gekatalyseerde regioselectiviteit van aromatische ring hydroxylering van fluorbenzeen.

sterische hindering van de Br en I atomen. Dit houdt in dat de cytochroom P450 gekatalyseerde aromatische ring hydroxylering van deze onderzochte benzeen derivaten voornamelijk verloopt via een electrofiele aanval van het $(FeO)^{3+}$ deeltje op de ring koolstof atomen (σ-additie). Dit σ-adduct legt vervolgens direkt, of via een keto intermediair, om naar de fenol. Dit betekent dat areenoxide intermediairen geen belangrijke rol spelen in de route die leidt tot fenol vorming. Dit laatste is in tegenstelling tot wat vaak in de literatuur wordt aangenomen.

Bij een serie benzeen verbindingen met een amino (NH_2) en methyl (CH_3) groep als substituenten in de aromatische ring (3-fluor(methyl)anilines), bleek dat de QSAR de regioselectiviteit van aromatische ring hydroxylering alleen qualitatief kon voorspellen (*Hoofdstuk 3*). De afwijkingen die gevonden werden tussen de voorspelde en gevonden regioselectiviteit kunnen worden toegeschreven aan een mogelijke interactie tussen het $(FeO)^{3+}$ deeltje en de amino groep in het substraat

resulterend in een stereoselectieve oriëntatie van het substraat in het actieve centrum van het cytochroom P450. Deze stereoselectieve oriëntatie van het substraat zorgt ervoor dat niet alle ring koolstof atomen even goed bereikbaar zijn voor aanval van het $(FeO)^{3+}$ deeltje. Deze hypothese werd ondersteund door resultaten van ^1H NMR T_1 relaxatiemetingen die lieten zien dat een serie fluormethylanilines in de actieve centra van microsomaal en gezuiverd cytochroom P4501A1 en 2B1 vrij draaibaar waren ten opzichte van het Fe^{3+} centrum (*Hoofdstuk 4*). De invloed van het actieve centrum op de regioselectiviteit van aromatische ring hydroxylering werd verder onderzocht met behulp van het mini-heem enzym microperoxidase (MP-8), hetgeen bestaat uit een ijzer porphyrine gebonden aan slechts acht aminozuren en dus een actief centrum mist. Resultaten van experimenten toonden aan dat de MP-8 gekatalyseerde aromatische ring hydroxylering verloopt via een cytochroom P450 type van zuurstof overdracht en dus kon dit MP-8 gebruikt worden als model systeem voor de invloed van het actieve centrum op de cytochroom P450 gekatalyseerde regioselectiviteit van aromatische hydroxylering (*Hoofdstuk 5*). Aangezien de MP-8 gekatalyseerde regioselectiviteit van aromatische ring hydroxylering van de 3-fluor(methyl)anilines vergelijkbaar is met die van de cytochroom P450 gekatalyseerde omzetting kan geconcludeerd worden dat de cytochroom P450 gekatalyseerde regioselectiviteit van aromatische ring hydroxylering van de 3-fluor(methyl)anilines niet het gevolg is van een stereoselectieve oriëntatie van de substraten in de actieve centra als gevolg van interacties tussen het substraat en de aminozuren in het actieve centrum.

Tijdens de aromatische ring hydroxylering van benzeen derivaten is het mogelijk dat halogeen atomen (b.v. Cl, Br, F) verschuiven naar het naast gelegen koolstof atoom (NIH shift). Deze NIH shift verloopt via areenoxide intermediairen (zie Figuur 2). Het blijkt dat tijdens de *in vivo* cytochroom P450 gekatalyseerde aromatische ring hydroxylering van polyfluorbenzenen fluor atomen nauwelijks shiften terwijl *in vitro* verschuiving van fluor atomen wel mogelijk is. Dit kan verklaard worden doordat *in vivo* GSH conjugatie van het areenoxide een efficiënt alternatief is voor areenoxide opening gekoppeld met een NIH shift (*Hoofdstuk 6*). Voor de chloor analogen van deze polyfluorbenzenen treedt zowel *in vivo* als *in vitro* aanzienlijk meer chloor NIH shift op. Uit computer berekeningen kon de volgende verklaring worden afgeleid voor de gevonden verschillen tussen de *in vivo* fluor en chloor shift in halogeen benzenen: voor fluorbenzenen is de areenoxide opening energetisch moeilijker dan voor de chloor analogen. Bovendien bleek ook nog dat de fluor areenoxiden sneller reageren in de alternatieve reactie route met glutathion dan de chloor analogen.

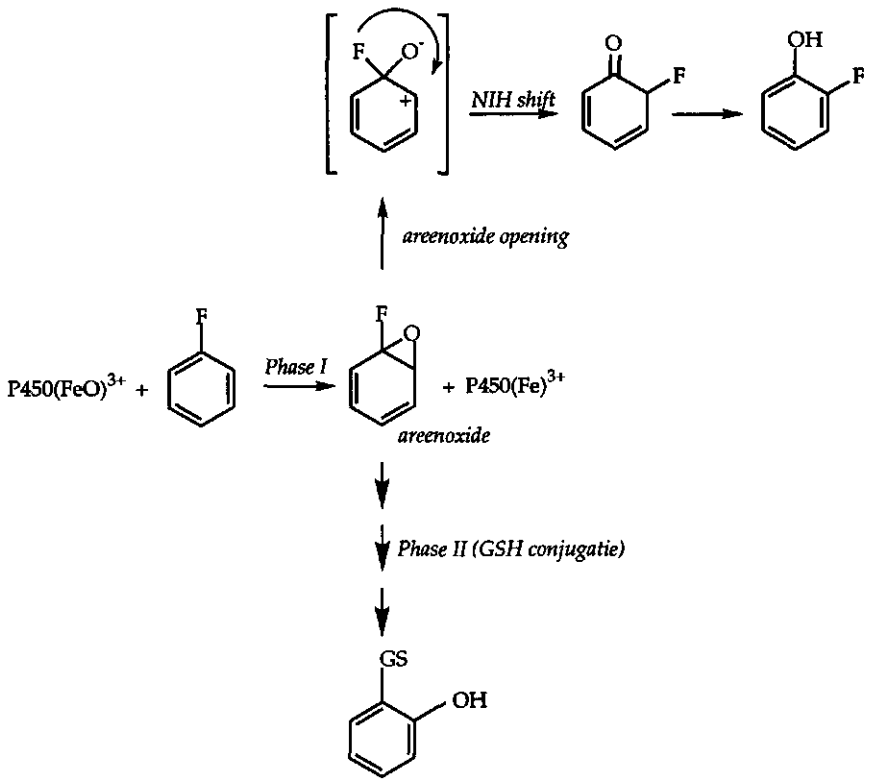

Figuur 2 Twee mogelijke metabole routes van areenoxiden.

Het effect van verschillende substituenten in benzeen derivaten op de biotransformatie route werd nogmaals geïllustreerd aan de hand van het insecticide teflubenzuron, dat is opgebouwd uit twee verschillend gesubstitueerde benzeen ringen verbonden door een ureum brug (*Hoofdstuk 7*). Ratten die oraal gedoseerd werden met deze verbinding namen slechts een klein percentage (10%) op uit het maag-darm kanaal, de rest werd ongemetaboliseerd uitgescheiden in de faeces. De ureum brug van het opgenomen teflubenzuron wordt gehydrolyseerd en de splitsingsprodukten, het benzoaat en aniline gedeelte, worden uitgescheiden in de urine. Het benzoaat deel wordt voornamelijk uitgescheiden als 2,6-difluorbenzoëzuur en het aniline gedeelte wordt uitgescheiden als metabolieten van 3,5-dichloor-2,4-difluoraniline en (3,5-dichloor-2,4-difluorfenyl)ureum. Hoewel een

gelijke hoeveelheid product is te verwachten van het benzoaat en aniline deel, wordt ongeveer 8 keer zoveel benzoaat als aniline product gevonden. Dosis-recovery studies van de splitsingsprodukten van teflubenzuron bevestigden deze resultaten daar urine recovery van het benzoaat gedeelte bijna 100% was terwijl dat van de aniline derivaten slechts ongeveer 50%. Dit verschil in recovery kan het best worden toegeschreven aan het feit dat het aniline gedeelte een cytochroom P450-gekatalyseerde dehalogenering op de C4 positie ondergaat waarbij mogelijk het zeer reactieve benzoquinonimine wordt gevormd. Dit benzoquinonimine kan binden aan celcomponenten en dus in het lichaam achterblijven. Dit laatste is vanuit toxicologisch oogpunt van belang omdat de vorming van een reactieve metaboliet in principe tot toxiciteit kan leiden.

Het onderzoek dat is uitgevoerd toont aan dat voor de onderzochte benzeen derivaten de chemische reaktiviteit van het substraat de belangrijkste rol speelt in het bepalen van het biotransformatie patroon. De chemische reaktiviteit kan gebruikt worden voor het opstellen van QSAR's zodat voorspellingen gedaan kunnen worden voor het biotransformatie patroon van nog niet onderzochte verbindingen. De vraag is nu in hoeverre deze QSAR's gebruikt kunnen worden voor verbindingen die qua structuur niet gerelateerd zijn aan de in deze studies onderzochte relatieve kleine niet polaire benzeen derivaten. Te verwachten is dat bij verbindingen met substituenten die specifieke interacties aangaan met de actieve centra of die zo groot zijn dat zij niet vrij draaibaar zijn in de actieve centra, een stereoselectieve oriëntatie van het substraat de regio/stereoselectieve katalyse zal bepalen naast de chemische reaktiviteit van het substraat. De consequentie is dat bij het opstellen van QSAR's voor dit soort verbindingen additionele parameters in rekening moeten worden gebracht zoals de (berekende of gemeten) optimale oriëntatie van het substraat in het actieve centrum.

Ook zijn QSARs van nut omdat zij meer inzicht kunnen geven in het mechanisme van reacties. Deze kennis kan mogelijk in de toekomst gebruikt worden om bijvoorbeeld een biotransformatie enzym als cytochroom P450 te gebruiken als biokatalysator. Deze mogelijkheid zal zeker steeds dichterbij komen als ook de techniek om enzymen te klonen verder ontwikkeld wordt en het dus ook economisch aantrekkelijker wordt om dit soort enzymen te gebruiken als katalysatoren bij de productie van chemische verbindingen. Via deze methode zullen minder afvalproducten ontstaan hetgeen uit milieuoogpunt zeer aantrekkelijk is.

Dankwoord

Een proefschrift schrijven kun je niet alleen, daarvoor heb je hulp nodig van vele mensen. Hierbij wil ik deze mensen bedanken voor hun bijdrage.
Allereerst mijn co-promotor Ivonne Rietjens voor de steun die je gaf om dit onderzoek uit te voeren. Hoewel je erg druk bent was er altijd de mogelijkheid om te komen praten over het onderzoek. De vele keren dat ik bij je kwam als het niet goed gestructureerd in mijn hoofd zat was je altijd in staat om dat te veranderen. Ik leerde er niet alleen veel van op wetenschappelijk gebied maar verliet je kamer ook vaak met tien keer zoveel energie. Jacques Vervoort bedank ik voor de hulp bij de vele NMR en computer problemen, en zijn levenswijsheden. Meestal kreeg ik deze wijsheden via stellingen gedoceerd. Hoewel ik sommige stellingen statistisch gezien nogal onverantwoord vond waren ze vaak wel verrassend nieuw voor mij en bleek het leven gelukkig toch niet altijd zo serieus te zijn.
Mijn promotor Prof. C. Veeger dank ik voor zijn inzet om dit onderzoek mogelijk te maken.
Veel dank aan Ans en Marelle voor de hulp en steun in het lab bij de vele HPLC en NMR monsters en de zoektocht naar een onbekende piek in het chromatogram of die ene verdwenen aniline ring. Minstens zo belangrijk, mede door jullie was het ook gezellig op het lab en kon ik mijn verhaal kwijt over niet alleen dat ene proefje maar ook over dingen die niets te maken hadden met cytochroom P450, MP-8 en benzeen derivaten. Dat geldt ook voor mijn mede lab-, kamer- en AIO-genoten, Jan-Willem, Lars, Marjon, Nicole, Petra, Sjaak, Sjef, Tatiana en Walter.
Ahmed Osman bedank ik voor het feit dat ik co-auteur mocht zijn van zijn artikel en dat dit artikel nu als Hoofdstuk 5 in mijn proefschrift kan staat.
Dank ook aan de studenten op het lab waaronder Sebastiaan Baks, Allart Stoop, Laura McRabeth, Henry van den Heijkant, Jan-Willem de Kraker en Martine Velraeds, die ook hun bijdrage hebben geleverd aan dit proefschrift.
Maria Faassen, Gerrit van Tintelen en Jo Haas bedank ik voor de uitstekende hulp bij de vele experimenten op het Centrum voor Kleine Proefdieren.
Tot slot wil ik een groep mensen bedanken die misschien niet direkt aan dit proefschrift hebben meegewerkt maar wel gezorgd hebben dat ik dat kon doen. Mijn vrienden, ouders, huisgenoten en kennissen bedank ik voor de interesse in mijn werk en de steun als ik dacht dat het allemaal niet zo goed verliep. Maar ook

belangrijk, jullie zorgen ervoor dat er nog meer in het leven is dan wetenschap; muziek, schaatsen en de fijne wandel- en fietsweekeinden/vakanties.

List of publications

- Koerts, J., Rietjens, I.M.C.M., Boersma, M.G., and Vervoort, J. (1995) ^{1}H NMR T_1 relaxation rate study on substrate orientation of fluoromethylanilines in the active sites of microsomal and purified cytochromes P4501A1 and 2B1. *FEBS Letters* 368, 279-284.

- Koerts, J., Boeren, S., Vervoort, J., Weiss, R., Veeger, C., and Rietjens, I.M.C.M. (1996) Interaction between the substrate and the high-valent-iron-oxo porphyrin cofactor as a possible factor influencing the regioselectivity of cytochrome P450-catalysed aromatic ring hydroxylation of 3-fluoro(methyl)anilines. *Chemico-Biological Interactions* 99, 129-146.

- Koerts, J., Velraeds, M.M.C., Soffers, A.E.M.F., Vervoort, J., and Rietjens, I.M.C.M. (1996) Influence of substituents in fluorobenzene derivatives on the cytochrome P450-catalysed hydroxylation at the adjacent *ortho* aromatic carbon centre. *Chemical Research in Toxicology*, accepted for publication.

- Koerts, J., Soffers, A.E.M.F., De Jager, A., and Rietjens, I.M.C.M. The occurrence of the NIH shift upon the cytochrome P450-catalysed *in vivo* and *in vitro* aromatic ring hydroxylation of fluorobenzenes. *Chemical Research in Toxicology*, submitted.

- Koerts, J., Soffers, A.E.M.F., De Kraker, J.-W., Cnubben, N.H.P., and Rietjens, I.M.C.M. Metabolism of the insecticide Teflubenzuron in rats. *Xenobiotica*, submitted.

- Rietjens, I.M.C.M., Koerts, J., Boeren, S., and Vervoort, J. (1991) Biosynthesis and chemical determination of polyfluoro-4-hydroxyanilines. *Recueil des Travaux Chimiques des Pays-Bas* 110, 216-221.

- Rietjens, I.M.C.M., Boersma, M.G., Soffers, A.E.M.F., Cnubben, N.H.P., Koerts, J., Peelen, S., Van Berkel, W.J.H., Veeger, C., and Vervoort, J. (1994) Use of molecular orbital calculations in studies on mechanisms of enzyme catalysis. In: Flavins and Flavoproteins 1993. (K. Yagi, Ed.), Walter de Gruyter and Co, Berlin.

- Vervoort, J., Boersma, M.G., Cnubben, N.H.P., Van Berkel, W.J.H., Koerts, J., and Rietjens, I.M.C.M. (1994) Mammalian flavin-containing monooxygenase catalysed conversion of 4-halo-N-methylanilines. In: Flavins and Flavoproteins 1993. (K. Yagi, Ed.), Walter de Gruyter and Co, Berlin.

- Osman, A.M., Koerts, J., Boersma, M.G., Boeren, S., Veeger, C., and Rietjens, I.M.C.M. (1996) Microperoxidase/H_2O_2-catalyzed aromatic hydroxylation proceeds by a cytochrome P450-type oxygen-transfer mechanism. *European Journal of Biochemistry* 240, 232-238.

Curriculum Vitae

Janneke Koerts werd geboren op 6 maart 1967 te Arnhem. In juni 1985 behaalde zij het Atheneum-b diploma aan de Katholieke Scholengemeenschap "De Breul" te Zeist. Daarna bracht zij een jaar door in Cambridge, Engeland, waar zij in juni 1986 het Cambridge Proficiency examen afgelegde.
In september 1986 begon zij met de studie Moleculaire Wetenschappen aan de Landbouwuniversiteit te Wageningen. Voor de doctoraalstudie verrichtte zij onderzoek bij de vakgroep Microbiologie (Prof. dr. A.J.B. Zehnder), Biochemie (Prof. dr. C. Veeger) en Milieutechnologie (Prof. dr. G. Lettinga). Vervolgens ging zij voor een stage naar de vakgroep Microbiologie van de Landbouwuniversiteit in Uppsala, Zweden. In maart 1992 studeerde zij af (met lof).
In april 1992 begon zij met een promotie-onderzoek bij de vakgroep Biochemie van de Landbouwuniversiteit Wageningen onder leiding van Prof. dr. C. Veeger, Dr. ir. I.M.C.M. Rietjens en Dr. ir. J. Vervoort. De resultaten van het promotie-onderzoek zijn beschreven in dit proefschrift. In deze periode volgde zij een deel van de doctoraal opleiding Bio-Pharmaceutische Wetenschappen aan de Rijksuniversiteit Leiden.
Vanaf augustus 1996 is zij werkzaam als post-doc bij de divisie Toxicologie van TNO Voeding te Zeist.